

Author Response for “Aqueous SOA formation from the photo-oxidation of vanillin: Direct photosensitized reactions and nitrate-mediated reactions” by Mabato et al.

We thank the reviewer for the thorough review and many constructive comments that helped improve the manuscript. Our point-by-point responses are below (changes to the original manuscript text and supporting information are in red, moved content in double-line strikethrough, and removed content in strikethrough). Please note that the line numbers in the responses refer to our revised manuscript with tracked changes. Also, please note that because we restructured the manuscript, the numbering of some figures and tables in the revised manuscript is different from those in the original manuscript.

## Reviewer 1

### Overview

The authors examined the aqueous photodegradation of vanillin (VL), a carbonyl-containing phenol emitted from biomass burning, and accompanying formation of aqueous SOA (aqSOA). They then measured the composition of the aqSOA using high-resolution mass spectrometry and UV/Vis absorption. They also determined the impact of purging solutions with N<sub>2</sub> (to remove dissolved oxygen) as well as the addition of ammonium nitrate (a photochemical source of hydroxyl radical, OH) and/or one of two hydroxyl radical scavengers (isopropyl alcohol or bicarbonate). They attempt to explain their results qualitatively based on a few dozen reactions, but there is little experimental attempt to test the mechanisms.

Vanillin has been studied in several past works, but this paper adds new information on the composition of the resulting aqSOA. The purging with N<sub>2</sub> is novel, but the interpretation of the results is not clear, and I disagree that these experiments show that secondary oxidants dominate VL loss. Unfortunately, the nitrate concentration added was too low to impact kinetics (because VL direct photodegradation is so fast), but it's interesting that it impacted the products formed. Finally, the authors seem compelled to try to mechanistically explain most of their results, but their explanations are very speculative and should be significantly cut. There are a several other major and minor issues, as described below.

Response: In this study, we aimed to investigate the photo-oxidation of VL at atmospherically relevant cloud and fog conditions. As mentioned in lines 112–116, ‘Although the concentration of VL in cloud/fog water has been estimated to be < 0.01 mM (Anastasio et al., 1996), a higher VL concentration (0.1 mM) was used in this study to guarantee sufficient signals for product identification (Vione et al., 2019). The chosen ammonium nitrate (AN) concentration (1 mM) was based on values observed in cloud and fog water (Munger et al., 1983; Collett et al., 1998; Zhang and Anastasio, 2003; Li et al., 2011; Giulianelli et al., 2014; Bianco et al., 2020).’ Our study is not intended to identify the concentrations of nitrate that would affect the kinetics. This sentence has been added to the text as follows:

Line 116: It should be noted that this study is not intended to identify the concentrations of nitrate that would affect the kinetics.

## Major Comments

1. The normalized abundance of products (line 131) is used throughout the paper as a key metric, but it's unclear if this is a robust endpoint, in part because its uncertainty is never discussed. (a) Based on the major products that have been identified (both via MS and IC), what is the likely range of ionization efficiencies (IEs) of the products and how much uncertainty does this introduce in the product abundance measure? (b) There is additional uncertainty in the quantification of VL, which is described on line 134 as semi-quantitative. (c) Altogether, what is the relative uncertainty in P from day to day and experiment to experiment? (d) This is an issue because there are several times when the normalized product abundance results are inconsistent with other, seemingly more quantitative metrics. For example, in section 3.1.3., the presence of OH scavengers had no significant effect upon VL decay or aqSOA light absorbance, but there were differences in the normalized abundance of products. Given the uncertainty in IE and other aspects of the product measure, I would be wary of attributing much significance to the normalized abundance of products as an endpoint when it's inconsistent with the more quantitative measures.

Response: The normalized abundance of products in this study is a semi-quantitative analysis intended to provide an overview of how the signal intensities (as normalized in Eq. 2) changed under different experimental conditions, but not to quantify the absolute concentration of products. Even if relative abundance (product peaks are normalized to the highest peak), which has been widely utilized (e.g., Lee et al., 2014, <https://pubs.acs.org/doi/10.1021/es502515r>; Romonosky et al., 2017, <https://pubs.acs.org/doi/10.1021/acs.jpca.6b10900>; Fleming et al., 2018, <https://doi.org/10.5194/acp-18-2461-2018>; Klodt et al., 2019, <https://pubs.acs.org/doi/pdf/10.1021/acsearchspacechem.9b00222>) in the literature is used instead of normalized abundance in our analysis, the major products detected as well as the conclusions of this study will remain the same. Regardless, we agree with the reviewer that we should emphasize the potential uncertainties in the normalized abundance of products. Detailed responses to the relevant sub-questions are as follows:

(a) Ionization efficiencies can indeed vary between different compounds. Unfortunately, the availability of measured relative ionization efficiencies (RIE) for different compounds is limited. We are not in a position to provide this information. The reviewer is correct that ESI ionization is not ideal for product quantification. Nevertheless, Nguyen et al. (2013) (<https://doi.org/10.1039/C2AY25682G>) found a positive correlation between ESI signal and "adjusted mass" (= molecular mass  $\times$  H: C). Based on that study, the uncertainty would be a factor of 2 – 4 if only the "adjusted mass" is considered, and further complications of matrix effect and polarity are disregarded. However, what we compared is not the absolute concentrations (or contributions) of the products observed. The comparison was based on how the signal intensities (as normalized in Eq. 2) changed under different experimental conditions. We compared the

responses of the same products (or at least the same class of products) as conditions varied, and their ionization efficiency might not be very different within the same class, according to the “adjusted mass” concept by Nguyen et al. (2013). We have revised Sect. 2.2 to highlight the inherent uncertainties for this metric due to ionization efficiencies which can vary for different compounds as follows:

Lines 146–167: Comparisons of peak abundance in mass spectrometry have been used in many recent studies (e.g., Lee et al., 2014; Romonosky et al., 2017; Wang et al., 2017; Fleming et al., 2018; Song et al., 2018; Klodt et al., 2019; Ning et al., 2019) to show the relative importance of different types of compounds (Wang et al., 2021). However, ionization efficiency may greatly vary for different classes of compounds (Kebarle, 2000; Schmidt et al., 2006; Leito et al., 2008; Perry et al., 2008; Krueve et al., 2014) and so uncertainties may arise from comparisons of peak areas among compounds. In this work, we assumed equal ionization efficiency of different compounds, which is commonly used to estimate O:C ratios of SOA (Bateman et al., 2012; Lin et al., 2012; De Haan et al., 2019), to calculate their normalized abundance. The normalized abundance of a product, [P] (unitless), was calculated as follows:

$$[P] = \frac{A_{P,t}}{A_{VL,t}} \cdot \frac{[VL]_t}{[VL]_0} \quad (\text{Eq. 2})$$

where  $A_{P,t}$  and  $A_{VL,t}$  are the extracted ion chromatogram (EIC) signal peak areas of the product P and VL from UHPLC-qToF-MS analyses at time  $t$ , respectively;  $[VL]_t$  and  $[VL]_0$  are the VL concentrations ( $\mu\text{M}$ ) determined using UHPLC at time  $t$  and 0, respectively. Here, we relied on the direct quantification more accurate measurements of [VL] using UHPLC (see Fig. S2 for VL calibration curve) for semi-quantification. ~~It should be noted that the ionization efficiency may greatly vary for different classes of compounds (Kebarle, 2000). Hence, we assumed equal ionization efficiency of different compounds to calculate their normalized abundance, which is commonly used to estimate O:C ratios of SOA (Bateman et al., 2012; Lin et al., 2012; De Haan et al., 2019).~~ It should be noted that the normalized abundance of products in this study is a semi-quantitative analysis intended to provide an overview of how the signal intensities changed under different experimental conditions but not to quantify the absolute concentration of products. Moreover, the major products detected in this study are probably those with high concentration or high ionization efficiency in the positive ESI mode. The use of relative abundance (product peaks are normalized to the highest peak) (e.g., Lee et al., 2014; Romonosky et al., 2017; Fleming et al., 2018; Klodt et al., 2019) would yield the same major products reported. Typical fragmentation behavior observed in MS/MS spectra for individual functional groups from Holčapek et al. (2010) are outlined in Table S1.

(b) The semi-quantification here refers to the normalized abundance of products, not the VL concentration. [VL] was directly quantified using UHPLC (see Fig. S2 for VL calibration curve). The reported [VL] are the average of results from triplicate experiments and the uncertainties from which and those from the MS signal intensities were propagated (now added in Table 2, formerly S2). This has been clarified in the text as follows:

Line 157: Here, we relied on the **direct quantification** ~~more accurate measurements~~ of [VL] using UHPLC (see Fig. S2 for VL calibration curve) ~~for semi-quantification~~.

(c) Given the same instrumental settings, the variations caused by the instrumental fluctuations would be smaller than the effects caused by the difference in ionization efficiency among different species. If there is any, it would be taken into account by the normalization in Eq. 2, which is why the normalized signal intensities were used instead of absolute signal intensities. For reference, relative uncertainties for MS signal peak areas of VL at the same concentration measured from different experiments range from 0.14 to 0.25. Moreover, the propagated uncertainties from the MS signal intensities and [VL] are now shown in Table 2 (formerly S2).

(d) For  $\cdot\text{OH}$  scavengers experiments, the insignificant changes for VL decay and absorbance enhancement might not be reflected in the products observed using UHPLC-qToF-MS in positive ESI mode. It is possible that the products observed might not have contributed significantly to all products formed and may not be the primary contributors to the absorbance enhancement. The absorbance enhancement may not necessarily correlate directly with the products detected. However, as mentioned in our response to major comment #4, we decided to omit the section for  $\cdot\text{OH}$  scavengers based on the likely minor contribution of  $\cdot\text{OH}$  to VL photo-oxidation in this study.

2. Throughout the manuscript, the low decay rate of  $\text{VL}^*$  under  $\text{N}_2$  is taken to mean that the triplet state of VL isn't involved in VL decay and that secondary,  $\text{O}_2$ -dependent, oxidants are responsible for VL decay. However, the  $\text{N}_2$ -purging control experiment result is ambiguous, since secondary steps in VL decay via triplets might require oxygen to proceed. For example, a major fate of the ketyl radical formed by the  $3\text{VL}^* + \text{VL}$  reaction is to add oxygen. In the absence of oxygen, the ketyl radical will still form, but its forward path ( $\text{O}_2$  addition) is blocked, possibly leading to eventual return to the reactants (and little apparent VL decay). So  $\text{N}_2$  purging is likely to not only remove secondary oxidants, but also to interfere with subsequent steps in the  $3\text{VL}^* - \text{VL}$  reactions. Thus the oft-stated conclusion that secondary oxidants from  $3\text{VL}^*$  are responsible for VL decay is not correct (e.g., on line 184). Without knowing the impact of  $\text{O}_2$  on the reaction intermediates in the triplet reaction, it is impossible to know what the  $\text{N}_2$ -purging result means.

Another strike against the "secondary oxidants" theory is that the proposed secondary oxidants are unlikely to be important for VL decay. For example, the  $1\text{O}_2^* + \text{VL}$  reaction is slow under the pH conditions here (where there is negligible phenolate). In air-saturated solutions, the  $1\text{O}_2^*$  and  $3\text{VL}^*$  concentrations should be roughly equal (see the McNeil and Canonica review in ESPI), but at pH 4 (and below) the rate constants for phenols with  $3\text{C}^*$  are much faster than the  $1\text{O}_2^*$  values. The bottom line is the  $1\text{O}_2^*$  is unlikely to be important. Similarly,  $\text{HO}_2/\text{O}_2^-$  was proposed as an oxidant for phenols, but these are very weak oxidants that react slowly with phenols. Finally,  $\text{OH}$  is apparently unimportant as well, based the  $\text{OH}$  scavengers having no significant impact on VL decay; however, it is possible that most of the IPA or bicarbonate was

purged from the sample prior to illumination (as discussed below). Regardless, photolysis of H<sub>2</sub>O<sub>2</sub> (formed from the <sup>3</sup>VL\* + VL reaction) will be slow, giving little OH.

Response: Thank you for this thorough and important analysis. We apologize for the confusion related to the role of VL triplets. The reviewer is correct that VL triplets are indeed important for VL decay and that the secondary oxidants generated in the presence of O<sub>2</sub> likely have only minor roles in the photo-oxidation of VL in this study. We also agree that without a detailed investigation of the effect of O<sub>2</sub> on the reactive intermediates, it is difficult to interpret the mechanism of the N<sub>2</sub> experiments. In principle, initial oxidation by triplets can proceed without O<sub>2</sub>, forming phenoxy (which is in resonance with a carbon-centered cyclohexadienyl radical that has a longer lifetime) and ketyl radicals (Neumann et al., 1986a, 1986b; Anastasio et al., 1996). The coupling of phenoxy radicals or phenoxy and cyclohexadienyl radicals can form oligomers, as observed for both N<sub>2</sub>- and air-saturated experiments. However, the little decay of VL under N<sub>2</sub>-saturated condition indicates that these radicals probably predominantly decayed via back-hydrogen transfer to regenerate VL (Lathioor et al., 1999). A possible explanation for this is the involvement of O<sub>2</sub> in the secondary steps of VL decay, likely concerning the fate of the ketyl radical, as the reviewer pointed out. We have amended the discussions to include these possibilities and to emphasize the importance of VL triplets as follows:

Line 187: ~~Effect of secondary oxidants from VL~~ VL photo-oxidation under N<sub>2</sub> and air-saturated conditions

Lines 188–220: ~~As mentioned earlier, secondary oxidants (<sup>1</sup>O<sub>2</sub>, O<sub>2</sub><sup>\*</sup>, <sup>•</sup>HO<sub>2</sub>, <sup>•</sup>OH) can be generated from <sup>3</sup>VL\* when O<sub>2</sub> is present (e.g., under air saturated conditions), while <sup>3</sup>VL\* is the only oxidant expected under N<sub>2</sub>-saturated conditions. The photo-oxidation of VL~~ To examine the contributions of <sup>3</sup>VL\* derived secondary oxidants and <sup>3</sup>VL\* only on VL photo-oxidation, experiments under both N<sub>2</sub>-air- and air-N<sub>2</sub>-saturated conditions (Fig. S3a) were carried out at pH 4, which is representative of moderately acidic aerosol and cloud pH values (Pye et al., 2020). No significant VL loss was observed for dark experiments. The oxidation of ground-state VL by <sup>3</sup>VL\* via H-atom abstraction or electron transfer can form phenoxy (which is in resonance with a carbon-centered cyclohexadienyl radical that has a longer lifetime) and ketyl radicals (Neumann et al., 1986a, 1986b; Anastasio et al., 1996). The coupling of phenoxy radicals or phenoxy and cyclohexadienyl radicals can form oligomers as observed for both N<sub>2</sub>- and air-saturated experiments (see discussions later). However, the little decay of VL under N<sub>2</sub>-saturated condition indicates that these radicals probably predominantly decayed via back-hydrogen transfer to regenerate VL (Lathioor et al., 1999). A possible explanation for this is the involvement of O<sub>2</sub> in the secondary steps of VL decay. For instance, a major fate of the ketyl radical is reaction with O<sub>2</sub> (Anastasio et al., 1996). In the absence of O<sub>2</sub>, radical formation occurs, but the forward reaction of ketyl radical and O<sub>2</sub> is blocked, leading to the regeneration of VL as suggested by the minimal VL decay. Aside from potential inhibition of secondary oxidants generation (Chen et al., 2020), N<sub>2</sub> purging may have also hindered the secondary steps for VL decay.

The low decay rate for VL\* under N<sub>2</sub>-saturated conditions suggests a minimal role for <sup>3</sup>VL\* in VL photo-oxidation. Contrastingly, the VL\* decay rate constant under air-saturated conditions was 4 times higher, revealing the importance of <sup>3</sup>VL\* derived secondary oxidants for photosensitized oxidation of VL. As mentioned earlier, secondary oxidants (<sup>1</sup>O<sub>2</sub>, O<sub>2</sub><sup>•-</sup>/<sup>•</sup>HO<sub>2</sub>, <sup>•</sup>OH) can be generated from <sup>3</sup>VL\* when O<sub>2</sub> is present (e.g., under air-saturated conditions). However, the photo-oxidation of VL in this study is likely mainly governed by <sup>3</sup>VL\* and that these secondary oxidants have only minor participation. Aside from <sup>•</sup>OH, O<sub>2</sub><sup>•-</sup>/<sup>•</sup>HO<sub>2</sub> and <sup>1</sup>O<sub>2</sub> can also promote VL photo-oxidation (Kaur and Anastasio, 2018; Chen et al., 2020). <sup>1</sup>O<sub>2</sub> is also a potential oxidant for phenols (Herrmann et al., 2010; Minella et al., 2011; Smith et al., 2014), but <sup>1</sup>O<sub>2</sub> reacts much faster (by ~60 times) with phenolate ions compared to neutral phenols (Tratnyek and Hoigne, 1991; Canonica et al., 1995; McNally et al., 2005). Under the pH values (pH 2.5 to 4) considered in this study, the amount of phenolate ion is negligible, so the reaction between VL and <sup>1</sup>O<sub>2</sub> should be slow. Interestingly, however, <sup>1</sup>O<sub>2</sub> has been shown to be important in the photo-oxidation of 4-ethylguaicol (pK<sub>a</sub> = 10.3) by <sup>3</sup>C\* of 3,4-dimethoxybenzaldehyde (solution with pH of ~3) (Chen et al., 2020). Furthermore, while the irradiation of other phenolic compounds can produce H<sub>2</sub>O<sub>2</sub>, a precursor for <sup>•</sup>OH (Anastasio et al., 1996), the amount of H<sub>2</sub>O<sub>2</sub> is small. Based on this, only trace amounts of H<sub>2</sub>O<sub>2</sub> were likely generated from VL\* (Li et al., 2014) under-air saturated conditions, suggesting that contribution from <sup>•</sup>OH was minor. Overall, these suggest that VL photo-oxidation in this study is driven by <sup>3</sup>VL\*. Further study on the impact of O<sub>2</sub> on the reactive intermediates involved is required to understand the exact mechanisms occurring under air-saturated conditions. Nonetheless, the VL\* decay trends clearly indicate that O<sub>2</sub> is important for efficient VL photo-oxidation an efficient oxidant for unsaturated organic compounds and has a lifetime that is much longer than <sup>3</sup>C\* (Chen et al., 2020).

Revisions made elsewhere in the text:

Line 23: The effects of oxygen (O<sub>2</sub>) secondary oxidants from <sup>3</sup>VL\*

Line 25: Our findings show that the secondary oxidants (<sup>1</sup>O<sub>2</sub>, O<sub>2</sub><sup>•-</sup>/<sup>•</sup>HO<sub>2</sub>, <sup>•</sup>OH) from the reactions of <sup>3</sup>VL\* and O<sub>2</sub> plays an essential role in VL photo-oxidation.

Line 91: The influences of O<sub>2</sub> secondary oxidants from VL triplets,

Line 184: In this work, the direct photosensitized oxidation of VL (by <sup>3</sup>VL\* or secondary oxidants from <sup>3</sup>VL\* and O<sub>2</sub> VL only experiments)

Lines 237–240: Although we have no quantification of the oxidants in our reaction systems as it is outside the scope of this study, these observations clearly substantiate that secondary oxidant from <sup>3</sup>VL\*, which are formed when O<sub>2</sub> is present, are required for efficient photosensitized oxidation of VL and nitrate-mediated VL photo-oxidation are more efficient in the presence of O<sub>2</sub>.

Lines 247–254: Compared to N<sub>2</sub>-saturated conditions, the normalized abundance of products such as oligomers, and functionalized monomers (e.g., demethylated VL; Fig. S4), and nitrogen-

containing compounds (e.g.,  $C_{16}H_{10}N_2O_9$ ; No. 33, Table S3, Table S2) (for VL+AN) had higher normalized abundance ~~were also more relatively abundant under air-saturated conditions were significantly higher under air saturated conditions~~ (Figs. 1c-d), likely due to **efficient the secondary oxidants from  $^3VL^*$ -initiated oxidation and enhanced VL nitration in the presence of and  $O_2$  and their interactions with nitrate photolysis products.** ~~The nitrogen-containing compounds (e.g.,  $C_{16}H_{10}N_2O_9$ ; No. 3, Table S3) were also more relatively abundant under air saturated conditions.~~ For both VL\* and VL+AN under air-saturated conditions, the most abundant product was  $C_{10}H_{10}O_5$  (No. 4, Table S23), a substituted VL.

Lines 287–289: Among experiments A5 to A8 (Table S2), VL+AN under air-saturated conditions (A7) had the highest normalized abundance of products and  $\langle OS_c \rangle$ , ~~most~~ probably due to the combined influence of ~~the secondary oxidants from  $^3VL^*$  and~~ **enhanced VL nitration in the presence of  $O_2$ , and nitrate photolysis products.**

Lines 295–300: In brief, the **presence of secondary oxidants from  $^3VL^*$  and  $O_2$  increased the normalized abundance of products and promoted the formation of more oxidized aqSOA.** ~~These trends were reinforced in the presence of nitrate, indicating synergistic effects between secondary oxidants from VL triplets and nitrate photolysis products.~~ **Compared to  $N_2$ -saturated condition, the higher normalized abundance of nitrogen-containing products under air-saturated condition for VL+AN (at pH 4) suggests a potential enhancement of VL nitration in the presence of  $O_2$ .**

Lines 324–326: Overall, these trends establish that ~~secondary oxidants from  $^3VL^*$  and  $O_2$  are~~ **is** necessary for the efficient formation of light-absorbing compounds from both VL\* and VL+AN.

Lines 493–495: Aside from the potential imidazole derivative ( $C_5H_5N_3O_2$ ; No. 510, Table S23),  $C_8H_9NO_3$  (No. 2, Table S2) was also observed from VL+AN but only under  $N_2$ -saturated conditions (Fig. 1b), probably due to further oxidation by ~~secondary oxidants from  $^3VL^*$ .~~

Line 512: This enhanced GUA decay rate **constant** may be due to the ~~following main reactions: oxidation of GUA by  $^3VL^*$  (or the secondary oxidants it generates upon reaction with  $O_2$ ),~~

Lines 520: which may be due to competition between ground-state VL and GUA for reactions with  $^3VL^*$  ~~(or the secondary oxidants it generates upon reaction with  $O_2$ )~~

Line 543: possibly due to both GUA and ground-state VL being available as oxidizable substrates for  $^3VL^*$  ~~and the secondary oxidants it can generate.~~

Line 601: Our results indicate that the photo-oxidation of VL is influenced by  $O_2$  ~~secondary oxidants from VL triplets, pH~~

Lines 602–612: ~~Compared to Under  $N_2$ -saturated conditions, the absence of  $O_2$  likely hindered the secondary steps in VL decay (e.g., reaction of ketyl radical and  $O_2$ ), regenerating VL as suggested by the minimal VL decay~~ **more efficient VL photo-oxidation was observed under air-**

~~saturated conditions ( $O_2$  is present), which can be attributed to the generation of secondary oxidants (e.g.,  $^1O_2$ ,  $O_2^{\bullet-}$ ,  $HO_2^{\bullet}$ ,  $^{\bullet}OH$ ) from  $^3VL^*$ . Further enhancement of VL photo-oxidation under air saturated conditions in the presence of nitrate indicates synergistic effects between secondary oxidants from VL triplets and nitrate photolysis products. In contrast,  $^3VL^*$ -initiated reactions proceeded rapidly under air-saturated conditions ( $O_2$  is present) as indicated by higher VL decay rate constant and increased normalized abundance of products. For pH 4 experiments, the presence of both  $O_2$  and nitrate resulted in the highest normalized abundance of products (including N-containing compounds) and  $\langle OS_C \rangle$ , which may be due to  $O_2$  promoting VL nitration. Nevertheless, further work is necessary to assess the effect of  $O_2$  on the reactive intermediates involved in  $^3VL^*$ -driven photo-oxidation and elucidate the mechanisms of VL photo-oxidation under air-saturated conditions.~~

3. Mechanism discussion. The authors seem compelled to try to explain all of their observations using one or more reactions, but since there is no quantitative examination of these mechanisms, they are all very speculative and mostly not useful. Worse, in some (many?) cases, the proposed mechanisms are inconsistent with some of the data. Fundamentally, without building a kinetic model of the mechanism and testing it against the observations, it is difficult to know whether the proposed reactions are important. The authors put too much emphasis on trying to mechanistically explain their observations and these explanations end up being mostly conjectures that are not grounded in data. These mechanistic speculations should be greatly reduced, especially if they are inconsistent with the kinetic or light absorption data and/or if they rely primarily upon the “normalized abundance of products” metric, which seems highly uncertain.

For example, on line 226, what trends were reinforced in the presence of nitrate? Looking at Table S2, ammonium nitrate has no effect on the kinetics, does not change the normalized product abundance at pH 2.5 or 3 (but does increase it at pH 4), and has no impact on  $OS(C)$ . Later, in Fig. 2, we see that the presence of nitrate only negligibly increased the long-wavelength absorbance of the products. Overall, the bulk of the observations suggest that nitrate has a minor impact on VL decay, consistent with the fast direct photodegradation of VL.

Response: We concur with the reviewer that the current manuscript contains several speculative reaction mechanisms. As building a kinetic model of the mechanisms is beyond the scope of this study, we proposed major pathways for aqSOA formation instead (Fig. 2, formerly 4). As suggested in major comment #7, Fig. 2 has been shown for the first time when potential aqSOA formation pathways were discussed, then referred to throughout the text.

The trends in line 297 (formerly 226) pertain to nitrate enhancing the increased normalized abundance of products and formation of more oxidized aqSOA from VL photo-oxidation in the presence of  $O_2$  ( $VL^*$  and  $VL+AN$  under air-saturated conditions) at pH 4, suggesting a potential enhancement of VL nitration in the presence of  $O_2$ . This has been revised as follows:

Lines 295–300: In brief, the ~~presence of secondary oxidants from  $^3VL^*$  and  $O_2$~~  increased the ~~normalized~~ abundance of products and promoted the formation of more oxidized aqSOA. ~~These~~



~~trends were reinforced in the presence of nitrate, indicating synergistic effects between secondary oxidants from VL triplets and nitrate photolysis products.~~ Compared to N<sub>2</sub>-saturated condition, the higher normalized abundance of nitrogen-containing products under air-saturated condition for VL+AN (at pH 4) suggests a potential enhancement of VL nitration in the presence of O<sub>2</sub>.

4. I am concerned that the authors purged IPA and bicarbonate from solution during each experiment since solutions were bubbled continuously. Do they have any way to know if these OH scavengers were removed before or during illumination? Similarly, guaiacol shouldn't undergo direct photochemical loss under illumination above 300 nm, so the apparent decay measured in the dark could be evaporation during purging. If the purging was slow enough, each bubble would achieve Henry's law equilibrium with the solution, which would allow you to estimate the rates of IPA and bicarbonate (lost as CO<sub>2</sub>) from the rate constant for GUA loss and the ratio of Henry's law constants for GUA and OH scavenger. For GUA, which can be measured by HPLC, the authors should report the fraction of the initial concentration (0.1 mM) that was lost after the 30 min of purging in the dark and the fraction then lost in the dark control for the illumination experiment. Then for IPA and bicarbonate, some estimate of their fraction lost during purging would be helpful. At the very least, this issue needs to be raised and addressed.

Response: The reviewer has correctly pointed out that the contribution of <sup>•</sup>OH to VL photo-oxidation in this study is likely minor, which is also suggested by other published literature (Anastasio et al., 1996; Li et al., 2014). We, therefore, decided to omit this section (and related sentences) and instead focus on the other findings of the paper.

5. Section 3.1.2. (a) Are VL (and GUA) decay rate constants normalized for photon fluxes? (b) Given the variability in kinetic decays, are the relative small differences in decay rate constants between pH 2.5 and 4 statistically different? (c) Do the authors have a good measure of the variability of the kinetics, e.g., the standard deviation of  $j(\text{VL})$  based on triplicate experiments? Given that the decays are not first order, it is more difficult to discern differences in rate constants, so I would be cautious.

Response: (a) We thank the reviewer for pointing this out. The decay rate constants were initially not normalized for photon fluxes, although the reported values are the average of results from triplicate experiments. The values have been updated to the photon flux-normalized decay rate constants, and the following information were added to the text:

Line 142: The decay rate constants were normalized to the photon flux measured for each experiment through dividing  $k'$  by the measured 2-nitrobenzaldehyde (2NB) decay rate constant,  $j(2\text{NB})$  (see Text S6 for more details).

(b) Yes, the differences in the decay rate constants between pH 2.5 and 4 (VL\*: decay rate constant at pH 2.5 is 1.6 times higher than at pH 4; VL+AN: decay rate constant at pH 2.5 is 1.4 times higher than at pH 4) are small but statistically significant ( $p < 0.05$ ). In addition, the variability for the decay rate constant measurements among triplicate experiments for all

conditions in this study is low (the standard deviation for each condition is now added in Table 2, formerly S2). We have added this in the text as follows:

Line 331: The decay rates constants for both VL\* and VL+AN increased as pH decreased (VL\* and VL+AN at pH 2.5: 1.65 and 1.43 times faster than at pH 4, respectively) (Fig. S3b). These differences in decay rate constants are small but statistically significant ( $p < 0.05$ ).

Other relevant changes in the text are as follows:

Line 510: The enhancement of GUA decay rate constant in the presence of VL is statistically significant ( $p < 0.05$ ), while that in the presence of AN is not ( $p > 0.05$ ).

(c) Yes, the reported decay rate constants are the average of results from triplicate experiments, and the standard deviation for each condition is now added in Table 2, formerly S2. The footnote of Table 2 has been revised as follows:

Table 2: <sup>b</sup>The data fitting was performed in the initial linear region. Each value is the average of results from triplicate experiments. Errors represent one standard deviation.

6. Lines 283-289. I would be surprised if deprotonation of phenols is responsible for the higher absorbance of the aqSOA at pH 4 compared to pH 3 and 2.5. For one, the pKa values of methoxy-substituted phenols are near 10, so there's no appreciable phenolate at pH 4. Nitro-substituted phenols can have much lower pKas, but absorbance of the aqSOA formed in the presence of nitrate is nearly the same as in the absence of nitrate, so it seems nitrophenols are a minor part of the light absorption. Another possibility is that different products are made at pH 2.5 compared to pH 4. Measuring the pH dependence of the aqSOA formed at pH 2.5 and 4 would allow you to determine whether the pH dependence is rooted in acid-base chemistry of the products or of the reactions.

Response: Thank you for the suggestion. As suggested, to understand the pH effect further, we measured the pH dependence of the aqSOA formed from VL\* at pH 4 and 2.5. The reviewer is correct that deprotonation of phenols does not sufficiently explain the higher absorbance enhancement observed at pH 4 compared to pH 2.5. Based on the comparable pH dependence of the aqSOA formed from VL\* at pH 4 and 2.5 (see figure below), the pH dependence observed is likely due to the acid-base chemistry of the reactions, probably involving <sup>3</sup>VL\* or the excimer of VL (Smith et al., 2016). Smith et al. (2016) reported that the direct photodegradation rate constants for 0.005 mM VL at  $pH \leq 3$  are nearly two times lower than at  $pH \geq 5$ . The opposite trend observed in this study for 0.1 mM VL (VL\* decay rate constant at pH 2.5 is 1.6 times higher than at pH 4) may be due to the reactivities of the protonated and neutral forms of the <sup>3</sup>VL\* being dependent on the VL concentration (Smith et al., 2016). Also, it has been reported that the quantum yield for direct VL photodegradation is higher at pH 5 than at pH 2 for 0.005 mM VL, but they are not statistically different for 0.03 mM VL (Smith et al., 2016). Changes on the text are as follows:

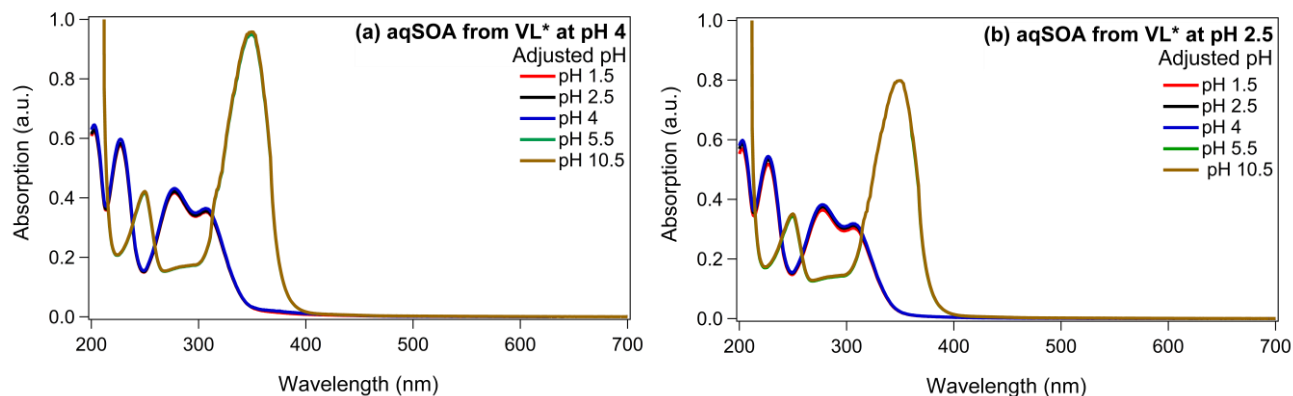


**Figure S10.** UV-Vis absorption spectra of VL\*-derived aqSOA formed at (a) pH 4 and (b) pH 2.5 over a range of pH conditions from 1.5 to 10.5.

Lines 375–386: ~~The higher absorbance enhancement for both VL\* and VL+AN (Fig. 32b) was observed as pH increased may be attributed to redshifts and increased visible light absorption of reaction products (Pang et al., 2019a). To determine whether the pH dependence is due to the acid-base chemistry of the products or of the reactions, we measured the pH dependence of the aqSOA formed from VL\* at pH 4 and 2.5 over a range of pH conditions from 1.5 to 10.5 (Fig. S10). For both cases, the intensity of absorption at longer wavelengths significantly increased as the pH of the solutions was raised. Moreover, the comparable pH dependence of the two solutions suggest that the observed pH dependence may be attributed to the acid-base chemistry of the reactions, which may involve <sup>3</sup>VL\* or the excimer of VL (Smith et al., 2016), as discussed earlier. When a phenolic molecule deprotonates at higher pH, an ortho or para electron withdrawing group, such as a nitro or aldehyde group, can attract a portion of the negative charge towards its oxygen atoms through induced and conjugated effects, leading to the extension of chromophore from the electron donating group (e.g., O<sup>-</sup>) to the electron withdrawing group via the aromatic ring (Carey, 2000; Williams and Fleming, 2008; Pang et al., 2019a). Hence, the delocalization of the negative charge in phenolates leads to significant redshifts (Mohr et al., 2013).~~

For reference, changes in the revised text that are relevant to lines 375–386 are shown below:

Lines 331–352: The decay rates constants for both VL\* and VL+AN increased as pH decreased (VL\* and VL+AN at pH 2.5: 1.65 and 1.43 times faster than at pH 4, respectively) (Fig. S3b). These differences in decay rate constants are small but statistically significant ( $p < 0.05$ ). The  $pK_a$  for the VL triplet has been reported to be 4.0 (Smith et al., 2016). As there are a greater fraction of VL triplets that are protonated at pH 2.5 (0.96) than at pH 4 (0.5), it is possible that the pH dependence of the decay rate constants observed in this study is due to <sup>3</sup>VL\* being more reactive in its protonated form. Smith et al. (2016) also observed a pH dependence for the direct photodegradation of VL (0.005 mM) (rate constants at  $pH \leq 3$  are ~two times lower than at  $pH \geq 5$ ) which they attributed to the sensitivity of the excimer of VL (i.e., the charge-transfer complex

formed between an excited state VL molecule and a separate ground state VL molecule; Birks, 1973, Turro et al., 2010) to acid-base chemistry. The opposite trend observed in this study for 0.1 mM VL may be due to the reactivities of the protonated and neutral forms of the  $^3\text{VL}^*$  being dependent on the VL concentration (Smith et al., 2016). For VL\*, this pH trend indicates that  $^3\text{VL}^*$  are more reactive in their protonated form, which is opposite to that reported for 0.005 mM VL (Smith et al., 2016), likely due to the concentration dependence of the relative reactivities of protonated and neutral forms of  $^3\text{VL}^*$ . It has been reported that the quantum yield for direct VL photodegradation is higher at pH 5 than at pH 2 for 0.005 mM VL, but they are not statistically different for 0.03 mM VL (Smith et al., 2016). Also, increases in hydrogen ion concentration can enhance the formation of  $\text{HO}_2^*$  and  $\text{H}_2\text{O}_2$  and in turn,  $^*\text{OH}$  formation (Du et al., 2011). In addition to these pH influences on VL\*, the dependence of N(III) ( $\text{NO}_2^- + \text{HONO}$ ) speciation on solution acidity (Pang et al., 2019a) also contributed to the observed pH effects for VL+AN. At pH 3.3, half of N(III) exists as HONO (Fischer and Warneck, 1996; Pang et al., 2019a), which has a higher quantum yield for  $^*\text{OH}$  formation than that of  $\text{NO}_2^-$  in the near-UV region (Arakaki et al., 1999; Kim et al., 2014). The increased  $^*\text{OH}$  formation rates as pH decreases can lead to faster VL decay (Pang et al., 2019a). Also,  $\text{NO}_2^-/\text{HONO}$  can generate  $^*\text{NO}_2$  via oxidation by  $^*\text{OH}$  (Reactions 4 and 15; Table 1) (Pang et al., 2019a). As pH decreases, the higher reactivity of  $^3\text{VL}^*$  and sensitivity of the excimer of VL to acid-base chemistry HONO being the dominant N(III) species can lead to faster VL photo-oxidation may have led to faster VL photo-oxidation.

7. Section 3.5. This section repeats what has been stated before. I would delete this section, show Figure 4 the first time discussing possible mechanisms, then refer to the Figure throughout the discussion of mechanisms (which is hopefully much shorter in the revised version).

Response: We agree with the reviewer. Section 3.5 has been deleted, and Fig. 4, now 2, has been shown for the first time when potential aqSOA formation pathways were discussed, then referred to throughout the text as follows:

Line 259: This compound was not observed in a parallel experiment in which AN was replaced with sodium nitrate (SN) (Fig. S6a; see Sect. 3.3 for discussion). The potential aqSOA formation most probable pathways via of direct photosensitized and nitrate-mediated photo-oxidation of VL photo-oxidation in this study are summarized in Fig. 2 were proposed (Fig. 4). In Scheme 1 (pH 4 and pH <4 under air-saturated conditions),  $^3\text{VL}^*$  and  $^*\text{OH}$  (from  $^3\text{VL}^*$  or nitrate photolysis) can initiate H atom abstraction to generate phenoxy or ketyl radicals (Huang et al., 2018; Vione et al., 2019). At pH 4, ring-opening products (Fig. S5) from fragmentation in both VL\* and VL+AN may have reacted with VL or dissolved ammonia to generate  $\text{C}_{10}\text{H}_{10}\text{O}_5$  (No. 4, Table S2) (Pang et al., 2019b) and a potential imidazole derivative ( $\text{C}_5\text{H}_5\text{N}_3\text{O}_2$ ; No. 5, Table S2), respectively. Moreover, nitrate photolysis products promoted functionalization and nitration (e.g.,  $\text{C}_{16}\text{H}_{10}\text{N}_2\text{O}_9$ ; No. 3, Table S2). At pH <4, the reactivity of  $^3\text{VL}^*$  increased as suggested by the abundance of oligomers (e.g.,  $\text{C}_{16}\text{H}_{14}\text{O}_6$ ) and increased normalized abundance of N-containing compounds.

Line 364: At pH < 4, <sup>3</sup>VL\* likely have higher reactivity as suggested by the increased normalized abundance of oligomers (e.g., C<sub>16</sub>H<sub>14</sub>O<sub>6</sub>; No. 6, Table S2 and C<sub>31</sub>H<sub>24</sub>O<sub>11</sub>) and N-containing compounds (e.g., C<sub>16</sub>H<sub>10</sub>N<sub>2</sub>O<sub>9</sub>; No. 3, Table S2 and C<sub>13</sub>H<sub>14</sub>N<sub>2</sub>O<sub>10</sub>) (Fig. 2).

### Minor Comments

1. Line 25. This notion of “efficiency” (i.e., which reaction path is faster) depends on the concentrations of the two oxidant precursors, VL and nitrate. Thus it’s not a universally true statement.

Response: Thank you for this suggestion. The apparent quantum efficiency of GUA photodegradation ( $\Phi_{\text{GUA}}$ ) in the presence of either VL or nitrate during simulated sunlight illumination can be defined as (Anastasio et al., 1996; Smith et al., 2014, 2016):

$$\Phi_{\text{GUA}} = \frac{\text{mol GUA destroyed}}{\text{mol photons absorbed}} \quad (\text{Eq. S9})$$

$\Phi_{\text{GUA}}$  was calculated using the measured rate of GUA decay and rate of light absorption by either VL or nitrate through the following equation:

$$\Phi_{\text{GUA}} = \frac{\text{rate of GUA decay}}{\text{rate of light absorption by VL or nitrate}} = \frac{k'_{\text{GUA}} \times [\text{GUA}]}{\sum[(1 - 10^{-\epsilon_{\lambda}[\text{C}]l}) \times I'_{\lambda}]} \quad (\text{Eq. S10})$$

where  $k'_{\text{GUA}}$  is the pseudo-first-order rate constant for GUA decay, [GUA] is the concentration of GUA (M),  $\epsilon_{\lambda}$  is the base-10 molar absorptivity (M<sup>-1</sup> cm<sup>-1</sup>) of VL or nitrate at wavelength  $\lambda$ , [C] is the concentration of VL or nitrate (M),  $l$  is the pathlength of the illumination cell (cm), and  $I'_{\lambda}$  is the volume-averaged photon flux (mol-photons L<sup>-1</sup> s<sup>-1</sup> nm<sup>-1</sup>) determined from 2NB actinometry:

$$j(2\text{NB}) = 2.303 \times \Phi_{2\text{NB}} \times l \times \sum_{300 \text{ nm}}^{350 \text{ nm}} (\epsilon_{2\text{NB},\lambda} \times I'_{\lambda} \times \Delta\lambda) \quad (\text{Eq. S11})$$

The  $\Phi_{\text{GUA}}$  in the presence of nitrate ( $1.3 \times 10^{-2} \pm 2.9 \times 10^{-3}$ ) is ~14 times larger than that in the presence of VL ( $9.0 \times 10^{-4} \pm 4.0 \times 10^{-4}$ ), suggesting that nitrate-mediated photo-oxidation of GUA is more efficient than that by photosensitized reactions of VL. We have revised this in the text as follows and added the information shown above in the supporting information: **Text S7. Estimation of the apparent quantum efficiency of guaiacol photodegradation.**

Line 29: Furthermore, comparisons of the apparent quantum efficiency of guaiacol photodegradation indicate that in this study, guaiacol oxidation by photosensitized reactions of VL ~~was observed to be more~~ is less efficient relative to nitrate-mediated photo-oxidation. Other relevant revisions in the text are as follows:

Line 514: As mentioned earlier, ~~the~~  $^3\text{VL}^*$  chemistry appears to be more important than that of nitrate photolysis even at 1:10 molar ratio of VL/nitrate on account of the much higher molar absorptivity of VL compared to that of nitrate (Fig. S1) and the high VL concentration (0.1 mM) used in this study. However, the apparent quantum efficiency of GUA photodegradation ( $\phi_{\text{GUA}}$ ) in the presence of nitrate ( $1.3 \times 10^{-2} \pm 2.9 \times 10^{-3}$ ) is  $\sim 14$  times larger than that in the presence of VL ( $9.0 \times 10^{-4} \pm 4.0 \times 10^{-4}$ ), suggesting that nitrate-mediated photo-oxidation of GUA is more efficient than that by photosensitized reactions of VL (see Text S7 for the more details).

Line 619: The oxidation of guaiacol, a non-carbonyl phenol, by photosensitized reactions of vanillin was also shown to be ~~more~~ less efficient than that by nitrate photolysis products based on its lower apparent quantum efficiency.

2. L. 42. “respectively” doesn’t serve a purpose in this sentence.

Response: Agree, we have deleted ‘respectively’ from line 50 (formerly 42).

3. Section 2.1. What was the initial volume of solution illuminated? Were solutions stirred? What was the flow rate of gas ( $\text{N}_2$  or air) through the solution before and during the experiment?

Response: The initial volume of the illuminated solution is 500 mL. The solutions were continuously mixed throughout the experiments. A constant flow rate of  $0.5 \text{ dm}^3/\text{min}$  was used before and during the experiments. These have been added to the text as follows:

Line 102: Photo-oxidation experiments were performed in a ~~500-mL~~ custom-built quartz photoreactor. The solutions (initial volume of 500 mL) were continuously mixed throughout the experiments using ~~equipped with~~ a magnetic stirrer. The solutions were bubbled with synthetic air or nitrogen ( $\text{N}_2$ ) (> 99.995%) ( $0.5 \text{ dm}^3/\text{min}$ ) for 30 min before irradiation to achieve air- and  $\text{N}_2$ -saturated conditions, respectively, and the bubbling was continued throughout the reactions (Du et al., 2011; Chen et al., 2020).

4. L. 100. Was there a difference in the temperature between the illuminated and dark solutions?

Response: For all experiments, the range in temperature fluctuations was  $27 \pm 2 \text{ }^\circ\text{C}$ .

5. L. 106. If the authors are going to abbreviate 2-propanol as IPA, it would be better to call it isopropyl alcohol to help readers remember the name of the abbreviation. NaBC is a poor choice for an abbreviation for sodium bicarbonate since BC stands for black carbon typically. Better to simply use its chemical formula,  $\text{NaHCO}_3$  or  $\text{HCO}_3^-$ , depending on the context.

Response: Sentences related to  $^{\bullet}\text{OH}$  scavengers have been deleted from the original manuscript.

6. L. 111. 2-propanol and bicarbonate were added in some experiments, but the description of why is odd. Their primary role will be OH scavengers, so it’s strange to call them a VOC and

inorganic anion, respectively. 2-propanol is not a common atmospheric gas, so it's a poor choice of model VOC. Similarly, calling bicarbonate an "inorganic anion" is a poor choice of words, since sulfate and nitrate are the classic inorganic ions. Better to refer to 2-propanol and bicarbonate as "OH scavengers" since that is their main role.

Response: Sentences related to  $\cdot\text{OH}$  scavengers have been deleted from the original manuscript.

7. L. 113. What does it mean that the OH scavengers were not added "in excess"? Since they're reacting with OH (which will have a very low concentration) they are technically in excess. Better to avoid this discussion, as it's not fruitful. If you want to dive more into the OH scavengers, you could calculate the fraction of OH each intercepts in their respective solutions or the amount that they suppress the OH concentration. (But, again, this depends on if the species were purged from solution.)

Response: Sentences related to  $\cdot\text{OH}$  scavengers have been deleted from the original manuscript.

8. L. 151. The disproportionation of  $\text{HO}_2/\text{O}_2^-$  is the same as the reaction of  $\text{HO}_2$  with  $\text{O}_2^-$ , so this sentence repeats itself.

Response: The reviewer is right. We have corrected this sentence as follows:

Line 181: The disproportionation of  $\text{HO}_2^*/\text{O}_2^*$  (Anastasio et al., 1996) ~~and reaction of  $\text{HO}_2^*$  with  $\text{O}_2^*$  (Du et al., 2011)~~ form hydrogen peroxide ( $\text{H}_2\text{O}_2$ ), which is a photolytic source of  $\cdot\text{OH}$ .

9. L. 163. It's unclear what the authors mean by "...a minimal role for  $^3\text{VL}^*$  in VL photo-oxidation". Do they mean that  $^3\text{VL}^* + \text{VL}$  is an unimportant reaction (but see above about this) or that the direct photodegradation of VL doesn't proceed through the triplet state?

Response: In this study, the photodegradation of VL is mainly governed by VL triplets, as explained in our response to major comment #2 (Please see this response for the revised text).

10. L. 167. It is not true that  $^1\text{O}_2$  has a much longer lifetime than  $^3\text{C}^*$ ; rather, the lifetimes are approximately the same. In cloud and fog drops, the lifetime of  $^1\text{O}_2$  is controlled by water deactivation and is approximately 5  $\mu\text{s}$  (see Bilski et al., 1997). The lifetime of  $^3\text{C}^*$  is controlled by reaction with dissolved  $\text{O}_2$  and is approximately  $1/((2\text{E}9 \text{ M}^{-1} \text{ s}^{-1}) * (250 \mu\text{M})) \sim 2 \mu\text{s}$ . Also, rather than the oxidant lifetime, it is the product of the oxidant concentration times its second-order rate constant that determines the relative importance of a given oxidant.

Response: We thank the reviewer for the correction. This sentence has been modified as part of the revision for major comment #2 (Please see this response for the revised text).

11. Page 7. This whole page is one paragraph. It should be trimmed to reduce speculative discussions of mechanisms, then broken into smaller pieces, focused on certain themes/points.

Response: We agree with the reviewer. Section 3.1.1 has been revised to reduce speculative discussions of mechanisms (Revisions for lines 188–220 are shown in response to major comment #2). Changes in the text are as follows:

Lines 220–240: ~~Similar to VL\*, the~~ decay rate **constant** for VL+AN under air-saturated conditions was **also higher faster** (6.6 times) than N<sub>2</sub>-saturated conditions; which **may can** be due to ~~several~~ reactions facilitated by nitrate photolysis products ~~and the enhancement of N(III)-mediated photo-oxidation that may have been enhanced~~ in the presence of O<sub>2</sub> as reported in early works (Vione et al., 2005; Kim et al., 2014; Pang et al., 2019a). **As shown later, more nitrogen-containing species were observed under air-saturated conditions.** An example is enhanced VL nitration likely from increased <sup>•</sup>NO<sub>2</sub> formation such as from the reaction of <sup>•</sup>OH and O<sub>2</sub><sup>•-</sup> with NO<sub>2</sub><sup>-</sup> (Reactions 4 and 5, respectively; Table 1) or the autoxidation of <sup>•</sup>NO from NO<sub>2</sub><sup>-</sup> photolysis (Reactions 6–9; Table 1) in aqueous solutions (Pang et al., 2019a). ~~Reactions involving <sup>•</sup>HO<sub>2</sub>/O<sub>2</sub><sup>•-</sup> which may originate from the photolysis of nitrate alone, likely from the production and subsequent photolysis of peroxyxynitrous acid (HOONO) (Reaction 10; Table 1) (Jung et al., 2017; Wang et al., 2021), or the reactions of <sup>3</sup>VL\* in the presence of O<sub>2</sub>, may have contributed as well. For instance, Wang et al. (2021) recently demonstrated that nitrate photolysis generates <sup>•</sup>HO<sub>2</sub>/O<sub>2</sub><sup>•-</sup><sub>(aq)</sub> and HONO<sub>(g)</sub> in the presence of dissolved aliphatic organic matter (e.g., nonanoic acid, ethanol), with the enhanced HONO<sub>(g)</sub> production caused by secondary photochemistry between <sup>•</sup>HO<sub>2</sub>/O<sub>2</sub><sup>•-</sup><sub>(aq)</sub> and photoproduced NO<sub>x(aq)</sub> (Reactions 11 and 12; Table 1), in agreement with Scharko et al. (2014). The significance of this increased HONO production is enhanced <sup>•</sup>OH formation (Reaction 13; Table 1). In addition, <sup>•</sup>HO<sub>2</sub> can react with <sup>•</sup>NO (Reaction 10; Table 1) from NO<sub>2</sub><sup>-</sup> photolysis (Reaction 6; Table 1) to form HOONO, and eventually <sup>•</sup>NO<sub>2</sub> and <sup>•</sup>OH (Reaction 14; Table 1) (Pang et al., 2019a).~~ Nevertheless, the comparable decay rates **constants** for VL\* and VL+AN imply that <sup>3</sup>VL\* chemistry still dominates even at 1:10 molar ratio of VL/nitrate, probably due to the much higher molar absorptivity of VL compared to that of nitrate (Fig. S1) and the high VL concentration (0.1 mM) used in this study. Although we have no quantification of the oxidants in our reaction systems as it is outside the scope of this study, these observations clearly substantiate that ~~secondary oxidants from <sup>3</sup>VL\*, which are formed when O<sub>2</sub> is present, are required for efficient~~ photosensitized oxidation of VL and nitrate-mediated VL photo-oxidation **are more efficient in the presence of O<sub>2</sub>.**

Lines 241–300: The products from VL\* under N<sub>2</sub>-saturated conditions were mainly oligomers (e.g., C<sub>16</sub>H<sub>14</sub>O<sub>4</sub>) (Fig. 1a), consistent with triplet-mediated oxidation forming higher molecular weight products, probably with less fragmentation relative to oxidation by <sup>•</sup>OH (Yu et al., 2014; Chen et al., 2020). A threefold increase in the normalized abundance of products was noted upon addition of nitrate (VL+AN under N<sub>2</sub>-saturated conditions; Fig. 1b), and in addition to oligomers, functionalized monomers (e.g., C<sub>8</sub>H<sub>6</sub>O<sub>5</sub>) and nitrogen-containing compounds (e.g., C<sub>8</sub>H<sub>9</sub>NO<sub>3</sub>; No. 2, Table S2) were also observed, in agreement with <sup>•</sup>OH-initiated oxidation yielding more functionalized/oxygenated products compared to triplet-mediated oxidation (Yu et al., 2014; Chen et al., 2020). ~~Compared to N<sub>2</sub>-saturated conditions, the normalized abundance of products such as oligomers, and functionalized monomers (e.g., demethylated VL; Fig. S4), and nitrogen-containing compounds (e.g., C<sub>16</sub>H<sub>10</sub>N<sub>2</sub>O<sub>9</sub>; No. 33, Table S3, Table S2) (for VL+AN) had higher normalized abundance were also more relatively abundant~~ under air-saturated conditions were



significantly higher under air-saturated conditions (Figs. 1c-d), likely due to efficient the secondary oxidants from  $^3\text{VL}^*$ -initiated oxidation and enhanced VL nitration in the presence of and  $\text{O}_2$  and their interactions with nitrate photolysis products. The nitrogen-containing compounds (e.g.,  $\text{C}_{16}\text{H}_{10}\text{N}_2\text{O}_9$ ; No. 3, Table S3) were also more relatively abundant under air-saturated conditions. For both  $\text{VL}^*$  and  $\text{VL}+\text{AN}$  under air-saturated conditions, the most abundant product was  $\text{C}_{10}\text{H}_{10}\text{O}_5$  (No. 4, Table S23), a substituted VL. Irradiation of VL by 254-nm lamp has also been reported to lead to VL dimerization and functionalization via ring-retaining pathways, as well as small oxygenates but only when  $^{\bullet}\text{OH}$  from  $\text{H}_2\text{O}_2$  were involved (Li et al., 2014). In this work, small organic acids (e.g., formic acid) were observed from both  $\text{VL}^*$  and  $\text{VL}+\text{AN}$  under air-saturated conditions (Fig. S5) due to simulated sunlight that could access the 308-nm VL band (Smith et al., 2016). Interestingly, we observed a potential imidazole derivative ( $\text{C}_5\text{H}_5\text{N}_3\text{O}_2$ ; Fig. 1d, No. 5, Table S2) from  $\text{VL}+\text{AN}$  under air-saturated conditions (Fig. 1d), which may have formed from reactions induced by ammonium. This compound was not observed in a parallel experiment in which AN was replaced with sodium nitrate (SN) (Fig. S6a; see Sect. 3.3 for discussion). The potential aqSOA formation most probable pathways via of direct photosensitized and nitrate-mediated photo-oxidation of VL photo-oxidation in this study are summarized in Fig. 2 were proposed (Fig. 4). In Scheme 1 (pH 4 and pH <4 under air-saturated conditions),  $^3\text{VL}^*$  and  $^{\bullet}\text{OH}$  (from  $^3\text{VL}^*$  or nitrate photolysis) can initiate H atom abstraction to generate phenoxy or ketyl radicals (Huang et al., 2018; Vione et al., 2019). At pH 4, ring-opening products (Fig. S5) from fragmentation in both  $\text{VL}^*$  and  $\text{VL}+\text{AN}$  may have reacted with VL or dissolved ammonia to generate  $\text{C}_{10}\text{H}_{10}\text{O}_5$  (No. 4, Table S2) (Pang et al., 2019b) or a potential imidazole derivative ( $\text{C}_5\text{H}_5\text{N}_3\text{O}_2$ ; No. 5, Table S2), respectively. Moreover, nitrate photolysis products promoted functionalization and nitration (e.g.,  $\text{C}_{16}\text{H}_{10}\text{N}_2\text{O}_9$ ; No. 3, Table S2). At pH <4, the reactivity of  $^3\text{VL}^*$  increased as suggested by the abundance of oligomers (e.g.,  $\text{C}_{16}\text{H}_{14}\text{O}_6$ ) and increased normalized abundance of N-containing compounds.

The molecular transformation of VL upon photo-oxidation was examined using the van Krevelen diagrams (Fig. S7). For all experiments (A1-159; Table S2) in this study, the O:C and H:C ratios of the products were mainly similar to those observed from the aging of other phenolics (Yu et al., 2014) and BB aerosols (Qi et al., 2019). Under  $\text{N}_2$ -saturated conditions, oligomers with O:C ratios  $\leq 0.6$  were dominant in  $\text{VL}^*$ , while smaller molecules ( $n_c \leq 8$ ) with higher O:C ratios (up to 0.8) were also observed for  $\text{VL}+\text{AN}$ . For  $\text{VL}+\text{AN}$  under air-saturated conditions, smaller molecules ( $n_c \leq 8$ ) with higher O:C ratios (up to 0.8) were also observed. In contrast, more products with higher O:C ratios ( $\geq 0.6$ ) were noted under air-saturated conditions for both  $\text{VL}^*$  and  $\text{VL}+\text{AN}$ . For experiments A5 to A8, the H:C ratios were mostly around 1.0 and double bond equivalent (DBE) values were typically (58% of the 50 most abundant products)  $> 7$ , indicating that the products for experiments A5 to A8 (Table S2) were mainly oxidized aromatic species compounds (Xie et al., 2020). Compounds with H:C  $\leq 1.0$  and O:C  $\leq 0.5$  are common for aromatic species, while compounds with H:C  $\geq 1.5$  and O:C  $\leq 0.5$  are typical for more aliphatic species (Mazzoleni et al., 2012; Kourtchev et al., 2014; Jiang et al., 2021). Moreover, majority of the products for experiments A5 to A8 have double bond equivalent (DBE) values  $> 7$ , which corresponds to oxidized aromatic compounds (Xie et al., 2020). In contrast, Loisel et al. (2021) reported mainly oxygenated aliphatic-like compounds (H:C,  $\geq 1.5$  and O:C,  $\leq 0.5$  ratios) from the direct irradiation of VL (0.1 mM), which may be probably due to

their use of ESI in the negative ion mode, which has higher sensitivity for detecting compounds such as carboxylic acids (Holčapek et al., 2010; Liigand et al., 2017), and solid-phase extraction (SPE) procedure causing the loss of some oligomers (LeClair et al., 2012; Zhao et al., 2013; Bianco et al., 2018). Among experiments A5 to A8 (Table S2), VL+AN under air-saturated conditions (A7) had the highest normalized abundance of products and  $\langle OS_c \rangle$ , most probably due to the combined influence of the secondary oxidants from  $^3VL^*$  and enhanced VL nitration in the presence of  $O_2$ , and nitrate photolysis products. In our calculations, the increase in  $\langle OS_c \rangle$  (except for VOCs and inorganic anions experiments; A9 to A12; Table S2) was lower than those in  $^*OH$  or triplet-mediated oxidation of phenolics (e.g., phenol, guaiacol) measured using an aerosol mass spectrometer (Sun et al., 2010; Yu et al., 2014). Our measured  $\langle OS_c \rangle$  range from -0.28 to +0.12, while other studies on phenolic aqSOA formation reported  $\langle OS_c \rangle$  ranging from -0.14 to +0.47 (Sun et al., 2010) and 0.04 to 0.74 (Yu et al., 2014). This is likely because we excluded contributions from ring-opening products, which may have higher  $OS_c$  values as these products are not detectable in the positive ion mode. Thus, the  $\langle OS_c \rangle$  in this study likely were lower estimates. In brief, the presence of secondary oxidants from  $^3VL^*$  and  $O_2$  increased the normalized abundance of products and promoted the formation of more oxidized aqSOA. These trends were reinforced in the presence of nitrate, indicating synergistic effects between secondary oxidants from VL triplets and nitrate photolysis products. Compared to  $N_2$ -saturated condition, the higher normalized abundance of nitrogen-containing products under air-saturated condition for VL+AN (at pH 4) suggests a potential enhancement of VL nitration in the presence of  $O_2$ .

12. L. 196. The text here and elsewhere discusses the abundance of specific products (not just the normalized product abundance). The abundance of each product should be added to Table S3, along with some estimate of the relative uncertainty of these values.

Response: The abundance mentioned in line 249 (formerly 196) pertains to the normalized abundance of all nitrogen-containing products for  $VL^*$  at pH 4 under air-saturated conditions, not for specific products.

13. L. 224. How much lower are  $OS(C)$  values here compared to previous work on aqSOA? Compare these values.

Response: Our measured  $\langle OS_c \rangle$  range from -0.28 to +0.12, while other studies on phenolic aqSOA formation reported  $\langle OS_c \rangle$  ranging from -0.14 to +0.47 (Sun et al., 2010) and 0.04 to 0.74 (Yu et al., 2014). This information has been added to the text as follows:

Line 286: Our measured  $\langle OS_c \rangle$  range from -0.28 to +0.12, while other studies on phenolic aqSOA formation reported  $\langle OS_c \rangle$  ranging from -0.14 to +0.47 (Sun et al., 2010) and 0.04 to 0.74 (Yu et al., 2014). This is likely because we excluded contributions from ring-opening products, which may have higher  $OS_c$  values as these products are not detectable in the positive ion mode.

14. L. 240. Is there any evidence that  $^3VL^* + O_2$  directly makes  $OH$ ? This would seem energetically unfavorable and also to be minor compared to energy transfer to make  $^1O_2$ .

Response: We do not have direct evidence of  $\cdot\text{OH}$  formation from  ${}^3\text{VL}^* + \text{O}_2$ , although trace amounts of  $\text{H}_2\text{O}_2$  were likely formed during VL photodegradation (Li et al., 2014) similar to the case of other phenolic compounds (Anastasio et al., 1996). This statement has been added to line 241.

Line 316: Trace amounts of  $\text{H}_2\text{O}_2$  were likely formed during VL photodegradation (Li et al., 2014), similar to the case of other phenolic compounds (Anastasio et al., 1996).

15. L. 242. In the presence of  $\text{O}_2$ , the ketyl radical is probably too short lived (it reacts with  $\text{O}_2$  to make an alpha-hydroxy peroxy radical) to combine appreciably with a phenoxy radical. But the phenoxy radical is in resonance with a carbon-centered cyclohexadienyl radical that is longer lived; these two species can couple (Yu et al., ACP, 2014).

Response: We thank the reviewer for the additional information. We have now revised line 311 to include this as follows:

Line 317: Oligomers can then form via the coupling of phenoxy radicals or phenoxy and cyclohexadienyl ketyl-radicals (Sun et al., 2010; Yu et al., 2014; Berto et al., 2016; Vione et al., 2019).

16. L. 261. The rate constant for  $\text{H}_2\text{O}_2$  formation is fastest near the pKa of  $\text{HO}_2$ , i.e., pH 4.8, so one wouldn't expect greater  $\text{H}_2\text{O}_2$  formation at pH 2.5 compared to pH 4. But this also depends on the pH dependence of the  $\text{HO}_2/\text{O}_2^-$  sources and sinks.

Response: Thank you for pointing this out. This statement has been deleted.

17. L. 264. This discussion of the pH dependence of N(III) photolysis doesn't seem applicable since the addition of nitrate makes a negligible contribution to VL decay. Just because N(III) photolysis is pH dependent doesn't mean it matters here.

Response: Thank you for pointing out this error. The reviewer is correct that the pH dependence of N(III) is not relevant for the discussion of pH effects on VL decay rate constants. Some of these statements have been transferred to the next paragraph (from line 360) to provide a potential explanation for the increased normalized abundance of nitrogen-containing compounds at lower pH. Revisions for lines 333–354 are shown in our response to major comment #6. Other changes in the text are as follows:

Line 359–364: For VL+AN, the normalized abundance of nitrogen-containing compounds was also higher-increased at lower pH (Table S2), likely due to increased  $\cdot\text{OH}$  and  $\cdot\text{NO}_2$  formation, which may be caused by the dependence of N(III) ( $\text{NO}_2^- + \text{HONO}$ ) speciation on solution acidity (Pang et al., 2019a). At pH 3.3, half of N(III) exists as HONO (Fischer and Warneck, 1996; Pang et al., 2019a), which has a higher quantum yield for  $\cdot\text{OH}$  formation than that of  $\text{NO}_2^-$  in the near-UV region

(Arakaki et al., 1999; Kim et al., 2014). Also,  $\text{NO}_2^-/\text{HONO}$  can generate  $\cdot\text{NO}_2$  via oxidation by  $\cdot\text{OH}$  (Reactions 4 and 105; Table 1) (Pang et al., 2019a).

Line 372: Essentially, the higher reactivity of  $^3\text{VL}^*$  and predominance of HONO over nitrite at lower pH may have resulted in increased formation of products mainly composed of oligomers and functionalized monomers.

18. L. 299. Why would the presence of  $\text{HO}_2$  lead to more dimer formation?  $\text{HO}_2$  (and  $\text{O}_2^-$ ) are too weak to oxidize phenols at any significant rate.

Response: Sentences related to  $\cdot\text{OH}$  scavengers have been deleted from the original manuscript.

19. Lines 298-301: This argument is circular: IPA cannot make more OH by scavenging OH and turning it into  $\text{HOOH}$ , which then photolyzes to make OH. Think of the associated stoichiometry. IPA will suppress  $[\text{OH}]$  because it is an OH sink, thus rendering OH an insignificant oxidant for VL. The observation that IPA has a negligible impact on VL decay (Fig. S3c) indicates that OH is not important as an oxidant for VL (with or without IPA) or that the IPA was mostly purged from the system.

Response: Sentences related to  $\cdot\text{OH}$  scavengers have been deleted from the original manuscript.

20. L. 310. IPA makes no difference in the VL kinetics, whether nitrate is present or not. So please don't make sweeping statements such as "...the role of nitrate in VL photo-oxidation is enhanced in the presence of IPA...". And don't suggest that OH is an important intermediate in the formation of a product in the presence of IPA (e.g., line 311), since IPA will greatly suppress the OH concentration.

Response: Sentences related to  $\cdot\text{OH}$  scavengers have been deleted from the original manuscript.

21. L. 313-322. It is hard to believe that 1 mM of IPA can significantly disrupt the structure of 55 M water. In any case, there is no increase in light absorption by the aqSOA formed in the presence of IPA (Fig. 2), so the Berke mechanism seems unimportant. Most of this should be deleted.

Response: Sentences related to  $\cdot\text{OH}$  scavengers have been deleted from the original manuscript.

22. L. 327. It is difficult to imagine that carbonate radical is a significant oxidant in these experiments: carbonate rate constants are relatively slow (compared to triplets or OH) and VL photodegradation is very fast. If the authors want to propose carbonate radical as an important sink, they need to do some calculations of its steady-state concentration and estimate the corresponding rate of VL loss. Again, the qualitative normalized abundance of products is driving these uncertain statements, while the quantitative photodecay rates and light absorption are showing there is no significant effect of bicarbonate. Lead with the latter observations, as they are more robust.

Response: Sentences related to  $\cdot\text{OH}$  scavengers have been deleted from the original manuscript.

23. L. 336. 1 mM IPA or bicarbonate is not high enough to reduce the cage effect from nitrate photolysis. In any case, IPA or bicarbonate are OH sinks, so they will suppress, not enhance, the OH concentration.

Response: Sentences related to  $\cdot\text{OH}$  scavengers have been deleted from the original manuscript.

24. L. 376. If this proposed mechanism was true, then VL decay would be significantly faster in the presence of nitrate, but this is not the case. It's not clear what the authors are trying to explain here - is it the increase in oligomerization at higher [VL]? The explanation for this is probably that the concentrations of phenoxy radicals (and the related, carbon-centered cyclohexadienyl radicals) increase with [VL], making radical-radical recombination to form oligomers a more significant fate.

Response: Thank you for pointing this out. We apologize for the confusion. There should have been an explanation here for the increased oligomerization observed at higher [VL]. We agree with the reviewer that a possible reason for this is the increased concentration of radicals with [VL] (added to the revised text). The succeeding lines are for comparing the potential pathways at 1:1 VL/nitrate and 1:100 VL/nitrate only at low [VL]. The text has been revised to clarify these as follows:

Lines 466–485: For both VL\* and VL+AN, the contribution of  $< 200$  m/z to the normalized abundance of products was higher at low [VL] than at high [VL], while the opposite was observed for  $> 300$  m/z (Fig. S123d). This indicates that functionalization was favored at low [VL], as supported by the higher  $\langle\text{OS}_c\rangle$ , while oligomerization was the dominant pathway at high [VL], consistent with more oligomers or polymeric products reported from high phenols concentration (e.g., 0.1 to 3 mM) (Li et al., 2014; Slikboer et al., 2015; Ye et al., 2019). **This is probably due to an increased concentration of phenoxy radicals (in resonance with a carbon-centered cyclohexadienyl radical) at high [VL], promoting radical-radical polymerization (Sun et al., 2010; Li et al., 2014).** ~~Moreover, At low [VL], the contribution of  $< 200$  m/z to the normalized abundance of products was higher for 1:1 than 1:100 VL/nitrate molar ratio, further suggesting the prevalence of functionalization for the former formation of more oxidized products. This may also be the reason why~~ **In addition, 1:1 VL/nitrate (A115; Table S2) had higher  $\langle\text{OS}_c\rangle$  than 1:100 VL/nitrate (A126; Table S2), indicating the formation of more oxidized products, but had fewer N-containing compounds compared to the latter. A possible explanation is that at 1:1 VL/nitrate, VL may efficiently competes with  $\text{NO}_2^-$  for  $\cdot\text{OH}$  (from nitrate or nitrite photolysis, Reaction 4; Table 1) and indirectly reduces  $\cdot\text{NO}_2$ . Similarly, hydroxylation has been suggested to be an more important pathway for 1:1 VL/nitrite than in 1:10 VL/nitrite (Pang et al., 2019a). ~~This may also be the reason why 1:1 VL/nitrate (A15; Table S2) had higher  $\langle\text{OS}_c\rangle$  than 1:100 (A16; Table S2) VL/nitrate but had fewer N-containing compounds compared to the latter. Moreover, the contribution of  $< 200$  m/z to the normalized abundance of products was higher for 1:1 than 1:100 VL/nitrate molar ratio, further suggesting the formation of more oxidized products.~~** **Fragmentation, which leads to the decomposition of previously formed oligomers and generation**

of small, oxygenated products such as organic acids (Huang et al., 2018), may also occur for the low [VL] experiments. However, its importance would likely be observed at longer irradiation times, similar to the high [VL] experiments.

25. L. 405. GUA should not undergo any direct photochemistry, so its decay in the absence of VL or AN suggests either that there is an oxidant-making contaminant in the system (that is consumed within a few hours) or that GUA is evaporating during illumination. But there is no GUA loss in the dark: is this because the temperature was cooler in the dark?

Response: Vione et al. (2019) also observed the direct photodegradation of GUA (0.1 mM) upon irradiation using Xe lamp. Moreover, Sun et al. (2010) reported an intermediate rate of direct photoreaction for GUA (0.1 mM), yielding aqSOA including GUA dimers (similar to what we observed). There was no significant loss of GUA both after 30 min of purging in the dark (-0.36%) and after 360 min of dark control experiments (-1.7%). Also, the temperature fluctuations ( $27 \pm 2$  °C) were minimal.

26. L. 498. This sentence mentions “Further enhancement of VL photo-oxidation...in the presence of nitrate...”, but VL photo-oxidation (i.e., photodegradation) was not enhanced in the presence of nitrate.

Response: This statement refers to the presence of both O<sub>2</sub> and nitrate resulting in the highest normalized abundance of products (including N-containing compounds) and <OS<sub>c</sub>> among experiments A5–A8. We have revised this as follows:

Line 606–611: ~~Further enhancement of VL photo-oxidation under air-saturated conditions in the presence of nitrate indicates synergistic effects between secondary oxidants from VL triplets and nitrate photolysis products. In contrast, <sup>3</sup>VL\*-initiated reactions proceeded rapidly under air-saturated conditions (O<sub>2</sub> is present) as indicated by higher VL decay rate constant and increased normalized abundance of products. For pH 4 experiments, the presence of both O<sub>2</sub> and nitrate resulted in the highest normalized abundance of products (including N-containing compounds) and <OS<sub>c</sub>>, which may be due to the presence of O<sub>2</sub> promoting VL nitration.~~

27. L. 1004. The author order is incorrect on the Tinel et al. ref.

Response: Thank you for the correction. We have now amended the author order for this reference as follows and revised the corresponding in-text citations:

George, C., Brüggemann, M., Hayeck, N., Tinel, L., and Donaldson, D. J.: Interfacial photochemistry: physical chemistry of gas-liquid interfaces, in: *Developments in Physical & Theoretical Chemistry*, edited by: Faust, J. A. and House, J. E., Elsevier, 435–457, <https://doi.org/10.1016/B978-0-12-813641-6.00014-5>, 2018.

28. Table 1. The quantum yield for Rxn 3 is not 0.001. This is a misperception based on the O(3P) result of Warneck and Wurzinger (J Phys Chem, 1988); their paper shows a value of ~0.01 for more direct (nitrite) measurements. Benedict et al. (Env Sci Technol., 2017) confirmed this higher

value. This error doesn't affect the current work, but it would be a shame to propagate the misperception.

Response: We thank the reviewer for the careful read. We now have corrected this value in Table 1:



29. Figure 4. (a) The resolution of the figure is poor, so it's fuzzy and hard to read. (b) Scheme 1 suggests that oligomers are only formed at pH < 4, which isn't true, as past work has shown oligomer formation in similar phenol systems at pH 5. (c) Ketyl radicals formed by  $^3\text{C}^*$  + phenol typically are shown as phenoxy OH group (a result of the triplet abstracting a hydrogen) and no double bond between the C and O. As stated earlier, their lifetimes are short in the presence of O<sub>2</sub>, so they're unlikely to do the coupling as shown here.

Response:

(a) This may be a formatting issue. We ensured that this is avoided in the revised version.

(b) The reviewer is right that oligomer formation in similar phenol systems was also observed at pH 5. However, the molecular formulas initially presented in Fig. 4 were the most abundant products or products with a significant increase in normalized abundance. To avoid this confusion, Fig. 4, now 2, has been revised to show the major products for each condition, with a marker for the most abundant products.

(c) Thank you for catching this error. Ketyl radical has been deleted in Fig. 2.

### Supplemental Material Notes

1. General note – it would have been helpful to have line numbers in the supplement.

Response: Line numbers have now been added to the supporting information as well.

2. Text S3. Were calibration curves only made once? Were they actually used in quantifying VL and GUA? (I don't see the need since absolute values are not needed in the kinetic plots.)

Response: No, the calibration curves were prepared weekly to account for potential changes in the detector response of UHPLC. These calibration curves were used to quantify VL and GUA as the calculated VL concentration was used for estimating the normalized abundance of products.

3. Text S6. (a) It's unclear what is meant by "Then, the average relative intensity absorbed by 2NB solution as a function of wavelength was calculated." Can you show this with an equation? (b) How much did the photon flux vary between experiments? Was this determined? If not, this variation is a source of variability in the kinetic measurements.

Response: (a) We apologize for the confusion. This statement pertains to a scaling factor (SF) that was used to determine the absolute photon flux in the reactor,  $I'_\lambda$ . Similar to Smith et al. (2014, 2016), we measured the spectral shape of the photon output of our illumination system (i.e., the relative flux at each wavelength) using a high-sensitivity spectrophotometer (Brolight Technology Co. Ltd, Hangzhou, China). Using an SF, this measured relative photon output,  $I_\lambda^{\text{relative}}$ , is related to  $I'_\lambda$  as follows:

$$I'_\lambda = I_\lambda^{\text{relative}} \times \text{SF} \quad (\text{Eq. S6})$$

Substitution of Eq. S6 into Eq. S5 and rearrangement yields:

$$j(2\text{NB}) = 2.303 \times (10^3 \text{ cm}^3 \text{ L}^{-1} \times 1 \text{ mol}/N_A \text{ mlc}) \times \sum(I'_\lambda \times \Delta\lambda \times \varepsilon_{2\text{NB},\lambda} \times \Phi_{2\text{NB}}) \quad (\text{Eq. S5})$$

Where  $j(2\text{NB})$  is the 2NB decay rate constant,  $N_A$  is Avogadro's number,  $I'_\lambda$  is the actinic flux (photons  $\text{cm}^{-2} \text{ s}^{-1} \text{ nm}^{-1}$ ),  $\Delta\lambda$  is the wavelength interval between actinic flux data points (nm), and  $\varepsilon_{2\text{NB},\lambda}$  and  $\Phi_{2\text{NB},\lambda}$  are the base-10 molar absorptivity ( $\text{M}^{-1} \text{ cm}^{-1}$ ) and quantum yield (molecule photon $^{-1}$ ) for 2NB, respectively. Values of  $\varepsilon_{2\text{NB},\lambda}$  (in water) at each wavelength under 298 K and a wavelength-independent  $\Phi_{2\text{NB}}$  value of 0.41 were adapted from Galbavy et al. (2010).

$$\text{SF} = \frac{j(2\text{NB})}{2.303 \times (10^3 \text{ cm}^3 \text{ L}^{-1} \times 1 \text{ mol}/N_A \text{ mlc}) \times \sum(I_\lambda^{\text{relative}} \times \Delta\lambda \times \varepsilon_{2\text{NB},\lambda} \times \Phi_{2\text{NB}})} \quad (\text{Eq. S7})$$

and substitution of (Eq. S6) into (Eq. S7) yields:

$$I'_\lambda = I_\lambda^{\text{relative}} \frac{j(2\text{NB})}{2.303 \times (10^3 \text{ cm}^3 \text{ L}^{-1} \times 1 \text{ mol}/N_A \text{ mlc}) \times \sum(I_\lambda^{\text{relative}} \times \Delta\lambda \times \varepsilon_{2\text{NB},\lambda} \times \Phi_{2\text{NB}})} \quad (\text{Eq. S8})$$

Finally,  $I'_\lambda$  was estimated through Eq. S8. The estimated photon flux in the aqueous reactor is shown in Figure S12.

We have added the above information to Text S6.

(b) The  $j(2\text{NB})$  in this study varied from 0.0021 to 0.0026  $\text{s}^{-1}$ . The decay rate constants have now been normalized to the photon flux, and the updated values are shown in Table 2, formerly S2.

4. Table S2. (a) VL (and GUA) decays are rate constants, not decay rates. (b) For reference, it would be helpful to give the OS(C) of VL. (c) What is pH of expt. A19?



Response: (a) Thank you for catching this error. This has been corrected in Table S2, now 2, as well as elsewhere in the text:

**Table S2.** Reaction conditions, initial VL (and GUA) decay rates ~~constants~~

Line 142: the calculation of GUA decay ~~rate constant~~.

Line 172: initial VL (and GUA) decay rates ~~constants~~,

Line 204: Contrastingly, the VL\* decay rate ~~constant~~ under air-saturated conditions

Line 220: ~~Similar to VL\*~~, ~~†~~The decay rate ~~constant~~ for VL+AN

Line 235: Nevertheless, the comparable decay rates ~~constants~~

Line 331: The decay rates ~~constants~~

Line 509: GUA decay ~~rate constant~~ was ~~faster~~ ~~higher~~ by 2.2 (GUA+VL)

Line 512: This enhanced GUA decay rate ~~constant~~

Line 574: Although nitrate did not substantially affect the VL decay rates ~~constants~~,

(b) Agree, we have now added the  $OS_c$  of VL (-0.25) to Table 2.

(c) The pH for exp 19, now 15, is 4, same with other experiments involving GUA. This is already listed in the second column of Table 2.

5. Figure S1. The vanillin spectrum has a problem around 305 nm - a large discontinuity that is probably caused by lamp switch. Either reacquire the spectrum or replace with a published value.

Response: Thank you for catching this. Fig. S1 has been revised to correct this.

6. Figure S3. Were the decays ever determined multiple times for the same condition? It would be helpful to show these results and derive a relative uncertainty for decay rate constants.

Response: Yes, the decays reported in Fig. S3 are the average of results from triplicate experiments, and the error bars for each data point are already shown. The photon flux-normalized decay rate constants have also been updated in Table S2, now 2, along with the standard deviation for each condition (Please see our response to major comment #5). The following sentence has been added in the methods section to clarify this:

Line 132: Each experiment was repeated independently at least three times and measurements were done in triplicate. The reported decay rate constants and absorbance enhancement are the average of results from triplicate experiments, and the corresponding errors represent one standard deviation.

We also added this note to figure captions when applicable: most error bars are smaller than the markers.

7. Figure S6. How can we tell that the imidazole formed in the AN experiment was not formed in the SN experiment? It would be helpful to put a marker on the two plots of Fig. S6 to show where the imidazole showed up in the AN experiment.

Response: Thank you for pointing this out. Fig. S6 has been revised to show a marker for the potential imidazole compound.

### Recommendation

I recommend that the manuscript be majorly revised and then reconsidered.

### References

Anastasio, C., Faust, B. C., and Rao, C. J.: Aromatic carbonyl compounds as aqueous-phase photochemical sources of hydrogen peroxide in acidic sulfate aerosols, fogs, and clouds. 1. Non-phenolic methoxybenzaldehydes and methoxyacetophenones with reductants (phenols), *Environ. Sci. Technol.*, 31, 218–232, <https://doi.org/10.1021/es960359g>, 1996.

Arakaki, T., Miyake, T., Hirakawa, T., and Sakugawa, H.: pH dependent photoformation of hydroxyl radical and absorbance of aqueous-phase N(III) ( $\text{HNO}_2$  and  $\text{NO}_2^-$ ), *Environ. Sci. Technol.*, 33, 2561–2565, <https://doi.org/10.1021/es980762i>, 1999.

Bateman, A. P., Laskin, J., Laskin, A., and Nizkorodov, S. A.: Applications of high-resolution electrospray ionization mass spectrometry to measurements of average oxygen to carbon ratios in secondary organic aerosols, *Environ. Sci. Technol.*, 46, 8315–8324, <https://doi.org/10.1021/es3017254>, 2012.

Bianco, A., Deguillaume, L., Vařtilingom, M., Nicol, E., Baray, J.-L., Chaumerliac, N., and Bridoux, M.: Chemical characterization of cloud water collected at Puy de Dôme by FT-ICR MS reveals the presence of SOA components, *Environ. Sci. Technol.*, 52, 10275–10285, <https://doi.org/10.1021/acsearthspacechem.9b00153>, 2018.

Bianco, A., Passananti, M., Brigante, M., and Mailhot, G.: Photochemistry of the cloud aqueous phase: a review, *Molecules*, 25, 423, <https://doi.org/10.3390/molecules25020423>, 2020.

Birks, J.B.: *Organic Molecular Photophysics*, John Wiley & Sons, 1973.

Canonica, S., Jans, U., Stemmler, K., and Hoigne, J.: Transformation kinetics of phenols in water: Photosensitization by dissolved natural organic material and aromatic ketones, *Environ. Sci. Technol.*, 29, 1822–1831, <https://doi.org/10.1021/es00007a020>, 1995.

Chen, Y., Li, N., Li, X., Tao, Y., Luo, S., Zhao, Z., Ma, S., Huang, H., Chen, Y., Ye, Z., and Ge, X.: Secondary organic aerosol formation from  $^3\text{C}^*$ -initiated oxidation of 4-ethylguaiaicol in atmospheric aqueous-phase, *Sci. Total Environ.*, 723, 137953, <https://doi.org/10.1016/j.scitotenv.2020.137953>, 2020.

Collett, J. L. Jr., Hoag, K. J., Sherman, D. E., Bator, A., and Richards, L. W.: Spatial and temporal variations in San Joaquin Valley fog chemistry, *Atmos. Environ.*, 33, 129–140, [https://doi.org/10.1016/S1352-2310\(98\)00136-8](https://doi.org/10.1016/S1352-2310(98)00136-8), 1998.

De Haan, D.O., Pajunoja, A., Hawkins, L. N., Welsh, H.G., Jimenez, N. G., De Loera, A., Zauscher, M., Andretta, A. D., Joyce, B. W., De Haan, A. C., Riva, M., Cui, T., Surratt, J. D., Cazaunau, M., Formenti, P., Gratien, A., Pangu, E., and Doussin, J-F.: Methylamine's effects on methylglyoxal-containing aerosol: chemical, physical, and optical changes, *ACS Earth Space Chem.*, 3, 1706–1716, <https://doi.org/10.1021/acsearthspacechem.9b00103>, 2019.

Du, Y., Fu, Q. S., Li, Y., and Su, Y.: Photodecomposition of 4-chlorophenol by reactive oxygen species in UV/air system, *J. Hazard. Mater.*, 186, 491–496, <https://doi.org/10.1016/j.jhazmat.2010.11.023>, 2011.

Fischer, M. and Warneck, P.: Photodecomposition of nitrite and undissociated nitrous acid in aqueous solution, *J. Phys. Chem.*, 100, 18749–18756, <https://doi.org/10.1021/jp961692+>, 1996.

Fleming, L. T., Lin, P., Laskin, A., Laskin, J., Weltman, R., Edwards, R. D., Arora, N. K., Yadav, A., Meinardi, S., Blake, D. R., Pillarisetti, A., Smith, K. R., and Nizkorodov, S. A.: Molecular composition of particulate matter emissions from dung and brushwood burning household cookstoves in Haryana, India, *Atmos. Chem. Phys.*, 18, 2461–2480, <https://doi.org/10.5194/acp-18-2461-2018>, 2018.

Galbavy, E. S., Ram, K., and Anastasio, C.: 2-Nitrobenzaldehyde as a chemical actinometer for solution and ice photochemistry, *J. Photochem. Photobiol. A*, 209, 186–192, <https://doi.org/10.1016/j.jphotochem.2009.11.013>, 2010.

George, C., Brüggemann, M., Hayeck, N., Tinel, L., and Donaldson, D. J.: Interfacial photochemistry: physical chemistry of gas-liquid interfaces, in: *Developments in Physical & Theoretical Chemistry*, edited by: Faust, J. A. and House, J. E., Elsevier, 435–457, <https://doi.org/10.1016/B978-0-12-813641-6.00014-5>, 2018.

Giulianelli, L., Gilardoni, S., Tarozzi, L., Rinaldi, M., Decesari, S., Carbone, C., Facchini, M. C., and Fuzzi, S.: Fog occurrence and chemical composition in the Po valley over the last twenty years, *Atmos. Environ.*, 98, 394–401, <https://doi.org/10.1016/j.atmosenv.2014.08.080>, 2014.

Herrmann, H., Hoffmann, D., Schaefer, T., Bräuer, P., and Tilgner, A.: Tropospheric aqueous-phase free-radical chemistry: Radical sources, spectra, reaction kinetics and prediction tools, *Chem. Phys. Chem.*, 11, 3796–3822, <https://doi.org/10.1002/cphc.201000533>, 2010.

Holčápek, M., Jirásko, R., and Lísa, M.: Basic rules for the interpretation of atmospheric pressure ionization mass spectra of small molecules, *J. Chromatogr. A*, 1217, 3908–3921, <https://doi.org/10.1016/j.chroma.2010.02.049>, 2010.

Huang, D. D., Zhang, Q., Cheung, H. H. Y., Yu, L., Zhou, S., Anastasio, C., Smith, J. D., and Chan, C. K.: Formation and evolution of aqSOA from aqueous-phase reactions of phenolic carbonyls: comparison between ammonium sulfate and ammonium nitrate solutions, *Environ. Sci. Technol.*, 52, 9215–9224, <https://doi.org/10.1021/acs.est.8b03441>, 2018.

Jiang, W., Misovich, M. V., Hettiyadura, A. P. S., Laskin, A., McFall, A. S., Anastasio, C., and Zhang, Q.: Photosensitized reactions of a phenolic carbonyl from wood combustion in the aqueous phase—chemical evolution and light absorption properties of aqSOA, *Environ. Sci. Technol.*, 55, 5199–5211, <https://doi.org/10.1021/acs.est.0c07581>, 2021.

Kebarle, P. A.: A brief overview of the mechanisms involved in electrospray mass spectrometry, *J. Mass Spectrom.*, 35, 804–817, <https://doi.org/10.1002/9783527628728.ch1>, 2000.

Kim, D.-h., Lee, J., Ryu, J., Kim, K., and Choi, W.: Arsenite oxidation initiated by the UV photolysis of nitrite and nitrate, *Environ. Sci. Technol.*, 48, 4030–4037, <https://doi.org/10.1021/es500001q>, 2014.

Klodt, A.L., Romonosky, D.E., Lin, P., Laskin, J., Laskin, A., and Nizkorodov, S.A.: Aqueous photochemistry of secondary organic aerosol of  $\alpha$ -pinene and  $\alpha$ -humulene in the presence of hydrogen peroxide or inorganic salts, *ACS Earth Space Chem.*, 3, 12, 2736–2746, <https://doi.org/10.1021/acsearthspacechem.9b00222>, 2019.

Kourtchev, I., Fuller, S. J., Giorio, C., Healy, R. M., Wilson, E., O'Connor, I., Wenger, J. C., McLeod, M., Aalto, J., Ruuskanen, T. M., Maenhaut, W., Jones, R., Venables, D. S., Sodeau, J. R., Kulmala, M., and Kalberer, M.: Molecular composition of biogenic secondary organic aerosols using ultrahigh-resolution mass spectrometry: comparing laboratory and field studies, *Atmos. Chem. Phys.*, 14, 2155–2167, <https://doi.org/10.5194/acp-14-2155-2014>, 2014.

Krueve, A., Kaupmees, K., Liigand, J., and Leito, I.: Negative electrospray ionization via deprotonation: predicting the ionization efficiency, *Anal. Chem.*, 86, 4822–4830, <https://doi.org/10.1021/ac404066v>, 2014.

Lathioor, E. C., Leigh, W. J., and St. Pierre, M. J.: Geometrical effects on intramolecular quenching of aromatic ketone ( $\pi,\pi^*$ ) triplets by remote phenolic hydrogen abstraction, *J. Am. Chem. Soc.*, 121, 11984–11992, <https://pubs.acs.org/doi/abs/10.1021/ja991207z>, 1999.

LeClair, J. P., Collett, J. L., and Mazzolen, L. R.: Fragmentation analysis of water-soluble atmospheric organic matter using ultrahigh-resolution FT-ICR mass spectrometry, *Environ. Sci. Technol.*, 46, 4312–4322, <https://doi.org/10.1021/es203509b>, 2012.

Lee, H. J., Aiona, P. K., Laskin, A., Laskin, J., and Nizkorodov, S. A.: Effect of solar radiation on the optical properties and molecular composition of laboratory proxies of atmospheric brown carbon, *Environ. Sci. Technol.*, 48, 10217–10226, <https://doi.org/10.1021/es502515r>, 2014.

Leito, I., Herodes, K., Huopola, M., Virro, K., Künnapas, A., Krueve, A., and Tanner, R.: Towards the electrospray ionization mass spectrometry ionization efficiency scale of organic compounds, *Rapid Commun. Mass Sp.*, 22, 379–384, <https://doi.org/10.1002/rcm.3371>, 2008.

Li, P., Li, X., Yang, C., Wang, X., Chen, J., and Collett, J. L. Jr.: Fog water chemistry in Shanghai, *Atmos. Environ.*, 45, 4034–4041, <https://doi.org/10.1016/j.atmosenv.2011.04.036>, 2011.

Li, Y. J., Huang, D. D., Cheung, H. Y., Lee, A. K. Y., and Chan, C. K.: Aqueous-phase photochemical oxidation and direct photolysis of vanillin - a model compound of methoxy phenols from biomass burning, *Atmos. Chem. Phys.*, 14, 2871–2885, <https://doi.org/10.5194/acp-14-2871-2014>, 2014.

Liigand, P., Kaupmees, K., Haav, K., Liigand, J., Leito, I., Girod, M., Antoine, R., and Krueve, A.: Think negative: finding the best electrospray ionization/MS mode for your analyte, *Anal. Chem.*, 89, 5665–5668, <https://doi.org/10.1021/acs.analchem.7>, 2017.

Lin, P., Yu, J. Z., Engling, G., and Kalberer, M.: Organosulfates in humic-like substance fraction isolated from aerosols at seven locations in East Asia: a study by ultra-high-resolution mass spectrometry, *Environ. Sci. Technol.*, 46, 13118–13127, <https://doi.org/10.1021/es303570v>, 2012.

Loisel, G., Mekic, M., Liu, S., Song, W., Jiang, B., Wang, Y., Deng, H., and Gligorovski, S.: Ionic strength effect on the formation of organonitrate compounds through photochemical degradation of vanillin in liquid water of aerosols, *Atmos. Environ.*, 246, 118140, <https://doi.org/10.1016/j.atmosenv.2020.118140>, 2021.

Mazzoleni, L. R., Saranjampour, P., Dalbec, M. M., Samburova, V., Hallar, A. G., Zielinska, B., Lowenthal, D. H., and Kohl, S.: Identification of water-soluble organic carbon in non-urban aerosols using ultrahigh-resolution FT-ICR mass spectrometry: organic anions, *Environ. Chem.*, 9, 285–297, <https://doi.org/10.1071/EN11167>, 2012.

McNally, A. M., Moody, E. C., and McNeill, K.: Kinetics and mechanism of the sensitized photodegradation of lignin model compounds, *Photochem. Photobiol. Sci.*, 4, 268–274, <https://doi.org/10.1039/B416956E>, 2005.

Minella, M., Romeo, F., Vione, D., Maurino, V., and Minero, C.: Low to negligible photoactivity of lake-water matter in the size range from 0.1 to 5  $\mu\text{m}$ , *Chemosphere*, 83, 1480–1485, <https://doi.org/10.1016/j.chemosphere.2011.02.093>, 2011.

Munger, J. W., Jacob, D. J., Waldman, J. M., and Hoffmann, M. R.: Fogwater chemistry in an urban atmosphere, *J. Geophys. Res. Oceans*, 88, 5109–5121, <https://doi.org/10.1029/JC088iC09p05109>, 1983.

Neumann, M. G., De Groote, R. A. M. C., and Machado, A. E. H.: Flash photolysis of lignin: Part 1. Deaerated solutions of dioxane-lignin, *Polym. Photochem.*, 7, 401–407, [https://doi.org/10.1016/0144-2880\(86\)90007-2](https://doi.org/10.1016/0144-2880(86)90007-2), 1986a.

Neumann, M. G., De Groote, R. A. M. C., and Machado, A. E. H.: Flash photolysis of lignin: II. Oxidative photodegradation of dioxane-lignin, *Polym. Photochem.*, 7, 461–468, [https://doi.org/10.1016/0144-2880\(86\)90015-1](https://doi.org/10.1016/0144-2880(86)90015-1), 1986b.

Nguyen, T. B., Nizkorodov, S. A., Laskin, A., and Laskin, J.: An approach toward quantification of organic compounds in complex environmental samples using high-resolution electrospray ionization mass spectrometry, *Anal. Methods*, 5, 72–80, <https://doi.org/10.1039/C2AY25682G>, 2013.

Ning, C., Gao, Y., Zhang, H., Yu, H., Wang, L., Geng, N., Cao, R., and Chen, J.: Molecular characterization of dissolved organic matters in winter atmospheric fine particulate matters ( $\text{PM}_{2.5}$ ) from a coastal city of northeast China, *Sci. Total Environ.*, 689, 312–321, <https://doi.org/10.1016/j.scitotenv.2019.06.418>, 2019.

Pang, H., Zhang, Q., Lu, X. H., Li, K., Chen, H., Chen, J., Yang, X., Ma, Y., Ma, J., and Huang, C.: Nitrite-mediated photooxidation of vanillin in the atmospheric aqueous phase, *Environ. Sci. Technol.*, 53, 14253–14263, <https://doi.org/10.1021/acs.est.9b03649>, 2019a.

Pang, H., Zhang, Q., Wang, H., Cai, D., Ma, Y., Li, L., Li, K., Lu, X., Chen, H., Yang, X., and Chen, J.: Photochemical aging of guaiacol by Fe(III)-oxalate complexes in atmospheric aqueous phase, *Environ. Sci. Technol.*, 53, 127–136, <https://doi.org/10.1021/acs.est.8b04507>, 2019b.

Perry, R. H., Cooks, R. G., and Noll, R. J.: Orbitrap mass spectrometry: instrumentation, ion motion and applications, *Mass Spectrom. Rev.*, 27, 661–699, <https://doi.org/10.1002/mas.20186>, 2008.

Pye, H., Nenes, A., Alexander, B., Ault, A. P., Barth, M. C., Clegg, S. L., Collett, J. L. Jr., Fahey, K. M., Hennigan, C. J., Herrmann, H., Kanakidou, M., Kelly, J. T., Ku, I. T., McNeill, V. F., Riemer, N., Schaefer, T., Shi, G., Tilgner, A., Walker, J. T., Wang, T., Weber, R., Xing, J., Zaveri, R. A., and Zuend,

A.: The acidity of atmospheric particles and clouds, *Atmos. Chem. Phys.*, 20, 4809–4888, <https://doi.org/10.5194/acp-20-4809-2020>, 2020.

Qi, L., Chen, M., Stefenelli, G., Pospisilova, V., Tong, Y., Bertrand, A., Hueglin, C., Ge, X., Baltensperger, U., Prévôt, A. S. H., and Slowik, J.G.: Organic aerosol source apportionment in Zurich using an extractive electrospray ionization time-of-flight mass spectrometer (EESI-TOF-MS) — Part 2: Biomass burning influences in winter, *Atmos. Chem. Phys.*, 19, 8037–8062, <https://doi.org/10.5194/acp-19-8037-2019>, 2019.

Romonosky, D. E., Li, Y., Shiraiwa, M., Laskin, A., Laskin, J., and Nizkorodov, S. A.: Aqueous photochemistry of secondary organic aerosol of  $\alpha$ -Pinene and  $\alpha$ -Humulene oxidized with ozone, hydroxyl radical, and nitrate radical, *J. Phys. Chem. A*, 121, 1298–1309, <https://doi.org/10.1021/acs.jpca.6b10900>, 2017.

Schmidt, A.-C., Herzsuh, R., Matysik, F.-M., and Engewald, W.: Investigation of the ionisation and fragmentation behaviour of different nitroaromatic compounds occurring as polar metabolites of explosives using electrospray ionisation tandem mass spectrometry, *Rapid Commun. Mass Sp.*, 20, 2293–2302, <https://doi.org/10.1002/rcm.2591>, 2006.

Slikboer, S., Grandy, L., Blair, S. L., Nizkorodov, S. A., Smith, R. W., and Al-Abadleh, H. A.: Formation of light absorbing soluble secondary organics and insoluble polymeric particles from the dark reaction of catechol and guaiacol with Fe(III), *Environ. Sci. Technol.*, 49, 7793–7801, <https://doi.org/10.1021/acs.est.5b01032>, 2015.

Smith, J. D., Sio, V., Yu, L., Zhang, Q., and Anastasio, C.: Secondary organic aerosol production from aqueous reactions of 973 atmospheric phenols with an organic triplet excited state, *Environ. Sci. Technol.*, 48, 1049–1057, <https://doi.org/10.1021/es4045715>, 2014.

Smith, J. D., Kinney, H., and Anastasio, C.: Phenolic carbonyls undergo rapid aqueous photodegradation to form low-volatility, light-absorbing products, *Atmos. Environ.*, 126, 36–44, <https://doi.org/10.1016/j.atmosenv.2015.11.035>, 2016.

Song, J., Li, M., Jiang, B., Wei, S., Fan, X., and Peng, P.: Molecular characterization of water-soluble humic like substances in smoke particles emitted from combustion of biomass materials and coal using ultrahigh-resolution electrospray ionization Fourier transform ion cyclotron resonance mass spectrometry, *Environ. Sci. Technol.*, 52, 2575–2585, <https://doi.org/10.1021/acs.est.7b06126>, 2018.

Sun, Y. L., Zhang, Q., Anastasio, C., and Sun, J.: Insights into secondary organic aerosol formed via aqueous-phase reactions of phenolic compounds based on high resolution mass spectrometry, *Atmos. Chem. Phys.*, 10, 4809–4822, <https://doi.org/10.5194/acp-10-4809-2010>, 2010.

Tratnyek, P. G. and Hoigne, J.: Oxidation of substituted phenols in the environment: a QSAR analysis of rate constants for reaction with singlet oxygen, *Environ. Sci. Technol.*, 25, 1596–1604, <https://doi.org/10.1021/es00021a011>, 1991.

Turro, N., Ramamurthy, V., and Scaiano, J.C.: *Modern Molecular Photochemistry*, University Science Book, 2010.

Vione, D., Maurino, V., Minero, C., and Pelizzetti, E.: Reactions induced in natural waters by irradiation of nitrate and nitrite ions, in: *The Handbook of Environmental Chemistry Vol. 2M - Environmental Photochemistry Part II*, Springer, Berlin, Heidelberg, Germany, 221–253, <https://doi.org/10.1007/b138185>, 2005.

Vione, D., Albinet, A., Barsotti, F., Mekic, M., Jiang, B., Minero, C., Brigante, M., and Gligorovski, S.: Formation of substances with humic-like fluorescence properties, upon photoinduced oligomerization of typical phenolic compounds emitted by biomass burning, *Atmos. Environ.*, 206, 197–207, <https://doi.org/10.1016/j.atmosenv.2019.03.005>, 2019.

Wang, K., Huang, R.-J., Brüggemann, M., Zhang, Y., Yang, L., Ni, H., Guo, J., Wang, M., Han, J., Bilde, M., Glasius, M., and Hoffmann, T.: Urban organic aerosol composition in eastern China differs from north to south: molecular insight from a liquid chromatography–mass spectrometry (Orbitrap) study, *Atmos. Chem. Phys.*, 21, 9089–9104, <https://doi.org/10.5194/acp-21-9089-2021>, 2021.

Wang, X., Hayeck, N., Brüggemann, M., Yao, L., Chen, H., Zhang, C., Emmelin, C., Chen, J., George, C., and Wang, L.: Chemical characterization of organic aerosols in Shanghai: A study by ultrahigh-performance liquid chromatography coupled with orbitrap mass spectrometry, *J. Geophys. Res. Atmos.*, 122, 11703–11722, <https://doi.org/10.1002/2017JD026930>, 2017.

Xie, Q., Su, S., Chen, S., Xu, Y., Cao, D., Chen, J., Ren, L., Yue, S., Zhao, W., Sun, Y., Wang, Z., Tong, H., Su, H., Cheng, Y., Kawamura, K., Jiang, G., Liu, C.-Q., and Fu, P.: Molecular characterization of firework-related urban aerosols using Fourier transform ion cyclotron resonance mass spectrometry, *Atmos. Chem. Phys.*, 20, 6803–6820, [10.5194/acp-20-6803-2020](https://doi.org/10.5194/acp-20-6803-2020), <https://doi.org/10.5194/acp-20-6803-2020>, 2020.

Ye, Z., Qu, Z., Ma, S., Luo, S., Chen, Y., Chen, H., Chen, Y., Zhao, Z., Chen, M., and Ge, X.: A comprehensive investigation of aqueous-phase photochemical oxidation of 4-ethylphenol, *Sci. Total Environ.*, 685, 976–985, <https://doi.org/10.1016/j.scitotenv.2019.06.276>, 2019.

Yu, L., Smith, J., Laskin, A., Anastasio, C., Laskin, J., and Zhang, Q.: Chemical characterization of SOA formed from aqueous-phase reactions of phenols with the triplet excited state of carbonyl and hydroxyl radical, *Atmos. Chem. Phys.*, 14, 13801–13816, <https://doi.org/10.5194/acp-14-13801-2014>, 2014.



Zhang, Q. and Anastasio, C.: Conversion of fogwater and aerosol organic nitrogen to ammonium, nitrate, and NO<sub>x</sub> during exposure to simulated sunlight and ozone, *Environ. Sci. Technol.*, 37, 3522–3530, <https://doi.org/10.1021/es034114x>, 2003.

Zhao, Y., Hallar, A.G., and Mazzoleni, L.R.: Atmospheric organic matter in clouds: exact masses and molecular formula identification using ultrahigh-resolution FT-ICR mass spectrometry, *Atmos. Chem. Phys.* 13, 12343–12362, <https://doi.org/10.5194/acp-13-12343-2013>, 2013.

Author Response for “Aqueous SOA formation from the photo-oxidation of vanillin: Direct photosensitized reactions and nitrate-mediated reactions” by Mabato et al.

We thank the reviewer for the thorough review and many constructive comments that helped improve the manuscript. Our point-by-point responses are below (changes to the original manuscript text and supporting information are in red, moved content in double-line strikethrough, and removed content in strikethrough). Please note that the line numbers in the responses refer to our revised manuscript with tracked changes. Also, please note that because we restructured the manuscript, the numbering of some figures and tables in the revised manuscript is different from those in the original manuscript.

## Reviewer 2

The manuscript describes very well-designed studies of vanillin photooxidation in bulk liquid solutions where pH, concentrations, reactant ratios, dissolved gases (N<sub>2</sub> or O<sub>2</sub>), ions (nitrate, bicarbonate) and other species (isopropanol) were varied in many combinations. The work is technically sound, with the loss of reactants, the identification and quantification of products, and the absorbance changes in solution all monitored hourly. The authors exhaustively discuss the differences between each experimental variation, pulling out as much detail as possible. This paper will be of interest to those interested in biomass burning aerosol and brown carbon formation, and is publishable after major revision to address the following points.

1. In places the discussion veers off into speculation, or suggests theories that aren't adequately explained enough to be convincing to the reader, as noted below. Generally the discussion is convincing and well-connected to the literature, but the discussion section reads like it has a thousand detailed conclusions, leaving the reader often feeling “lost in the weeds” and blunting the impact of the work. In general, the focus of the paper could be improved by moving Table 1 to the SI, removing a lot of speculative discussion, and bringing Tables S2 and maybe S3 from the SI to the main paper. These tables are more vital to the discussion at many points, in my opinion.

Response: Thank you for the suggestion. Speculative discussions have been removed from the revised text. First, Section 3.1.1 has been amended to emphasize the importance of VL triplets:

Line 187: ~~Effect of secondary oxidants from VL-VL photo-oxidation under N<sub>2</sub> and air-saturated conditions~~

Lines 188–240: ~~As mentioned earlier, secondary oxidants (<sup>1</sup>O<sub>2</sub>, O<sub>2</sub><sup>•-</sup>, <sup>•</sup>HO<sub>2</sub>, <sup>•</sup>OH) can be generated from <sup>3</sup>VL\* when O<sub>2</sub> is present (e.g., under air-saturated conditions), while <sup>3</sup>VL\* is the only oxidant expected under N<sub>2</sub>-saturated conditions. The photo-oxidation of VL To examine the contributions of <sup>3</sup>VL\* derived secondary oxidants and <sup>3</sup>VL\* only on VL photo-oxidation, experiments under both N<sub>2</sub>-air- and air-N<sub>2</sub>-saturated conditions (Fig. S3a) were carried out at pH 4, which is representative of moderately acidic aerosol and cloud pH values (Pye et al., 2020). No significant VL loss was observed for dark experiments. The oxidation of ground-state VL by <sup>3</sup>VL\* via H-atom~~

abstraction or electron transfer can form phenoxy (which is in resonance with a carbon-centered cyclohexadienyl radical that has a longer lifetime) and ketyl radicals (Neumann et al., 1986a, 1986b; Anastasio et al., 1996). The coupling of phenoxy radicals or phenoxy and cyclohexadienyl radicals can form oligomers as observed for both N<sub>2</sub>- and air-saturated experiments (see discussions later). However, the little decay of VL under N<sub>2</sub>-saturated condition indicates that these radicals probably predominantly decayed via back-hydrogen transfer to regenerate VL (Lathioor et al., 1999). A possible explanation for this is the involvement of O<sub>2</sub> in the secondary steps of VL decay. For instance, a major fate of the ketyl radical is reaction with O<sub>2</sub> (Anastasio et al., 1996). In the absence of O<sub>2</sub>, radical formation occurs, but the forward reaction of ketyl radical and O<sub>2</sub> is blocked, leading to the regeneration of VL as suggested by the minimal VL decay. Aside from potential inhibition of secondary oxidants generation (Chen et al., 2020), N<sub>2</sub> purging may have also hindered the secondary steps for VL decay.

~~The low decay rate for VL\* under N<sub>2</sub>-saturated conditions suggests a minimal role for <sup>3</sup>VL\* in VL photo-oxidation. Contrastingly, the VL\* decay rate constant under air-saturated conditions was 4 times higher, revealing the importance of <sup>3</sup>VL\* derived secondary oxidants for photosensitized oxidation of VL. As mentioned earlier, secondary oxidants (<sup>1</sup>O<sub>2</sub>, O<sub>2</sub><sup>-</sup>/<sup>•</sup>HO<sub>2</sub>, <sup>•</sup>OH) can be generated from <sup>3</sup>VL\* when O<sub>2</sub> is present (e.g., under air-saturated conditions). However, the photo-oxidation of VL in this study is likely mainly governed by <sup>3</sup>VL\* and that these secondary oxidants have only minor participation. Aside from <sup>•</sup>OH, O<sub>2</sub><sup>-</sup>/<sup>•</sup>HO<sub>2</sub> and <sup>1</sup>O<sub>2</sub> can also promote VL photo-oxidation (Kaur and Anastasio, 2018; Chen et al., 2020). <sup>1</sup>O<sub>2</sub> is also a potential oxidant for phenols (Herrmann et al., 2010; Minella et al., 2011; Smith et al., 2014), but <sup>1</sup>O<sub>2</sub> reacts much faster (by ~60 times) with phenolate ions compared to neutral phenols (Tratnyek and Hoigne, 1991; Canonica et al., 1995; McNally et al., 2005). Under the pH values (pH 2.5 to 4) considered in this study, the amount of phenolate ion is negligible, so the reaction between VL and <sup>1</sup>O<sub>2</sub> should be slow. Interestingly, however, <sup>1</sup>O<sub>2</sub> has been shown to be important in the photo-oxidation of 4-ethylguaiaicol (pK<sub>a</sub> = 10.3) by <sup>3</sup>C\* of 3,4-dimethoxybenzaldehyde (solution with pH of ~3) (Chen et al., 2020). Furthermore, while the irradiation of other phenolic compounds can produce H<sub>2</sub>O<sub>2</sub>, a precursor for <sup>•</sup>OH (Anastasio et al., 1996), the amount of H<sub>2</sub>O<sub>2</sub> is small. Based on this, only trace amounts of H<sub>2</sub>O<sub>2</sub> were likely generated from VL\* (Li et al., 2014) under-air saturated conditions, suggesting that contribution from <sup>•</sup>OH was minor. Overall, these suggest that VL photo-oxidation in this study is driven by <sup>3</sup>VL\*. Further study on the impact of O<sub>2</sub> on the reactive intermediates involved is required to understand the exact mechanisms occurring under air-saturated conditions. Nonetheless, the VL\* decay trends clearly indicate that O<sub>2</sub> is important for efficient VL photo-oxidation an efficient oxidant for unsaturated organic compounds and has a lifetime that is much longer than <sup>3</sup>C\* (Chen et al., 2020). Similar to VL\*, the decay rate constant for VL+AN under air-saturated conditions was also higher faster (6.6 times) than N<sub>2</sub>-saturated conditions, which may can be due to several reactions facilitated by nitrate photolysis products and the enhancement of N(III)-mediated photo-oxidation that may have been enhanced in the presence of O<sub>2</sub> as reported in early works (Vione et al., 2005; Kim et al., 2014; Pang et al., 2019a). As shown later, more nitrogen-containing species were observed under air-saturated conditions. An example is enhanced VL nitration likely from increased <sup>•</sup>NO<sub>2</sub> formation such as from the reaction of <sup>•</sup>OH and O<sub>2</sub><sup>-</sup> with NO<sub>2</sub> (Reactions 4 and 5, respectively; Table 1) or the autoxidation of <sup>•</sup>NO from NO<sub>2</sub><sup>-</sup> photolysis (Reactions 6–9; Table 1) in aqueous solutions (Pang et al., 2019a).~~

Reactions involving  $\text{HO}_2/\text{O}_2$  which may originate from the photolysis of nitrate alone, likely from the production and subsequent photolysis of peroxyxynitrous acid ( $\text{HOONO}$ ) (Reaction 10; Table 1) (Jung et al., 2017; Wang et al., 2021), or the reactions of  $^3\text{VL}^*$  in the presence of  $\text{O}_2$ , may have contributed as well. For instance, Wang et al. (2021) recently demonstrated that nitrate photolysis generates  $\text{HO}_2/\text{O}_2$  and  $\text{HONO}_{(g)}$  in the presence of dissolved aliphatic organic matter (e.g., nonanoic acid, ethanol), with the enhanced  $\text{HONO}_{(g)}$  production caused by secondary photochemistry between  $\text{HO}_2/\text{O}_2$  and photoproducted  $\text{NO}_x$  (Reactions 11 and 12; Table 1), in agreement with Scharko et al. (2014). The significance of this increased  $\text{HONO}$  production is enhanced  $\text{OH}$  formation (Reaction 13; Table 1). In addition,  $\text{HO}_2$  can react with  $\text{NO}$  (Reaction 10; Table 1) from  $\text{NO}_2$  photolysis (Reaction 6; Table 1) to form  $\text{HOONO}$ , and eventually  $\text{NO}_2$  and  $\text{OH}$  (Reaction 14; Table 1) (Pang et al., 2019a). Nevertheless, the comparable decay rates constants for  $\text{VL}^*$  and  $\text{VL}+\text{AN}$  imply that  $^3\text{VL}^*$  chemistry still dominates even at 1:10 molar ratio of  $\text{VL}$ /nitrate, probably due to the much higher molar absorptivity of  $\text{VL}$  compared to that of nitrate (Fig. S1) and the high  $\text{VL}$  concentration (0.1 mM) used in this study. Although we have no quantification of the oxidants in our reaction systems as it is outside the scope of this study, these observations clearly substantiate that secondary oxidants from  $^3\text{VL}^*$ , which are formed when  $\text{O}_2$  is present, are required for efficient photosensitized oxidation of  $\text{VL}$  and nitrate-mediated  $\text{VL}$  photo-oxidation are more efficient in the presence of  $\text{O}_2$ .

Moreover, Section 3.1.3 (Effect of VOCs and inorganic anions) and related sentences have also been deleted based on the likely minor contribution of  $\text{OH}$  to  $\text{VL}$  photo-oxidation in this study as pointed out by Reviewer 1 and suggested by other published literature (Anastasio et al., 1996; Li et al., 2014). Also, Section 3.5 has been deleted and Fig. 4, now 2, has been shown for the first time when potential aqSOA formation pathways were discussed, then referred to throughout the text. Table 1, which was reduced to half, was maintained in the revised version, while Table S2 (now 2) was moved to the main text, as suggested by the reviewer.

2. I do not trust using results for IPA to make generalizations about the effect of all VOCs on vanillin photooxidation. The authors repeat this questionable generalization several times throughout the manuscript, including twice in the abstract. Especially because the authors' explanation for the effect of IPA on their results relies on alcohol / water microstructure arguments, generalization to all VOCs seems unwarranted. Plus, IPA would be present only at very low concentrations in aqueous aerosol or cloud droplets due to its high volatility. It would be more appropriate if the authors remove (or heavily qualify) all statements about VOCs.

Response: We concur with the reviewer that the initial generalization for the effect of all VOCs on  $\text{VL}$  photo-oxidation based on IPA results is unsubstantiated. Moreover, the contribution of  $\text{OH}$  to  $\text{VL}$  photo-oxidation in this study is likely minimal, as pointed out by Reviewer 1 and suggested by other published literature (Anastasio et al., 1996; Li et al., 2014). Section 3.1.3 (Effect of VOCs and inorganic anions) and related sentences have been deleted altogether. Nonetheless, we maintain that it would be worthwhile to explore the effects of other potential aerosol constituents on aqSOA formation and photo-oxidation studies (lines 627–631).

3. At several points, the authors discuss rather small differences between experiments (factors of 1.2 to 1.5) as significant, but the uncertainties in the parameter values being compared are never quantified. This raises doubts in readers' minds about which differences are actually statistically significant. Some discussion of uncertainties and random error is needed.

Response: Thank you for pointing this out. We have added relevant statements to discuss these uncertainties as follows:

Line 132: Each experiment was repeated independently at least three times and measurements were done in triplicate. The reported decay rate constants and absorbance enhancement are the average of results from triplicate experiments, and the corresponding errors represent one standard deviation.

The footnote of Table S2, now 2, has been revised as follows:

Table 2: <sup>b</sup>The data fitting was performed in the initial linear region. Each value is the average of results from triplicate experiments. Errors represent one standard deviation.

The revised text also now indicates whether a difference of less than a factor of 2 is statistically significant or not:

Line 331: The decay rates constants for both VL\* and VL+AN increased as pH decreased (VL\* and VL+AN at pH 2.5: 1.65 and 1.43 times faster than at pH 4, respectively) (Fig. S3b). These differences in decay rate constants are small but statistically significant ( $p < 0.05$ ).

Line 510: The enhancement of GUA decay rate constant in the presence of VL is statistically significant ( $p < 0.05$ ), while that in the presence of AN is not ( $p > 0.05$ ).

4. The argument that <sup>3</sup>VL\* is more reactive in its protonated form as an explanation for the observed pH effects does not make sense to me. The pK<sub>a</sub> of VL is 7.4, which means that more than 99.9% of it is protonated in all experiments, negating the possibility of any detectable acceleration at low pH by this mechanism. Furthermore, the authors describe reasonable alternative explanations for their observed pH effects, such as the more efficient photolysis of HONO vs NO<sub>2</sub>- producing more OH radicals at low pH. However, the questionable claim that <sup>3</sup>VL\* is more reactive in its protonated form is repeated several times throughout the manuscript (for example, lines 267, 270, 280, 449 and 500). This claim needs to be convincingly justified or removed from the manuscript.

Response: The pK<sub>a</sub> (7.4) mentioned by the reviewer is for ground state VL, while the pK<sub>a</sub> for the VL triplet has been reported to be 4.0 (Smith et al., 2016). As there are a greater fraction of VL triplets that are protonated at pH 2.5 (0.96) than at pH 4 (0.5), it is possible that the pH dependence observed in this study is due to <sup>3</sup>VL\* being more reactive in its protonated form. Smith et al. (2016) also observed a pH dependence for the direct photodegradation of VL (0.005 mM) (rate constants at pH ≤ 3 are ~two times lower than at pH ≥ 5) which they attributed to the

sensitivity of the excimer of VL (i.e., the charge-transfer complex formed between an excited state VL molecule and a separate ground state VL molecule; Birks, 1973, Turro et al., 2010) to acid-base chemistry. The opposite trend observed in this study for 0.1 mM VL may be due to the reactivities of the protonated and neutral forms of the  $^3\text{VL}^*$  being dependent on the VL concentration (Smith et al., 2016). It has been reported that the quantum yield for direct VL photodegradation is higher at pH 5 than at pH 2 for 0.005 mM VL, but they are not statistically different for 0.03 mM VL (Smith et al., 2016). We have added a statement to include the sensitivity of the excimer of VL to acid-base chemistry as another possibility for the observed pH dependence. In addition, we have removed the discussion of N(III) photolysis as an alternative explanation for the effects of pH on VL decay kinetics as there is no significant difference between the decay rate constants of  $\text{VL}^*$  and  $\text{VL}+\text{AN}$ . Changes in the text are as follows:

Lines 331–352: The decay rates **constants** for both  $\text{VL}^*$  and  $\text{VL}+\text{AN}$  increased as pH decreased ( $\text{VL}^*$  and  $\text{VL}+\text{AN}$  at pH 2.5: **1.65** and **1.43** times faster than at pH 4, respectively) (Fig. S3b). **These differences in decay rate constants are small but statistically significant ( $p < 0.05$ ). The  $pK_a$  for the VL triplet has been reported to be 4.0 (Smith et al., 2016). As there are a greater fraction of VL triplets that are protonated at pH 2.5 (0.96) than at pH 4 (0.5), it is possible that the pH dependence of the decay rate constants observed in this study is due to  $^3\text{VL}^*$  being more reactive in its protonated form. Smith et al. (2016) also observed a pH dependence for the direct photodegradation of VL (0.005 mM) (rate constants at  $\text{pH} \leq 3$  are ~two times lower than at  $\text{pH} \geq 5$ ) which they attributed to the sensitivity of the excimer of VL (i.e., the charge-transfer complex formed between an excited state VL molecule and a separate ground state VL molecule; Birks, 1973, Turro et al., 2010) to acid-base chemistry. The opposite trend observed in this study for 0.1 mM VL may be due to the reactivities of the protonated and neutral forms of the  $^3\text{VL}^*$  being dependent on the VL concentration (Smith et al., 2016). For  $\text{VL}^*$ , this pH trend indicates that  $^3\text{VL}^*$  are more reactive in their protonated form, which is opposite to that reported for 0.005 mM VL (Smith et al., 2016), likely due to the concentration dependence of the relative reactivities of protonated and neutral forms of  $^3\text{VL}^*$ . It has been reported that the quantum yield for direct VL photodegradation is higher at pH 5 than at pH 2 for 0.005 mM VL, but they are not statistically different for 0.03 mM VL (Smith et al., 2016). Also, increases in hydrogen ion concentration can enhance the formation of  $\text{HO}_2^*$  and  $\text{H}_2\text{O}_2$  and in turn,  $^*\text{OH}$  formation (Du et al., 2011). In addition to these pH influences on  $\text{VL}^*$ , the dependence of N(III) ( $\text{NO}_2^- + \text{HONO}$ ) speciation on solution acidity (Pang et al., 2019a) also contributed to the observed pH effects for  $\text{VL}+\text{AN}$ . At pH 3.3, half of N(III) exists as  $\text{HONO}$  (Fischer and Warneck, 1996; Pang et al., 2019a), which has a higher quantum yield for  $^*\text{OH}$  formation than that of  $\text{NO}_2^-$  in the near-UV region (Arakaki et al., 1999; Kim et al., 2014). The increased  $^*\text{OH}$  formation rates as pH decreases can lead to faster VL decay (Pang et al., 2019a). Also,  $\text{NO}_2^-/\text{HONO}$  can generate  $^*\text{NO}_2$  via oxidation by  $^*\text{OH}$  (Reactions 4 and 15; Table 1) (Pang et al., 2019a). As pH decreases, the higher reactivity of  $^3\text{VL}^*$  and **sensitivity of the excimer of VL to acid-base chemistry**  ~~$\text{HONO}$  being the dominant N(III) species can lead to faster VL photo-oxidation~~ **may have led** to faster VL photo-oxidation.**

Line 356: further indicating that  $^3\text{VL}^*$  ~~are~~ **may be** more reactive in their protonated form.

Line 372: Essentially, the higher reactivity of  $^3\text{VL}^*$  and predominance of HONO over nitrite at lower pH **may have resulted** in increased formation of products mainly composed of oligomers and functionalized monomers.

**Specific comments:**

1. Line 25: The authors conclude that photosensitized reactions of VL were “more efficient” relative to nitrate-mediated photo-oxidation. However, as pointed out by the authors, VL is much more light-absorbing than nitrate. Can the authors make a comparative statement after taking this difference into account? Which is more efficient on a per-photon-absorbed basis? This would be a more appropriate comparison of reaction efficiency.

Response: Thank you for this suggestion. The apparent quantum efficiency of GUA photodegradation ( $\Phi_{\text{GUA}}$ ) in the presence of either VL or nitrate during simulated sunlight illumination can be defined as (Anastasio et al., 1996; Smith et al., 2014, 2016):

$$\Phi_{\text{GUA}} = \frac{\text{mol GUA destroyed}}{\text{mol photons absorbed}} \quad (\text{Eq. S9})$$

$\Phi_{\text{GUA}}$  was calculated using the measured rate of GUA decay and rate of light absorption by either VL or nitrate through the following equation:

$$\Phi_{\text{GUA}} = \frac{\text{rate of GUA decay}}{\text{rate of light absorption by VL or nitrate}} = \frac{k'_{\text{GUA}} \times [\text{GUA}]}{\sum[(1 - 10^{-\epsilon_{\lambda}[\text{C}]l}) \times I'_{\lambda}]} \quad (\text{Eq. S10})$$

where  $k'_{\text{GUA}}$  is the pseudo-first-order rate constant for GUA decay,  $[\text{GUA}]$  is the concentration of GUA (M),  $\epsilon_{\lambda}$  is the base-10 molar absorptivity ( $\text{M}^{-1} \text{cm}^{-1}$ ) of VL or nitrate at wavelength  $\lambda$ ,  $[\text{C}]$  is the concentration of VL or nitrate (M),  $l$  is the pathlength of the illumination cell (cm), and  $I'_{\lambda}$  is the volume-averaged photon flux ( $\text{mol-photons L}^{-1} \text{s}^{-1} \text{nm}^{-1}$ ) determined from 2NB actinometry:

$$j(2\text{NB}) = 2.303 \times \Phi_{2\text{NB}} \times l \times \sum_{300 \text{ nm}}^{350 \text{ nm}} (\epsilon_{2\text{NB},\lambda} \times I'_{\lambda} \times \Delta\lambda) \quad (\text{Eq. S11})$$

The  $\Phi_{\text{GUA}}$  in the presence of nitrate ( $1.3 \times 10^{-2} \pm 2.9 \times 10^{-3}$ ) is ~14 times larger than that in the presence of VL ( $9.0 \times 10^{-4} \pm 4.0 \times 10^{-4}$ ), suggesting that nitrate-mediated photo-oxidation of GUA is more efficient than that by photosensitized reactions of VL. We have revised this in the text as follows and added the information shown above in the supporting information: **Text S7. Estimation of the apparent quantum efficiency of guaiacol photodegradation.**

Line 29: Furthermore, **comparisons of the apparent quantum efficiency of guaiacol photodegradation indicate that in this study, guaiacol oxidation by photosensitized reactions of VL was observed to be more is less** efficient relative to nitrate-mediated photo-oxidation.

Other relevant revisions in the text are as follows:

Line 514: As mentioned earlier, ~~the~~  $^3\text{VL}^*$  chemistry appears to be more important than that of nitrate photolysis even at 1:10 molar ratio of VL/nitrate on account of the much higher molar absorptivity of VL compared to that of nitrate (Fig. S1) and the high VL concentration (0.1 mM) used in this study. However, the apparent quantum efficiency of GUA photodegradation ( $\phi_{\text{GUA}}$ ) in the presence of nitrate ( $1.3 \times 10^{-2} \pm 2.9 \times 10^{-3}$ ) is  $\sim 14$  times larger than that in the presence of VL ( $9.0 \times 10^{-4} \pm 4.0 \times 10^{-4}$ ), suggesting that nitrate-mediated photo-oxidation of GUA is more efficient than that by photosensitized reactions of VL (see Text S7 for the more details).

Line 619: The oxidation of guaiacol, a non-carbonyl phenol, by photosensitized reactions of vanillin was also shown to be ~~more~~ less efficient than that by nitrate photolysis products based on its lower apparent quantum efficiency.

2. Line 226: The authors at several points claim that VL triplet states and nitrate photolysis products have a “synergistic effect,” but evidence in support of this claim is lacking, or at best the evidence supporting it is not adequately explained. The inadequately supported claim is repeated in line 497.

Response: Thank you for this point. The trends in line 297 (formerly 226) pertain to nitrate enhancing the increased normalized abundance of products and formation of more oxidized aqSOA from VL photo-oxidation in the presence of  $\text{O}_2$  ( $\text{VL}^*$  and  $\text{VL}+\text{AN}$  under air-saturated conditions) at pH 4, suggesting a potential enhancement of VL nitration in the presence of  $\text{O}_2$ . This has been revised as follows:

Lines 295–300: In brief, the presence of ~~secondary oxidants from  $^3\text{VL}^*$  and  $\text{O}_2$~~  increased the normalized abundance of products and promoted the formation of more oxidized aqSOA. ~~These trends were reinforced in the presence of nitrate, indicating synergistic effects between secondary oxidants from VL triplets and nitrate photolysis products.~~ Compared to  $\text{N}_2$ -saturated condition, the higher normalized abundance of nitrogen-containing products under air-saturated condition for  $\text{VL}+\text{AN}$  (at pH 4) suggests a potential enhancement of VL nitration in the presence of  $\text{O}_2$ .

Line 606–611: ~~Further enhancement of VL photo-oxidation under air-saturated conditions in the presence of nitrate indicates synergistic effects between secondary oxidants from VL triplets and nitrate photolysis products.~~ In contrast,  $^3\text{VL}^*$ -initiated reactions proceeded rapidly under air-saturated conditions ( $\text{O}_2$  is present) as indicated by higher VL decay rate constant and increased normalized abundance of products. For pH 4 experiments, the presence of both  $\text{O}_2$  and nitrate resulted in the highest normalized abundance of products (including N-containing compounds) and  $\langle \text{OS}_c \rangle$ , which may be due to the presence of  $\text{O}_2$  promoting VL nitration.

3. Line 258: This explanation of opposite pH trends at 0.1 and 0.005 mM VL is extremely speculative.



Response: Smith et al. (2016) reported that the relative reactivities of the protonated and neutral forms of VL triplets depend on the VL concentration. Specifically, they found that the quantum yield for direct VL photodegradation is higher at pH 5 than at pH 2 for 0.005 mM VL, but they are not statistically different for 0.03 mM VL (Smith et al., 2016). The opposite trend observed in our study may then be due to this concentration dependence of the reactivities of the protonated and neutral forms of  $^3\text{VL}^*$ . Moreover, as mentioned in our response to major comment #6 by Reviewer 1, the comparable pH dependence of the aqSOA formed from  $\text{VL}^*$  at pH 4 and 2.5 over a range of pH conditions from 1.5 to 10.5 suggests that the pH dependence observed is likely due to the acid-base chemistry of the reactions which may involve  $^3\text{VL}^*$  or the excimer of VL (Smith et al., 2016). Please see our response to your major comment #4 for relevant changes made in the text.

4. Line 272: For greater clarity, it would be helpful if the manuscript would always match product formulas mentioned in the text to the structures shown in Table S3. Is this product structure #21 in Table S3?

Response: We thank the reviewer for this suggestion. We have added the product structures (if applicable) to the formulas mentioned in the text. No, product structure #21, now #12, refers to a GUA tetramer that was observed only in the GUA+VL experiment (Line 544). Unfortunately, we do not have a product structure for the tetramer mentioned in Line 358 (formerly 272), although we have now added the proposed formula for this tetramer as follows:

Line 358: Furthermore, a tetramer ( $\text{C}_{31}\text{H}_{24}\text{O}_{11}$ ) was observed only in  $\text{VL}^*$  at pH 2.5.

5. Line 297: is this dimer product structure #5 in Table S3?

Response: Sentences related to  $^{\bullet}\text{OH}$  scavengers have been deleted from the original manuscript.

6. Line 334: The solvent cage effect explanation seems questionable. Why would two negatively charged ions share a solvent cage, given their electrostatic repulsion? Furthermore, in line 339 the authors state that “NaBC did not cause any substantial change in the decay of VL,” thus making this whole solvent cage discussion irrelevant to the data at hand.

Response: Sentences related to  $^{\bullet}\text{OH}$  scavengers have been deleted from the original manuscript.

7. Line 341 – 346: the authors state that “no tetramers were observed in  $\text{VL}^*+\text{NaBC}$ ” and “ $\text{VL}+\text{AN}+\text{IPA}$  had more oligomers,” and then go on to suggest that the formation of oligomers can be promoted by inorganic ions, likely via the generation of radicals such as  $\cdot\text{CO}_3$ . No evidence has been provided, as far as I can tell, that NaBC promotes oligomer formation, so I was confused by the authors’ claim here that bicarbonate does in fact promote oligomer formation via  $\cdot\text{CO}_3$  radicals.

Response: Sentences related to  $^{\bullet}\text{OH}$  scavengers have been deleted from the original manuscript.

8. Line 363: ESI-MS is routinely used to detect macromolecules in biochemistry. This suggestion that the method cannot detect molecules with more than 25 carbons is an erroneous conclusion to draw from Lin et al. (2018).

Response: Lin et al. (2018) also studied BrC from BBOA, similar to our experiments. As they reported that majority of ESI-detected compounds in their study are smaller molecules with fewer than 25 carbon atoms, we raise the possibility that this may also be the case for our study.

9. Line 379: The logic needs to be better spelled out here. Why is the formation of more oxidized products suggested by a larger fraction of small-mass products observed for 1:1 VL/nitrate mixtures compared to 1:100? Do small product masses imply fragmentation, or is there a competition with oligomerization?

Response: We apologize for the confusion. The larger fraction of small product masses (< 200 m/z) observed for 1:1 compared to 1:100 VL/nitrate suggests the prevalence of functionalization for the former. In addition, the higher  $\langle OS_c \rangle$  for 1:1 VL/nitrate indicates the formation of more oxidized products compared to 1:100 VL/nitrate. The small product masses (< 200 m/z) imply functionalization, while the contribution of > 300 m/z suggests oligomerization. Fragmentation was indicated by the observed small organic acids (analyzed using IC), but not the mass spectrometric analyses as the small organic acids are not detectable in the positive ion mode. Fragmentation, which leads to the decomposition of previously formed oligomers and generation of small, oxygenated products such as organic acids (Huang et al., 2018), may also occur for the low [VL] experiments. However, its importance would likely be observed at longer irradiation times, similar to the high [VL] experiments. Oligomerization probably occurred for both 1:1 and 1:100 VL/nitrate as suggested by the observed contribution of > 300 m/z, although to a lesser extent than functionalization based on the higher contribution of < 200 m/z. Lines 466–485 have been revised as follows:

Lines 466–485: For both VL\* and VL+AN, the contribution of < 200 m/z to the normalized abundance of products was higher at low [VL] than at high [VL], while the opposite was observed for > 300 m/z (Fig. S123d). This indicates that functionalization was favored at low [VL], as supported by the higher  $\langle OS_c \rangle$ , while oligomerization was the dominant pathway at high [VL], consistent with more oligomers or polymeric products reported from high phenols concentration (e.g., 0.1 to 3 mM) (Li et al., 2014; Slikboer et al., 2015; Ye et al., 2019). This is probably due to an increased concentration of phenoxy radicals (in resonance with a carbon-centered cyclohexadienyl radical) at high [VL], promoting radical-radical polymerization (Sun et al., 2010; Li et al., 2014). Moreover At low [VL], the contribution of < 200 m/z to the normalized abundance of products was higher for 1:1 than 1:100 VL/nitrate molar ratio, further suggesting the prevalence of functionalization for the former ~~formation of more oxidized products. This may also be the reason why~~ In addition, 1:1 VL/nitrate (A115; Table S2) had higher  $\langle OS_c \rangle$  than 1:100 VL/nitrate (A126; Table S2), indicating the formation of more oxidized products, but had fewer N-containing compounds compared to the latter. A possible explanation is that at 1:1 VL/nitrate, VL may efficiently competes with  $NO_2^-$  for  $^*OH$  (from nitrate or nitrite photolysis, Reaction 4; Table 1) and indirectly reduces  $^*NO_2$ . Similarly, hydroxylation has been suggested to be a more

important pathway for 1:1 VL/nitrite than in 1:10 VL/nitrite (Pang et al., 2019a). ~~This may also be the reason why 1:1 VL/nitrate (A15; Table S2) had higher  $\langle OS_n \rangle$  than 1:100 (A16; Table S2) VL/nitrate but had fewer N-containing compounds compared to the latter. Moreover, the contribution of  $<200$  m/z to the normalized abundance of products was higher for 1:1 than 1:100 VL/nitrate molar ratio, further suggesting the formation of more oxidized products.~~ Fragmentation, which leads to the decomposition of previously formed oligomers and generation of small, oxygenated products such as organic acids (Huang et al., 2018), may also occur for the low [VL] experiments. However, its importance would likely be observed at longer irradiation times, similar to the high [VL] experiments.

10. Line 389:  $C_8H_9NO_3$  should be identified as product structure #2 (an amine) on Table S3.

Response: Thank you for this suggestion. We have now added the structure number to  $C_8H_9NO_3$  in line 494 (formerly 389) as follows:

Line 494: ...  $C_8H_9NO_3$  (No. 2, Table S2) was also...

11. Line 408: The nitrate photolysis explanations may not be needed, given that the observed enhancement of nitrate on guaiacol decay rates was only a factor of 1.2. Is this a statistically significant change?

Response: Thank you for pointing this out. The reviewer is correct that the nitrate photolysis explanation is not needed in this case, given that the observed enhancement for GUA+AN is not statistically significant. Changes in the text are as follows:

Line 510: ~~The enhancement of GUA decay rate constant in the presence of VL is statistically significant ( $p < 0.05$ ), while that in the presence of AN is not ( $p > 0.05$ ).~~

12. Line 418: The word “Similarly” is being used to relate two seemingly dissimilar observations, causing needless confusion. In the previous sentence, VL shows much higher absorbance enhancement than nitrate, but in this sentence nitrate is being compared to an experiment without nitrate.

Response: The reviewer is correct. The word ‘similarly’ has been removed in Line 525 (formerly 418) to avoid confusion.

Line 525: ~~Similarly,~~ Yang et al. (2021) also observed greater light absorption during nitrate-mediated photo-oxidation relative to direct GUA photodegradation.

13. Line 471: This sentence is confusing. Doesn’t this work address (among other things) the effects of nitration on triplet-generating aromatics?

Response: Thank you for catching this. We have clarified this sentence as follows:

Line 574: Although nitrate did not substantially affect the VL decay rates **constants**, likely due to much higher molar absorptivity of VL than nitrate and high VL concentration used in this work, the presence of nitrate promoted functionalization and nitration, indicating the significance of nitrate photolysis in this aqSOA formation pathway. **While This work demonstrates that nitration, which is can be an important process for producing light-absorbing organics or BrC (Jacobson, 1999; Kahnt et al., 2013; Mohr et al., 2013; Laskin et al., 2015; Teich et al., 2017; Li et al., 2020), its effect on can also affect the aqueous-phase processing of triplet-generating aromatics has not yet been examined in detail.**

14. Line 481: Why would VL photodegrade 10 times slower in ALW relative to dilute cloudwater? This effect is important for applying this work to the atmosphere. Could the authors provide some theory or explanation here?

Response: There is no generalization yet for these increased or decreased photodegradation of methoxyphenols and by far, only VL has been observed to exhibit decreased photodegradation in ALW. The study for VL in ALW (Loisel et al., 2021) stated that the nature of inorganic ions would affect the photodegradation of organic compounds. Further work on the effects of inorganic ions on photodegradation of VL in ALW is warranted.

15. (a) On Table S2, experiments without nitrate are listed as “—” in the column of normalized abundances of N-containing compounds. Is this because no N-containing compounds were detected in the top 50, or because these samples were not analyzed for N-containing compounds? (b) It would be helpful to map the reactant molecule onto the Figure S12 graph.

Response: (a) The reviewer is right. The samples for experiments without nitrate were not analyzed for N-containing compounds. This information has been added to the footnote of Table S2 as follows:

...<sup>d</sup>The normalized abundance of products was calculated using Eq. 2. **The samples for experiments without nitrate (marked with N/A ↯) were not analyzed for N-containing compounds.**

(b) VL has now been added to Fig. S12, now S11.

#### **Technical Corrections:**

1. Line 349: “increased” should be “increase”

Response: Sentences related to \*OH scavengers have been deleted from the original manuscript.

2. Line 377: “an important” should be “a more important”

Response: Thank you for pointing this out. Line 478 (formerly 377) has been revised accordingly:

Line 478: Similarly, hydroxylation has been suggested to be a **more** important pathway for 1:1 VL/nitrite than in 1:10 VL/nitrite (Pang et al., 2019a).

3. Line 459: “decompose” should be “decomposes”

Response: Sentences related to  $\cdot\text{OH}$  scavengers have been deleted from the original manuscript.

4. Sodium nitrate in my opinion would be better abbreviated “NaN” to be more consistent with other abbreviations such as “NaBC.”

Response: Sentences related to  $\cdot\text{OH}$  scavengers have been deleted from the original manuscript.

5. Table S3: Compound number 4, the most abundant product in some studies, is missing an oxygen atom. It should be clarified that structure #1 is the reactant molecule vanillin rather than a product.

Response: Thank you for the correction and suggestion. We have corrected these on Table S2, formerly S3.

## References

Anastasio, C., Faust, B. C., and Rao, C. J.: Aromatic carbonyl compounds as aqueous-phase photochemical sources of hydrogen peroxide in acidic sulfate aerosols, fogs, and clouds. 1. Non-phenolic methoxybenzaldehydes and methoxyacetophenones with reductants (phenols), *Environ. Sci. Technol.*, 31, 218–232, <https://doi.org/10.1021/es960359g>, 1996.

Birks, J.B.: *Organic Molecular Photophysics*, John Wiley & Sons, 1973.

Canonica, S., Jans, U., Stemmler, K., and Hoigne, J.: Transformation kinetics of phenols in water: Photosensitization by dissolved natural organic material and aromatic ketones, *Environ. Sci. Technol.*, 29, 1822–1831, <https://doi.org/10.1021/es00007a020>, 1995.

Chen, Y., Li, N., Li, X., Tao, Y., Luo, S., Zhao, Z., Ma, S., Huang, H., Chen, Y., Ye, Z., and Ge, X.: Secondary organic aerosol formation from  $^3\text{C}^*$ -initiated oxidation of 4-ethylguaiaicol in atmospheric aqueous-phase, *Sci. Total Environ.*, 723, 137953, <https://doi.org/10.1016/j.scitotenv.2020.137953>, 2020.

Herrmann, H., Hoffmann, D., Schaefer, T., Bräuer, P., and Tilgner, A.: Tropospheric aqueous-phase free-radical chemistry: Radical sources, spectra, reaction kinetics and prediction tools, *Chem. Phys. Chem.*, 11, 3796–3822, <https://doi.org/10.1002/cphc.201000533>, 2010.

Huang, D. D., Zhang, Q., Cheung, H. H. Y., Yu, L., Zhou, S., Anastasio, C., Smith, J. D., and Chan, C. K.: Formation and evolution of aqSOA from aqueous-phase reactions of phenolic carbonyls:

comparison between ammonium sulfate and ammonium nitrate solutions, *Environ. Sci. Technol.*, 52, 9215–9224, <https://doi.org/10.1021/acs.est.8b03441>, 2018.

Jacobson, M. Z.: Isolating nitrated and aromatic aerosols and nitrated aromatic gases as sources of ultraviolet light absorption, *J. Geophys. Res.*, 104, 3527–3542, <https://doi.org/10.1029/1998JD100054>, 1999.

Kahnt, A., Behrouzi, S., Vermeylen, R., Shalamzari, M. S., Vercauteren, J., Roekens, E., Claeys, M., and Maenhaut, W.: One-year study of nitro-organic compounds and their relation to wood burning in PM<sub>10</sub> aerosol from a rural site in Belgium, *Atmos. Environ.*, 81, 561–568, <https://doi.org/10.1016/j.atmosenv.2013.09.041>, 2013.

Kim, D.-h., Lee, J., Ryu, J., Kim, K., and Choi, W.: Arsenite oxidation initiated by the UV photolysis of nitrite and nitrate, *Environ. Sci. Technol.*, 48, 4030–4037, <https://doi.org/10.1021/es500001q>, 2014.

Laskin, A., Laskin, J., and Nizkorodov, S.A.: Chemistry of atmospheric brown carbon, *Chem. Rev.*, 115, 4335–4382, <https://doi.org/10.1021/cr5006167>, 2015.

Lathioor, E. C., Leigh, W. J., and St. Pierre, M. J.: Geometrical effects on intramolecular quenching of aromatic ketone ( $\pi,\pi^*$ ) triplets by remote phenolic hydrogen abstraction, *J. Am. Chem. Soc.*, 121, 11984–11992, <https://pubs.acs.org/doi/abs/10.1021/ja991207z>, 1999.

Li, F., Tang, S., Tsona, N. T., and Du, L.: Kinetics and mechanism of OH-induced  $\alpha$ -terpineol oxidation in the atmospheric aqueous phase, *Atmos. Environ.*, 237, 117650, <https://doi.org/10.1016/j.atmosenv.2020.117650>, 2020.

Li, Y. J., Huang, D. D., Cheung, H. Y., Lee, A. K. Y., and Chan, C. K.: Aqueous-phase photochemical oxidation and direct photolysis of vanillin - a model compound of methoxy phenols from biomass burning, *Atmos. Chem. Phys.*, 14, 2871–2885, <https://doi.org/10.5194/acp-14-2871-2014>, 2014.

Lin, P., Fleming, L. T., Nizkorodov, S. A., Laskin, J., and Laskin, A.: Comprehensive molecular characterization of atmospheric brown carbon by high resolution mass spectrometry with electrospray and atmospheric pressure photoionization, *Anal. Chem.*, 90, 12493–12502, <https://doi.org/10.1021/acs.analchem.8b02177>, 2018.

Loisel, G., Mekic, M., Liu, S., Song, W., Jiang, B., Wang, Y., Deng, H., and Gligorovski, S.: Ionic strength effect on the formation of organonitrate compounds through photochemical degradation of vanillin in liquid water of aerosols, *Atmos. Environ.*, 246, 118140, <https://doi.org/10.1016/j.atmosenv.2020.118140>, 2021.

McNally, A. M., Moody, E. C., and McNeill, K.: Kinetics and mechanism of the sensitized photodegradation of lignin model compounds, *Photochem. Photobiol. Sci.*, 4, 268–274, <https://doi.org/10.1039/B416956E>, 2005.

Minella, M., Romeo, F., Vione, D., Maurino, V., and Minero, C.: Low to negligible photoactivity of lake-water matter in the size range from 0.1 to 5  $\mu\text{m}$ , *Chemosphere*, 83, 1480–1485, <https://doi.org/10.1016/j.chemosphere.2011.02.093>, 2011.

Mohr, C., Lopez-Hilfiker, F. D., Zotter, P., Prévôt, A. S. H., Xu, L., Ng, N. L., Herndon, S. C., Williams, L. R., Franklin, J. P., Zahniser, M. S., Worsnop, D. R., Knighton, W. B., Aiken, A. C., Gorkowski, K. J., Dubey, M. K., Allan, J. D., and Thornton, J. A.: Contribution of nitrated phenols to wood burning brown carbon light absorption in Detling, United Kingdom during winter time, *Environ. Sci. Technol.*, 47, 6316–6324, <https://doi.org/10.1021/es400683v>, 2013.

Neumann, M. G., De Groote, R. A. M. C., and Machado, A. E. H.: Flash photolysis of lignin: Part 1. Deaerated solutions of dioxane-lignin, *Polym. Photochem.*, 7, 401–407, [https://doi.org/10.1016/0144-2880\(86\)90007-2](https://doi.org/10.1016/0144-2880(86)90007-2), 1986a.

Neumann, M. G., De Groote, R. A. M. C., and Machado, A. E. H.: Flash photolysis of lignin: II. Oxidative photodegradation of dioxane-lignin, *Polym. Photochem.*, 7, 461–468, [https://doi.org/10.1016/0144-2880\(86\)90015-1](https://doi.org/10.1016/0144-2880(86)90015-1), 1986b.

Pang, H., Zhang, Q., Lu, X. H., Li, K., Chen, H., Chen, J., Yang, X., Ma, Y., Ma, J., and Huang, C.: Nitrite-mediated photooxidation of vanillin in the atmospheric aqueous phase, *Environ. Sci. Technol.*, 53, 14253–14263, <https://doi.org/10.1021/acs.est.9b03649>, 2019a.

Pye, H., Nenes, A., Alexander, B., Ault, A. P., Barth, M. C., Clegg, S. L., Collett, J. L. Jr., Fahey, K. M., Hennigan, C. J., Herrmann, H., Kanakidou, M., Kelly, J. T., Ku, I. T., McNeill, V. F., Riemer, N., Schaefer, T., Shi, G., Tilgner, A., Walker, J. T., Wang, T., Weber, R., Xing, J., Zaveri, R. A., and Zuend, A.: The acidity of atmospheric particles and clouds, *Atmos. Chem. Phys.*, 20, 4809–4888, <https://doi.org/10.5194/acp-20-4809-2020>, 2020.

Slikboer, S., Grandy, L., Blair, S. L., Nizkorodov, S. A., Smith, R. W., and Al-Abadleh, H. A.: Formation of light absorbing soluble secondary organics and insoluble polymeric particles from the dark reaction of catechol and guaiacol with Fe(III), *Environ. Sci. Technol.*, 49, 7793–7801, <https://doi.org/10.1021/acs.est.5b01032>, 2015.

Smith, J. D., Sio, V., Yu, L., Zhang, Q., and Anastasio, C.: Secondary organic aerosol production from aqueous reactions of 973 atmospheric phenols with an organic triplet excited state, *Environ. Sci. Technol.*, 48, 1049–1057, <https://doi.org/10.1021/es4045715>, 2014.

Smith, J. D., Kinney, H., and Anastasio, C.: Phenolic carbonyls undergo rapid aqueous photodegradation to form low-volatility, light-absorbing products, *Atmos. Environ.*, 126, 36–44, <https://doi.org/10.1016/j.atmosenv.2015.11.035>, 2016.

Sun, Y. L., Zhang, Q., Anastasio, C., and Sun, J.: Insights into secondary organic aerosol formed via aqueous-phase reactions of phenolic compounds based on high resolution mass spectrometry, *Atmos. Chem. Phys.*, 10, 4809–4822, <https://doi.org/10.5194/acp-10-4809-2010>, 2010.

Teich, M., van Pinxteren, D., Wang, M., Kecorius, S., Wang, Z., Müller, T., Močnik, G., and Herrmann, H.: Contributions of nitrated aromatic compounds to the light absorption of water-soluble and particulate brown carbon in different atmospheric environments in Germany and China, *Atmos. Chem. Phys.*, 17, 1653–1672, <https://doi.org/10.5194/acp-17-1653-2017>, 2017.

Tratnyek, P. G. and Hoigne, J.: Oxidation of substituted phenols in the environment: a QSAR analysis of rate constants for reaction with singlet oxygen, *Environ. Sci. Technol.*, 25, 1596–1604, <https://doi.org/10.1021/es00021a011>, 1991.

Turro, N., Ramamurthy, V., and Scaiano, J.C.: *Modern Molecular Photochemistry*, University Science Book, 2010.

Vione, D., Maurino, V., Minero, C., and Pelizzetti, E.: Reactions induced in natural waters by irradiation of nitrate and nitrite ions, in: *The Handbook of Environmental Chemistry Vol. 2M - Environmental Photochemistry Part II*, Springer, Berlin, Heidelberg, Germany, 221–253, <https://doi.org/10.1007/b138185>, 2005.

Yang, J., Au, W. C., Law, H., Lam, C. H., and Nah, T.: Formation and evolution of brown carbon during aqueous-phase nitrate-mediated photooxidation of guaiacol and 5-nitroguaiacol, *Atmos. Environ.*, 254, 118401, <https://doi.org/10.1016/j.atmosenv.2020.118140>, 2021.

Ye, Z., Qu, Z., Ma, S., Luo, S., Chen, Y., Chen, H., Chen, Y., Zhao, Z., Chen, M., and Ge, X.: A comprehensive investigation of aqueous-phase photochemical oxidation of 4-ethylphenol, *Sci. Total Environ.*, 685, 976–985, <https://doi.org/10.1016/j.scitotenv.2019.06.276>, 2019.



Author Response for “Aqueous SOA formation from the photo-oxidation of vanillin: Direct photosensitized reactions and nitrate-mediated reactions” by Mabato et al.

We thank the reviewer for the thorough review and many constructive comments that helped improve the manuscript. Our point-by-point responses are below (changes to the original manuscript text and supporting information are in red, moved content in double-line strikethrough, and removed content in strikethrough). Please note that the line numbers in the responses refer to our revised manuscript with tracked changes. Also, please note that because we restructured the manuscript, the numbering of some figures and tables in the revised manuscript is different from those in the original manuscript.

### Reviewer 3

This study investigated the aqueous photo-oxidation of vanillin (VL) via both direct photosensitized reaction and nitrate-mediated photo-oxidation and discussed the influence of secondary oxidants from triplet excited states ( $^3\text{VL}^*$ ), solution pH, VOCs, and inorganic anions, etc. in detail. The experiments and data analysis are well done, and the mechanisms that are proposed are plausible. This study provides valuable information about the chemical composition, optical properties, and possible reaction mechanisms for SOA formed from the VL photo-oxidation under different conditions. However, there are a few major and minor comments I would like the authors to address before it is considered for publication in ACP.

### Major comments

(1) With the experiment design, it is difficult to directly compare  $^3\text{VL}^*$  pathway and nitrated-mediated pathway, as also mentioned by the authors that the VL concentration was very high, and  $^3\text{VL}^*$  chemistry dominated in all the VL + ammonium nitrate (AN) experiments. Maybe more precisely, what was compared was photo-oxidation of VL via  $^3\text{VL}^*$  chemistry with and without nitrate. However, both the title and some places in the manuscript are misleading.

Response: We agree with the reviewer that  $^3\text{VL}^*$  chemistry dominated in VL+AN experiments, as mentioned throughout the manuscript. However, we did not intend to compare  $^3\text{VL}^*$  and nitrated-mediated pathways either. It is our opinion that the current title does not have such connotation. Despite the high VL concentration, the VL+AN experiments showed some differences in the aqSOA formed. Hence, we would like to keep the current title. With the revised abstract, we hope it will not confuse readers into expecting a comparison.

(2) I suggest the authors restructure the manuscript: on the one hand, to move part of the figures and tables from the SI to the manuscript, e.g. Table S2 and Figure S12, to make it easier to follow. On the other hand, to simplify the article by cutting some “maybe interesting” but not that important/related findings/discussions to make the main storyline clearer.

Response: Thank you for the suggestion. Speculative discussions have been removed from the revised text. First, Section 3.1.1 has been amended to emphasize the importance of VL triplets:

Line 187: ~~Effect of secondary oxidants from VL-VL photo-oxidation under N<sub>2</sub> and air-saturated conditions~~

Lines 188–240: ~~As mentioned earlier, secondary oxidants (<sup>1</sup>O<sub>2</sub>, O<sub>2</sub><sup>\*</sup>/<sup>\*</sup>HO<sub>2</sub>, <sup>\*</sup>OH) can be generated from <sup>3</sup>VL\* when O<sub>2</sub> is present (e.g., under air-saturated conditions), while <sup>3</sup>VL\* is the only oxidant expected under N<sub>2</sub>-saturated conditions. The photo-oxidation of VL To examine the contributions of <sup>3</sup>VL\* derived secondary oxidants and <sup>3</sup>VL\* only on VL photo-oxidation, experiments under both N<sub>2</sub>-air- and air-N<sub>2</sub>-saturated conditions (Fig. S3a) were carried out at pH 4, which is representative of moderately acidic aerosol and cloud pH values (Pye et al., 2020). No significant VL loss was observed for dark experiments. The oxidation of ground-state VL by <sup>3</sup>VL\* via H-atom abstraction or electron transfer can form phenoxy (which is in resonance with a carbon-centered cyclohexadienyl radical that has a longer lifetime) and ketyl radicals (Neumann et al., 1986a, 1986b; Anastasio et al., 1996). The coupling of phenoxy radicals or phenoxy and cyclohexadienyl radicals can form oligomers as observed for both N<sub>2</sub>- and air-saturated experiments (see discussions later). However, the little decay of VL under N<sub>2</sub>-saturated condition indicates that these radicals probably predominantly decayed via back-hydrogen transfer to regenerate VL (Lathioor et al., 1999). A possible explanation for this is the involvement of O<sub>2</sub> in the secondary steps of VL decay. For instance, a major fate of the ketyl radical is reaction with O<sub>2</sub> (Anastasio et al., 1996). In the absence of O<sub>2</sub>, radical formation occurs, but the forward reaction of ketyl radical and O<sub>2</sub> is blocked, leading to the regeneration of VL as suggested by the minimal VL decay. Aside from potential inhibition of secondary oxidants generation (Chen et al., 2020), N<sub>2</sub> purging may have also hindered the secondary steps for VL decay.~~

~~The low decay rate for VL\* under N<sub>2</sub>-saturated conditions suggests a minimal role for <sup>3</sup>VL\* in VL photo-oxidation. Contrastingly, the VL\* decay rate constant under air-saturated conditions was 4 times higher, revealing the importance of <sup>3</sup>VL\* derived secondary oxidants for photosensitized oxidation of VL. As mentioned earlier, secondary oxidants (<sup>1</sup>O<sub>2</sub>, O<sub>2</sub><sup>\*</sup>/<sup>\*</sup>HO<sub>2</sub>, <sup>\*</sup>OH) can be generated from <sup>3</sup>VL\* when O<sub>2</sub> is present (e.g., under air-saturated conditions). However, the photo-oxidation of VL in this study is likely mainly governed by <sup>3</sup>VL\* and that these secondary oxidants have only minor participation. Aside from <sup>\*</sup>OH, O<sub>2</sub><sup>\*</sup>/<sup>\*</sup>HO<sub>2</sub> and <sup>1</sup>O<sub>2</sub> can also promote VL photo-oxidation (Kaur and Anastasio, 2018; Chen et al., 2020). <sup>1</sup>O<sub>2</sub> is also a potential oxidant for phenols (Herrmann et al., 2010; Minella et al., 2011; Smith et al., 2014), but <sup>1</sup>O<sub>2</sub> reacts much faster (by ~60 times) with phenolate ions compared to neutral phenols (Tratnyek and Hoigne, 1991; Canonica et al., 1995; McNally et al., 2005). Under the pH values (pH 2.5 to 4) considered in this study, the amount of phenolate ion is negligible, so the reaction between VL and <sup>1</sup>O<sub>2</sub> should be slow. Interestingly, however, <sup>1</sup>O<sub>2</sub> has been shown to be important in the photo-oxidation of 4-ethylguaicol (pK<sub>a</sub> = 10.3) by <sup>3</sup>C\* of 3,4-dimethoxybenzaldehyde (solution with pH of ~3) (Chen et al., 2020). Furthermore, while the irradiation of other phenolic compounds can produce H<sub>2</sub>O<sub>2</sub>, a precursor for <sup>\*</sup>OH (Anastasio et al., 1996), the amount of H<sub>2</sub>O<sub>2</sub> is small. Based on this, only trace amounts of H<sub>2</sub>O<sub>2</sub> were likely generated from VL\* (Li et al., 2014) under-air saturated conditions, suggesting that contribution from <sup>\*</sup>OH was minor. Overall, these suggest that VL photo-oxidation~~

in this study is driven by  $^3\text{VL}^*$ . Further study on the impact of  $\text{O}_2$  on the reactive intermediates involved is required to understand the exact mechanisms occurring under air-saturated conditions. Nonetheless, the  $\text{VL}^*$  decay trends clearly indicate that  $\text{O}_2$  is important for efficient VL photo-oxidation ~~an efficient oxidant for unsaturated organic compounds and has a lifetime that is much longer than  $^3\text{C}^*$  (Chen et al., 2020). Similar to  $\text{VL}^*$ , t~~ The decay rate constant for VL+AN under air-saturated conditions was also higher faster (6.6 times) than  $\text{N}_2$ -saturated conditions, which may can be due to several reactions facilitated by nitrate photolysis products and the enhancement of N(III) mediated photo-oxidation that may have been enhanced in the presence of  $\text{O}_2$  as reported in early works (Vione et al., 2005; Kim et al., 2014; Pang et al., 2019a). As shown later, more nitrogen-containing species were observed under air-saturated conditions. An example is enhanced VL nitration likely from increased  $^*\text{NO}_2$  formation such as from the reaction of  $^*\text{OH}$  and  $\text{O}_2^{\cdot-}$  with  $\text{NO}_2^-$  (Reactions 4 and 5, respectively; Table 1) or the autoxidation of  $^*\text{NO}$  from  $\text{NO}_2^-$  photolysis (Reactions 6–9; Table 1) in aqueous solutions (Pang et al., 2019a). Reactions involving  $^*\text{HO}_2/\text{O}_2^{\cdot-}$  which may originate from the photolysis of nitrate alone, likely from the production and subsequent photolysis of peroxyxynitrous acid ( $\text{HOONO}$ ) (Reaction 10; Table 1) (Jung et al., 2017; Wang et al., 2021), or the reactions of  $^3\text{VL}^*$  in the presence of  $\text{O}_2$ , may have contributed as well. For instance, Wang et al. (2021) recently demonstrated that nitrate photolysis generates  $^*\text{HO}_2/\text{O}_2^{\cdot-}(\text{aq})$  and  $\text{HONO}(\text{g})$  in the presence of dissolved aliphatic organic matter (e.g., nonanoic acid, ethanol), with the enhanced  $\text{HONO}(\text{g})$  production caused by secondary photochemistry between  $^*\text{HO}_2/\text{O}_2^{\cdot-}(\text{aq})$  and photoproducted  $\text{NO}_x(\text{aq})$  (Reactions 11 and 12; Table 1), in agreement with Scharko et al. (2014). The significance of this increased  $\text{HONO}$  production is enhanced  $^*\text{OH}$  formation (Reaction 13; Table 1). In addition,  $^*\text{HO}_2$  can react with  $^*\text{NO}$  (Reaction 10; Table 1) from  $\text{NO}_2^-$  photolysis (Reaction 6; Table 1) to form  $\text{HOONO}$ , and eventually  $^*\text{NO}_2$  and  $^*\text{OH}$  (Reaction 14; Table 1) (Pang et al., 2019a). Nevertheless, the comparable decay rates constants for  $\text{VL}^*$  and VL+AN imply that  $^3\text{VL}^*$  chemistry still dominates even at 1:10 molar ratio of VL/nitrate, probably due to the much higher molar absorptivity of VL compared to that of nitrate (Fig. S1) and the high VL concentration (0.1 mM) used in this study. Although we have no quantification of the oxidants in our reaction systems as it is outside the scope of this study, these observations clearly substantiate that secondary oxidants from  $^3\text{VL}^*$ , which are formed when  $\text{O}_2$  is present, are required for efficient photosensitized oxidation of VL and nitrate-mediated VL photo-oxidation are more efficient in the presence of  $\text{O}_2$ .

Moreover, Section 3.1.3 (Effect of VOCs and inorganic anions) and related sentences have also been deleted based on the likely minor contribution of  $^*\text{OH}$  to VL photo-oxidation in this study as pointed out by Reviewer 1 and suggested by other published literature (Anastasio et al., 1996; Li et al., 2014). Also, Section 3.5 has been deleted and Fig. 4, now 2, has been shown for the first time when potential aqSOA formation pathways were discussed, then referred to throughout the text. Table 1, which was reduced to half, was maintained in the revised version, while Table S2 (now 2) was moved to the main text, as suggested by the reviewer.

(3) (a) It is very interesting to see the changes in optical properties, and their relation to the changes in chemical composition. However, I only see very general discussions about it (e.g. line 234-238 and line 282-289). It will be nice to discuss the specific compounds, possible chromophores, and to explain the changes in the optical properties.

(b) To explain the pH-dependency, the authors cited Pang et al. 2019a, which reported the pH-dependent light absorbance of nitrophenols. However, the dominating products in this study were those without N, different from those in Pang et al. 2019a. In addition, the chemical composition of SOA with pH 4 and pH < 4 are quite different, which could also lead to different functional group/chromophores, and changes in optical properties.

Response:

(a) Thank you for this suggestion. We agree that identifying the BrC chromophores would enrich the discussion for the changes in the optical properties. However, it is possible that the products detected using UHPLC-qToF-MS in positive ESI mode might not have contributed significantly to all products formed and hence may not be the primary contributors to the absorbance enhancement. In other words, the absorbance enhancement may not necessarily correlate directly with the products detected. Detailed characterization of specific chromophores is indeed interesting, but it is outside of the scope of this study. Instead, the changes in the optical properties for this study are based on the integrated area of the absorption spectra from 350 to 550 nm in order to consider the contributions of all potentially light-absorbing products.

(b) The reviewer is correct that the dominant products in this study do not contain nitrogen. We have revised this explanation based on the comparable pH dependence of the aqSOA formed from VL\* at pH 2.5 and 4 over a range of pH conditions from 1.5 to 10.5. This suggests that the observed pH dependence is due to the acid-base chemistry of the reactions, which may involve <sup>3</sup>VL\* or the excimer of VL (Smith et al., 2016). Changes in the text are as follows:

Lines 375–386: ~~The higher absorbance enhancement for both VL\* and VL+AN (Fig. 32b) was observed as pH increased may be attributed to redshifts and increased visible light absorption of reaction products (Pang et al., 2019a). To determine whether the pH dependence is due to the acid-base chemistry of the products or of the reactions, we measured the pH dependence of the aqSOA formed from VL\* at pH 4 and 2.5 over a range of pH conditions from 1.5 to 10.5 (Fig. S10). For both cases, the intensity of absorption at longer wavelengths significantly increased as the pH of the solutions was raised. Moreover, the comparable pH dependence of the two solutions suggest that the observed pH dependence may be attributed to the acid-base chemistry of the reactions, which may involve <sup>3</sup>VL\* or the excimer of VL (Smith et al., 2016), as discussed earlier. When a phenolic molecule deprotonates at higher pH, an ortho or para electron withdrawing group, such as a nitro or aldehyde group, can attract a portion of the negative charge towards its oxygen atoms through induced and conjugated effects, leading to the extension of chromophore from the electron donating group (e.g., O<sup>-</sup>) to the electron withdrawing group via the aromatic ring (Carey, 2000; Williams and Fleming, 2008; Pang et al., 2019a). Hence, the delocalization of the negative charge in phenolates leads to significant redshifts (Mohr et al., 2013).~~

For reference, changes in the revised text that are relevant to lines 375–386 are shown below:

Lines 331–352: The decay rate constants for both VL\* and VL+AN increased as pH decreased (VL\* and VL+AN at pH 2.5: 1.65 and 1.43 times faster than at pH 4, respectively) (Fig. S3b). These differences in decay rate constants are small but statistically significant ( $p < 0.05$ ). The  $pK_a$  for the VL triplet has been reported to be 4.0 (Smith et al., 2016). As there are a greater fraction of VL triplets that are protonated at pH 2.5 (0.96) than at pH 4 (0.5), it is possible that the pH dependence of the decay rate constants observed in this study is due to  $^3\text{VL}^*$  being more reactive in its protonated form. Smith et al. (2016) also observed a pH dependence for the direct photodegradation of VL (0.005 mM) (rate constants at  $\text{pH} \leq 3$  are ~two times lower than at  $\text{pH} \geq 5$ ) which they attributed to the sensitivity of the excimer of VL (i.e., the charge-transfer complex formed between an excited state VL molecule and a separate ground state VL molecule; Birks, 1973, Turro et al., 2010) to acid-base chemistry. The opposite trend observed in this study for 0.1 mM VL may be due to the reactivities of the protonated and neutral forms of the  $^3\text{VL}^*$  being dependent on the VL concentration (Smith et al., 2016). For VL\*, this pH trend indicates that  $^3\text{VL}^*$  are more reactive in their protonated form, which is opposite to that reported for 0.005 mM VL (Smith et al., 2016), likely due to the concentration dependence of the relative reactivities of protonated and neutral forms of  $^3\text{VL}^*$ . It has been reported that the quantum yield for direct VL photodegradation is higher at pH 5 than at pH 2 for 0.005 mM VL, but they are not statistically different for 0.03 mM VL (Smith et al., 2016). Also, increases in hydrogen ion concentration can enhance the formation of  $\text{HO}_2^*$  and  $\text{H}_2\text{O}_2$  and in turn,  $^*\text{OH}$  formation (Du et al., 2011). In addition to these pH influences on VL\*, the dependence of N(III) ( $\text{NO}_2^- \rightleftharpoons \text{HONO}$ ) speciation on solution acidity (Pang et al., 2019a) also contributed to the observed pH effects for VL+AN. At pH 3.3, half of N(III) exists as HONO (Fischer and Warneck, 1996; Pang et al., 2019a), which has a higher quantum yield for  $^*\text{OH}$  formation than that of  $\text{NO}_2^-$  in the near UV region (Arakaki et al., 1999; Kim et al., 2014). The increased  $^*\text{OH}$  formation rates as pH decreases can lead to faster VL decay (Pang et al., 2019a). Also,  $\text{NO}_2^-/\text{HONO}$  can generate  $^*\text{NO}_2$  via oxidation by  $^*\text{OH}$  (Reactions 4 and 15; Table 1) (Pang et al., 2019a). As pH decreases, the higher reactivity of  $^3\text{VL}^*$  and sensitivity of the excimer of VL to acid-base chemistry HONO being the dominant N(III) species can lead to faster VL photo-oxidation may have led to faster VL photo-oxidation.

(4) Adding the experiments of guaiacol (GUA) is a little bit confusing, as the title is the photo-oxidation of VL. I understand it is a good addition to the manuscript, and these experiments nicely compared the photo-oxidation of GUA via the two pathways. However, the conclusion (line 25-26) “guaiacol oxidation by photosensitized reactions of VL was observed to be more efficient relative to nitrate-mediated photo-oxidation” is still problematic, as the concentration of VL in GUA + VL experiment was still 10 times higher than the observed value in the cloud and fog but the concentration of AN in GUA + AN experiments was similar to the observed concentration.

Response: Thank you for this suggestion. The apparent quantum efficiency of GUA photodegradation ( $\Phi_{\text{GUA}}$ ) in the presence of either VL or nitrate during simulated sunlight illumination can be defined as (Anastasio et al., 1996; Smith et al., 2014, 2016):

$$\Phi_{\text{GUA}} = \frac{\text{mol GUA destroyed}}{\text{mol photons absorbed}} \quad (\text{Eq. S9})$$

$\Phi_{\text{GUA}}$  was calculated using the measured rate of GUA decay and rate of light absorption by either VL or nitrate through the following equation:

$$\Phi_{\text{GUA}} = \frac{\text{rate of GUA decay}}{\text{rate of light absorption by VL or nitrate}} = \frac{k'_{\text{GUA}} \times [\text{GUA}]}{\sum[(1 - 10^{-\epsilon_{\lambda}[\text{C}]l}) \times I'_{\lambda}]} \quad (\text{Eq. S10})$$

where  $k'_{\text{GUA}}$  is the pseudo-first-order rate constant for GUA decay,  $[\text{GUA}]$  is the concentration of GUA (M),  $\epsilon_{\lambda}$  is the base-10 molar absorptivity ( $\text{M}^{-1} \text{cm}^{-1}$ ) of VL or nitrate at wavelength  $\lambda$ ,  $[\text{C}]$  is the concentration of VL or nitrate (M),  $l$  is the pathlength of the illumination cell (cm), and  $I'_{\lambda}$  is the volume-averaged photon flux ( $\text{mol-photons L}^{-1} \text{s}^{-1} \text{nm}^{-1}$ ) determined from 2NB actinometry:

$$j(2\text{NB}) = 2.303 \times \Phi_{2\text{NB}} \times l \times \sum_{300 \text{ nm}}^{350 \text{ nm}} (\epsilon_{2\text{NB},\lambda} \times I'_{\lambda} \times \Delta\lambda) \quad (\text{Eq. S11})$$

The  $\phi_{\text{GUA}}$  in the presence of nitrate ( $1.3 \times 10^{-2} \pm 2.9 \times 10^{-3}$ ) is ~14 times larger than that in the presence of VL ( $9.0 \times 10^{-4} \pm 4.0 \times 10^{-4}$ ), suggesting that nitrate-mediated photo-oxidation of GUA is more efficient than that by photosensitized reactions of VL. We have revised this in the text as follows and added the information shown above in the supporting information: **Text S7. Estimation of the apparent quantum efficiency of guaiacol photodegradation.**

Line 29: Furthermore, comparisons of the apparent quantum efficiency of guaiacol photodegradation indicate that in this study, guaiacol oxidation by photosensitized reactions of VL ~~was observed to be more~~ is less efficient relative to nitrate-mediated photo-oxidation.

Other relevant revisions in the text are as follows:

Line 514: As mentioned earlier, ~~the~~  $^3\text{VL}^*$  chemistry appears to be more important than that of nitrate photolysis even at 1:10 molar ratio of VL/nitrate on account of the much higher molar absorptivity of VL compared to that of nitrate (Fig. S1) and the high VL concentration (0.1 mM) used in this study. However, the apparent quantum efficiency of GUA photodegradation ( $\phi_{\text{GUA}}$ ) in the presence of nitrate ( $1.3 \times 10^{-2} \pm 2.9 \times 10^{-3}$ ) is ~14 times larger than that in the presence of VL ( $9.0 \times 10^{-4} \pm 4.0 \times 10^{-4}$ ), suggesting that nitrate-mediated photo-oxidation of GUA is more efficient than that by photosensitized reactions of VL (see Text S7 for the more details).

Line 619: The oxidation of guaiacol, a non-carbonyl phenol, by photosensitized reactions of vanillin was also shown to be ~~more~~ less efficient than that by nitrate photolysis products based on its lower apparent quantum efficiency.

## Minor comments

1. Line 27-28 In the abstract, the sentence “which nitrate photolysis products can further enhance” sounds not clear to me.

Response: We apologize for the confusion. This sentence was supposed to convey two things: a) the direct photosensitized oxidation of VL may be an important aqSOA source and b) the addition of nitrate photolysis products to (a) can initiate further reactions that can enhance aqSOA formation. We have revised this sentence as follows:

Line 32: This study indicates that the direct photosensitized oxidation of VL, **and nitrate-mediated photo-oxidation of VL** ~~which nitrate photolysis products can further enhance~~, may be an important aqSOA sources in areas influenced by biomass burning emissions.

2. Line 121 Did you average these replicates for mass spectra and/or decay rates? Please clarify it.

Response: Yes, the reported mass spectra are based on the average of results from duplicate experiments, while the decay rate constants and absorbance enhancement are average of results from triplicate experiments. We have added the following sentence in the methods to clarify this:

Line 132: Each experiment was repeated independently at least three times and measurements were done in triplicate. **The reported decay rate constants and absorbance enhancement are the average of results from triplicate experiments, and the corresponding errors represent one standard deviation.**

The footnote of Table S2, now 2, has been revised as follows:

Table 2: <sup>b</sup>The data fitting was performed in the initial linear region. **Each value is the average of results from triplicate experiments. Errors represent one standard deviation.**

3. Line 168-169 It would be nice to explain it together with the chemical composition shown in Figure 1.

Response: This paragraph discusses the VL decay trends. Line 249 (formerly 196) already includes an example for this ( $C_{16}H_{10}N_2O_9$ ; No. 3, Table S2). Changes in the text are as follows:

Lines 220: ~~Similar to VL\*, the~~ **The decay rate constant** for VL+AN under air-saturated conditions was **also higher faster** (6.6 times) than  $N_2$ -saturated conditions, which **may can** be due to ~~several reactions facilitated by nitrate photolysis products and the enhancement of N(III)-mediated photo-oxidation that may have been enhanced~~ in the presence of  $O_2$  ~~as reported in early works~~ (Vione et al., 2005; Kim et al., 2014; Pang et al., 2019a).

Lines 247–254: ~~Compared to N<sub>2</sub>-saturated conditions, the normalized abundance of products such as oligomers, and functionalized monomers (e.g., demethylated VL; Fig. S4), and nitrogen-containing compounds (e.g., C<sub>16</sub>H<sub>10</sub>N<sub>2</sub>O<sub>9</sub>; No. 33, Table S3, Table S2) (for VL+AN) had higher normalized abundance were also more relatively abundant under air-saturated conditions were significantly higher under air-saturated conditions (Figs. 1c-d), likely due to efficient the secondary oxidants from <sup>3</sup>VL\*-initiated oxidation and enhanced VL nitration in the presence of and O<sub>2</sub> and their interactions with nitrate photolysis products. The nitrogen-containing compounds (e.g., C<sub>16</sub>H<sub>10</sub>N<sub>2</sub>O<sub>9</sub>; No. 3, Table S3) were also more relatively abundant under air-saturated conditions.~~ For both VL\* and VL+AN under air-saturated conditions, the most abundant product was C<sub>10</sub>H<sub>10</sub>O<sub>5</sub> (No. 4, Table S2), a substituted VL.

4. Line 181 “VL\*” should be “<sup>3</sup>VL\*”?

Response: Thank you for catching this error. This has been corrected as follows:

Line 235: Nevertheless, the comparable decay rates constants for VL\* and VL+AN imply that <sup>3</sup>VL\* chemistry

5. Line 187 In both VL\* and VL + AN under N<sub>2</sub>-saturated conditions (Fig. 1(a) and (b)), trimer signals are very high. Any explanations?

Response: N<sub>2</sub>-saturated experiments would inhibit the formation of secondary oxidants, which can lead to <sup>3</sup>VL\*-driven reactions (Chen et al., 2020) (line 107). Compared to •OH-mediated oxidation which yields more functionalized/oxygenated products, triplet-driven oxidation has been suggested to produce higher molecular weight products, probably with less fragmentation (Yu et al., 2014; Chen et al., 2020), as mentioned in lines 241–243. This likely explains the prevalence of dimers and trimers for the N<sub>2</sub>-saturated experiments.

6. Line 212 Could you give some numbers to show “majority”?

Response: It is 58% of the 50 most abundant products for experiments A5 to A8. This has been added to the text as follows:

Lines 277–279: ~~F~~for experiments A5 to A8, ~~The~~H:C ratios were mostly around 1.0 and double bond equivalent (DBE) values were typically (58% of the 50 most abundant products) > 7, indicating that the products ~~for experiments A5 to A8 (Table S2)~~ were mainly oxidized aromatic species-compounds (Xie et al., 2020).

7. Line 255 Should it be pH 4?

Response: Thank you for catching this error. The text has now been corrected as follows:

Line 331: the range of 2.5 to 4.5



## References

Anastasio, C., Faust, B. C., and Rao, C. J.: Aromatic carbonyl compounds as aqueous-phase photochemical sources of hydrogen peroxide in acidic sulfate aerosols, fogs, and clouds. 1. Non-phenolic methoxybenzaldehydes and methoxyacetophenones with reductants (phenols), *Environ. Sci. Technol.*, 31, 218–232, <https://doi.org/10.1021/es960359g>, 1996.

Birks, J.B.: *Organic Molecular Photophysics*, John Wiley & Sons, 1973.

Canonica, S., Jans, U., Stemmler, K., and Hoigne, J.: Transformation kinetics of phenols in water: Photosensitization by dissolved natural organic material and aromatic ketones, *Environ. Sci. Technol.*, 29, 1822–1831, <https://doi.org/10.1021/es00007a020>, 1995.

Herrmann, H., Hoffmann, D., Schaefer, T., Brüer, P., and Tilgner, A.: Tropospheric aqueous-phase free-radical chemistry: Radical sources, spectra, reaction kinetics and prediction tools, *Chem. Phys. Chem.*, 11, 3796–3822, <https://doi.org/10.1002/cphc.201000533>, 2010.

Kim, D.-h., Lee, J., Ryu, J., Kim, K., and Choi, W.: Arsenite oxidation initiated by the UV photolysis of nitrite and nitrate, *Environ. Sci. Technol.*, 48, 4030–4037, <https://doi.org/10.1021/es500001q>, 2014.

Lathioor, E. C., Leigh, W. J., and St. Pierre, M. J.: Geometrical effects on intramolecular quenching of aromatic ketone ( $\pi,\pi^*$ ) triplets by remote phenolic hydrogen abstraction, *J. Am. Chem. Soc.*, 121, 11984–11992, <https://pubs.acs.org/doi/abs/10.1021/ja991207z>, 1999.

Li, Y. J., Huang, D. D., Cheung, H. Y., Lee, A. K. Y., and Chan, C. K.: Aqueous-phase photochemical oxidation and direct photolysis of vanillin - a model compound of methoxy phenols from biomass burning, *Atmos. Chem. Phys.*, 14, 2871–2885, <https://doi.org/10.5194/acp-14-2871-2014>, 2014.

McNally, A. M., Moody, E. C., and McNeill, K.: Kinetics and mechanism of the sensitized photodegradation of lignin model compounds, *Photochem. Photobiol. Sci.*, 4, 268–274, <https://doi.org/10.1039/B416956E>, 2005.

Minella, M., Romeo, F., Vione, D., Maurino, V., and Minero, C.: Low to negligible photoactivity of lake-water matter in the size range from 0.1 to 5  $\mu\text{m}$ , *Chemosphere*, 83, 1480–1485, <https://doi.org/10.1016/j.chemosphere.2011.02.093>, 2011.

Neumann, M. G., De Groote, R. A. M. C., and Machado, A. E. H.: Flash photolysis of lignin: Part 1. Deaerated solutions of dioxane-lignin, *Polym. Photochem.*, 7, 401–407, [https://doi.org/10.1016/0144-2880\(86\)90007-2](https://doi.org/10.1016/0144-2880(86)90007-2), 1986a.

Neumann, M. G., De Groote, R. A. M. C., and Machado, A. E. H.: Flash photolysis of lignin: II. Oxidative photodegradation of dioxane-lignin, *Polym. Photochem.*, 7, 461–468, [https://doi.org/10.1016/0144-2880\(86\)90015-1](https://doi.org/10.1016/0144-2880(86)90015-1), 1986b.

Pang, H., Zhang, Q., Lu, X. H., Li, K. , Chen, H., Chen, J. , Yang, X., Ma, Y., Ma, J., and Huang, C.: Nitrite-mediated photooxidation of vanillin in the atmospheric aqueous phase, *Environ. Sci. Technol.*, 53, 14253–14263, <https://doi.org/10.1021/acs.est.9b03649>, 2019a.

Pye, H., Nenes, A., Alexander, B., Ault, A. P., Barth, M. C., Clegg, S. L., Collett, J. L. Jr., Fahey, K. M., Hennigan, C. J., Herrmann, H., Kanakidou, M., Kelly, J. T., Ku, I. T., McNeill, V. F., Riemer, N., Schaefer, T., Shi, G., Tilgner, A., Walker, J. T., Wang, T., Weber, R., Xing, J., Zaveri, R. A., and Zuend, A.: The acidity of atmospheric particles and clouds, *Atmos. Chem. Phys.*, 20, 4809–4888, <https://doi.org/10.5194/acp-20-4809-2020>, 2020.

Smith, J. D., Sio, V., Yu, L., Zhang, Q., and Anastasio, C.: Secondary organic aerosol production from aqueous reactions of 973 atmospheric phenols with an organic triplet excited state, *Environ. Sci. Technol.*, 48, 1049–1057, <https://doi.org/10.1021/es4045715>, 2014.

Smith, J. D., Kinney, H., and Anastasio, C.: Phenolic carbonyls undergo rapid aqueous photodegradation to form low-volatility, light-absorbing products, *Atmos. Environ.*, 126, 36–44, <https://doi.org/10.1016/j.atmosenv.2015.11.035>, 2016.

Tratnyek, P. G. and Hoigne, J.: Oxidation of substituted phenols in the environment: a QSAR analysis of rate constants for reaction with singlet oxygen, *Environ. Sci. Technol.*, 25, 1596–1604, <https://doi.org/10.1021/es00021a011>, 1991.

Turro, N., Ramamurthy, V., and Scaiano, J.C.: *Modern Molecular Photochemistry*, University Science Book, 2010.

Vione, D., Maurino, V., Minero, C., and Pelizzetti, E.: Reactions induced in natural waters by irradiation of nitrate and nitrite ions, in: *The Handbook of Environmental Chemistry Vol. 2M - Environmental Photochemistry Part II*, Springer, Berlin, Heidelberg, Germany, 221–253, <https://doi.org/10.1007/b138185>, 2005.

Xie, Q., Su, S., Chen, S., Xu, Y., Cao, D., Chen, J., Ren, L., Yue, S., Zhao, W., Sun, Y., Wang, Z., Tong, H., Su, H., Cheng, Y., Kawamura, K., Jiang, G., Liu, C-Q., and Fu, P.: Molecular characterization of firework-related urban aerosols using Fourier transform ion cyclotron resonance mass spectrometry, *Atmos. Chem. Phys.*, 20, 6803–6820, [10.5194/acp-20-6803-2020](https://doi.org/10.5194/acp-20-6803-2020), <https://doi.org/10.5194/acp-20-6803-2020>, 2020.

# 1 Aqueous SOA formation from the photo-oxidation of vanillin: Direct 2 photosensitized reactions and nitrate-mediated reactions

3 Beatrix Rosette Go Mabato<sup>1</sup>, Yan Lyu<sup>1</sup>, Yan Ji<sup>1</sup>, Yong Jie Li<sup>2</sup>, Dan Dan Huang<sup>32</sup>, Xue Li<sup>43</sup>, Theodora  
4 Nah<sup>1</sup>, Chun Ho Lam<sup>1</sup>, and Chak K. Chan<sup>1\*</sup>

5 <sup>1</sup>School of Energy and Environment, City University of Hong Kong, Hong Kong, China

6 <sup>2</sup>Department of Civil and Environmental Engineering, and Centre for Regional Ocean, Faculty of Science and Technology,  
7 University of Macau, Macau, China

8

9 <sup>32</sup>Shanghai Academy of Environmental Sciences, Shanghai 200233, China

10

11 <sup>43</sup>Institute of Mass Spectrometry and Atmospheric Environment, Jinan University No. 601 Huangpu Avenue West, Guangzhou  
12 510632, China

13

14 *Correspondence to:* Chak K. Chan (Chak.K.Chan@cityu.edu.hk)

15 **Abstract.** Vanillin (VL), a phenolic aromatic carbonyl abundant in biomass burning emissions, forms triplet excited states  
16 (<sup>3</sup>VL\*) under simulated sunlight leading to aqueous secondary organic aerosol (aqSOA) formation. This direct photosensitized  
17 oxidation of VL was compared with nitrate-mediated VL photo-oxidation under atmospherically relevant cloud and fog  
18 conditions, through examining the VL decay kinetics, product compositions, and light absorbance changes. The majority of  
19 the most abundant products from both VL photo-oxidation pathways were potential Brown carbon (BrC) chromophores. In  
20 addition, both pathways generated oligomers, functionalized monomers, and oxygenated ring-opening products, but nitrate  
21 promoted functionalization and nitration, which can be ascribed to its photolysis products (<sup>•</sup>OH, <sup>•</sup>NO<sub>2</sub>, and N(III), NO<sub>2</sub><sup>-</sup> or  
22 HONO). Moreover, a potential imidazole derivative observed from nitrate-mediated VL photo-oxidation suggested that  
23 ammonium may be involved in the reactions. The effects of ~~oxygen (<sup>•</sup>O<sub>2</sub>) secondary oxidants from <sup>3</sup>VL\*~~, pH, ~~the presence of~~  
24 ~~volatile organic compounds (VOCs) and inorganic anions~~, and reactants concentration and molar ratios on VL photo-oxidation  
25 were also explored. Our findings show that ~~the secondary oxidants (<sup>•</sup>O<sub>2</sub>, O<sub>2</sub><sup>-•</sup>, <sup>•</sup>HO<sub>2</sub>, <sup>•</sup>OH) from the reactions of <sup>3</sup>VL\* and O<sub>2</sub>~~  
26 ~~plays~~ an essential role in VL photo-oxidation, ~~and~~ ~~Enhanced~~ oligomer formation was ~~enhanced~~ ~~noted~~ at pH < 4 ~~and in the~~  
27 ~~presence of VOCs and inorganic anions, probably due to additional generation of radicals (<sup>•</sup>HO<sub>2</sub> and CO<sub>3</sub><sup>•+</sup>)~~. Also,  
28 functionalization was dominant at low VL concentration, whereas oligomerization was favored at high VL concentration.  
29 Furthermore, ~~comparisons of the apparent quantum efficiency of guaiacol photodegradation indicate that in this study,~~ guaiacol  
30 oxidation by photosensitized reactions of VL ~~was observed to be more is less~~ efficient relative to nitrate-mediated photo-  
31 oxidation. Lastly, potential ~~aqSOA formation VL photo-oxidation~~ pathways ~~via VL photo-oxidation under different reaction~~  
32 ~~conditions~~ were proposed. This study indicates that the direct photosensitized oxidation of VL ~~and nitrate-mediated VL photo-~~

33 ~~oxidation, which nitrate photolysis products can further enhance,~~ may be an important aqSOA sources in areas influenced by  
34 biomass burning emissions.

35

36

## 37 **1 Introduction**

38 Aqueous reactions can be an important source of secondary organic aerosols (SOA) (Blando and Turpin, 2000; Volkamer et  
39 al., 2009; Lim et al., 2010; Ervens et al., 2011; Huang et al., 2011; Lee et al., 2011; Smith et al., 2014) such as highly-  
40 oxygenated and low-volatility organics (Hoffmann et al., 2018; Liu et al., 2019) which may affect aerosol optical properties  
41 due to contributions to Brown Carbon (BrC) (Gilardoni et al., 2016). BrC refers to organic aerosols that absorb radiation  
42 efficiently in the near-ultraviolet (UV) and visible regions (Laskin et al., 2015). The formation of aqueous SOA (aqSOA) via  
43 photochemical reactions involves oxidation, with hydroxyl radical ( $\cdot\text{OH}$ ) usually considered as the primary oxidant (Herrmann  
44 et al., 2010; Smith et al., 2014). The significance of photosensitized chemistry in atmospheric aerosols has recently been  
45 reviewed (George et al., 2015). For instance, triplet excited states of organic compounds ( $^3\text{C}^*$ ) from the irradiation of light-  
46 absorbing organics such as non-phenolic aromatic carbonyls (Canonica et al., 1995; Anastasio et al., 1996; Vione et al., 2006;  
47 Smith et al., 2014) have been reported to oxidize phenols at faster rates and with higher aqSOA yields compared to  $\cdot\text{OH}$  (Sun  
48 et al., 2010; Smith et al., 2014; Yu et al., 2014; Smith et al., 2016). Aside from being an oxidant,  $^3\text{C}^*$  can also be a precursor  
49 of singlet oxygen ( $^1\text{O}_2$ ), superoxide ( $\text{O}_2^{\cdot-}$ ) or hydroperoxyl ( $\cdot\text{HO}_2$ ) radical, and  $\cdot\text{OH}$  (via  $\text{HO}_2^{\cdot}/\text{O}_2^{\cdot-}$  formation) upon reactions  
50 with  $\text{O}_2$  and substrates (e.g., phenols), ~~respectively~~ (TinelGeorge et al., 2018). The  $^3\text{C}^*$  concentration in typical fog water has  
51 been estimated to be  $>_{25}$  times than that of  $\cdot\text{OH}$ , making  $^3\text{C}^*$  the primary photo-oxidant for biomass burning phenolic  
52 compounds (Kaur and Anastasio, 2018; Kaur et al., 2019). Recent works on triplet-driven oxidation of phenols have mainly  
53 focused on changes of physicochemical properties (e.g., light absorption) and aqSOA yield (e.g., Smith et al., 2014, 2015,  
54 2016), with few reports on reaction mechanisms and characterization of reaction products (e.g., Yu et al., 2014; Chen et al.,  
55 2020; Jiang et al., 2021).

56 Inorganic nitrate is a major component of aerosols and cloud/fog water. In cloud and fog water, the concentrations of  
57 inorganic nitrate can vary from  $50\ \mu\text{M}$  to  $>_{1000}\ \mu\text{M}$ , with higher levels typically noted under polluted conditions (Munger et  
58 al., 1983; Collett et al., 1998; Zhang and Anastasio, 2003; Li et al., 2011; Giulianelli et al., 2014; Bianco et al., 2020). Upon  
59 photolysis (Vione et al., 2006; Herrmann, 2007; Scharko et al., 2014), inorganic nitrate in cloud and fog water can contribute  
60 to BrC (Minero et al., 2007) and aqSOA formation (Huang et al., 2018; Klodt et al., 2019; Zhang et al., 2021) by generating  
61  $\cdot\text{OH}$  and nitrating agents (e.g.,  $\cdot\text{NO}_2$ ). For example, the aqSOA yields from the photo-oxidation of phenolic carbonyls in nitrate  
62 are twice as high as that in sulfate solution (Huang et al., 2018). Nitration is a significant process in the formation of light-  
63 absorbing organics or BrC in the atmosphere (Jacobson, 1999; Kahnt et al., 2013; Mohr et al., 2013; Laskin et al., 2015; Teich  
64 et al., 2017; Li et al., 2020). Furthermore, nitrate photolysis has been proposed to be a potentially important process for  $\text{SO}_2$

65 oxidation via the generation of  $\cdot\text{OH}$ ,  $\text{NO}_2$ , and  $\text{N(III)}$  within particles (Gen et al., 2019a, 2019b), and it can also potentially  
66 change the morphology of atmospheric viscous particles (Liang et al., 2021). Accordingly, both  $^3\text{C}^*$  and inorganic nitrate can  
67 contribute to aqSOA and BrC formation.

68 ~~————~~ Biomass burning (BB) is a significant atmospheric source of both phenolic and non-phenolic aromatic carbonyls  
69 (Rogge et al., 1998; Nolte et al., 2001; Schauer et al., 2001; Bond et al., 2004). ~~For An~~ example, ~~is~~ vanillin (VL) (Henry's law  
70 constant of  $4.56 \times 10^5 \text{ M atm}^{-1}$ ; Yaws, 1994), a model compound for methoxyphenols which are abundant in BB emissions  
71 (Pang et al., 2019a), ~~which~~ has been shown to yield low-volatility products (Li et al., 2014) via aqueous  $\cdot\text{OH}$  oxidation and  
72 direct photodegradation. ~~—~~ Photodegradation kinetics and aqSOA yields have been reported for direct VL photodegradation  
73 (Smith et al., 2016), with oxygenated aliphatic-like compounds (high H:C,  $\geq 1.5$  and low O:C,  $\leq 0.5$  ratios) reported as the  
74 most likely products (Loisel et al., 2021). Additionally, aqueous-phase reactions of phenols with reactive nitrogen species have  
75 been proposed to be a significant source of nitrophenols and SOA (Grosjean, 1985; Kitanovski et al., 2014; Kroflič et al., 2015;  
76 Pang et al., 2019a; Kroflič et al., 2021; Yang et al., 2021). For instance, nitrite-mediated VL photo-oxidation can generate  
77 nitrophenols, and the reactions are influenced by nitrite/VL molar ratios, pH, and the presence of  $\cdot\text{OH}$  scavengers (Pang et al.,  
78 2019a). As BB aerosols are typically internally mixed with other aerosol components (Zielinski et al., 2020), VL may coexist  
79 with nitrate in BB aerosols. The aqueous-phase photo-oxidation of VL and nitrate may then reveal insights into the atmospheric  
80 processing of BB aerosols.

81 ~~As BB aerosols are typically internally mixed with other aerosol components (Zielinski et al., 2020), VL may coexist~~  
82 ~~with nitrate in BB aerosols. The aqueous phase photo-oxidation of VL and nitrate may then reveal insights into the atmospheric~~  
83 ~~processing of BB aerosols. In addition, pollution from large BB events in central Amazonia has been reported to interact with~~  
84 ~~volatile organic compounds (VOCs) and soil dust (Rizzo et al., 2010). Moreover, the production, growth, and chemical~~  
85 ~~complexity of SOA can be influenced by the uptake and aerosol phase reactions of VOCs (Pöschl, 2005; De Gouw and~~  
86 ~~Jimenez, 2009; Ziemann and Atkinson, 2012). Accordingly, studies incorporating other atmospherically relevant species (e.g.,~~  
87 ~~VOCs and inorganic anions) in photo-oxidation experiments are warranted.~~

88 To evaluate the potential significance of VL and its reactions with nitrate in aqSOA formation in cloud/fog water, we  
89 studied the direct photosensitized oxidation of VL and nitrate-mediated VL photo-oxidation under atmospherically relevant  
90 conditions. In this work, reactions were characterized based on VL decay kinetics, light absorbance changes, and products.  
91 The influences of  ~~$\text{O}_2$  secondary oxidants from VL triplets~~, solution pH, ~~the presence of VOCs and inorganic anions~~, and  
92 reactants concentration and molar ratios on these two photo-oxidation pathways were also assessed. The  $^3\text{C}^*$  of non-phenolic  
93 aromatic carbonyls (e.g., 3-4-dimethoxybenzaldehyde, DMB; a non-phenolic aromatic carbonyl) (Smith et al., 2014; Yu et al.,  
94 2014; Jiang et al., 2021) and phenolic aromatic carbonyls (e.g., acetosyringone, vanillin) (Smith et al., 2016) have been shown  
95 to oxidize phenols, but the reaction products from the latter are unknown. We then examined the photo-oxidation of guaiacol,  
96 another non-carbonyl phenol, in the presence of VL and compared it with nitrate-mediated photo-oxidation. Finally, we  
97 proposed aqSOA formation pathways via VL photo-oxidation pathways of VL under different reaction conditions. This work  
98 presents a comprehensive comparison of VL photo-oxidation by VL photosensitization and in the presence of inorganic nitrate.

## 100 2 Methods

### 101 2.1 Aqueous phase photo-oxidation experiments

102 Photo-oxidation experiments were performed in a ~~500 mL~~ custom-built quartz photoreactor. ~~The solutions (initial volume of~~  
103 ~~500 mL) were continuously mixed throughout the experiments using~~ ~~equipped with~~ a magnetic stirrer. The solutions were  
104 bubbled with synthetic air or nitrogen (N<sub>2</sub>) (>99.995%) (~~0.5 dm<sup>3</sup>/min~~) for 30 min before irradiation to achieve air- and N<sub>2</sub>-  
105 saturated conditions, respectively, and the bubbling was continued throughout the reactions (Du et al., 2011; Chen et al., 2020).  
106 The aim of the air-saturated experiments was to enable the generation of secondary oxidants (<sup>1</sup>O<sub>2</sub>, O<sub>2</sub><sup>•-</sup>/<sup>•</sup>HO<sub>2</sub>, <sup>•</sup>OH) from <sup>3</sup>VL\*  
107 as O<sub>2</sub> is present. Conversely, the N<sub>2</sub>-saturated experiments would inhibit the formation of these secondary oxidants, which can  
108 leading to <sup>3</sup>VL\*-driven reactions (Chen et al., 2020). Solutions were irradiated through the quartz window of the reactor using  
109 a xenon lamp (model 6258, Ozone free xenon lamp, 300 W, Newport) equipped with a longpass filter (20CGA-305 nm cut-  
110 on filter, Newport) to eliminate light below 300 nm. Cooling fans positioned around the photoreactor and lamp housing  
111 maintained reaction temperatures at 27 ± 2 °C. The averaged initial photon flux in the reactor from 300 to 380 nm measured  
112 using a chemical actinometer (2-nitrobenzaldehyde) was 2.6 × 10<sup>15</sup> photons cm<sup>-2</sup> s<sup>-1</sup> nm<sup>-1</sup> (Fig. S1). Although the concentration  
113 of VL in cloud/fog water has been estimated to be < 0.01 mM (Anastasio et al., 1996), a higher VL concentration (0.1 mM)  
114 was used in this study to guarantee sufficient signals for product identification (Vione et al., 2019). The chosen ammonium  
115 nitrate (AN) concentration (1 mM) was based on values observed in cloud and fog water (Munger et al., 1983; Collett et al.,  
116 1998; Zhang and Anastasio, 2003; Li et al., 2011; Giulianelli et al., 2014; Bianco et al., 2020). It should be noted that this study  
117 is not intended to identify the concentrations of nitrate that would affect the kinetics. ~~We also examined the role of VOCs (2-~~  
118 ~~propanol, IPA) (1 mM) and inorganic anions (sodium bicarbonate, NaBC) (1 mM) in these reactions. IPA can be classified as~~  
119 ~~both a biogenic (from grass, Olofsson et al., 2003) and anthropogenic VOC (e.g., from solvents and industrial processes,~~  
120 ~~Hippelein, 2004; Lewis et al., 2020), while bicarbonate is an inorganic anion observed in fog water from both urban and rural~~  
121 ~~locations (Collett et al., 1999; Straub et al., 2012; Straub, 2017). IPA and NaBC are particularly interesting also because they~~  
122 ~~can produce other radicals (e.g., <sup>•</sup>HO<sub>2</sub> and carbonate radical, CO<sub>3</sub><sup>•-</sup>) that may react with nitrate photolysis products (Vione et~~  
123 ~~al., 2009; Wang et al., 2021) and they can act as <sup>•</sup>OH scavengers (Warneck and Wurzinger, 1988; Vione et al., 2009; Gen et~~  
124 ~~al., 2019b; Pang et al., 2019a), although it must be noted that these compounds were not added in excess for our experiments.~~  
125 Moreover, comparisons were made between the photo-oxidation of guaiacol (0.1 mM), a non-carbonyl phenol, in the presence  
126 of VL (0.1 mM) or AN (1 mM). Samples (10 mL) were collected hourly for a total of 6 h for offline optical and chemical  
127 analyses. Absorbance measurements, VL (and GUA) decay kinetics (calibration curves for VL and GUA standard solutions;  
128 Fig. S2), small organic acids measurements, and product characterization were conducted using UV-Vis spectrophotometry,  
129 ultra-high-performance liquid chromatography with photodiode array detector (UHPLC-PDA), ion chromatography (IC), and  
130 UHPLC coupled with quadrupole time-of-flight mass spectrometry (UHPLC-qToF-MS) equipped with an electrospray

131 ionization (ESI) source and operated in the positive ion mode (the negative ion mode signals were too low for our analyses),  
132 respectively. Each experiment was repeated independently at least three times and measurements were done in triplicate. The  
133 reported decay rate constants and absorbance enhancement are the average of results from triplicate experiments, and the  
134 corresponding errors represent one standard deviation. The mass spectra are based on the average of results from duplicate  
135 experiments. Details on the materials and analytical procedures are provided in the Supporting Information (Text S1 to S6)The  
136 Supporting Information (Text S1 to S7) provides details on the materials and analytical procedures. The pseudo-first-order  
137 rate constant ( $k'$ ) for VL decay was determined using the following equation (Huang et al., 2018):

$$138 \ln ([VL]_t/[VL]_0) = -k't \quad (\text{Eq. 1})$$

141 where  $[VL]_t$  and  $[VL]_0$  are the concentrations of VL at time  $t$  and 0, respectively. Replacing VL with GUA in Eq. 1 enabled  
142 the calculation of GUA decay rate constant. The decay rate constants were normalized to the photon flux measured for each  
143 experiment through dividing  $k'$  by the measured 2-nitrobenzaldehyde (2NB) decay rate constant,  $j(2NB)$  (see Text S6 for more  
144 details).

## 145 2.2 Calculation of normalized abundance of products

146 Comparisons of peak abundance in mass spectrometry have been used in many recent studies (e.g., Lee et al., 2014;  
147 Romonosky et al., 2017; Wang et al., 2017; Fleming et al., 2018; Song et al., 2018; Klodt et al., 2019; Ning et al., 2019) to  
148 show the relative importance of different types of compounds (Wang et al., 2021). However, ionization efficiency may greatly  
149 vary for different classes of compounds (Kearle, 2000; Schmidt et al., 2006; Leito et al., 2008; Perry et al., 2008; Krueve et  
150 al., 2014); and so uncertainties may arise from comparisons of peak areas among compounds. In this work, we assumed equal  
151 ionization efficiency of different compounds, which is commonly used to estimate O:C ratios of SOA (Bateman et al., 2012;  
152 Lin et al., 2012; De Haan et al., 2019), to calculate their normalized abundance. The normalized abundance of a product, [P]  
153 (unitless), was calculated as follows:

$$154 [P] = \frac{A_{P,t}}{A_{VL,t}} \cdot \frac{[VL]_t}{[VL]_0} \quad (\text{Eq. 2})$$

155 where  $A_{P,t}$  and  $A_{VL,t}$  are the extracted ion chromatogram (EIC) ~~signal~~ peak areas of the product P and VL from UHPLC-qToF-  
156 MS analyses at time  $t$ , respectively;  $[VL]_t$  and  $[VL]_0$  are the VL concentrations ( $\mu\text{M}$ ) determined using UHPLC at time  $t$  and  
157 0, respectively. Here, we relied on the direct quantification more accurate measurements of [VL] using UHPLC (see Fig. S2  
158 for VL calibration curve)for semi-quantification. It should be noted that the ionization efficiency may greatly vary for different  
159 classes of compounds (Kearle, 2000). Hence, we assumed equal ionization efficiency of different compounds to calculate  
160 their normalized abundance, which is commonly used to estimate O:C ratios of SOA (Bateman et al., 2012; Lin et al., 2012;  
161 De Haan et al., 2019). It should be noted that the normalized abundance of products in this study is a semi-quantitative analysis  
162 intended to provide an overview of how the signal intensities changed under different experimental conditions but not to

163 quantify the absolute concentration of products. Moreover, the major products detected in this study are probably those with  
164 high concentration or high ionization efficiency in the positive ESI mode. The use of relative abundance (product peaks are  
165 normalized to the highest peak) (e.g., Lee et al., 2014; Romonosky et al., 2017; Fleming et al., 2018; Klodt et al., 2019) would  
166 yield the same major products reported. Typical fragmentation behavior observed in MS/MS spectra for individual functional  
167 groups from Holčapek et al. (2010) are outlined in Table S1.

168

## 169 **3 Results and Discussion**

### 170 **3.1 Kinetics, mass spectrometric, and absorbance changes analyses during aqueous phase photo-oxidation of vanillin**

171 For clarity purposes, the reactions involving reactive species referred to in the following discussions are provided in Table 1.  
172 Table S2 summarizes the reaction conditions, initial VL (and GUA) decay rates constants, normalized abundance of products,  
173 and average carbon oxidation state ( $\langle OS_c \rangle$ ) (of the 50 most abundant products). In general, the 50 most abundant products  
174 contributed more than half of the total normalized abundance of products. ~~For clarity purposes, the reactions involving reactive~~  
175 ~~species referred to in the following discussions are provided in Table 1.~~

176 As shown in Figure S3, VL underwent oxidation both directly and in the presence of nitrate upon simulated sunlight  
177 illumination. VL absorbs light and is promoted to its excited singlet state ( $^1VL^*$ ), then undergoes intersystem crossing (ISC)  
178 to the excited triplet state,  $^3VL^*$ . In principle,  $^3VL^*$  can oxidize ground-state VL (Type I photosensitized reactions) via H-  
179 atom abstraction/electron transfer and form  $O_2^{\cdot-}$  or  $HO_2^{\cdot}$  in the presence of  $O_2$  (TinelGeorge et al., 2018), or react with  $O_2$  (Type  
180 II photosensitized reactions) to yield  $^1O_2$  via energy transfer or  $O_2^{\cdot-}$  via electron transfer (Lee et al., 1987; Foote et al., 1991).  
181 The disproportionation of  $HO_2^{\cdot}/O_2^{\cdot-}$  (Anastasio et al., 1996) ~~and reaction of  $HO_2^{\cdot}$  with  $O_2^{\cdot-}$  (Du et al., 2011)~~ form hydrogen  
182 peroxide ( $H_2O_2$ ), which is a photolytic source of  $\cdot OH$ . Overall, air-saturated conditions, in which  $O_2$  is present, enable the  
183 generation of secondary oxidants from  $^3VL^*$  ( $^1O_2$ ,  $O_2^{\cdot-}/HO_2^{\cdot}$ ,  $\cdot OH$ ). Moreover,  $\cdot OH$ ,  $\cdot NO_2$ , and  $NO_2^{\cdot}/HNO_2$ , i.e., N(III),  
184 generated via nitrate photolysis (Reactions 1--3; Table 1), can also oxidize or nitrate VL. In this work, the direct  
185 photosensitized oxidation of VL (~~(by  $^3VL^*$  or secondary oxidants from  $^3VL^*$  and  $O_2$  VL only experiments)~~) and nitrate-  
186 mediated VL photo-oxidation are referred to as VL\* and VL+AN, respectively.

#### 187 **3.1.1 Effect of secondary oxidants from VL triplets VL photo-oxidation under $N_2$ and air-saturated conditions**

188 ~~As mentioned earlier, secondary oxidants ( $^1O_2$ ,  $O_2^{\cdot-}/HO_2^{\cdot}$ ,  $\cdot OH$ ) can be generated from  $^3VL^*$  when  $O_2$  is present (e.g., under~~  
189 ~~air-saturated conditions), while  $^3VL^*$  is the only oxidant expected under  $N_2$ -saturated conditions. The photo-oxidation of VL  
190 To examine the contributions of  $^3VL^*$ -derived secondary oxidants and  $^3VL^*$  only on VL photo-oxidation, experiments under  
191 both  $N_2$ -air and air- $N_2$ -saturated conditions (Fig. S3a) were carried out at pH 4, which is representative of moderately acidic  
192 aerosol and cloud pH values (Pye et al., 2020). No significant VL loss was observed for dark experiments. The oxidation of  
193 ground-state VL by  $^3VL^*$  via H-atom abstraction or electron transfer can form phenoxy (which is in resonance with a carbon-~~



194 centered cyclohexadienyl radical that has a longer lifetime) and ketyl radicals (Neumann et al., 1986a, 1986b; Anastasio et al.,  
195 1996). The coupling of phenoxy radicals or phenoxy and cyclohexadienyl radicals can form oligomers as observed for both  
196 N<sub>2</sub>- and air-saturated experiments (see discussions later). However, the little decay of VL under N<sub>2</sub>-saturated condition  
197 indicates that these radicals probably predominantly decayed via back-hydrogen transfer to regenerate VL (Lathioor et al.,  
198 1999). A possible explanation for this is the involvement of O<sub>2</sub> in the secondary steps of VL decay. For instance, a major fate  
199 of the ketyl radical is reaction with O<sub>2</sub> (Anastasio et al., 1996). In the absence of O<sub>2</sub>, radical formation occurs, but the forward  
200 reaction of ketyl radical and O<sub>2</sub> is blocked, leading to the regeneration of VL as suggested by the minimal VL decay. Aside  
201 from potential inhibition of secondary oxidants generation (Chen et al., 2020), N<sub>2</sub> purging may have also hindered the  
202 secondary steps for VL decay.

203 ~~The low decay rate for VL\* under N<sub>2</sub>-saturated conditions suggests a minimal role for <sup>3</sup>VL\* in VL photo-oxidation.~~  
204 Contrastingly, the VL\* decay rate constant under air-saturated conditions was 4 times higher, ~~revealing the importance of~~  
205 ~~<sup>3</sup>VL\* derived secondary oxidants for photosensitized oxidation of VL. As mentioned earlier, secondary oxidants (<sup>1</sup>O<sub>2</sub>, O<sub>2</sub><sup>=</sup>~~  
206 ~~/HO<sub>2</sub>, \*OH) can be generated from <sup>3</sup>VL\* when O<sub>2</sub> is present (e.g., under air-saturated conditions). However, the photo-~~  
207 ~~oxidation of VL in this study is likely mainly governed by <sup>3</sup>VL\* and that these secondary oxidants have only minor~~  
208 ~~participation. Aside from \*OH, O<sub>2</sub><sup>=</sup>/HO<sub>2</sub> and <sup>1</sup>O<sub>2</sub> can also promote VL photo-oxidation (Kaur and Anastasio, 2018; Chen et~~  
209 ~~al., 2020). <sup>1</sup>O<sub>2</sub> is also a potential oxidant for phenols (Herrmann et al., 2010; Minella et al., 2011; Smith et al., 2014), but <sup>1</sup>O<sub>2</sub>~~  
210 ~~reacts much faster (by ~60 times) with phenolate ions compared to neutral phenols (Tratnyek and Hoigne, 1991; Canonica et~~  
211 ~~al., 1995; McNally et al., 2005). Under the pH values (pH 2.5 to 4) considered in this study, the amount of phenolate ion is~~  
212 ~~negligible, so the reaction between VL and <sup>1</sup>O<sub>2</sub> should be slow. Interestingly, however, <sup>1</sup>O<sub>2</sub> has been shown to be important in~~  
213 ~~the photo-oxidation of 4-ethylguaicol (pK<sub>a</sub> = 10.3) by <sup>3</sup>C\* of 3,4-dimethoxybenzaldehyde (solution with pH of ~3) (Chen et~~  
214 ~~al., 2020). Furthermore, while the irradiation of other phenolic compounds can produce H<sub>2</sub>O<sub>2</sub>, a precursor for \*OH (Anastasio~~  
215 ~~et al., 1996), the amount of H<sub>2</sub>O<sub>2</sub> is small. Based on this, only trace amounts of H<sub>2</sub>O<sub>2</sub> were likely generated from VL\* (Li et~~  
216 ~~al., 2014) under-air saturated conditions, suggesting that contribution from \*OH was minor. Overall, these suggest that VL~~  
217 ~~photo-oxidation in this study is driven by <sup>3</sup>VL\*. Further study on the impact of O<sub>2</sub> on the reactive intermediates involved is~~  
218 ~~required to understand the exact mechanisms occurring under air-saturated conditions. Nonetheless, the VL\* decay trends~~  
219 ~~clearly indicate that O<sub>2</sub> is important for efficient VL photo-oxidation an efficient oxidant for unsaturated organic compounds~~  
220 ~~and has a lifetime that is much longer than <sup>3</sup>C\* (Chen et al., 2020). Similar to VL\*, ~~†~~The decay rate constant for VL+AN under  
221 air-saturated conditions was ~~also higher faster~~ (6.6 times) than N<sub>2</sub>-saturated conditions, which ~~may can~~ be due to ~~several~~  
222 reactions facilitated by nitrate photolysis products ~~and the enhancement of N(III) mediated photo-oxidation that may have~~  
223 ~~been enhanced~~ in the presence of O<sub>2</sub> ~~as reported in early works~~ (Vione et al., 2005; Kim et al., 2014; Pang et al., 2019a). ~~As~~  
224 ~~shown later, more nitrogen-containing species were observed under air-saturated conditions. An example is enhanced VL~~  
225 nitration likely from increased \*NO<sub>2</sub> formation such as from the reaction of \*OH and O<sub>2</sub><sup>=</sup> with NO<sub>2</sub><sup>=</sup> (Reactions 4 and 5,  
226 respectively; Table 1) or the autoxidation of \*NO from NO<sub>2</sub><sup>=</sup> photolysis (Reactions 6–9; Table 1) in aqueous solutions (Pang~~

227 et al., 2019a). ~~Reactions involving  $^1\text{HO}_2/\text{O}_2^+$  which may originate from the photolysis of nitrate alone, likely from the~~  
228 ~~production and subsequent photolysis of peroxyxynitrous acid (HOONO) (Reaction 10; Table 1) (Jung et al., 2017; Wang et al.,~~  
229 ~~2021), or the reactions of  $^3\text{VL}^*$  in the presence of  $\text{O}_2$ , may have contributed as well. For instance, Wang et al. (2021) recently~~  
230 ~~demonstrated that nitrate photolysis generates  $^1\text{HO}_2/\text{O}_2^+$  and  $\text{HONO}_{(\text{g})}$  in the presence of dissolved aliphatic organic matter~~  
231 ~~(e.g., nonanoic acid, ethanol), with the enhanced  $\text{HONO}_{(\text{g})}$  production caused by secondary photochemistry between  $^1\text{HO}_2/\text{O}_2^+$~~   
232 ~~( $_{(\text{aq})}$ ) and photoproduced  $\text{NO}_{\text{x}(\text{aq})}$  (Reactions 11 and 12; Table 1), in agreement with Seharko et al. (2014). The significance of this~~  
233 ~~increased  $\text{HONO}$  production is enhanced  $^1\text{OH}$  formation (Reaction 13; Table 1). In addition,  $^1\text{HO}_2$  can react with  $^1\text{NO}$  (Reaction~~  
234 ~~10; Table 1) from  $\text{NO}_2^-$  photolysis (Reaction 6; Table 1) to form HOONO, and eventually  $^1\text{NO}_2$  and  $^1\text{OH}$  (Reaction 14; Table~~  
235 ~~1) (Pang et al., 2019a). Nevertheless, the comparable decay rates constants for  $\text{VL}^*$  and  $\text{VL}+\text{AN}$  imply that  $^3\text{VL}^*$  chemistry~~  
236 still dominates even at 1:10 molar ratio of VL/nitrate, probably due to the much higher molar absorptivity of VL compared to  
237 that of nitrate (Fig. S1) and the high VL concentration (0.1 mM) used in this study. Although we have no quantification of the  
238 oxidants in our reaction systems as it is outside the scope of this study, these observations clearly substantiate that ~~secondary~~  
239 ~~oxidants from  $^3\text{VL}^*$ , which are formed when  $\text{O}_2$  is present, are required for efficient~~ photosensitized oxidation of VL and  
240 nitrate-mediated VL photo-oxidation are more efficient in the presence of  $\text{O}_2$ .

241 The products from  $\text{VL}^*$  under  $\text{N}_2$ -saturated conditions were mainly oligomers (e.g.,  $\text{C}_{16}\text{H}_{14}\text{O}_4$ ) (Fig. 1a), consistent  
242 with triplet-mediated oxidation forming higher molecular weight products, probably with less fragmentation relative to  
243 oxidation by  $^1\text{OH}$  (Yu et al., 2014; Chen et al., 2020). A threefold increase in the normalized abundance of products was noted  
244 upon addition of nitrate ( $\text{VL}+\text{AN}$  under  $\text{N}_2$ -saturated conditions; Fig. 1b), and in addition to oligomers, functionalized  
245 monomers (e.g.,  $-\text{C}_8\text{H}_6\text{O}_5$ ) and nitrogen-containing compounds (e.g.,  $\text{C}_8\text{H}_6\text{NO}_3$ ; No. 2, Table S23) were also observed, in  
246 agreement with  $^1\text{OH}$ -initiated oxidation yielding more functionalized/oxygenated products compared to triplet-mediated  
247 oxidation (Yu et al., 2014; Chen et al., 2020). ~~Compared to  $\text{N}_2$ -saturated conditions, the normalized abundance of products~~  
248 ~~such as  $\text{O}$  oligomers, and functionalized monomers (e.g., demethylated VL; Fig. S4), and the nitrogen-containing compounds~~  
249 ~~(e.g.,  $\text{C}_{16}\text{H}_{10}\text{N}_2\text{O}_9$ ; No. 33, Table S3, Table S2) (for  $\text{VL}+\text{AN}$ ) had higher normalized abundance were also more relatively~~  
250 ~~abundant under air-saturated conditions, were significantly higher under air saturated conditions~~ (Figs. 1c-d), likely due to  
251 ~~efficient the secondary oxidants from  $^3\text{VL}^*$ -initiated oxidation and enhanced VL nitration in the presence of  $^1\text{O}_2$  and their~~  
252 ~~interactions with nitrate photolysis products. The nitrogen-containing compounds (e.g.,  $\text{C}_{16}\text{H}_{10}\text{N}_2\text{O}_9$ ; No. 3, Table S3) were~~  
253 ~~also more relatively abundant under air saturated conditions.~~ For both  $\text{VL}^*$  and  $\text{VL}+\text{AN}$  under air-saturated conditions, the  
254 most abundant product was  $\text{C}_{10}\text{H}_{10}\text{O}_5$  (No. 4, Table S23), a substituted VL. Irradiation of VL by 254-nm lamp has also been  
255 reported to lead to VL dimerization and functionalization via ring-retaining pathways, as well as small oxygenates but only  
256 when  $^1\text{OH}$  from  $\text{H}_2\text{O}_2$  were involved (Li et al., 2014). In this work, small organic acids (e.g., formic acid) were observed from  
257 both  $\text{VL}^*$  and  $\text{VL}+\text{AN}$  under air-saturated conditions (Fig. S5) due to simulated sunlight that could access the 308-nm VL  
258 band (Smith et al., 2016). Interestingly, we observed a potential imidazole derivative ( $\text{C}_5\text{H}_5\text{N}_3\text{O}_2$ ; Fig. 1d, No. 5, Table S2) from  
259  $\text{VL}+\text{AN}$  under air-saturated conditions (Fig. 1d), which may have formed from reactions induced by ammonium. This  
260 compound was not observed in a parallel experiment in which AN was replaced with sodium nitrate (SN) (Fig. S6a; see Sect.

261 3.3 for discussion). The potential aqSOA formation most probable pathways via of direct photosensitized and nitrate-mediated  
262 photo-oxidation of VL, photo-oxidation in this study are summarized in Fig. 2 were proposed (Fig. 4). In Scheme 1 (pH 4 and  
263 pH <4 under air saturated conditions),  $^3\text{VL}^*$  and  $^{\bullet}\text{OH}$  (from  $^3\text{VL}^*$  or nitrate photolysis) can initiate H atom abstraction to  
264 generate phenoxy or ketyl radicals (Huang et al., 2018; Vione et al., 2019). At pH 4, ring-opening products (Fig. S5) from  
265 fragmentation in both VL\* and VL+AN may have reacted with VL or dissolved ammonia to generate C<sub>10</sub>H<sub>10</sub>O<sub>5</sub> (No. 4, Table  
266 S2) (Pang et al., 2019b) or and a potential imidazole derivative (C<sub>5</sub>H<sub>5</sub>N<sub>3</sub>O<sub>2</sub>; No. 5, Table S2), respectively. Moreover, nitrate  
267 photolysis products promoted functionalization and nitration (e.g., C<sub>16</sub>H<sub>10</sub>N<sub>2</sub>O<sub>9</sub>; No. 3, Table S2). At pH <4, the reactivity of  
268  $^3\text{VL}^*$  increased as suggested by the abundance of oligomers (e.g., C<sub>16</sub>H<sub>14</sub>O<sub>6</sub>) and increased normalized abundance of N-  
269 containing compounds.

270

271 The molecular transformation of VL upon photo-oxidation was examined using the van Krevelen diagrams (Fig. S7).  
272 For all experiments (A1-159; Table S2) in this study, the O:C and H:C ratios of the products were mainly similar to those  
273 observed from the aging of other phenolics (Yu et al., 2014) and BB aerosols (Qi et al., 2019). Under N<sub>2</sub>-saturated conditions,  
274 oligomers with O:C ratios ≤0.6 were dominant in VL\* under N<sub>2</sub>-saturated conditions, while smaller molecules (n<sub>c</sub> ≤ 8) with  
275 higher O:C ratios (up to 0.8) were also observed ~~For VL+AN. For VL+AN under N<sub>2</sub>-saturated conditions, smaller molecules~~  
276 ~~(n<sub>c</sub> ≤ 8) with higher O:C ratios (up to 0.8) were also observed.~~ In contrast, M ~~more~~ products with higher O:C ratios (≥0.6) were  
277 noted under air-saturated conditions for both VL\* and VL+AN. For experiments A5 to A8, The H:C ratios were mostly around  
278 1.0 and double bond equivalent (DBE) values were typically (58% of the 50 most abundant products) ≥ 7, indicating that the  
279 products ~~for experiments A5 to A8 (Table S2)~~ were mainly oxidized aromatic ~~aromatic species~~ compounds (Xie et al., 2020).  
280 Compounds with H:C ≤ 1.0 and O:C ≤ 0.5 are common for aromatic species, while compounds with H:C ≥ 1.5 and O:C ≤ 0.5  
281 are typical for more aliphatic species (Mazzoleni et al., 2012; Kourtchev et al., 2014; Jiang et al., 2021). ~~Moreover, majority~~  
282 ~~of the products for experiments A5 to A8 have double bond equivalent (DBE) values >7, which corresponds to oxidized~~  
283 ~~aromatic compounds (Xie et al., 2020).~~ In contrast, Loisel et al. (2021) reported mainly oxygenated aliphatic-like compounds  
284 ~~(H:C, ≥1.5 and O:C, ≤0.5 ratios)~~ from the direct irradiation of VL (0.1 mM), which may be probably due to their use of ESI in  
285 the negative ion mode, which has higher sensitivity for detecting compounds such as carboxylic acids (Holčapek et al., 2010;  
286 Liigand et al., 2017), and solid-phase extraction (SPE) procedure causing the loss of some oligomers (LeClair et al., 2012;  
287 Zhao et al., 2013; Bianco et al., 2018). Among experiments A5 to A8 ~~(Table S2)~~, VL+AN under air-saturated conditions (A7)  
288 had the highest normalized abundance of products and <OS<sub>c</sub>>, most probably due to the combined influence of the secondary  
289 oxidants from  $^3\text{VL}^*$  and enhanced VL nitration in the presence of O<sub>2</sub>, and nitrate photolysis products. In our calculations, the  
290 increase in <OS<sub>c</sub>> (except for VOCs and inorganic anions experiments; A9 to A12; Table S2) was lower than those in  $^{\bullet}\text{OH}$ -  
291 or triplet mediated oxidation of phenolics (e.g., phenol, guaiacol) measured using an aerosol mass spectrometer (Sun et al.,  
292 2010; Yu et al., 2014). Our measured <OS<sub>c</sub>> for all experiments range from -0.28 to +0.12, while other studies on phenolic  
293 aqSOA formation reported <OS<sub>c</sub>> ranging from -0.14 to +0.47 (Sun et al., 2010) and 0.04 to 0.74 (Yu et al., 2014). This is  
294 likely because we excluded contributions from ring-opening products, which may have higher OS<sub>c</sub> values as these products

295 are not detectable in the positive ion mode. Thus, the  $\langle OS_c \rangle$  in this study likely were lower estimates. In brief, the presence of  
296 secondary oxidants from  $^3VL^*$  and  $O_2$  increased the normalized abundance of products and promoted the formation of more  
297 oxidized aqSOA. These trends were reinforced in the presence of nitrate, indicating synergistic effects between secondary  
298 oxidants from VL triplets and nitrate photolysis products. Compared to  $N_2$ -saturated condition, the higher normalized  
299 abundance of nitrogen-containing products under air-saturated condition for VL+AN (at pH 4) suggests a potential  
300 enhancement of VL nitration in the presence of  $O_2$ .

301 Illumination of phenolic aromatic carbonyls with high molar absorptivities ( $\epsilon_{\lambda, \max}$ ) ( $\sim 8$  to  $22 \times 10^3 \text{ M}^{-1} \text{ cm}^{-1}$ ) leads to  
302 an overall loss of light absorption but increased absorbance at longer wavelengths ( $> 350 \text{ nm}$ ), where the carbonyls did not  
303 initially absorb light (Smith et al., 2016). Fig. 32a illustrates the changes in total absorbance from 350 to 550 nm of  $VL^*$  and  
304 VL+AN under  ~~$N_2$ -air~~ and  ~~$N_2$ -air~~-saturated conditions. The absorption spectra of  $VL^*$  under air- and  $N_2$ - saturated conditions  
305 (pH 4) at different time intervals are shown in Fig. S8. For both  $VL^*$  and VL+AN, evident absorbance enhancement was  
306 observed under air-saturated conditions, while the absorbance changes under  $N_2$ -saturated conditions were minimal, consistent  
307 with the VL decay trends. This absorbance enhancement can be explained by the formation of oligomers with large, conjugated  
308  $\pi$ -electron systems (Chang and Thompson, 2010) and hydroxylated products (Li et al., 2014; Zhao et al., 2015), in agreement  
309 with the observed reaction products. In this work, phenoxy radicals (in resonance with a carbon-centered cyclohexadienyl  
310 radical) can be generated from several processes such as the oxidation ~~(Vione et al., 2019)~~-of ground-state VL by  $^3VL^*$  via H-  
311 atom abstraction ~~(Huang et al., 2018)~~ or electron transfer coupled with proton transfer from the phenoxy radical cation or from  
312 solvent water (Neumann et al., 1986a, 1986b; Anastasio et al., 1996) and photoinduced O-H bond-breaking (Berto et al., 2016).  
313 ~~Moreover,  $^3VL^*$  can initiate H atom abstraction from the CHO group of VL, generating ketyl radicals via Norrish type~~  
314 ~~reactions (Vione et al., 2019).~~ Also, similar reactions can be initiated by  $\cdot OH$  (Gelencsér et al., 2003; Hoffer et al., 2004; Chang  
315 and Thompson, 2010; Sun et al., 2010), which in this study can be generated from the reaction between  $^3VL^*$  and  $O_2$ , as well  
316 as nitrate photolysis. Trace amounts of  $H_2O_2$  were likely formed during VL photodegradation (Li et al., 2014), similar to the  
317 case of other phenolic compounds (Anastasio et al., 1996). Oligomers can then form via the coupling of phenoxy radicals or  
318 phenoxy and cyclohexadienyl ketyl radicals (Sun et al., 2010; Yu et al., 2014 Berto et al., 2016; Vione et al., 2019). Absorbance  
319 increase at  $> 350 \text{ nm}$  has also been reported for photosensitized oxidation of phenol and 4-phenoxyphenol (De Laurentiis et  
320 al., 2013a, 2013b) and direct photolysis of tyrosine and 4-phenoxyphenol (Bianco et al., 2014) in which dimers have been  
321 identified as initial substrates. The continuous absorbance enhancement throughout 6 h of irradiation correlated with the  
322 observation of oligomers and nitrated compounds after irradiation. However, the increasing concentration of small organic  
323 acids (Fig. S5) throughout the experiments suggests that fragmentation, which results in the decomposition of initially formed  
324 oligomers and formation of smaller oxygenated products (Huang et al., 2018), is important at longer irradiation times. Overall,  
325 these trends establish that ~~secondary oxidants from  $^3VL^*$  and  $O_2$  are is~~ necessary for the efficient formation of light-absorbing  
326 compounds from both  $VL^*$  and VL+AN.

### 327 3.1.2 Effect of pH

328 The reactivity of  $^3\text{C}^*$  (Smith et al., 2014, 2015, 2016), aromatic photonitration by nitrate (Machado and Boule, 1995; Dzenge  
329 et al., 1999; Vione et al., 2005; Minero et al., 2007), and N(III)-mediated VL photo-oxidation (Pang et al., 2019a) have been  
330 demonstrated to be pH-dependent. In this study, the effect of pH on VL photo-oxidation was investigated within the range of  
331 2.5 to ~~4.5~~, corresponding to typical cloud ~~(2-7)~~ pH values (2-7) (Pye et al., 2020). The decay rates ~~constants~~ for both VL\* and  
332 VL+AN increased as pH decreased (VL\* and VL+AN at pH 2.5: 1.~~65~~ and 1.~~43~~ times faster than at pH 4, respectively) (Fig.  
333 S3b). These differences in decay rate constants are small but statistically significant ( $p < 0.05$ ). The  $pK_a$  for the VL triplet has  
334 been reported to be 4.0 (Smith et al., 2016). As there are a greater fraction of VL triplets that are protonated at pH 2.5 (0.96)  
335 than at pH 4 (0.5), it is possible that the pH dependence of the decay rate constants observed in this study is due to  $^3\text{VL}^*$  being  
336 more reactive in its protonated form. Smith et al. (2016) also observed a pH dependence for the direct photodegradation of VL  
337 (0.005 mM) (rate constants at  $\text{pH} < 3$  are ~two times lower than at  $\text{pH} \geq 5$ ) which they attributed to the sensitivity of the  
338 excimer of VL (i.e., the charge-transfer complex formed between an excited state VL molecule and a separate ground state VL  
339 molecule; Birks, 1973, Turro et al., 2010) to acid-base chemistry. The opposite trend observed in this study for 0.1 mM VL  
340 may be due to the reactivities of the protonated and neutral forms of the  $^3\text{VL}^*$  being dependent on the VL concentration (Smith  
341 et al., 2016). For VL\*, this pH trend indicates that  $^3\text{VL}^*$  are more reactive in their protonated form, which is opposite to that  
342 reported for 0.005 mM VL (Smith et al., 2016), likely due to the concentration dependence of the relative reactivities of  
343 protonated and neutral forms of  $^3\text{VL}^*$ . It has been reported that the quantum yield for direct VL photodegradation is higher at  
344 pH 5 than at pH 2 for 0.005 mM VL, but they are not statistically different for 0.03 mM VL (Smith et al., 2016). Also, increases  
345 in hydrogen ion concentration can enhance the formation of  $\text{HO}_2^*$  and  $\text{H}_2\text{O}_2$  and in turn,  $^*\text{OH}$  formation (Du et al., 2011). In  
346 addition to these pH influences on VL\* the dependence of N(III) ( $\text{NO}_2^- + \text{HONO}$ ) speciation on solution acidity (Pang et al.,  
347 2019a) also contributed to the observed pH effects for VL+AN. At pH 3.3, half of N(III) exists as HONO (Fischer and  
348 Warneck, 1996; Pang et al., 2019a), which has a higher quantum yield for  $^*\text{OH}$  formation than that of  $\text{NO}_2^-$  in the near-UV  
349 region (Arakaki et al., 1999; Kim et al., 2014). The increased  $^*\text{OH}$  formation rates as pH decreases can lead to faster VL decay  
350 (Pang et al., 2019a). Also,  $\text{NO}_2^-/\text{HONO}$  can generate  $^*\text{NO}_2$  via oxidation by  $^*\text{OH}$  (Reactions 4 and 15; Table 1) (Pang et al.,  
351 2019a). As pH decreases, the higher reactivity of  $^3\text{VL}^*$  and sensitivity of the excimer of VL to acid-base chemistry HONO  
352 being the dominant N(III) species can lead ~~may have led~~ to faster VL photo-oxidation. Similar to pH 4 experiments, comparable  
353 decay rate constants between VL\* and VL+AN were also noted at  $\text{pH} < 4$ , again suggesting the predominant role of  $^3\text{VL}^*$   
354 chemistry compared to nitrate, likely due to the high VL concentration (0.1 mM) used in this study.

355 As pH decreased, the normalized abundance of products, particularly oligomers and functionalized monomers, was  
356 higher for both VL\* and VL+AN, further indicating that  $^3\text{VL}^*$  ~~are~~ may be more reactive in their protonated form. The most  
357 abundant products observed were a substituted VL ( $\text{C}_{10}\text{H}_{10}\text{O}_5$ ; No. 4, Table S2) and VL dimer ( $\text{C}_{16}\text{H}_{14}\text{O}_6$ ; No. ~~65~~, Table  
358 S3 Table S2) at pH 4 and  $\text{pH} < 4$ , respectively (Figs. 1c-h). Furthermore, a tetramer ( $\text{C}_{31}\text{H}_{24}\text{O}_{11}$ ) was observed only in VL\* at  
359 pH 2.5. For VL+AN, the normalized abundance of nitrogen-containing compounds was also higher increased at lower pH

360 (Table S2), likely due to increased  $\cdot\text{OH}$  and  $\cdot\text{NO}_2$  formation, which may be caused by the dependence of N(III) ( $\text{NO}_2^- + \text{HONO}$ )  
361 speciation on solution acidity (Pang et al., 2019a). At pH 3.3, half of N(III) exists as HONO (Fischer and Warneck, 1996; Pang  
362 et al., 2019a), which has a higher quantum yield for  $\cdot\text{OH}$  formation than that of  $\text{NO}_2^-$  in the near-UV region (Arakaki et al.,  
363 1999; Kim et al., 2014). Also,  $\text{NO}_2^-/\text{HONO}$  can generate  $\cdot\text{NO}_2$  via oxidation by  $\cdot\text{OH}$  (Reactions 4 and 105; Table 1) (Pang et  
364 al., 2019a). At pH < 4,  $^3\text{VL}^*$  likely have higher reactivity as suggested by the increased normalized abundance of oligomers  
365 (e.g.,  $\text{C}_{16}\text{H}_{14}\text{O}_6$ ; No. 6, Table S2 and  $\text{C}_{31}\text{H}_{24}\text{O}_{11}$ ) and N-containing compounds (e.g.,  $\text{C}_{16}\text{H}_{10}\text{N}_2\text{O}_9$ ; No. 3, Table S2 and  
366  $\text{C}_{13}\text{H}_{14}\text{N}_2\text{O}_{10}$ ) (Fig. 2). The potential imidazole derivative ( $\text{C}_3\text{H}_5\text{N}_3\text{O}_2$ , No. 5, Table S2) was observed only at pH 4, possibly  
367 due to the pH dependence of ammonium speciation ( $\text{pK}_a = 9.25$ ). Imidazole formation requires the nucleophilic attack of  
368 ammonia on the carbonyl group (Yu et al., 2011), and at pH 4, the concentration of dissolved ammonia in VL+AN was about  
369 10 or 30 times higher than that at pH 3 or pH 2.5, respectively. At different pH, the O:C and H:C ratios in VL\* and VL+AN  
370 had no significant differences (Figs. S7c–d and S9), but molecules with higher O:C ratios (> 0.6) were more abundant at pH  
371 < 4. Accordingly, the  $\langle\text{OS}_c\rangle$  at pH < 4 for both VL\* and VL+AN were higher than that at pH 4, consistent with higher  $\langle\text{OS}_c\rangle$   
372 observed at pH 5 compared to pH 7 for the  $\cdot\text{OH}$ -mediated photo-oxidation of syringol (Sun et al., 2010). Essentially, the higher  
373 reactivity of  $^3\text{VL}^*$  and predominance of HONO over nitrite at lower pH may have resulted in increased formation of products  
374 mainly composed of oligomers and functionalized monomers.

375 ~~The higher absorbance enhancement for both VL\* and VL+AN (Fig. 32b) was observed as pH increased may be~~  
376 ~~attributed to redshifts and increased visible light absorption of reaction products (Pang et al., 2019a). To determine whether~~  
377 ~~the pH dependence is due to the acid-base chemistry of the products or of the reactions, we measured the pH dependence of~~  
378 ~~the aqSOA formed from VL\* at pH 4 and 2.5 over a range of pH conditions from 1.5 to 10.5 (Fig. S10). For both cases, the~~  
379 ~~intensity of absorption at longer wavelengths significantly increased as the pH of the solutions was raised. Moreover, the~~  
380 ~~comparable pH dependence of the two solutions suggests that the observed pH dependence may be attributed to the acid-base~~  
381 ~~chemistry of the reactions, which may involve  $^3\text{VL}^*$  or the excimer of VL (Smith et al., 2016), as discussed earlier. When a~~  
382 ~~phenolic molecule deprotonates at higher pH, an ortho or para electron withdrawing group, such as a nitro or aldehyde group,~~  
383 ~~can attract a portion of the negative charge towards its oxygen atoms through induced and conjugated effects, leading to the~~  
384 ~~extension of chromophore from the electron donating group (e.g.,  $\text{O}^-$ ) to the electron withdrawing group via the aromatic ring~~  
385 ~~(Carey, 2000; Williams and Fleming, 2008; Pang et al., 2019a). Hence, the delocalization of the negative charge in phenolates~~  
386 ~~leads to significant redshifts (Mohr et al., 2013).~~

### 387 **3.1.3 Effect of VOCs and inorganic anions**

388 ~~Aerosols are a complex mix of organic and inorganic compounds (Kanakidou et al., 2005). We explored the photo-oxidation~~  
389 ~~behavior of VL, with and without nitrate, in the presence of VOCs (2-propanol, IPA) and inorganic anions (sodium bicarbonate,~~  
390 ~~NaBC). For both VL\* and VL+AN, there was no significant change in VL decay (Figs. S3c–d), and comparable absorbance~~  
391 ~~enhancements (Figs. 2c–d) were observed upon the addition of IPA and NaBC. However, the characterization of reaction~~  
392 ~~products revealed the distinct effects of these compounds on the photo-oxidation of VL. Both IPA and NaBC increased the~~

393 normalized abundance of products from VL\* (by a factor of 2.4 and 1.4, respectively) and VL+AN (by a factor of 4) (Table  
394 S2). The major product observed in VL\*+IPA (Fig. S10a) was a dimer (C<sub>16</sub>H<sub>14</sub>O<sub>6</sub>). Also, higher oligomers up to tetramers  
395 (e.g., C<sub>31</sub>H<sub>22</sub>O<sub>12</sub>) not observed in VL\* were noted. A possible explanation may be the additional generation of <sup>•</sup>HO<sub>2</sub> from the  
396 reaction of IPA with <sup>•</sup>OH (Warneck and Wurzinger, 1988) (Reactions 16 and 17; Table 1), which can originate from <sup>3</sup>VL\* or  
397 nitrate photolysis, inducing reactions such as oxidation and nitration. As discussed earlier, <sup>•</sup>HO<sub>2</sub> can form H<sub>2</sub>O<sub>2</sub>, a photolytic  
398 source of <sup>•</sup>OH (Anastasio et al., 1996; Du et al., 2011). In the presence of IPA, the increase in normalized abundance of products  
399 (VL+AN+IPA: 3.8 times vs. VL\*+IPA: 2.4 times; Table S2) and <OS<sub>e</sub>> (VL+AN+IPA: 0.13 to 0.08 vs. VL\*+IPA: 0.16 to  
400 0.10; Table S2) being more evident for VL+AN compared to VL\* also supports the potential importance of reactions  
401 involving <sup>•</sup>HO<sub>2</sub> and nitrate photolysis products such as the secondary photochemistry between <sup>•</sup>HO<sub>2</sub>/O<sub>2</sub><sup>•-</sup><sub>(aq)</sub> and photoproducted  
402 NO<sub>x(aq)</sub> enhancing HONO<sub>(g)</sub> production from nitrate photolysis in the presence of dissolved aliphatic organic matter (Wang et  
403 al., 2021) as discussed in Sect. 3.1.1. This chemistry may have operated in VL+AN+IPA considering that <sup>•</sup>HO<sub>2</sub>/O<sub>2</sub><sup>•-</sup> may  
404 originate from multiple sources in this experiment: nitrate photolysis (Reaction 10; Table 1) (Jung et al., 2017; Wang et al.,  
405 2021), the reactions of <sup>3</sup>VL\* in the presence of O<sub>2</sub> (see Sect. 3.1), or reaction of IPA with <sup>•</sup>OH (Warneck and Wurzinger, 1988)  
406 (Reactions 16 and 17; Table 1). In other words, the role of nitrate in VL photo-oxidation is enhanced in the presence of IPA,  
407 likely due to additional <sup>•</sup>HO<sub>2</sub>/O<sub>2</sub><sup>•-</sup> formation. In VL+AN+IPA, nitrate photolysis likely converted C<sub>16</sub>H<sub>14</sub>O<sub>6</sub> (from VL\*+IPA)  
408 to C<sub>15</sub>H<sub>12</sub>O<sub>8</sub> (Figs. S10a-b) via demethylation and then multiple hydroxylations. Nitrate photolysis generates <sup>•</sup>OH, and  
409 demethylation has been reported to be enhanced at high <sup>•</sup>OH exposure (Gold et al., 1983). Moreover, alcohols can affect the  
410 structure of water, causing a localized patterning or organization that changes the solvation environment, which can account  
411 for reactivity enhancement in the presence of alcohol containing solvents (Berke et al., 2019). Berke et al. (2019) has  
412 demonstrated that IPA and other alcohols (e.g., ethanol) can promote the production of light absorbing compounds, i.e.,  
413 imidazoles, from the reactions between glyoxal and ammonium sulfate. This phenomenon has been attributed to the formation  
414 of micro heterogeneities of hydrated alcohol molecules in a complex solution environment composed of solvated sulfate ions  
415 and a mixture of reactants and products upon the addition of alcohols. As proposed by an earlier study (Onori and Santucci,  
416 1996), if the water in the SOA mimicking solutions exists in two forms, bulk and hydrating, the micro heterogeneities may  
417 interact with water/nitrate matrix to sequester the reactants and products, concentrating them within a smaller effective solvent  
418 volume and consequently resulting in increased normalized abundance of products (Berke et al., 2019).

419 ——— For NaBC which does not produce <sup>•</sup>HO<sub>2</sub> upon reactions with <sup>•</sup>OH under air saturated conditions (Gen et al., 2019b),  
420 the increased normalized abundance of products may be due to other reactions promoted by the carbonate radical (CO<sub>3</sub><sup>•-</sup>),  
421 which can be generated from the reactions of bicarbonate/carbonate with <sup>•</sup>OH (Reactions 18 and 19; Table 1) (Neta et al.,  
422 1988; Wojnárovits et al., 2020) or <sup>3</sup>VL\* (Reactions 20 and 21; Table 1) (Canonica et al., 2005). CO<sub>3</sub><sup>•-</sup> is a selective oxidant  
423 that reacts with organic molecules at a lower rate than <sup>•</sup>OH and readily reacts with electron rich parts of phenols, aromatic  
424 amines, and sulfur containing compounds (e.g., glutathione) through both electron transfer and H abstraction (Huang and  
425 Mabury, 2000; Wojnárovits et al., 2020). Similar to IPA, the enhancement of normalized abundance of products  
426 (VL+AN+NaBC: 4.3 times vs. VL\*+NaBC: 1.4 times; Table S2) and <OS<sub>e</sub>> (VL+AN+NaBC: 0.13 to 0.08 vs. VL\*+NaBC:

427 -0.16 to -0.11; Table S2) was more obvious for VL+AN+NaBC than VL\*+NaBC, further underlining the contributions of  
428 nitrate photolysis products. For example, it has been reported that carbonate and bicarbonate can substantially increase the  
429 photodegradation of electron rich compounds (e.g., catechol) by nitrate (Vione et al., 2009). Bicarbonate can enhance the  
430 photolysis of nitrate via a solvent-cage effect, reacting with photolysis-derived  $^{\bullet}\text{OH}$  before it escapes the surrounding cage of  
431 the water molecules. This prevents the recombination of  $^{\bullet}\text{OH}$  and  $^{\bullet}\text{NO}_2$  inside the solvent cage that otherwise would yield back  
432  $\text{NO}_3^- + \text{H}^+$ , which reduces the quantum yield of  $^{\bullet}\text{OH}$  photoproduction (Bouillon and Miller, 2005). This scavenging of in-cage  
433  $^{\bullet}\text{OH}$  by bicarbonate would then hinder recombination, resulting in a higher generation rate of  $\text{CO}_3^{\bullet-} + ^{\bullet}\text{OH}$  with bicarbonate  
434 compared to  $^{\bullet}\text{OH}$  alone without bicarbonate. However, in our experiments, NaBC did not cause any substantial change in the  
435 decay of VL for both VL\* and VL+AN, although it promoted higher normalized abundance of products. The major product in  
436 VL\*+NaBC was a functionalized monomer ( $\text{C}_7\text{H}_4\text{O}_4$ ; No. 6, Table S3; Fig. S10c). Unlike VL\*+IPA, no tetramers were  
437 observed in VL\*+NaBC. Similar to VL+AN+IPA, the addition of NaBC to VL+AN resulted in trimers and a high abundance  
438 dimer ( $\text{C}_{15}\text{H}_{12}\text{O}_8$ ; No. 7, Table S3) (Figs. S10b and S10d). Overall, VL+AN+IPA had more oligomers while VL+AN+NaBC  
439 had more functionalized monomers (e.g.,  $\text{C}_8\text{H}_6\text{O}_4$ ; No. 8, Table S3). These findings suggest that aside from low pH (<4), the  
440 formation of oligomers from VL photo-oxidation can also be promoted by presence of VOCs and inorganic anions likely via  
441 the generation of radicals such as  $^{\bullet}\text{HO}_2$  and  $\text{CO}_3^{\bullet-}$  which can also interact with nitrate photolysis products.

442 The addition of IPA or NaBC to VL\* resulted in products with higher O:C and H:C ratios (Figs. S11a and S11c).  
443 Although the products were more abundant in VL\*+IPA than with NaBC, the distribution of their products in van Krevelen  
444 diagrams was rather similar. The increased in  $\langle \text{OS}_e \rangle$  in the presence of IPA or NaBC was more significant for VL+AN than  
445 VL\*, likely due to the interactions of nitrate photolysis products with  $^{\bullet}\text{HO}_2$  and  $\text{CO}_3^{\bullet-}$ . For VL+AN, IPA and NaBC also  
446 increased the O:C and H:C ratios (Figs. S11b and S11d), and most products had  $\text{OS}_e > 0$ , similar to less volatile and semi-  
447 volatile oxygenated organic aerosols (LV-OOA and SV-OOA) (Kroll et al., 2011).

### 448 3.1.34 Distribution of potential BrC compounds

449 Figure S112 plots the DBE values vs. number of carbons ( $n_c$ ) (Lin et al., 2018) for the 50 most abundant products from pH 4  
450 experiments under air-saturated conditions, along with reference to DBE values corresponding to fullerene-like hydrocarbons  
451 (Lobodin et al., 2012), cata-condensed polycyclic aromatic hydrocarbons (PAHs) (Siegmann and Sattler, 2000), and linear  
452 conjugated polyenes with a general formula  $\text{C}_x\text{H}_{x+2}$ . As light absorption by BrC requires uninterrupted conjugation across a  
453 significant part of the molecular structure, compounds with DBE/ $n_c$  ratios (shaded area in Fig. S112) greater than that of linear  
454 conjugated polyenes are potential BrC compounds (Lin et al., 2018). Based on this criterion and the observed absorbance  
455 enhancement at  $> 350$  nm (Fig. 32), the majority of the 50 most abundant products from pH 4 experiments under air-saturated  
456 conditions were potential BrC chromophores composed of monomers and oligomers up to tetramers. However, as ESI-detected  
457 compounds in BB organic aerosols has been reported to be mainly molecules with  $n_c < 25$  (Lin et al., 2018), there may be  
458 higher oligomers that were not detected in our reaction systems.



### 459 3.2 Effect of reactants concentration and molar ratios on the aqueous photo-oxidation of vanillin

460 To examine the influence of VL and nitrate concentration and their molar ratios on VL photo-oxidation, we also characterized  
461 the reaction products from lower [VL] (0.01 mM VL\*; A104; Table S2), lower ~~[VL] concentrations~~ and an equal molar ratio  
462 of VL/nitrate (0.01 mM VL + 0.01 mM AN; A115; Table S2), and lower [VL] and 1:100 molar ratio of VL/nitrate (0.01 mM  
463 VL + 1 mM AN; A126; Table S2) at pH 4. The normalized abundance of products from low [VL] experiments (A104-A126;  
464 Table S2) were up to 1.4 times higher than that of high [VL] experiments (A5 and A7; Table S2). Nevertheless, the major  
465 products for both low and high [VL] experiments were functionalized monomers (Figs. 1c-d and S123a-c) such as C<sub>8</sub>H<sub>6</sub>O<sub>4</sub>  
466 (No. 7, Table S2) and C<sub>10</sub>H<sub>10</sub>O<sub>5</sub> (No. 4, Table S2). For both VL\* and VL+AN, the contribution of <200 m/z to the normalized  
467 abundance of products was higher at low [VL] than at high [VL], while the opposite was observed for >300 m/z (Fig. S123d).  
468 This indicates that functionalization was favored at low [VL], as supported by the higher <OS<sub>c</sub>>, while oligomerization was  
469 the dominant pathway at high [VL], consistent with more oligomers or polymeric products reported from high phenols  
470 concentration (e.g., 0.1 to 3 mM) (Li et al., 2014; Slikboer et al., 2015; Ye et al., 2019). This is probably due to an increased  
471 concentration of phenoxy radicals (in resonance with a carbon-centered cyclohexadienyl radical) at high [VL], promoting  
472 radical-radical polymerization (Sun et al., 2010; Li et al., 2014). ~~Moreover At low [VL], the contribution of <200 m/z to the~~  
473 ~~normalized abundance of products was higher for 1:1 than 1:100 VL/nitrate molar ratio, further suggesting the prevalence of~~  
474 ~~functionalization for the former formation of more oxidized products. This may also be the reason why~~ In addition, 1:1  
475 VL/nitrate (A115; Table S2) had higher <OS<sub>c</sub>> than 1:100 VL/nitrate (A126; Table S2) VL/nitrate, indicating the formation  
476 of more oxidized products, but had fewer N-containing compounds compared to the latter. A possible explanation is that at  
477 1:1 VL/nitrate, VL ~~may efficiently~~ competes with NO<sub>2</sub><sup>-</sup> for <sup>•</sup>OH (from nitrate or nitrite photolysis, Reaction 4; Table 1) and  
478 indirectly reduces <sup>•</sup>NO<sub>2</sub>. Similarly, hydroxylation has been suggested to be ~~an~~ more important pathway for 1:1 VL/nitrite than  
479 in 1:10 VL/nitrite (Pang et al., 2019a). ~~This may also be the reason why 1:1 VL/nitrate (A15; Table S2) had higher <OS<sub>c</sub>> than~~  
480 ~~1:100 (A16; Table S2) VL/nitrate but had fewer N-containing compounds compared to the latter. Moreover, the contribution~~  
481 ~~of <200 m/z to the normalized abundance of products was higher for 1:1 than 1:100 VL/nitrate molar ratio, further suggesting~~  
482 ~~the formation of more oxidized products.~~ Fragmentation, which leads to the decomposition of previously formed oligomers  
483 and generation of small, oxygenated products such as organic acids (Huang et al., 2018), may also occur for the low [VL]  
484 experiments. However, its importance would likely be observed at longer irradiation times, similar to the high [VL]  
485 experiments.

### 486 3.3 Participation of ammonium in the aqueous photo-oxidation of vanillin

487 Imidazole and imidazole derivatives have been reported to be the major products of glyoxal and ammonium sulfate reactions  
488 at pH 4 (Galloway et al., 2009; Yu et al., 2011; Sedehi et al., 2013; Gen et al., 2018; Mabato et al., 2019). Here, we compared  
489 VL+AN and VL+SN at pH 4 in terms of reaction products and oxidative characteristics to confirm the participation of  
490 ammonium in the aqueous photo-oxidation of VL. ~~In both experiments~~ The normalized abundance of the products was

491 comparable ~~in both experiments~~ (A7 and A913; Table S2), with C<sub>10</sub>H<sub>10</sub>O<sub>5</sub> (No. 4, Table S2) as the most abundant product  
492 (Figs. 1d and S6a), but in VL+SN, there was a significant amount of a VL dimer (C<sub>15</sub>H<sub>12</sub>O<sub>8</sub>; No. 89, Table S3Table S2).  
493 Moreover, the nitrogen-containing compounds were distinct. Aside from the potential imidazole derivative (C<sub>5</sub>H<sub>5</sub>N<sub>3</sub>O<sub>2</sub>; No.  
494 540, Table S23), C<sub>8</sub>H<sub>9</sub>NO<sub>3</sub> (No. 2, Table S2) was also observed from VL+AN but only under N<sub>2</sub>-saturated conditions (Fig.  
495 1b), probably due to further oxidation by ~~secondary oxidants from~~<sup>3</sup>VL\*. The product analysis suggests the participation of  
496 ammonium in the aqueous-phase reactions. Ammonium salts are an important constituent of atmospheric aerosols particles  
497 (Jimenez et al., 2009), and reactions between dicarbonyls (e.g., glyoxal) and ammonia or primary amines have been  
498 demonstrated to form BrC (De Haan et al., 2009, 2011; Nozière et al., 2009; Shapiro et al., 2009; Lee et al., 2013; Powelson  
499 et al., 2014; Gen et al., 2018; Mabato et al., 2019). Relative to VL+AN, the products from VL+SN had higher O:C ratios (e.g.,  
500 C<sub>7</sub>H<sub>4</sub>N<sub>2</sub>O<sub>7</sub>; No. 944, Table S23), OS<sub>c</sub>, and <OS<sub>c</sub>> values (Table S2).

### 501 3.4 Oxidation of guaiacol by photosensitized reactions of vanillin and photolysis of nitrate

502 The oxidation of phenols by <sup>3</sup>C\* has been mainly studied using non-phenolic aromatic carbonyls (Anastasio et al., 1996; Smith  
503 et al., 2014, 2015; Yu et al., 2014; Chen et al., 2020) and aromatic ketones (Canonica et al., 2000) as triplet precursors. Recently,  
504 <sup>3</sup>VL\* have also been shown to oxidize syringol (Smith et al., 2016), a non-carbonyl phenol, although the reaction products  
505 remain unknown. In this section, we discussed the photo-oxidation of guaiacol (GUA), a lignocellulosic BB pollutant (Kroflíč  
506 et al., 2015) that is also a non-carbonyl phenol, in the presence of VL (GUA+VL) or nitrate (GUA+AN). The dark experiments  
507 did not show any substantial loss of VL or GUA (Fig. S3ce). Due to its poor light absorption in the solar range, GUA is not an  
508 effective photosensitizer (Smith et al., 2014; Yu et al., 2014). Accordingly, the direct GUA photodegradation resulted in  
509 minimal decay, which plateaued after ~3 hours. However, in the presence of VL or nitrate, the GUA decay rate constant was  
510 faster/higher by 2.2 (GUA+VL) and 1.32 (GUA+AN) times, respectively, than for direct GUA photodegradation. The  
511 enhancement of GUA decay rate constant in the presence of VL is statistically significant ( $p < 0.05$ ), while that in the presence  
512 of AN is not ( $p > 0.05$ ). This enhanced GUA decay rate constant may be due to the ~~following main reactions~~: oxidation of  
513 GUA by <sup>3</sup>VL\* ~~(or the secondary oxidants it generates upon reaction with O<sub>2</sub>)~~, oxidation by <sup>\*</sup>OH ~~produced from nitrate~~  
514 ~~photolysis, or nitration by <sup>\*</sup>NO<sub>2</sub> from nitrate photolysis~~. As mentioned earlier, ~~the~~<sup>3</sup>VL\* chemistry appears to be more important  
515 than that of nitrate photolysis even at 1:10 molar ratio of VL/nitrate on account of the much higher molar absorptivity of VL  
516 compared to that of nitrate (Fig. S1) and the high VL concentration (0.1 mM) used in this study. However, the apparent  
517 quantum efficiency of GUA photodegradation ( $\phi_{\text{GUA}}$ ) in the presence of nitrate ( $1.3 \times 10^{-2} \pm 2.9 \times 10^{-3}$ ) is ~14 times larger than  
518 that in the presence of VL ( $9.0 \times 10^{-4} \pm 4.0 \times 10^{-4}$ ), suggesting that nitrate-mediated photo-oxidation of GUA is more efficient  
519 than that by photosensitized reactions of VL (see Text S7 for more details). The decay of VL in GUA+VL (A148; Table S2)  
520 was 3 times slower than that of VL\* (A5; Table S2), which may be due to competition between ground-state VL and GUA for  
521 reactions with <sup>3</sup>VL\* ~~(or the secondary oxidants it generates upon reaction with O<sub>2</sub>)~~ or increased conversion of <sup>3</sup>VL\* back to  
522 the ground state through the oxidation of GUA (Anastasio et al., 1996; Smith et al., 2014). The corresponding absorbance  
523 changes for the GUA experiments (Fig. 34ce) were consistent with the observed decay trends. The minimal absorbance changes

524 for the direct GUA photodegradation also plateaued after ~3 hours. Moreover, the difference between GUA photo-oxidation  
525 in the presence of VL or nitrate was more evident, with the former showing much higher absorbance enhancement. ~~Similarly,~~  
526 Yang et al. (2021) also observed greater light absorption during nitrate-mediated photo-oxidation relative to direct GUA  
527 photodegradation.

528 For the direct GUA photodegradation, GUA+VL, and GUA+AN, the normalized abundance of products was  
529 calculated only for GUA+VL (2.2; Table S2), as the GUA signal from the UHPLC-qToF-MS in the positive ion mode was  
530 weak, which may introduce large uncertainties during normalization. Nonetheless, the number of products detected from these  
531 experiments (178, 266, and 844 for the direct GUA photodegradation, GUA+AN, and GUA+VL, respectively) corroborates  
532 the kinetics and absorbance results. The major products (Fig. 43a) from the direct photodegradation of GUA were C<sub>14</sub>H<sub>14</sub>O<sub>4</sub>  
533 (No. 109, ~~Table S3~~Table S2), a typical GUA dimer, and a trimer (C<sub>21</sub>H<sub>20</sub>O<sub>6</sub>; No. 1120, ~~Table S3~~Table S2) which likely  
534 originated from photoinduced O-H bond-breaking (Berto et al., 2016). In general, higher absolute signals ~~areas were~~ noted  
535 for oligomers (e.g., C<sub>14</sub>H<sub>14</sub>O<sub>4</sub>, ~~No. 10 and C<sub>21</sub>H<sub>20</sub>O<sub>6</sub>, No. 11, Table S2~~) and hydroxylated products (e.g., C<sub>7</sub>H<sub>8</sub>O<sub>4</sub>) in both  
536 GUA+VL and GUA+AN, similar to those observed from GUA oxidation by triplets of 3,4-dimethoxybenzaldehyde (DMB; a  
537 non-phenolic aromatic carbonyl) or <sup>•</sup>OH (from H<sub>2</sub>O<sub>2</sub> photolysis) (Yu et al., 2014). In contrast to the GUA aqSOA reported by  
538 Yu et al. (2014), the photo-oxidation of GUA in this study yielded nitrated compounds (e.g., C<sub>9</sub>H<sub>14</sub>N<sub>2</sub>O<sub>6</sub>, C<sub>11</sub>H<sub>14</sub>N<sub>2</sub>O<sub>9</sub>) from  
539 GUA+AN and VL dimers (e.g., C<sub>16</sub>H<sub>12</sub>O<sub>6</sub>) from GUA+VL. However, based on a recent work on the aqueous photo-oxidation  
540 of guaiacyl acetone (another aromatic phenolic carbonyl) by DMB triplets, the hydroxylation and dimerization of DMB can  
541 also contribute to aqSOA (Jiang et al., 2021). The contributions from DMB-participated reactions were only minor due to the  
542 low initial DMB concentration (0.005 mM). Relative to GUA+AN, higher signals for dimers such as C<sub>14</sub>H<sub>14</sub>O<sub>4</sub> (~~No. 10, Table~~  
543 ~~S2~~) and C<sub>16</sub>H<sub>12</sub>O<sub>6</sub> were noted in GUA+VL, possibly due to both GUA and ground-state VL being available as oxidizable  
544 substrates for <sup>3</sup>VL\* ~~and the secondary oxidants it can generate~~. Also, a potential GUA tetramer (C<sub>28</sub>H<sub>24</sub>O<sub>8</sub>, No. 1221, Table  
545 ~~S23~~) was observed only in GUA+VL, consistent with higher oligomer formation from the triplets-mediated photo-oxidation  
546 of phenolics relative to <sup>•</sup>OH-assisted photo-oxidation (Yu et al., 2014). In general, the products from the direct GUA  
547 photodegradation, GUA+VL, and GUA+AN had similar OS<sub>c</sub> values (-0.5 to 0.5) (Figs. 43b-d), falling into the criterion of  
548 BBOA and SV-OOA (Kroll et al., 2011). In this work, ~~efficient~~ GUA photo-oxidation was observed in the presence of VL  
549 ~~and~~ AN, forming aqSOA composed of oligomers, hydroxylated products, and nitrated compounds (for GUA+AN). The  
550 higher product signals from GUA+VL compared to GUA+AN is likely due to the availability of both GUA and ground-state  
551 VL as aqSOA precursors.

### 552 ~~3.5 Photo-oxidation pathways of vanillin via direct photosensitization and in the presence of nitrate~~

553 ~~The most probable pathways of direct photosensitized and nitrate-mediated photo-oxidation of VL were proposed (Fig. 4). In~~  
554 ~~Scheme 1 (pH 4 and pH <4 under air saturated conditions), <sup>3</sup>VL\* and <sup>•</sup>OH (from <sup>3</sup>VL\* or nitrate photolysis) can initiate H-~~  
555 ~~atom abstraction to generate phenoxy or ketyl radicals (Huang et al., 2018; Vione et al., 2019). At pH 4, ring-opening products~~

556 (~~Fig. S5~~) from fragmentation in both VL\* and VL+AN may have reacted with VL or dissolved ammonia to generate C<sub>10</sub>H<sub>14</sub>O<sub>8</sub>  
557 (~~Pang et al., 2019b~~) and a potential imidazole derivative (C<sub>8</sub>H<sub>8</sub>N<sub>2</sub>O<sub>9</sub>), respectively. Moreover, nitrate photolysis products  
558 promoted functionalization and nitration (e.g., C<sub>16</sub>H<sub>14</sub>N<sub>2</sub>O<sub>9</sub>). At pH < 4, the reactivity of <sup>3</sup>VL\* increased as suggested by the  
559 abundance of oligomers (e.g., C<sub>16</sub>H<sub>14</sub>O<sub>6</sub>) and increased normalized abundance of N-containing compound  
560 ——— In Scheme 2 (pH 4, IPA or NaBC, under air saturated conditions), additional radicals generated (<sup>•</sup>HO<sub>2</sub> and CO<sub>3</sub><sup>•-</sup>)  
561 likely promoted more reactions. An abundant dimer (C<sub>16</sub>H<sub>14</sub>O<sub>6</sub>) and higher oligomers (e.g., tetramers, C<sub>31</sub>H<sub>22</sub>O<sub>12</sub>) were  
562 identified in VL\*+IPA, possibly due to <sup>•</sup>HO<sub>2</sub>-initiated reactions, while a functionalized monomer (C<sub>7</sub>H<sub>4</sub>O<sub>4</sub>) was abundant in  
563 VL\*+NaBC. In general, nitrate enhanced both oligomerization and functionalization in VL+IPA or VL+NaBC. In  
564 VL+AN+IPA, C<sub>15</sub>H<sub>12</sub>O<sub>8</sub> likely originated from C<sub>16</sub>H<sub>14</sub>O<sub>6</sub> via demethylation and multiple hydroxylations. In VL+AN+NaBC,  
565 C<sub>8</sub>H<sub>6</sub>O<sub>4</sub> was possibly generated via H atom abstraction from -OCH<sub>3</sub> by <sup>•</sup>OH, and further addition with O<sub>2</sub> is energy barrierless  
566 (Priya and Lakshmipathi, 2017; Sun et al., 2019), generating a hydroperoxide (-OCH<sub>2</sub>OOH) that readily decompose to form  
567 OCH<sub>2</sub>O<sup>•</sup> and <sup>•</sup>OH (Yaremenko et al., 2016). OCH<sub>2</sub>O<sup>•</sup> is finally transformed into -OCHO with the elimination of HO<sub>2</sub> in the  
568 presence of O<sub>2</sub> (Sun et al., 2019). Moreover, the abundance of C<sub>15</sub>H<sub>12</sub>O<sub>8</sub> was higher in VL+AN+NaBC than in VL\*+NaBC.

#### 569 4 Conclusions and atmospheric implications

570 This study shows that the photo-oxidation of VL via its direct photosensitized reactions and in the presence of nitrate can  
571 generate aqSOA composed of oligomers, functionalized monomers, oxygenated ring-opening products, and nitrated  
572 compounds (for nitrate-mediated reactions). The characterization of products presented in this work complements earlier  
573 studies (e.g., Smith et al. 2014, 2015, 2016) that mainly discussed the kinetics and aqSOA yield of triplet-driven oxidation of  
574 phenols. Although nitrate did not substantially affect the VL decay rates constants, likely due to much higher molar absorptivity  
575 of VL than nitrate and high VL concentration used in this work, the presence of nitrate promoted functionalization and nitration,  
576 indicating the significance of nitrate photolysis in this aqSOA formation pathway. ~~While~~ This work demonstrates that nitration,  
577 which is can be an important process for producing light-absorbing organics or BrC (Jacobson, 1999; Kahnt et al., 2013; Mohr  
578 et al., 2013; Laskin et al., 2015; Teich et al., 2017; Li et al., 2020), ~~its effect on~~ can also affect the aqueous-phase processing of  
579 triplet-generating aromatics ~~has not yet been examined in detail~~. On a related note, a recent work (Ma et al., 2021) mimicking  
580 phenol oxidation by DMB (a non-phenolic aromatic carbonyl) triplets in more concentrated conditions in aerosol liquid water  
581 (ALW) showed that significantly higher AN concentration (0.5 M) increased the photodegradation rate constant for guaiacyl  
582 acetone (an aromatic phenolic carbonyl with high Henry's law constant, 1.2 × 10<sup>6</sup> M atm<sup>-1</sup>; McFall et al., 2020) by >20 times  
583 which was ascribed to <sup>•</sup>OH formation from nitrate photolysis (Brezonik and Fulkerson-Brekken, 1998; Chu and Anastasio,  
584 2003). The same study also estimated that reactions of phenols with high Henry's law constants (10<sup>6</sup> to 10<sup>9</sup> M atm<sup>-1</sup>) can be  
585 important for SOA formation in ALW, with mechanisms mainly governed by <sup>3</sup>C\* and <sup>1</sup>O<sub>2</sub> (Ma et al., 2021). Likewise, Zhou  
586 et al. (2019) reported that the direct photodegradation of acetosyringone was faster by about 6 times in the presence of 2 M  
587 NaClO<sub>4</sub>. However, the opposite was noted for the photodegradation of VL in sodium sulfate or sodium nitrate, which would

588 occur slower ( $\approx 2$  times slower in 0.5 M sodium sulfate and  $\sim 10$  times slower in 0.124 M sodium nitrate) in ALW relative to  
589 dilute aqueous phase in clouds. These suggest that the nature of inorganic ions may have an essential role in the  
590 photodegradation of organic compounds in the aqueous phase (Loisel et al., 2021).

591 Furthermore, a potential imidazole derivative observed from the VL+AN (A7; Table S2) experiment suggests that  
592 ammonium may participate in aqSOA formation from the photo-oxidation of phenolic aromatic carbonyls. Also, the oligomers  
593 from these reaction systems may be rather recalcitrant to fragmentation based on their high abundance, even at the  
594 longest irradiation time used in this study. Nonetheless, the increasing concentration of small organic acids over time implies  
595 that fragmentation becomes important at extended irradiation times. Aromatic carbonyls and nitrophenols have been reported  
596 to be the most important classes of BrC in cloud water heavily affected by biomass burning in the North China Plain  
597 (Desyaterik et al., 2013). Correspondingly, the most abundant products from our reaction systems (pH 4, air-saturated  
598 solutions) are mainly potential BrC chromophores. These suggest that aqSOA generated in cloud/fog water from the oxidation  
599 of biomass burning aerosols via direct photosensitized reactions and nitrate photolysis products can impact aerosol optical  
600 properties and radiative forcing, particularly for areas where biomass burning is intensive.

601 Our results indicate that the photo-oxidation of VL is influenced by ~~O<sub>2</sub> secondary oxidants from VL triplets~~, pH, ~~the~~  
602 ~~presence of VOCs and inorganic anions~~, and reactants concentration and molar ratios. ~~Compared to Under N<sub>2</sub>-saturated~~  
603 ~~conditions, - the absence of O<sub>2</sub> likely hindered the secondary steps in VL decay (e.g., reaction of ketyl radical and O<sub>2</sub>),~~  
604 ~~regenerating VL as suggested by the minimal VL decay~~ ~~more efficient VL photo-oxidation was observed under air saturated~~  
605 ~~conditions (O<sub>2</sub> is present), which can be attributed to the generation of secondary oxidants (e.g., <sup>1</sup>O<sub>2</sub>, O<sub>2</sub><sup>-</sup>/<sup>\*</sup>HO<sub>2</sub>, <sup>\*</sup>OH) from~~  
606 ~~<sup>3</sup>VL\*.~~ ~~Further enhancement of VL photo-oxidation under air saturated conditions in the presence of nitrate indicates~~  
607 ~~synergistic effects between secondary oxidants from VL triplets and nitrate photolysis products.~~ ~~In contrast, <sup>3</sup>VL\*-initiated~~  
608 ~~reactions proceeded rapidly under air-saturated conditions (O<sub>2</sub> is present) as indicated by higher VL decay rate constant and~~  
609 ~~increased normalized abundance of products. For pH 4 experiments, the presence of both O<sub>2</sub> and nitrate resulted in the highest~~  
610 ~~normalized abundance of products (including N-containing compounds) and <OS<sub>c</sub>>, which may be due to O<sub>2</sub> promoting VL~~  
611 ~~nitration. Nevertheless, further work is necessary to assess the effect of O<sub>2</sub> on the reactive intermediates involved in <sup>3</sup>VL\*-~~  
612 ~~driven photo-oxidation and elucidate the mechanisms of VL photo-oxidation under air-saturated conditions.~~ ~~Additionally, the~~  
613 ~~formation of oligomers from VL photo-oxidation was~~ ~~observed to be promoted at low pH (<4) or in the presence of IPA/NaBC,~~  
614 ~~which likely generated additional radicals such as <sup>\*</sup>HO<sub>2</sub> and CO<sub>3</sub><sup>\*</sup>.~~ ~~As aerosols comprise more complex mixtures of organic~~  
615 ~~and inorganic compounds, it is worthwhile to explore the impacts of other potential aerosol constituents on aqSOA formation~~  
616 ~~and photo-oxidation studies. This can also be beneficial in understanding the interplay among different reaction mechanisms~~  
617 ~~during photo-oxidation.~~ ~~Moreover, l~~ ~~ow VL concentration favored functionalization, while oligomerization prevailed at high~~  
618 ~~VL concentration, consistent with past works (Li et al., 2014; Slikboer et al., 2015; Ye et al., 2019). Hydroxylation was~~  
619 ~~observed to be important for equal molar ratios of VL and nitrate, likely due to VL competing with nitrite for <sup>\*</sup>OH. The~~  
620 ~~oxidation of guaiacol, a non-carbonyl phenol, by photosensitized reactions of vanillin was also shown to be~~ ~~moreless~~ ~~efficient~~  
621 ~~than that by nitrate photolysis products~~ ~~based on its lower apparent quantum efficiency.~~

622 In this study, we investigated reactions of VL and nitrate at concentrations in cloud/fog water. The concentrations of  
623 VL and nitrate can be significantly higher in aqueous aerosol particles. As a major component of aerosols, the concentration  
624 of nitrate can be as high as sulfate (Huang et al., 2014). More studies should then explore the direct photosensitized oxidation  
625 and nitrate-mediated photo-oxidation of other biomass burning-derived phenolic aromatic carbonyls, particularly those with  
626 high molar absorption coefficients and can generate  $^3C^*$ . The influences of reaction conditions should also be investigated to  
627 better understand the oxidation pathways. [As aerosols comprise more complex mixtures of organic and inorganic compounds,](#)  
628 [it is worthwhile to explore the impacts of other potential aerosol constituents on aqSOA formation and photo-oxidation studies.](#)  
629 [This can also be beneficial in understanding the interplay among different reaction mechanisms during photo-oxidation.](#)  
630 Considering that biomass burning emissions are expected to increase continuously, further studies on these aqSOA formation  
631 pathways are strongly suggested.

632

633 *Data availability.*

634 The data used in this publication are available to the community and can be accessed by request to the corresponding author.

635 *Author contributions.*

636 BRGM designed and conducted the experiments; YL provided assistance in measurements and helped to analyze experimental  
637 data; YJ provided assistance in measurements; BRGM, YL, and CKC wrote the paper. All co-authors contributed to the  
638 discussion of the manuscript.

639 *Competing interests.*

640 The authors declare that they have no conflict of interest.

641 *Acknowledgments.*

642 This work was financially supported by the National Natural Science Foundation of China (41875142 and 42075100). [Y.J.L.](#)  
643 [acknowledges support from the Science and Technology Development Fund, Macau SAR \(File no. 0019/2020/A1\), the Multi-](#)  
644 [Year Research grant \(No. MYRG2018-00006-FST\) from the University of Macau.](#) D.D.H. acknowledges support from the  
645 National Natural Science Foundation of China (21806108). X.L. acknowledges support from the Local Innovative and  
646 Research Teams Project of Guangdong Pearl River Talents Program (2019BT02Z546). T.N. acknowledges support from the  
647 Hong Kong Research Grants Council (21304919) and City University of Hong Kong (9610409). C.H.L. acknowledges support  
648 from the City University of Hong Kong (9610458 and 7005576).

## 649 **References**

650 ~~Abida, O., Mielke, L. H., and Osthoff, H. D.: Observation of gas phase peroxyxynitrous and peroxyxynitric acid during the~~  
651 ~~photolysis of nitrate in acidified frozen solutions, Chem. Phys. Lett., 511, 187–192,~~  
652 ~~<https://doi.org/10.1016/j.eplett.2011.06.055>, 2011.~~

- 654 Anastasio, C., Faust, B. C., and Rao, C. J.: Aromatic carbonyl compounds as aqueous-phase photochemical sources of  
655 hydrogen peroxide in acidic sulfate aerosols, fogs, and clouds. 1. Non-phenolic methoxybenzaldehydes and  
656 methoxyacetophenones with reductants (phenols), *Environ. Sci. Technol.*, 31, 218–232, <https://doi.org/10.1021/es960359g>,  
657 1996.
- 658
- 659 Arakaki, T., Miyake, T., Hirakawa, T., and Sakugawa, H.: pH dependent photoformation of hydroxyl radical and absorbance  
660 of aqueous-phase N(III) ( $\text{HNO}_2$  and  $\text{NO}_2$ ), *Environ. Sci. Technol.*, 33, 2561–2565, <https://doi.org/10.1021/es980762i>, 1999.
- 661
- 662 Bateman, A. P., Laskin, J., Laskin, A., and Nizkorodov, S. A.: Applications of high-resolution electrospray ionization mass  
663 spectrometry to measurements of average oxygen to carbon ratios in secondary organic aerosols, *Environ. Sci. Technol.*, 46,  
664 8315–8324, <https://doi.org/10.1021/es3017254>, 2012.
- 665 [Benedict, K. B., McFall, A. S., and Anastasio, C.: Quantum yield of nitrite from the photolysis of aqueous nitrate above 300  
666 nm, \*Environ. Sci. Technol.\*, 51, 4387–4395, <https://doi.org/10.1021/acs.est.6b06370>, 2017.](#)
- 667
- 668 ~~[Berke, A. E., Bhat, T. A., Myers, H., Gubbins, E. F., Nwankwo, A. A. O., Lu, K., Timpane, L., and Keller, C.: Effect of short-  
669 chain alcohols on the bulk phase reaction between glyoxal and ammonium sulfate, \*Atmos. Environ.\*, 198, 407–416,  
670 <https://doi.org/10.1016/j.atmosenv.2018.11.015>, 2019.](#)~~
- 671
- 672 Berto, S., De Laurentiis, E., Tota, T., Chiavazza, E., Daniele, P.G., Minella, M., Isaia, M., Brigante, M., and Vione, D.:  
673 Properties of the humic-like material arising from the photo-transformation of L-tyrosine, *Sci. Total Environ.*, 434–444,  
674 <https://doi.org/10.1016/j.scitotenv.2015.12.047>, 2016.
- 675
- 676 Bianco, A., Minella, M., De Laurentiis, E., Maurino, V., Minero, C., and Vione, D.: Photochemical generation of photoactive  
677 compounds with fulvic-like and humic-like fluorescence in aqueous solution, *Chemosphere*, 111, 529–536,  
678 <https://doi.org/10.1016/j.chemosphere.2014.04.035>, 2014.
- 679
- 680 Bianco, A., Deguillaume, L., Väitilingom, M., Nicol, E., Baray, J.-L., Chaumerliac, N., and Bridoux, M.: Chemical  
681 characterization of cloud water collected at Puy de Dôme by FT-ICR MS reveals the presence of SOA components, *Environ.*  
682 *Sci. Technol.*, 52, 10275–10285, <https://doi.org/10.1021/acsearthspacechem.9b00153>, 2018.
- 683
- 684 Bianco, A., Passananti, M., Brigante, M., and Mailhot, G.: Photochemistry of the cloud aqueous phase: a review, *Molecules*,  
685 25, 423, <https://doi.org/10.3390/molecules25020423>, 2020.
- 686
- 687 [Birks, J.B.: \*Organic Molecular Photophysics\*, John Wiley & Sons, 1973.](#)
- 688
- 689 Blando, J. D. and Turpin, B. J.: Secondary organic aerosol formation in cloud and fog droplets: a literature evaluation of  
690 plausibility, *Atmos. Environ.*, 34, 1623–1632, [https://doi.org/10.1016/S1352-2310\(99\)00392-1](https://doi.org/10.1016/S1352-2310(99)00392-1), 2000.
- 691
- 692 Bond, T. C., Streets, D. G., Yarber, K. F., Nelson, S. M., Woo, J.-H., and Klimont, Z.: A technology-based global inventory of  
693 black and organic carbon emissions from combustion, *J. Geophys. Res.*, 109, <https://doi.org/10.1029/2003JD003697>, 2004.
- 694 [Bouillon, R.C. and Miller, W.L.: Photodegradation of dimethyl sulfide \(DMS\) in natural waters: laboratory assessment of the  
695 nitrate photolysis induced DMS oxidation, \*Environ. Sci. Technol.\*, 39, 9471–9477, <https://doi.org/10.1021/es048022z>, 2005.](#)
- 696
- 697 Brezonik, P. L. and Fulkerson-Brekken, J.: Nitrate-induced photolysis in natural waters: controls on concentrations of hydroxyl  
698 radical photo-intermediates by natural scavenging agents, *Environ. Sci. Technol.*, 32, 3004–3010,  
699 [mhttps://doi.org/10.1021/es9802908](https://doi.org/10.1021/es9802908), 1998.
- 700

701 Canonica, S., Jans, U., Stemmler, K., and Hoigne, J.: Transformation kinetics of phenols in water: Photosensitization by  
702 dissolved natural organic material and aromatic ketones, *Environ. Sci. Technol.*, 29, 1822–1831,  
703 <https://doi.org/10.1021/es00007a020>, 1995.  
704  
705 Canonica, S., Hellrung, B., and Wirz, J.: Oxidation of phenols by triplet aromatic ketones in aqueous solution, *J. Phys. Chem.*,  
706 104, 1226–1232, <https://doi.org/10.1021/jp9930550>, 2000.  
707  
708 ~~Canonica, S., Kohn, T., Mac, M., Real, F.J., Wirz, J., and Von Gunten, U.: Photosensitizer method to determine rate constants~~  
709 ~~for the reaction of carbonate radical with organic compounds, *Environ. Sci. Technol.*, 39, 9182–9188,~~  
710 ~~<https://doi.org/10.1021/es051236b>, 2005.~~  
711 ~~Carey, F. A.: *Organic Chemistry*, 4th Ed., McGraw-Hill, USA, 2000.~~  
712  
713 Chang, J. L. and Thompson, J. E.: Characterization of colored products formed during irradiation of aqueous solutions  
714 containing H<sub>2</sub>O<sub>2</sub> and phenolic compounds, *Atmos. Environ.*, 44, 541–551, <https://doi.org/10.1016/j.atmosenv.2009.10.042>,  
715 2010.



716  
717  
718 Chen, Y., Li, N., Li, X., Tao, Y., Luo, S., Zhao, Z., Ma, S., Huang, H., Chen, Y., Ye, Z., and Ge, X.: Secondary organic aerosol  
719 formation from  $^3\text{C}^*$ -initiated oxidation of 4-ethylguaiacol in atmospheric aqueous-phase, *Sci. Total Environ.*, 723, 137953,  
720 <https://doi.org/10.1016/j.scitotenv.2020.137953>, 2020.  
721  
722 Chu, L. and Anastasio, C.: Quantum yields of hydroxyl radical and nitrogen dioxide from the photolysis of nitrate on ice, *J.*  
723 *Phys. Chem. A*, 107, 9594–9602, <https://doi.org/10.1021/jp0349132>, 2003.  
724  
725 Collett, J. L. Jr., Hoag, K. J., Sherman, D. E., Bator, A., and Richards, L. W.: Spatial and temporal variations in San Joaquin  
726 Valley fog chemistry, *Atmos. Environ.*, 33, 129–140, [https://doi.org/10.1016/S1352-2310\(98\)00136-8](https://doi.org/10.1016/S1352-2310(98)00136-8), 1998.  
727  
728 ~~Collett, J. L. Jr., Hoag, K. J., Rao, X., and Pandis, S. N.: Internal acid buffering in San Joaquin Valley fog drops and its~~  
729 ~~influence on aerosol processing, *Atmos. Environ.*, 33, 4833–4847, [https://doi.org/10.1016/S1352-2310\(99\)00221-6](https://doi.org/10.1016/S1352-2310(99)00221-6), 1999.~~  
730  
731 ~~De Gouw, J. and Jimenez, J. L.: Organic aerosols in the Earth's atmosphere, *Environ. Sci. Technol.*, 43, 7614–7618,~~  
732 ~~<https://doi.org/10.1021/es9006004>, 2009.~~  
733  
734 De Haan, D. O., Corrigan, A. L., Tolbert, M. A., Jimenez, J. L., Wood, S. E., and Turley, J. J.: Secondary organic aerosol  
735 formation by self-reactions of methylglyoxal and glyoxal in evaporating droplets, *Environ. Sci. Technol.*, 43, 8184–8190,  
736 <https://doi.org/10.1021/es902152t>, 2009.  
737  
738 De Haan, D. O., Hawkins, L. N., Kononenko, J. A., Turley, J. J., Corrigan, A. L., Tolbert, M. A., and Jimenez, J. L.: Formation  
739 of nitrogen-containing oligomers by methylglyoxal and amines in simulated evaporating cloud droplets, *Environ. Sci. Technol.*,  
740 45, 984–991, <https://doi.org/10.1021/es102933x>, 2011.  
741  
742 De Haan, D.O., Pajunoja, A., Hawkins, L. N., Welsh, H.G., Jimenez, N. G., De Loera, A., Zauscher, M., Andretta, A. D.,  
743 Joyce, B. W., De Haan, A. C., Riva, M., Cui, T., Surratt, J. D., Cazaunau, M., Formenti, P., Gratién, A., Panguí, E., and  
744 Doussin, J-F.: Methylamine's effects on methylglyoxal-containing aerosol: chemical, physical, and optical changes, *ACS*  
745 *Earth Space Chem.*, 3, 1706–1716, <https://doi.org/10.1021/acsearthspacechem.9b00103>, 2019.  
746  
747 De Laurentiis, E., Socorro, J., Vione, D., Quivet, E., Brigante, M., Mailhot, G., Wortham, H., and Gligorovski, S.:  
748 Phototransformation of 4-phenoxyphenol sensitised by 4-carboxybenzophenone: Evidence of new photochemical pathways in  
749 the bulk aqueous phase and on the surface of aerosol deliquescent particles, *Atmos. Environ.*, 81, 569–578,  
750 <https://doi.org/10.1016/j.atmosenv.2013.09.036>, 2013a.  
751  
752 De Laurentiis, E., Sur, B., Pazzi, M., Maurino, V., Minero, C., Mailhot, G., Brigante, M., and Vione, D.: Phenol transformation  
753 and dimerisation, photosensitised by the triplet state of 1-nitronaphthalene: A possible pathway to humic-like substances  
754 (HULIS) in atmospheric waters, *Atmos. Environ.*, 70, 318–327, <https://doi.org/10.1016/j.atmosenv.2013.01.014>, 2013b.  
755  
756 Desyaterik, Y., Sun, Y., Shen, X., Lee, T., Wang, X., Wang, T., and Collett, J. L. Jr.: Speciation of “brown” carbon in cloud  
757 water impacted by agricultural biomass burning in eastern China, *J. Geophys. Res. Atmos.*, 118, 7389–7399,  
758 <https://doi.org/10.1002/jgrd.50561>, 2013.  
759  
760 Du, Y., Fu, Q. S., Li, Y., and Su, Y.: Photodecomposition of 4-chlorophenol by reactive oxygen species in UV/air system, *J.*  
761 *Hazard. Mater.*, 186, 491–496, <https://doi.org/10.1016/j.jhazmat.2010.11.023>, 2011.  
762  
763 Dzengel, J., Theurich, J., and Bahnemann, D. W.: Formation of nitroaromatic compounds in advanced oxidation processes:  
764 photolysis versus photocatalysis, *Environ. Sci. Technol.*, 33, 294–300, <https://doi.org/10.1021/es980358j>, 1999.

765  
766  
767 Evrens, B., Turpin, B. J., and Weber, R. J.: Secondary organic aerosol formation in cloud droplets and aqueous particles  
768 (aqSOA): a review of laboratory, field and model studies, *Atmos. Chem. Phys.*, 11, 11069–11102, [https://doi.org/10.5194/acp-](https://doi.org/10.5194/acp-11-11069-2011)  
769 11-11069-2011, 2011.  
770  
771 Fischer, M. and Warneck, P.: Photodecomposition of nitrite and undissociated nitrous acid in aqueous solution, *J. Phys. Chem.*,  
772 100, 18749–18756, <https://doi.org/10.1021/jp961692+>, 1996.  
773  
774 [Fleming, L. T., Lin, P., Laskin, A., Laskin, J., Weltman, R., Edwards, R. D., Arora, N. K., Yadav, A., Meinardi, S., Blake, D.](https://doi.org/10.5194/acp-18-2461-2018)  
775 [R., Pillarisetti, A., Smith, K. R., and Nizkorodov, S. A.: Molecular composition of particulate matter emissions from dung and](https://doi.org/10.5194/acp-18-2461-2018)  
776 [brushwood burning household cookstoves in Haryana, India, \*Atmos. Chem. Phys.\*, 18, 2461–2480,](https://doi.org/10.5194/acp-18-2461-2018)  
777 <https://doi.org/10.5194/acp-18-2461-2018>, 2018.  
778  
779  
780 Foote, C.S.: Definition of type I and type II photosensitized oxidation, *Photochem. Photobiol.*, 54, 659,  
781 <https://doi.org/10.1111/j.1751-1097.1991.tb02071.x>, 1991.  
782  
783 Galloway, M. M., Chhabra, P. S., Chan, A. W. H., Surratt, J. D., Flagan, R. C., Seinfeld, J. H., and Keutsch, F. N.: Glyoxal  
784 uptake on ammonium sulphate seed aerosol: reaction products and reversibility of uptake under dark and irradiated conditions,  
785 *Atmos. Chem. Phys.*, 9, 3331–3345, <https://doi.org/10.5194/acp-9-3331-2009>, 2009.  
786  
787 Gelencsér, A., Hoffer, A., Kiss, G., Tombácz, E., Kurdi, R., and Bencze, L.: In-situ formation of light-absorbing organic matter  
788 in cloud water, *J. Atmos. Chem.*, 45, 25–33, <https://doi.org/10.1023/A:1024060428172>, 2003.  
789  
790 Gen, M., Huang, D. D., and Chan, C. K.: Reactive uptake of glyoxal by ammonium-containing salt particles as a function of  
791 relative humidity, *Environ. Sci. Technol.*, 52, 6903–6911, <https://doi.org/10.1021/acs.est.8b00606>, 2018.  
792  
793 Gen, M., Zhang, R., Huang, D. D., Li, Y., and Chan, C. K.: Heterogeneous SO<sub>2</sub> oxidation in sulfate formation by photolysis  
794 of particulate nitrate, *Environ. Sci. Technol. Lett.*, 6, 86–91, <https://doi.org/10.1021/acs.estlett.8b00681>, 2019a.  
795  
796 Gen, M., Zhang, R., Huang, D. D., Li, Y., and Chan, C. K.: Heterogeneous oxidation of SO<sub>2</sub> in sulfate production during nitrate  
797 photolysis at 300 nm: Effect of pH, relative humidity, irradiation intensity, and the presence of organic compounds, *Environ.*  
798 *Sci. Technol.*, 53, 8757–8766, <https://doi.org/10.1021/acs.est.9b01623>, 2019b.  
799  
800 George, C., Ammann, M., D’Anna, B., Donaldson, D.J., and Nizkorodov, S.A.: Heterogeneous photochemistry in the  
801 atmosphere, *Chem. Rev.*, 115, 4218–4258, <https://doi.org/10.1021/cr500648z>, 2015.  
802  
803 [George, C., Brüggemann, M., Hayeck, N., Tinel, L., and Donaldson, D. J.: Interfacial photochemistry: physical chemistry of](https://doi.org/10.1016/B978-0-12-813641-6.00014-5)  
804 [gas-liquid interfaces, in: \*Developments in Physical & Theoretical Chemistry\*, edited by: Faust, J. A. and House, J. E., Elsevier,](https://doi.org/10.1016/B978-0-12-813641-6.00014-5)  
805 [435–457, https://doi.org/10.1016/B978-0-12-813641-6.00014-5](https://doi.org/10.1016/B978-0-12-813641-6.00014-5), 2018.  
806  
807  
808 Gilardoni, S., Massoli, P., Paglione, M., Giulianelli, L., Carbone, C., Rinaldi, M., Decesari, S., Sandrini, S., Costabile, F.,  
809 Gobbi, G.P., Pietrogrande, M.C., Visentin, M., Scotto, F., Fuzzi, S., and Facchini, M.C.: Direct observation of aqueous  
810 secondary organic aerosol from biomass-burning emissions, *PNAS.*, 113, 10013–10018,  
811 <https://doi.org/10.1073/pnas.1602212113>, 2016.  
812

813 Giulianelli, L., Gilardoni, S., Tarozzi, L., Rinaldi, M., Decesari, S., Carbone, C., Facchini, M. C., and Fuzzi, S.: Fog occurrence  
814 and chemical composition in the Po valley over the last twenty years, *Atmos. Environ.*, 98, 394–401,  
815 <https://doi.org/10.1016/j.atmosenv.2014.08.080>, 2014.

~~816 Gold, M. H., Kutsuki, H., and Morgan, M. A.: Oxidative degradation of lignin by photochemical and chemical radical  
817 generating systems, *Photochem. Photobiol.*, 38, 647–651, <https://doi.org/10.1111/j.1751-1097.1983.tb03595.x>, 1983.~~

818

819 Goldstein, S. and Czapski, G.: Kinetics of nitric oxide autoxidation in aqueous solution in the absence and presence of various  
820 reductants. The nature of the oxidizing intermediates, *J. Am. Chem. Soc.*, 117, 12078–12084,  
821 <https://doi.org/10.1021/ja00154a007>, 1995a.

822

~~823 Goldstein, S. and Czapski, G.: The reaction of  $\cdot\text{NO}$  with  $\text{O}_2^-$  and  $\cdot\text{HO}_2$ : a pulse radiolysis study, *Free Radical Biol. Med.*, 19,  
824 505–510, [https://doi.org/10.1016/0891-5849\(95\)00034-U](https://doi.org/10.1016/0891-5849(95)00034-U), 1995b.~~

825

~~826 Goldstein, S., Czapski, G., Lind, J., and Merényi, G.: Mechanism of decomposition of peroxyxynitric Ion ( $\text{O}_2\text{NOO}^-$ ): Evidence  
827 for the formation of  $\text{O}_2^-$  and  $\cdot\text{NO}_2$  radicals, *Inorg. Chem.*, 37, 3943–3947, <https://doi.org/10.1021/ic980051i>, 1998.~~

828

~~829 Goldstein, S., Lind, J., and Merényi, G.: Chemistry of peroxyxynitrites as compared to peroxyxynitrates, *Chem. Rev.*, 10, 2457–  
830 2470, <https://doi.org/10.1021/cr0307087>, 2005.~~

831

832 Grosjean, D.: Reactions of o-cresol and nitrocresol with nitrogen oxides ( $\text{NO}_x$ ) in sunlight and with ozone–nitrogen dioxide  
833 mixtures in the dark, *Environ. Sci. Technol.*, 19, 968–974, <https://doi.org/10.1021/es00140a014>, 1985.

834

835 Herrmann, H.: On the photolysis of simple anions and neutral molecules as sources of  $\text{O}^-/\text{OH}$ ,  $\text{SO}_x^-$  and  $\text{Cl}$  in aqueous solution,  
836 *Phys. Chem. Chem. Phys.*, 9, 3935–3964, <https://doi.org/10.1039/B618565G>, 2007.

837

838 Herrmann, H., Hoffmann, D., Schaefer, T., Brüner, P., and Tilgner, A.: Tropospheric aqueous-phase free-radical chemistry:  
839 Radical sources, spectra, reaction kinetics and prediction tools, *Chem Phys Chem.*, 11, 3796–3822,  
840 <https://doi.org/10.1002/cphc.201000533>, 2010.

841

~~842 Hippelein, M.: Background concentrations of individual and total volatile organic compounds in residential indoor air of  
843 Schleswig-Holstein, Germany, *J. Environ. Monit.*, 6, 745–752, <https://doi.org/10.1039/b401139m>, 2004.~~

844

845 Hoffer, A., Kiss, G., Blazsó, M., and Gelencsér, A.: Chemical characterization of humic-like substances (HULIS) formed from  
846 a lignin-type precursor in model cloud water, *Geophys. Res. Lett.*, 31, <https://doi.org/10.1029/2003GL018962>, 2004.

847

848 Hoffmann, E.H., Tilgner, A., Wolke, R., Böge, O., Walter, A., and Herrmann, H.: Oxidation of substituted aromatic  
849 hydrocarbons in the tropospheric aqueous phase: kinetic mechanism development and modelling, *Phys. Chem. Chem. Phys.*,  
850 20, 10960–10977, <https://doi.org/10.1039/C7CP08576A>, 2018.

851

852 Holčapek, M., Jirásko, R., and Lísa, M.: Basic rules for the interpretation of atmospheric pressure ionization mass spectra of  
853 small molecules, *J. Chromatogr. A*, 1217, 3908–3921, <https://doi.org/10.1016/j.chroma.2010.02.049>, 2010.

854

855 Huang, D. D., Zhang, Q., Cheung, H. H. Y., Yu, L., Zhou, S., Anastasio, C., Smith, J. D., and Chan, C. K.: Formation and  
856 evolution of aqSOA from aqueous-phase reactions of phenolic carbonyls: comparison between ammonium sulfate and  
857 ammonium nitrate solutions, *Environ. Sci. Technol.*, 52, 9215–9224, <https://doi.org/10.1021/acs.est.8b03441>, 2018.

~~858 Huang, J. P. and Mabury, S. A.: The role of carbonate radical in limiting the persistence of sulfur-containing chemicals in  
859 sunlit natural waters, *Chemosphere*, 41, 1775–1782, [https://doi.org/10.1016/S0045-6535\(00\)00042-4](https://doi.org/10.1016/S0045-6535(00)00042-4), 2000.~~

860

861 Huang, R.-J., Zhang, Y., Bozzetti, C., Ho, K.-F., Cao, J.-J., Han, Y., Daellenbach, K. R., Slowik, J. G., Platt, S. M., Canonaco,  
862 F., Zotter, P., Wolf, R., Pieber, S. M., Bruns, E. A., Crippa, M., Ciarelli, G., Piazzalunga, A., Schwikowski, M., Abbaszade,

863 G., Schnelle-Kreis, J., Zimmermann, R., An, Z., Szidat, S., Baltensperger, U., El Haddad, I., and Prévôt, A. S. H.: High  
864 secondary aerosol contribution to particulate pollution during haze events in China, *Nature*, 514, 218–222,  
865 <https://doi.org/10.1038/nature13774>, 2014.

866

867 Huang, X. H. H., Ip, H. S. S., and Yu, J. Z.: Secondary organic aerosol formation from ethylene in the urban atmosphere of  
868 Hong Kong: A multiphase chemical modeling study, *J. Geophys. Res.*, 116, D03206, <https://doi.org/10.1029/2010JD014121>,  
869 2011.

870

871 Jacobson, M. Z.: Isolating nitrated and aromatic aerosols and nitrated aromatic gases as sources of ultraviolet light absorption,  
872 *J. Geophys. Res.*, 104, 3527–3542, <https://doi.org/10.1029/1998JD100054>, 1999.

873

874 Jiang, W., Misovich, M. V., Hettiyadura, A. P. S., Laskin, A., McFall, A. S., Anastasio, C., and Zhang, Q.: Photosensitized  
875 reactions of a phenolic carbonyl from wood combustion in the aqueous phase—chemical evolution and light absorption  
876 properties of aqSOA, *Environ. Sci. Technol.*, 55, 5199–5211, <https://doi.org/10.1021/acs.est.0c07581>, 2021.

877

878 Jimenez, J. L., Canagaratna, M. R., Donahue, N. M., Prevot, A.S.H., Zhang, Q., Kroll, J. H., DeCarlo, P. F., Allan, J. D., Coe,  
879 H., Ng, N. L., Aiken, A.C., Docherty, K.S., Ulbrich, I. M., Grieshop, A. P., Robinson, A. L., Duplissy, J., Smith, J. D., Wilson,  
880 K. R., Lanz, V.A., Hueglin, C., Sun, Y. L., Tian, J., Laaksonen, A., Raatikainen, T., Rautiainen, J., Vaattovaara, P., Ehn, M.,  
881 Kulmala, M., Tomlinson, J. M., Collins, D. R., Cubison, M. J., Dunlea, E., J., Huffman, J. A., Onasch, T. B., Alfarra, M. R.,  
882 Williams, P. I., Bower, K., Kondo, Y., Schneider, J., Drewnick, F., Borrmann, S., Weimer, S., Demerjian, K., Salcedo, D.,  
883 Cottrell, L., Griffin, R., Takami, A., Miyoshi, T., Hatakeyama, S., Shimono, A., Sun, J. Y., Zhang, Y. M., Dzepina, K., Kimmel,  
884 J. R., Sueper, D., Jayne, J. T., Herndon, S. C., Trimborn, A. M., Williams, L. R., Wood, E. C., Middlebrook, A. M., Kolb, C.  
885 E., Baltensperger, U., and Worsnop, D. R.: Evolution of organic aerosols in the atmosphere, *Science*, 326, 1525–1529,  
886 <https://doi.org/10.1126/science.1180353>, 2009.

887 ~~Jung, H., Chadha, T. S., Kim, D., Biswas, P., and Jun, Y. S.: Photochemically assisted fast abiotic oxidation of manganese and~~  
888 ~~formation of  $\delta$ -MnO<sub>2</sub> nanosheets in nitrate solution, *Chem. Commun.*, 53, 4445–4448, <https://doi.org/10.1039/C7CC00754J>,~~  
889 ~~2017.~~

890

891 Kahnt, A., Behrouzi, S., Vermeylen, R., Shalamzari, M. S., Vercauteren, J., Roekens, E., Claeys, M., and Maenhaut, W.: One-  
892 year study of nitro-organic compounds and their relation to wood burning in PM<sub>10</sub> aerosol from a rural site in Belgium, *Atmos.*  
893 *Environ.*, 81, 561–568, <https://doi.org/10.1016/j.atmosenv.2013.09.041>, 2013.

894 ~~Kanakidou, M., Seinfeld, J. H., Pandis, S. N., Barnes, I., Dentener, F. J., Facchini, M. C., Van Dingenen, R., Ervens, B., Nenes,~~  
895 ~~A., Nielsen, C. J., Swietlicki, E., Putaud, J. P., Balkanski, Y., Fuzzi, S., Horth, J., Moortgat, G. K., Winterhalter, R., Myhre,~~  
896 ~~C. E. L., Tsigaridis, K., Vignati, E., Stephanou, E. G., and Wilson, J.: Organic aerosol and global climate modelling: a review,~~  
897 ~~*Atmos. Chem. Phys.*, 5, 1053–1123, <https://doi.org/10.5194/acp-5-1053-2005>, 2005.~~

898

899

900 Kaur, R. and Anastasio, C.: First measurements of organic triplet excited states in atmospheric waters, *Environ. Sci. Technol.*,  
901 52, 5218–5226., <https://doi.org/10.1021/acs.est.7b06699>, 2018.

902

903 Kaur, R., Labins, J. R., Helbock, S. S., Jiang, W., Bein, K. J., Zhang, Q., and Anastasio, C.: Photooxidants from brown carbon  
904 and other chromophores in illuminated particle extracts, *Atmos. Chem. Phys.*, 19, 6579–6594, [https://doi.org/10.5194/acp-19-](https://doi.org/10.5194/acp-19-6579-2019)  
905 [6579-2019](https://doi.org/10.5194/acp-19-6579-2019), 2019.

906

907 Kebarle, P. A.: A brief overview of the mechanisms involved in electrospray mass spectrometry, *J. Mass Spectrom.*, 35,  
908 804–817, <https://doi.org/10.1002/9783527628728.ch1>, 2000.

909

910 Kim, D.-h., Lee, J., Ryu, J., Kim, K., and Choi, W.: Arsenite oxidation initiated by the UV photolysis of nitrite and nitrate,  
911 *Environ. Sci. Technol.*, 48, 4030–4037, <https://doi.org/10.1021/es500001q>, 2014.

912

913 Kitanovski, Z., Čusak, A., Grgić, I., and Claeys, M.: Chemical characterization of the main products formed through aqueous-  
914 phase photonitration of guaiacol, *Atmos. Meas. Tech.*, 7, 2457–2470, <https://doi.org/10.5194/amt-7-2457-2014>, 2014.  
915

916 Klodt, A.L., Romonosky, D.E., Lin, P., Laskin, J., Laskin, A., and Nizkorodov, S.A.: Aqueous photochemistry of secondary  
917 organic aerosol of  $\alpha$ -pinene and  $\alpha$ -humulene in the presence of hydrogen peroxide or inorganic salts, *ACS Earth Space Chem.*,  
918 3, 12, 2736–2746, <https://doi.org/10.1021/acsearthspacechem.9b00222>, 2019.  
919

920 Kourtchev, I., Fuller, S. J., Giorio, C., Healy, R. M., Wilson, E., O'Connor, I., Wenger, J. C., McLeod, M., Aalto, J.,  
921 Ruuskanen, T. M., Maenhaut, W., Jones, R., Venables, D. S., Sodeau, J. R., Kulmala, M., and Kalberer, M.: Molecular  
922 composition of biogenic secondary organic aerosols using ultrahigh-resolution mass spectrometry: comparing laboratory and  
923 field studies, *Atmos. Chem. Phys.*, 14, 2155–2167, <https://doi.org/10.5194/acp-14-2155-2014>, 2014.  
924

925 Kroflić, A., Grilc, M., and Grgić, I.: Unraveling pathways of guaiacol nitration in atmospheric waters: nitrite, a source of  
926 reactive nitronium ion in the atmosphere, *Environ. Sci. Technol.*, 49, 9150–9158, <https://doi.org/10.1021/acs.est.5b01811>,  
927 2015.  
928

929 Kroflić, A., Anders, J., Drventić, I., Mettke, P., Böge, O., Mutzel, A., Kleffmann, J., and Herrmann, H.: Guaiacol nitration in  
930 a simulated atmospheric aerosol with an emphasis on atmospheric nitrophenol formation mechanisms, *ACS Earth Space Chem.*,  
931 <https://doi.org/10.1021/acsearthspacechem.1c00014>, 2021.  
932

933 Kroll, J. H., Donahue, N. M., Jimenez, J. L., Kessler, S. H., Canagaratna, M. R., Wilson, K. R., Altieri, K. E., Mazzoleni, L.  
934 R., Wozniak, A. S., Bluhm, H., Mysak, E. R., Smith, J. D., Kolb, C. E., and Worsnop, D. R.: Carbon oxidation state as a metric  
935 for describing the chemistry of atmospheric organic aerosol, *Nat. Chem.*, 3, 133–139, <https://doi.org/10.1038/nchem.948>, 2011.  
936

937 [Kruve, A., Kaupmees, K., Liigand, J., and Leito, I.: Negative electrospray ionization via deprotonation: predicting the  
938 ionization efficiency. \*Anal. Chem.\*, 86, 4822–4830, <https://doi.org/10.1021/ac404066v>, 2014.](https://doi.org/10.1021/ac404066v)  
939

940 [Lammel, G., Perner, D., and Warneck, P.: Decomposition of pernitric acid in aqueous solution, \*J. Phys. Chem.\*, 94, 6141–6144,  
941 <https://doi.org/10.1021/j100378a091>, 1990.](https://doi.org/10.1021/j100378a091)  
942

943 Laskin, A., Laskin, J., and Nizkorodov, S.A.: Chemistry of atmospheric brown carbon, *Chem. Rev.*, 115, 4335–4382,  
944 <https://doi.org/10.1021/cr5006167>, 2015.  
945

946 [Lathioor, E. C., Leigh, W. J., and St. Pierre, M. J.: Geometrical effects on intramolecular quenching of aromatic ketone \( \$\pi,\pi^\*\$ \)  
947 triplets by remote phenolic hydrogen abstraction, \*J. Am. Chem. Soc.\*, 121, 11984–11992,  
948 <https://pubs.acs.org/doi/abs/10.1021/ja991207z>, 1999.](https://pubs.acs.org/doi/abs/10.1021/ja991207z)  
949

950 LeClair, J. P., Collett, J. L., and Mazzoleni, L. R.: Fragmentation analysis of water-soluble atmospheric organic matter using  
951 ultrahigh-resolution FT-ICR mass spectrometry, *Environ. Sci. Technol.*, 46, 4312–4322, <https://doi.org/10.1021/es203509b>,  
952 2012.  
953

954 Lee, A. K. Y., Herckes, P., Leaitch, W. R., Macdonald, A. M., and Abbatt, J. P. D.: Aqueous OH oxidation of ambient organic  
955 aerosol and cloud water organics: Formation of highly oxidized products, *Geophys. Res. Lett.*, 38, L11805,  
956 <https://doi.org/10.1029/2011GL047439>, 2011.  
957

958 Lee, A. K. Y., Zhao, R., Li, R., Liggió, J., Li, S.-M., and Abbatt, J. P. D.: Formation of light absorbing organo-nitrogen species  
959 from evaporation of droplets containing glyoxal and ammonium sulfate, *Environ. Sci. Technol.*, 47, 12819–12826,  
960 <https://doi.org/10.1021/es402687w>, 2013.  
961

962 [Lee, H. J., Aiona, P. K., Laskin, A., Laskin, J., and Nizkorodov, S. A.: Effect of solar radiation on the optical properties and](#)  
963 [molecular composition of laboratory proxies of atmospheric brown carbon, \*Environ. Sci. Technol.\*, 48, 10217–](#)  
964 [10226, <https://doi.org/10.1021/es502515r>, 2014.](#)

965

966 Lee, P. C. C. and Rodgers, M. A. J.: Laser flash photokinetic studies of Rose Bengal sensitized photodynamic interactions of  
967 nucleotides and DNA, *Photochem. Photobiol.*, 45, 79–86, <https://doi.org/10.1111/j.1751-1097.1987.tb08407.x>, 1987.

968

969 [Leito, I., Herodes, K., Huopola, M., Virro, K., Künnapas, A., Krueve, A., and Tanner, R.: Towards the electrospray](#)  
970 [ionization mass spectrometry ionization efficiency scale of organic compounds, \*Rapid Commun. Mass Sp.\*, 22, 379–](#)  
971 [384, <https://doi.org/10.1002/rcm.3371>, 2008.](#)

972 ~~[Lewis, A. C., Hopkins, J. R., Carslaw, D. C., Hamilton, J. F., Nelson, B. S., Stewart, G., Dorn, J., Passant, N., and Murrells,](#)~~  
973 ~~[T.: An increasing role for solvent emissions and implications for future measurements of volatile organic compounds, \*Philos.\*](#)~~  
974 ~~[Trans. R. Soc.](#), 378, <https://doi.org/10.1098/rsta.2019.0328>, 2020.~~

975

976 Li, F., Tang, S., Tsona, N. T., and Du, L.: Kinetics and mechanism of OH-induced  $\alpha$ -terpineol oxidation in the atmospheric  
977 aqueous phase, *Atmos. Environ.*, 237, 117650, <https://doi.org/10.1016/j.atmosenv.2020.117650>, 2020.

978

979 Li, P., Li, X., Yang, C., Wang, X., Chen, J., and Collett, J. L. Jr.: Fog water chemistry in Shanghai, *Atmos. Environ.*, 45,  
980 4034–4041, <https://doi.org/10.1016/j.atmosenv.2011.04.036>, 2011.

981

982 Li, Y. J., Huang, D. D., Cheung, H. Y., Lee, A. K. Y., and Chan, C. K.: Aqueous-phase photochemical oxidation and direct  
983 photolysis of vanillin - a model compound of methoxy phenols from biomass burning, *Atmos. Chem. Phys.*, 14, 2871–2885,  
984 <https://doi.org/10.5194/acp-14-2871-2014>, 2014.

985

986 Liang, Z., Zhang, R., Gen, M., Chu, Y., and Chan, C. K.: Nitrate photolysis in mixed sucrose–nitrate–sulfate particles at  
987 different relative humidities, *J. Phys. Chem. A*, 125, 3739–3747, <https://doi.org/10.1021/acs.jpca.1c00669>, 2021.

988

989 Liigand, P., Kaupmees, K., Haav, K., Liigand, J., Leito, I., Girod, M., Antoine, R., and Krueve, A.: Think negative: finding the  
990 best electrospray ionization/MS mode for your analyte, *Anal. Chem.*, 89, 5665–5668, <https://doi.org/10.1021/acs.analchem.7>,  
991 2017.

992

993 Lim, Y. B., Tan, Y., Perri, M. J., Seitzinger, S. P., and Turpin, B. J.: Aqueous chemistry and its role in secondary organic  
994 aerosol (SOA) formation, *Atmos. Chem. Phys.*, 10, 10521–10539, <https://doi.org/10.5194/acp-10-10521-2010>, 2010.

995

996 ~~[Lin, P., Fleming, L. T., Nizkorodov, S. A., Laskin, J., and Laskin, A.: Comprehensive molecular characterization of](#)~~  
997 ~~[atmospheric brown carbon by high resolution mass spectrometry with electrospray and atmospheric pressure photoionization,](#)~~  
998 ~~[Anal. Chem.](#), 90, 12493–12502, <https://doi.org/10.1021/acs.analchem.8b02177>, 2018.~~

999

1000 Lin, P., Yu, J. Z., Engling, G., and Kalberer, M.: Organosulfates in humic-like substance fraction isolated from aerosols at  
1001 seven locations in East Asia: a study by ultra-high-resolution mass spectrometry, *Environ. Sci. Technol.*, 46, 13118–13127,  
1002 <https://doi.org/10.1021/es303570v>, 2012.

1003

1004 ~~[Lin, P., Fleming, L. T., Nizkorodov, S. A., Laskin, J., and Laskin, A.: Comprehensive molecular characterization of](#)~~  
1005 ~~[atmospheric brown carbon by high resolution mass spectrometry with electrospray and atmospheric pressure photoionization,](#)~~  
1006 ~~[Anal. Chem.](#), 90, 12493–12502, <https://doi.org/10.1021/acs.analchem.8b02177>, 2018.~~

1007

1008 Liu, C., Liu, J., Liu, Y., Chen, T., and He, H.: Secondary organic aerosol formation from the OH-initiated oxidation of guaiacol  
1009 under different experimental conditions, *Atmos. Environ.*, 207, 30–37, <https://doi.org/10.1016/j.atmosenv.2019.03.021>, 2019.

1010

1011 Lobodin, V. V., Marshall, A. G., and Hsu, C. S.: Compositional space boundaries for organic compounds, *Anal. Chem.*, 84,  
1012 3410–3416, <https://doi.org/10.1021/ac300244f>, 2012.

1013

1014 Loisel, G., Mekic, M., Liu, S., Song, W., Jiang, B., Wang, Y., Deng, H., and Gligorovski, S.: Ionic strength effect on the  
1015 formation of organonitrate compounds through photochemical degradation of vanillin in liquid water of aerosols, *Atmos.*  
1016 *Environ.*, 246, 118140, <https://doi.org/10.1016/j.atmosenv.2020.118140>, 2021.

1017

1018 Ma, L., Guzman, C., Niedek, C., Tran, T., Zhang, Q., and Anastasio, C.: Kinetics and mass yields of aqueous secondary organic  
1019 aerosol from highly substituted phenols reacting with a triplet excited state, *Environ. Sci. Technol.*, 55, 5772–5781,  
1020 <https://doi.org/10.1021/acs.est.1c00575>, 2021.

1021

1022 Mabato, B. R. G., Gen, M., Chu, Y., and Chan, C. K.: Reactive uptake of glyoxal by methylammonium-containing salts as a  
1023 function of relative humidity, *ACS Earth Space Chem.*, 3, 150–157, <https://doi.org/10.1021/acsearthspacechem.8b00154>, 2019.

1024

1025 Machado, F. and Boule, P.: Photonitration and photonitrosation of phenolic derivatives induced in aqueous solution by  
1026 excitation of nitrite and nitrate ions, *J. Photochem. Photobiol. A: Chem.*, 86, 73–80, [https://doi.org/10.1016/1010-1027-6030\(94\)03946-R](https://doi.org/10.1016/1010-1027-6030(94)03946-R), 1995.

1028

1029 Mack, J. and Bolton, J.R.: Photochemistry of nitrite and nitrate in aqueous solution: a review, *J. Photochem. Photobiol. Chem.*,  
1030 128, 1–13, [https://doi.org/10.1016/S1010-6030\(99\)00155-0](https://doi.org/10.1016/S1010-6030(99)00155-0), 1999.

1031

1032 Mazzoleni, L. R., Saranjampour, P., Dalbec, M. M., Samburova, V., Hallar, A. G., Zielinska, B., Lowenthal, D. H., and Kohl,  
1033 S.: Identification of water-soluble organic carbon in non-urban aerosols using ultrahigh-resolution FT-ICR mass spectrometry:  
1034 organic anions, *Environ. Chem.*, 9, 285–297, <https://doi.org/10.1071/EN11167>, 2012.

1035

1036 McFall, A. S., Johnson, A. W., and Anastasio, C.: Air–water partitioning of biomass-burning phenols and the effects of  
1037 temperature and salinity, *Environ. Sci. Technol.*, 54, 3823–3830, <https://doi.org/10.1021/acs.est.9b06443>, 2020.

1038

1039 [McNally, A. M., Moody, E. C., and McNeill, K.: Kinetics and mechanism of the sensitized photodegradation of lignin model](#)  
1040 [compounds, \*Photochem. Photobiol. Sci.\*, 4, 268–274, <https://doi.org/10.1039/B416956E>, 2005.](#)

1041

1042 [Minella, M., Romeo, F., Vione, D., Maurino, V., and Minero, C.: Low to negligible photoactivity of lake-water matter in the](#)  
1043 [size range from 0.1 to 5  \$\mu\text{m}\$ , \*Chemosphere\*, 83, 1480–1485, <https://doi.org/10.1016/j.chemosphere.2011.02.093>, 2011.](#)

1044

1045 Minero, C., Bono, F., Rubertelli, F., Pavino, D., Maurino, V., Pelizzetti, E., and Vione, D.: On the effect of pH in aromatic  
1046 photonitration upon nitrate photolysis, *Chemosphere*, 66, 650–656, <https://doi.org/10.1016/j.chemosphere.2006.07.082>, 2007.

1047

1048 Mohr, C., Lopez-Hilfiker, F. D., Zotter, P., Prévôt, A. S. H., Xu, L., Ng, N. L., Herndon, S. C., Williams, L. R., Franklin, J.  
1049 P., Zahniser, M. S., Worsnop, D. R., Knighton, W. B., Aiken, A. C., Gorkowski, K. J., Dubey, M. K., Allan, J. D., and Thornton,  
1050 J. A.: Contribution of nitrated phenols to wood burning brown carbon light absorption in Detling, United Kingdom during  
1051 winter time, *Environ. Sci. Technol.*, 47, 6316–6324, <https://doi.org/10.1021/es400683v>, 2013.

1052

1053 Munger, J. W., Jacob, D. J., Waldman, J. M., and Hoffmann, M. R.: Fogwater chemistry in an urban atmosphere, *J. Geophys.*  
1054 *Res. Oceans*, 88, 5109–5121, <https://doi.org/10.1029/JC088iC09p05109>, 1983.

1055 [Neta, P., Huie, R. E., and Ross, A.: Rate constants for reactions of inorganic radicals in aqueous solution, \*J. Phys. Chem. Ref. Data\*, 17, 1027–1284, <https://doi.org/10.1063/1.555808>, 1988.](#)

1056

1057 [Neumann, M. G., De Groote, R. A. M. C., and Machado, A. E. H.: Flash photolysis of lignin: Part 1. Deaerated solutions of](#)  
1058 [dioxane-lignin, \*Polym. Photochem.\*, 7, 401–407, \[https://doi.org/10.1016/0144-2880\\(86\\)90007-2\]\(https://doi.org/10.1016/0144-2880\(86\)90007-2\), 1986a.](#)

1059

1060 [Neumann, M. G., De Groot, R. A. M. C., and Machado, A. E. H.: Flash photolysis of lignin: II. Oxidative photodegradation](#)  
1061 [of dioxane-lignin, Polym. Photochem., 7, 461–468, \[https://doi.org/10.1016/0144-2880\\(86\\)90015-1\]\(https://doi.org/10.1016/0144-2880\(86\)90015-1\), 1986b.](#)  
1062  
1063 [Ning, C., Gao, Y., Zhang, H., Yu, H., Wang, L., Geng, N., Cao, R., and Chen, J.: Molecular characterization of dissolved](#)  
1064 [organic matters in winter atmospheric fine particulate matters \(PM<sub>2.5</sub>\) from a coastal city of northeast China, Sci. Total](#)  
1065 [Environ., 689, 312–321, <https://doi.org/10.1016/j.scitotenv.2019.06.418>, 2019.](#)  
1066  
1067 Nolte, C. G., Schauer, J. J., Cass, G. R., and Simoneit, B. R. T.: Highly polar organic compounds present in wood smoke and  
1068 in the ambient atmosphere, Environ. Sci. Technol., 35, <https://doi.org/10.1021/es001420r>, 1912–1919, 2001.  
1069  
1070 Nozière, B., Dziedzic, P., and Córdova, A.: Products and kinetics of the liquid-phase reaction of glyoxal catalyzed by  
1071 ammonium ions (NH<sub>4</sub><sup>+</sup>), J. Phys. Chem. A, 113, 231–237, <https://doi.org/10.1021/jp8078293>, 2009.  
1072  
1073 [Olofsson, M., Ek-Olausson, B., Ljungström, E., and Langer, S.: Flux of organic compounds from grass measured by relaxed](#)  
1074 [eddy accumulation technique, J. Environ. Monit., 5, 963–970, <https://doi.org/10.1039/B303329E>, 2003.](#)  
1075 [Onori, G. and Santucci, A.: Dynamical and structural properties of water/alcohol mixtures, J. Mol. Liq., 69, 161–181,](#)  
1076 [https://doi.org/10.1016/S0167-7322\(96\)90012-4, 1996.](#)  
1077  
1078 Pang, H., Zhang, Q., Lu, X. H., Li, K., Chen, H., Chen, J., Yang, X., Ma, Y., Ma, J., and Huang, C.: Nitrite-mediated  
1079 photooxidation of vanillin in the atmospheric aqueous phase, Environ. Sci. Technol., 53, 14253–14263,  
1080 <https://doi.org/10.1021/acs.est.9b03649>, 2019a.  
1081  
1082 Pang, H., Zhang, Q., Wang, H., Cai, D., Ma, Y., Li, L., Li, K., Lu, X., Chen, H., Yang, X., and Chen, J.: Photochemical aging  
1083 of guaiacol by Fe(III)-oxalate complexes in atmospheric aqueous phase, Environ. Sci. Technol., 53, 127–136,  
1084 <https://doi.org/10.1021/acs.est.8b04507>, 2019b.  
1085  
1086 [Perry, R. H., Cooks, R. G., and Noll, R. J.: Orbitrap mass spectrometry: instrumentation, ion motion and applications, Mass](#)  
1087 [Spectrom. Rev., 27, 661–699, <https://doi.org/10.1002/mas.20186>, 2008.](#)  
1088  
1089 Powelson, M. H., Espelien, B. M., Hawkins, L. N., Galloway, M. M., and De Haan, D. O.: Brown carbon formation by  
1090 aqueous-phase carbonyl compound reactions with amines and ammonium sulfate, Environ. Sci. Technol., 48, 985–993,  
1091 <https://doi.org/10.1021/es4038325>, 2014.  
1092  
1093 [Pöschl, U.: Atmospheric aerosols: composition, transformation, climate, and health effects, Angew. Chem. Int., 44, 7520–](#)  
1094 [7540, <https://doi.org/10.1002/anie.200501122>, 2005.](#)  
1095 [Priya, A. M. and Lakshmi pathi, S.: DFT study on abstraction reaction mechanism of OH radical with 2-methoxyphenol, J. Phys.](#)  
1096 [Org. Chem., 30, <https://doi.org/10.1002/poc.3713>, 2017.](#)  
1097  
1098 Pye, H., Nenes, A., Alexander, B., Ault, A. P., Barth, M. C., Clegg, S. L., Collett, J. L. Jr., Fahey, K. M., Hennigan, C. J.,  
1099 Herrmann, H., Kanakidou, M., Kelly, J. T., Ku, I. T., McNeill, V. F., Riemer, N., Schaefer, T., Shi, G., Tilgner, A., Walker, J.  
1100 T., Wang, T., Weber, R., Xing, J., Zaveri, R. A., and Zuend, A.: The acidity of atmospheric particles and clouds, Atmos. Chem.  
1101 Phys., 20, 4809–4888, <https://doi.org/10.5194/acp-20-4809-2020>, 2020.



1102  
1103  
1104 Qi, L., Chen, M., Stefenelli, G., Pospisilova, V., Tong, Y., Bertrand, A., Hueglin, C., Ge, X., Baltensperger, U., Prévôt, A. S.  
1105 H., and Slowik, J.G.: Organic aerosol source apportionment in Zurich using an extractive electrospray ionization time-of-flight  
1106 mass spectrometer (EESI-TOF-MS) — Part 2: Biomass burning influences in winter, *Atmos. Chem. Phys.*, 19, 8037–8062,  
1107 <https://doi.org/10.5194/acp-19-8037-2019>, 2019.

1108  
1109 Rizzo, L.V., Artaxo, P., Karl, T., Guenther, A.B., and Greenberg, J.: Aerosol properties, in canopy gradients, turbulent fluxes  
1110 and VOC concentrations at a pristine forest site in Amazonia, *Atmos. Environ.*, 44, 503–511,  
1111 <https://doi.org/10.1016/j.atmosenv.2009.11.002>, 2010.

1112  
1113 Rogge, W. F., Hildemann, L. M., Mazurek, M. A., Cass, G. R., and Simoneit, B. R. T.: Sources of fine organic aerosol. 9. Pine,  
1114 oak, and synthetic log combustion in residential fireplaces, *Environ. Sci. Technol.*, 32, 13–22,  
1115 <https://doi.org/10.1021/es960930b>, 1998.

1116  
1117 Romonosky, D. E., Li, Y., Shiraiwa, M., Laskin, A., Laskin, J., and Nizkorodov, S. A.: Aqueous photochemistry of secondary  
1118 organic aerosol of  $\alpha$ -Pinene and  $\alpha$ -Humulene oxidized with ozone, hydroxyl radical, and nitrate radical, *J. Phys. Chem. A*, 121,  
1119 1298–1309, <https://doi.org/10.1021/acs.jpca.6b10900>, 2017.

1120  
1121 Scharko, N. K., Berke, A. E., and Raff, J. D.: Release of nitrous acid and nitrogen dioxide from nitrate photolysis in acidic  
1122 aqueous solutions, *Environ. Sci. Technol.*, 48, 20, 11991–1200, <https://doi.org/10.1021/es503088x>, 2014.

1123  
1124 Schauer, J. J., Kleeman, M. J., Cass, G. R., and Simoneit, B. R. T.: Measurement of emissions from air pollution sources. 3.  
1125 C<sub>1</sub>–C<sub>29</sub> organic compounds from fireplace combustion of wood, *Environ. Sci. Technol.*, 35, 1716–1728,  
1126 <https://doi.org/10.1021/es001331e>, 2001.

1127  
1128  
1129 Schmidt, A.-C., Herzsuh, R., Matysik, F.-M., and Engewald, W.: Investigation of the ionisation and fragmentation behaviour  
1130 of different nitroaromatic compounds occurring as polar metabolites of explosives using electrospray ionisation tandem mass  
1131 spectrometry, *Rapid Commun. Mass Sp.*, 20, 2293–2302, <https://doi.org/10.1002/rcm.2591>, 2006.

1132  
1133 Sedehi, N., Takano, H., Blasic, V. A., Sullivan, K. A., and De Haan, D. O.: Temperature- and pH-dependent aqueous-phase  
1134 kinetics of the reactions of glyoxal and methylglyoxal with atmospheric amines and ammonium sulfate, *Atmos. Environ.*, 77,  
1135 656–663, <https://doi.org/10.1016/j.atmosenv.2013.05.070>, 2013.

1136  
1137 Shapiro, E. L., Szprengiel, J., Sareen, N., Jen, C. N., Giordano, M. R., and McNeill, V. F.: Light-absorbing secondary organic  
1138 material formed by glyoxal in aqueous aerosol mimics, *Atmos. Chem. Phys.*, 9, 2289–2300, [https://doi.org/10.5194/acp-9-](https://doi.org/10.5194/acp-9-2289-2009)  
1139 [2289-2009](https://doi.org/10.5194/acp-9-2289-2009), 2009.

1140  
1141 Siegmann, K. and Sattler, K. D.: Formation mechanism for polycyclic aromatic hydrocarbons in methane flames, *J. Chem.*  
1142 *Phys.*, 112, 698–709, <https://doi.org/10.1063/1.480648>, 2000.

1143  
1144 Slikboer, S., Grandy, L., Blair, S. L., Nizkorodov, S. A., Smith, R. W., and Al-Abadleh, H. A.: Formation of light absorbing  
1145 soluble secondary organics and insoluble polymeric particles from the dark reaction of catechol and guaiacol with Fe(III),  
1146 *Environ. Sci. Technol.*, 49, 7793–7801, <https://doi.org/10.1021/acs.est.5b01032>, 2015.

1147  
1148 Smith, J. D., Sio, V., Yu, L., Zhang, Q., and Anastasio, C.: Secondary organic aerosol production from aqueous reactions of  
1149 atmospheric phenols with an organic triplet excited state, *Environ. Sci. Technol.*, 48, 1049–1057,  
1150 <https://doi.org/10.1021/es4045715>, 2014.

1151

1152 Smith, J. D., Kinney, H., and Anastasio, C.: Aqueous benzene-diols react with an organic triplet excited state and hydroxyl  
1153 radical to form secondary organic aerosol, *Phys. Chem. Chem. Phys.*, 17, 10227–10237, <https://doi.org/10.1039/C4CP06095D>,  
1154 2015.

1155

1156 Smith, J. D., Kinney, H., and Anastasio, C.: Phenolic carbonyls undergo rapid aqueous photodegradation to form low-volatility,  
1157 light-absorbing products, *Atmos. Environ.*, 126, 36–44, <https://doi.org/10.1016/j.atmosenv.2015.11.035>, 2016.

1158

1159 ~~Straub, D. J.: Radiation fog chemical composition and its temporal trend over an eight year period, *Atmos. Environ.*, 148, 49–~~  
1160 ~~61, <https://doi.org/10.1016/j.atmosenv.2016.10.031>, 2017.~~

1161 ~~Straub, D. J., Hutchings, J. W., and Herekes, P.: Measurements of fog composition at a rural site, *Atmos. Environ.*, 47, 195–~~  
1162 ~~205., <https://doi.org/10.1016/j.atmosenv.2011.11.014>, 2012.~~

1163

1164 Song, J., Li, M., Jiang, B., Wei, S., Fan, X., and Peng, P.: Molecular characterization of water-soluble humic like substances  
1165 in smoke particles emitted from combustion of biomass materials and coal using ultrahigh-resolution electrospray ionization  
1166 Fourier transform ion cyclotron resonance mass spectrometry, *Environ. Sci. Technol.*, 52, 2575–2585,  
1167 <https://doi.org/10.1021/acs.est.7b06126>, 2018.

1168

1169 ~~Sturzbecher Höhne, M., Nauser, T., Kissner, R., and Koppenol, W. H.: Photon initiated homolysis of peroxyxynitrous acid,~~  
1170 ~~*Inorg. Chem.*, 48, 7307–7312, <https://doi.org/10.1021/ie900614e>, 2009.~~

1171 ~~Sun, Y., Xu, F., Li, X., Zhang, Q., and Gu, Y.: Mechanisms and kinetic studies of OH-initiated atmospheric oxidation of~~  
1172 ~~methoxyphenols in the presence of O<sub>2</sub> and NO<sub>x</sub>, *Phys. Chem. Chem. Phys.*, 21, 21856–21866,~~  
1173 ~~<https://doi.org/10.1039/C9CP03246K>, 2019.~~

1174

1175 Sun, Y. L., Zhang, Q., Anastasio, C., and Sun, J.: Insights into secondary organic aerosol formed via aqueous-phase reactions  
1176 of phenolic compounds based on high resolution mass spectrometry, *Atmos. Chem. Phys.*, 10, 4809–4822,  
1177 <https://doi.org/10.5194/acp-10-4809-2010>, 2010.

1178

1179 Teich, M., van Pinxteren, D., Wang, M., Kecorius, S., Wang, Z., Müller, T., Močnik, G., and Herrmann, H.: Contributions of  
1180 nitrated aromatic compounds to the light absorption of water-soluble and particulate brown carbon in different atmospheric  
1181 environments in Germany and China, *Atmos. Chem. Phys.*, 17, 1653–1672, <https://doi.org/10.5194/acp-17-1653-2017>.

1182

1183 ~~Tinel, L., George, C., Brüggemann, M., Hayeck, N., Tinel, L., and Donaldson, D. J.: Interfacial photochemistry: physical~~  
1184 ~~chemistry of gas liquid interfaces, in: *Developments in Physical & Theoretical Chemistry*, edited by: Faust, J. A. and House,~~  
1185 ~~J. E., Elsevier, 435–457, <https://doi.org/10.1016/B978-0-12-813641-6.00014-5>, 2018.~~

1186 Tratnyek, P. G. and Hoigne, J.: Oxidation of substituted phenols in the environment: a QSAR analysis of rate constants for  
1187 reaction with singlet oxygen, *Environ. Sci. Technol.*, 25, 1596–1604, <https://doi.org/10.1021/es00021a011>, 1991.

1188

1189 Turro, N., Ramamurthy, V., and Scaiano, J.C.: *Modern Molecular Photochemistry*. University Science Book, 2010.

1190

1191 Vione, D., Maurino, V., Minero, C., and Pelizzetti, E.: Phenol photonitration upon UV irradiation of nitrite in aqueous solution  
1192 I: effects of oxygen and 2-propanol, *Chemosphere*, 45, 893–902, [https://doi.org/10.1016/S0045-6535\(01\)00035-2](https://doi.org/10.1016/S0045-6535(01)00035-2), 2001.

1193

1194 Vione, D., Maurino, V., Minero, C., and Pelizzetti, E.: Reactions induced in natural waters by irradiation of nitrate and nitrite  
1195 ions, in: *The Handbook of Environmental Chemistry Vol. 2M - Environmental Photochemistry Part II*, Springer, Berlin,  
1196 Heidelberg, Germany, 221–253, <https://doi.org/10.1007/b138185>, 2005.

1197

1198 Vione, D., Maurino, V., Minero, C., Pelizzetti, E., Harrison, M. A. J., Olariu, R., and Arsene, C.: Photochemical reactions in  
1199 the tropospheric aqueous phase and on particulate matter, *Chem. Soc. Rev.*, 35, 441–453, <https://doi.org/10.1039/B510796M>,  
1200 2006.

1201

1202 ~~Vione, D., Khanra, S., Cucu-Man, S., Maddigapu, P. R., Das, R., Arsene, C., Olariu, R-I., Maurino, V., and Minero, C.:  
1203 Inhibition vs. enhancement of the nitrate induced phototransformation of organic substrates by the  $\cdot\text{OH}$  scavengers bicarbonate  
1204 and carbonate, *Water Res.*, 43, 4718–4728, <https://doi.org/10.1016/j.watres.2009.07.032>, 2009.~~  
1205  
1206 Vione, D., Albinet, A., Barsotti, F., Mekic, M., Jiang, B., Minero, C., Brigante, M., and Gligorovski, S.: Formation of  
1207 substances with humic-like fluorescence properties, upon photoinduced oligomerization of typical phenolic compounds  
1208 emitted by biomass burning, *Atmos. Environ.*, 206, 197–207, <https://doi.org/10.1016/j.atmosenv.2019.03.005>, 2019.  
1209  
1210 Volkamer, R., Ziemann, P. J., Molina, and M. J.: Secondary organic aerosol formation from acetylene ( $\text{C}_2\text{H}_2$ ): seed effect on  
1211 SOA yields due to organic photochemistry in the aerosol aqueous phase, *Atmos. Chem. Phys.*, 9, 1907–1928,  
1212 <https://doi.org/10.5194/acp-9-1907-2009>, 2009.  
1213  
1214 ~~Wang, X., Dalton, E. Z., Payne, Z. C., Perrier, S., Riva, M., Raff, J. D., and George, C.: Superoxide and nitrous acid production  
1215 from nitrate photolysis is enhanced by dissolved aliphatic organic matter, *Environ. Sci. Technol. Lett.*, 8, 53–58,  
1216 <https://doi.org/10.1021/aes.estlett.0c00806>, 2021.~~  
1217 ~~Warneck, P. and Wurzinger, C.: Product quantum yields for the 305 nm photodecomposition of nitrate in aqueous solution, *J.*  
1218 *Phys. Chem.*, 92, 6278–6283, <https://doi.org/10.1021/j100333a022>, 1988.~~  
1219  
1220 Wang, K., Huang, R-J., Brüggemann, M., Zhang, Y., Yang, L., Ni, H., Guo, J., Wang, M., Han, J., Bilde, M., Glasius, M., and  
1221 Hoffmann, T.: Urban organic aerosol composition in eastern China differs from north to south: molecular insight from a liquid  
1222 chromatography–mass spectrometry (Orbitrap) study, *Atmos. Chem. Phys.*, 21, 9089–9104, [https://doi.org/10.5194/acp-21-](https://doi.org/10.5194/acp-21-9089-2021)  
1223 9089-2021, 2021.  
1224  
1225 Wang, X., Hayeck, N., Brüggemann, M., Yao, L., Chen, H., Zhang, C., Emmelin, C., Chen, J., George, C., and Wang, L.:  
1226 Chemical characterization of organic aerosols in Shanghai: A study by ultrahigh-performance liquid chromatography coupled  
1227 with orbitrap mass spectrometry, *J. Geophys. Res. Atmos.*, 122, 11703–11722, <https://doi.org/10.1002/2017JD026930>, 2017.  
1228 ~~Williams, D. H. and Fleming, I.: Spectroscopic methods in organic chemistry, 6th Ed., McGraw Hill Education, London, 2008.~~  
1229 ~~Wojnárovits, L., Tóth, T., and Takács, E.: Rate constants of carbonate radical anion reactions with molecules of environmental~~  
1230 ~~interest in aqueous solution: a review, *Sci. Total Environ.*, 717, 137219, <https://doi.org/10.1016/j.scitotenv.2020.137219>, 2020.~~  
1231  
1232 Xie, Q., Su, S., Chen, S., Xu, Y., Cao, D., Chen, J., Ren, L., Yue, S., Zhao, W., Sun, Y., Wang, Z., Tong, H., Su, H., Cheng,  
1233 Y., Kawamura, K., Jiang, G., Liu, C-Q., and Fu, P.: Molecular characterization of firework-related urban aerosols using Fourier  
1234 transform ion cyclotron resonance mass spectrometry, *Atmos. Chem. Phys.*, 20, 6803–6820, 10.5194/acp-2019-1180,  
1235 <https://doi.org/10.5194/acp-20-6803-2020>, 2020.  
1236  
1237 Yang, J., Au, W. C., Law, H., Lam, C. H., and Nah, T.: Formation and evolution of brown carbon during aqueous-phase nitrate-  
1238 mediated photooxidation of guaiacol and 5-nitroguaiacol, *Atmos. Environ.*, 254, 118401,  
1239 <https://doi.org/10.1016/j.atmosenv.2020.118140>, 2021.  
1240 ~~Yaremenko, I. A., Vil', V. A., Demchuk, D. V., and Terent'ev, A. O.: Rearrangements of organic peroxides and related~~  
1241 ~~processes, *Beilstein J. Org. Chem.*, 12, 1647–1748, <https://doi.org/10.3762/bjoc.12.162>, 2016.~~  
1242  
1243 Yaws, C. L.: Handbook of vapor pressure: Volume 3: Organic compounds  $\text{C}_8$  to  $\text{C}_{28}$ , Gulf Professional Publishing, USA, 1994.  
1244  
1245 Ye, Z., Qu, Z., Ma, S., Luo, S., Chen, Y., Chen, H., Chen, Y., Zhao, Z., Chen, M., and Ge, X.: A comprehensive investigation  
1246 of aqueous-phase photochemical oxidation of 4-ethylphenol, *Sci. Total Environ.*, 685, 976–985,  
1247 <https://doi.org/10.1016/j.scitotenv.2019.06.276>, 2019.  
1248  
1249 Yu, G., Bayer, A. R., Galloway, M. M., Korshavn, K. J., Fry, C. G., and Keutsch, F. N.: Glyoxal in aqueous ammonium sulfate  
1250 solutions: products, kinetics and hydration effects, *Environ. Sci. Technol.*, 45, 6336–6342, <https://doi.org/10.1021/es200989n>,  
1251 2011.

1252 Yu, L., Smith, J., Laskin, A., Anastasio, C., Laskin, J., and Zhang, Q.: Chemical characterization of SOA formed from aqueous-  
1253 phase reactions of phenols with the triplet excited state of carbonyl and hydroxyl radical, *Atmos. Chem. Phys.*, 14,  
1254 13801–13816, <https://doi.org/10.5194/acp-14-13801-2014>, 2014.

1255  
1256  
1257 Zhang, Q. and Anastasio, C.: Conversion of fogwater and aerosol organic nitrogen to ammonium, nitrate, and NO<sub>x</sub> during  
1258 exposure to simulated sunlight and ozone, *Environ. Sci. Technol.*, 37, 3522–3530, <https://doi.org/10.1021/es034114x>, 2003.

1259  
1260  
1261 Zhang, R., Gen, M., Fu, T-M., and Chan, C. K.: Production of formate via oxidation of glyoxal promoted by particulate nitrate  
1262 photolysis, *Environ. Sci. Technol.*, 55, 5711–5720, <https://doi.org/10.1021/acs.est.0c08199>, 2021.

1263  
1264 Zhao, R., Lee, A. K. Y., Huang, L., Li, X., Yang, F., and Abbatt, J. P. D.: Photochemical processing of aqueous atmospheric  
1265 brown carbon, *Atmos. Chem. Phys.*, 15, 6087–6100, <https://doi.org/10.5194/acp-15-6087-2015>, 2015.

1266  
1267 Zhao, Y., Hallar, A.G., and Mazzoleni, L.R.: Atmospheric organic matter in clouds: exact masses and molecular formula  
1268 identification using ultrahigh-resolution FT-ICR mass spectrometry, *Atmos. Chem. Phys.* 13, 12343–12362,  
1269 <https://doi.org/10.5194/acp-13-12343-2013>, 2013.

1270  
1271 Zhou, W., Mekic, M., Liu, J., Loisel, G., Jin, B., Vione, D., and Gligorovski, S.: Ionic strength effects on the photochemical  
1272 degradation of acetosyringone in atmospheric deliquescent aerosol particles, *Atmos. Environ.*, 198, 83–88,  
1273 <https://doi.org/10.1016/j.atmosenv.2018.10.047>, 2019.

1274  
1275 Zielinski, T., Bolzacchini, E., Cataldi, M., Ferrero, L., Graßl, S., Hansen, G., Mateos, D., Mazzola, M., Neuber, R., Pakszys,  
1276 P., Posyniak, M., Ritter, C., Severi, M., Sobolewski, P., Traversi, R., and Velasco-Merino, C.: Study of chemical and optical  
1277 properties of biomass burning aerosols during long-range transport events toward the Arctic in summer 2017, *Atmosphere*, 11,  
1278 84, <https://doi.org/10.3390/atmos11010084>, 2020.

1279  
1280 ~~Ziemann, P. J. and Atkinson, R.: Kinetics, products, and mechanisms of secondary organic aerosol formation, *Chem. Soc.*  
1281 *Rev.*, 41, 6582–6605, <https://doi.org/10.1039/C2CS35122F>, 2012.~~

1282 **Table 1.** List of reactions involving reactive species relevant to this study.

No.	Reactions	References
1	$\text{NO}_3^- + h\nu \rightarrow \cdot\text{NO}_2 + \text{O}^-; \phi = 0.01$	Vione et al., 2006; <a href="#">Scharko et al., 2014</a> ; <a href="#">Benedict et al., 2017</a>
2	$\text{O}^- + \text{H}_3\text{O}^+ \leftrightarrow \cdot\text{OH} + \text{H}_2\text{O}$	
3	$\text{NO}_3^- + h\nu \rightarrow \text{NO}_2^- + \text{O}(\text{^3P}); \phi = 0.0011$	
4	$\text{NO}_2^- + \cdot\text{OH} \rightarrow \cdot\text{NO}_2 + \text{OH}^- (k = 1.0 \times 10^{10} \text{ M}^{-1} \text{ s}^{-1})$	Mack and Bolton, 1999; Pang et al., 2019a
5	$\text{O}_2^{\cdot-} + \text{NO}_2^- + 2\text{H}^+ \rightarrow \cdot\text{NO}_2 + \text{H}_2\text{O}_2$	Vione et al., 2001; Pang et al., 2019a
6	$\text{NO}_2^- + h\nu \rightarrow \cdot\text{NO} + \text{O}^-; \phi_{\text{OH},300} = 6.7 (\pm 0.9)\%$	Fischer and Warneck, 1996; Mack and Bolton, 1999; Pang et al., 2019a
7	$\cdot\text{NO} + \text{O}_2 \leftrightarrow \cdot\text{ONOO}$	
8	$\cdot\text{ONOO} + \cdot\text{NO} \rightarrow \text{ONOONO}$	
9	$\text{ONOONO} \rightarrow 2\cdot\text{NO}_2$	Goldstein and Czapski, 1995a; Pang et al., 2019a
10	$\text{NO}_3^- + h\nu \rightarrow \cdot\text{NO}_2 + \text{OH}^- \text{ (reactions 1 \& 2)} \rightarrow \text{HOONO} \xrightarrow{h\nu} \cdot\text{NO} + \cdot\text{HO}_2$ $(\text{p}K_a = 6.8)$	<del>Goldstein et al., 2005; Vione et al., 2005; Sturzbecher-Höhne et al., 2009; Abida et al., 2011; Wang et al., 2021</del>
11	$\cdot\text{HO}_2 \rightleftharpoons \text{H}^+ + \text{O}_2^{\cdot-} \xrightarrow{\text{NO}_2} \cdot\text{OONO}_2 \xrightarrow{\text{H}_2\text{O}} \cdot\text{O}_2 + \text{NO}_2^- \xrightarrow{+\text{H}^+} \text{HOONO}_2$ $\text{HOONO} \xrightarrow{+\text{H}^+} \text{HOONO}_2$ $(\text{p}K_a = 4.8)$ $(\text{p}K_a = 3.2)$	<del>mmel et al., 1990; Goldstein et al., 1998; Wang et al., 2021</del>
12	$\cdot\text{OONO}_2 + \text{H}^+ \rightleftharpoons \text{HOONO}_2$ $\text{O}_2^{\cdot-} + \text{NO} \rightleftharpoons \text{OONO}^- \xrightarrow{\text{HOONO}} \cdot\text{NO}_2 + \text{HOONO}_2$ $(\text{p}K_a = 5.9)$ $\text{NO}_3^-$	Goldstein and Czapski, 1995b; Wang et al., 2021
13	$\text{HNO}_2 + h\nu \rightarrow \cdot\text{NO} + \text{OH}^-; \phi_{\text{OH},300} = 36.2 (\pm 4.7)\%$	Fischer and Warneck, 1996; Kim et al., 2014; Pang et al., 2019a
14	$\text{HOONO} \rightarrow \cdot\text{NO}_2 + \cdot\text{OH} (k = 0.35 \pm 0.03 \text{ s}^{-1})$	Goldstein et al., 2005; Pang et al., 2019a
105	$\text{HNO}_2 + \cdot\text{OH} \rightarrow \cdot\text{NO}_2 + \text{H}_2\text{O} (k = 2.6 \times 10^9 \text{ M}^{-1} \text{ s}^{-1})$	Kim et al., 2014; Pang et al., 2019a
16	$(\text{CH}_3)_2\text{CHOH} + \cdot\text{OH} \rightarrow (\text{CH}_3)_2\text{COH} + \text{H}_2\text{O}$	Warneck and Wurzinger, 1988; Pang et al., 2019a
17	$(\text{CH}_3)_2\text{COH} + \text{O}_2 \rightarrow (\text{CH}_3)_2\text{CO} + \cdot\text{HO}_2$	
18	$\cdot\text{OH} + \text{HCO}_3^- \rightarrow \text{CO}_3^{\cdot-} + \text{H}_2\text{O} (k = 8.5 \times 10^6 \text{ M}^{-1} \text{ s}^{-1})$	Wojnárovits et al., 2020
19	$\cdot\text{OH} + \text{CO}_3^{2-} \rightarrow \text{CO}_3^{\cdot-} + \text{OH}^- (k = 3.9 \times 10^8 \text{ M}^{-1} \text{ s}^{-1})$	
20	$^3\text{C}^* + \text{HCO}_3^- \rightarrow \text{CO}_3^{\cdot-} + \text{H}^+ + \text{C}^-$ $(k = 10^6 - 10^7 \text{ M}^{-1} \text{ s}^{-1}; ^3\text{C}^*: \text{triplet aromatic ketones})$	Canonica et al., 2005
21	$^3\text{C}^* + \text{CO}_3^{2-} \rightarrow \text{CO}_3^{\cdot-} + \text{C}^-$ $(k = 10^6 - 10^7 \text{ M}^{-1} \text{ s}^{-1}; ^3\text{C}^*: \text{triplet aromatic ketones})$	

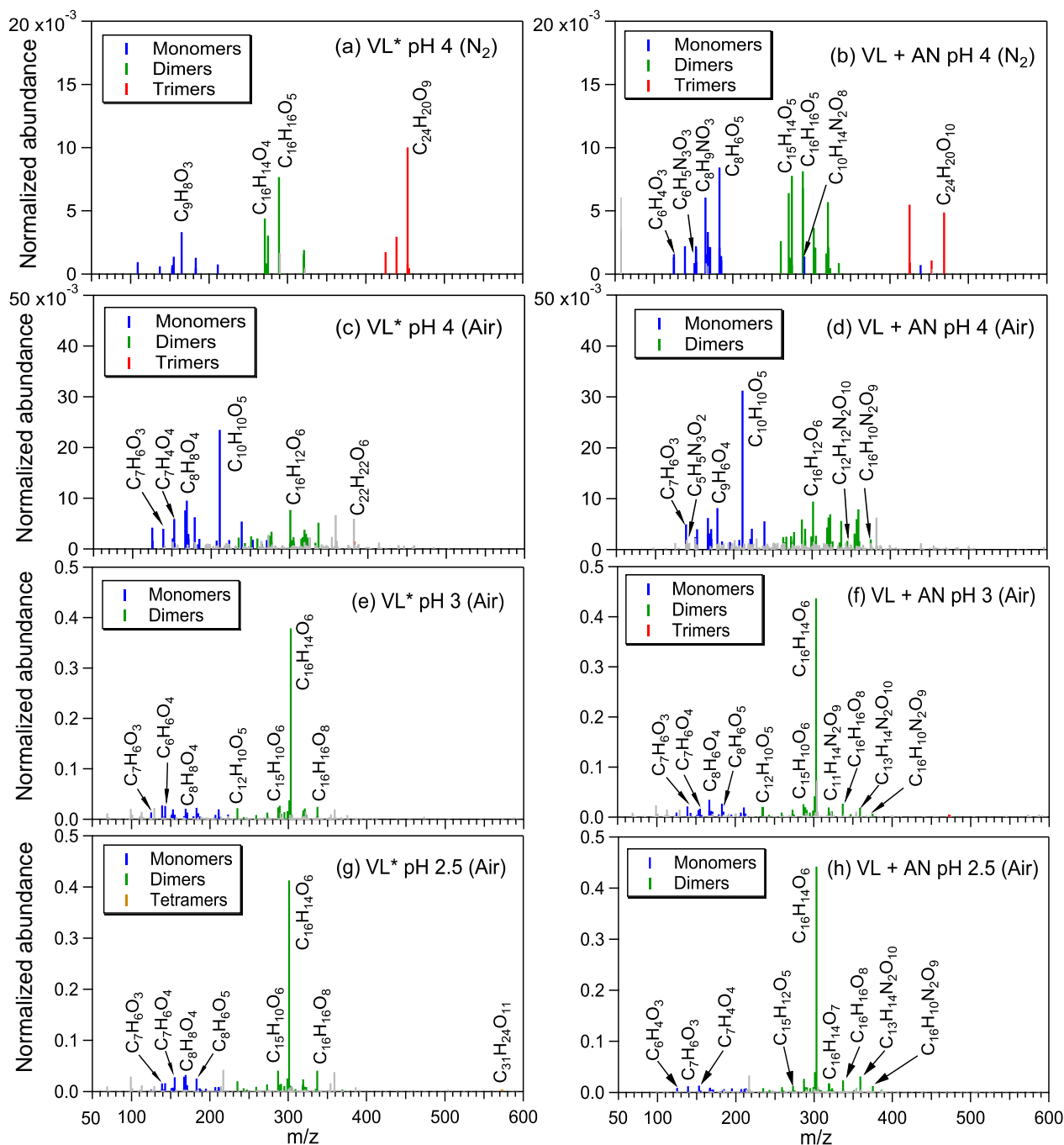
1284  
1285  
1286  
1287  
1288  
1289  
1290  
1291  
1292  
1293  
1294  
1295  
1296  
1297  
1298  
1299  
1300  
1301  
1302  
1303  
1304  
1305  
1306  
1307  
1308  
1309  
1310  
1311  
1312  
1313  
1314  
1315  
1316  
1317  
1318  
1319  
1320  
1321  
1322  
1323  
1324  
1325  
1326  
1327  
1328  
1329  
1330  
1331

**Table 2.** Reaction conditions, initial VL (and GUA) decay rate constants, normalized abundance of products, and average carbon oxidation state ( $\langle OS_c \rangle$ ) in each experiment. Except where noted, the reaction systems consisted of VL (0.1 mM); GUA (0.1 mM), AN (1 mM); sodium nitrate (SN) (1 mM) under air-saturated conditions after 6 h of simulated sunlight irradiation. Analyses were performed using UHPLC-qToF-MS equipped with an ESI source and operated in the positive ion mode.

<u>Exp no.</u>	<u>pH</u>	<u>Reaction conditions</u>	<u>Initial VL (and GUA) decay rate constants (min<sup>-1</sup>)<sup>b</sup></u>	<u>Ratio of 50 most abundant products to total products<sup>c</sup></u>	<u>Normalized abundance of products<sup>d</sup></u>	<u>Normalized abundance of N-containing compounds<sup>d</sup></u>	<u>&lt;OS<sub>c</sub>&gt;<sup>e</sup> (OS<sub>c</sub> of VL: -0.25)</u>
<u>A1</u>	<u>2.5</u>	<u>VL*</u>	<u><math>2.0 \times 10^{-2} + 5.8 \times 10^{-5}</math></u>	<u>0.59</u>	<u><math>1.7 \pm 0.16</math></u>	<u>N/A</u>	<u>-0.05</u>
<u>A2</u>		<u>VL+AN</u>	<u><math>1.7 \times 10^{-2} + 7.3 \times 10^{-4}</math></u>	<u>0.63</u>	<u><math>1.4 \pm 0.19</math></u>	<u><math>5.3 \times 10^{-2}</math></u>	<u>-0.04</u>
<u>A3</u>	<u>3</u>	<u>VL*</u>	<u><math>1.5 \times 10^{-2} + 4.2 \times 10^{-4}</math></u>	<u>0.53</u>	<u><math>1.9 \pm 0.33</math></u>	<u>N/A</u>	<u>-0.04</u>
<u>A4</u>		<u>VL+AN</u>	<u><math>1.5 \times 10^{-2} + 2.3 \times 10^{-4}</math></u>	<u>0.56</u>	<u><math>1.9 \pm 0.30</math></u>	<u><math>3.6 \times 10^{-2}</math></u>	<u>-0.05</u>
<u>A5</u>	<u>4</u>	<u>VL*</u>	<u><math>1.2 \times 10^{-2} + 5.9 \times 10^{-4}</math></u>	<u>0.58</u>	<u><math>0.26 \pm 0.42</math></u>	<u>N/A</u>	<u>-0.16</u>
<u>A6</u>		<u>VL*</u> <u>(N<sub>2</sub>-saturated)</u>	<u><math>3.2 \times 10^{-3} + 1.1 \times 10^{-3}</math></u>	<u>0.96</u>	<u><math>4.7 \times 10^{-2}</math> <u><math>\pm 0.0027</math></u></u>	<u>N/A</u>	<u>-0.24</u>
<u>A7</u>		<u>VL+AN</u>	<u><math>1.2 \times 10^{-2} + 8.8 \times 10^{-4}</math></u>	<u>0.53</u>	<u><math>0.37 \pm 0.38</math></u>	<u><math>1.7 \times 10^{-2}</math></u>	<u>-0.13</u>
<u>A8</u>		<u>VL+AN</u> <u>(N<sub>2</sub>-saturated)</u>	<u><math>1.9 \times 10^{-3} + 9.2 \times 10^{-5}</math></u>	<u>0.89</u>	<u><math>0.12 \pm 0.0095</math></u>	<u><math>6.3 \times 10^{-3}</math></u>	<u>-0.21</u>
<u>A9</u>		<u>VL+SN</u>	<u>N/A</u>	<u>0.51</u>	<u><math>0.42 \pm 0.33</math></u>	<u><math>1.7 \times 10^{-2}</math></u>	<u>-0.07</u>
<u>A10</u>		<u>VL* (0.01 mM)<sup>a</sup></u>	<u>N/A</u>	<u>0.90</u>	<u><math>0.37 \pm 0.018</math></u>	<u>N/A</u>	<u>-0.07</u>
<u>A11</u>		<u>VL (0.01 mM) + AN (0.01 mM)</u>	<u>N/A</u>	<u>0.77</u>	<u><math>0.40 \pm 0.074</math></u>	<u><math>8.6 \times 10^{-3}</math></u>	<u>0.12</u>
<u>A12</u>		<u>VL (0.01 mM) + AN</u>	<u>N/A</u>	<u>0.42</u>	<u><math>0.45 \pm 0.025</math></u>	<u><math>1.2 \times 10^{-2}</math></u>	<u>-0.06</u>
<u>A13</u>		<u>GUA only</u>	<u><math>6.2 \times 10^{-3} + 2.5 \times 10^{-4}</math></u>	<u>0.77</u>	<u>N/A</u>	<u>N/A</u>	<u>-0.28</u>
<u>A14</u>		<u>GUA+VL</u>	<u>GUA: <math>1.4 \times 10^{-2} + 4.0 \times 10^{-4}</math> VL: <math>4.3 \times 10^{-3} + 2.2 \times 10^{-4}</math></u>	<u>0.60</u>	<u><math>2.2 \pm 0.47</math></u>	<u>N/A</u>	<u>-0.27</u>
<u>A15</u>	<u>GUA+AN</u>	<u><math>8.0 \times 10^{-3} + 2.9 \times 10^{-3}</math></u>	<u>0.77</u>	<u>N/A</u>	<u>N/A</u>	<u>-0.26</u>	

1332  
1333 <sup>a</sup>Irradiation time for VL\* (0.01 mM, A10) was 3 h. <sup>b</sup>The data fitting was performed in the initial linear region. Each value is  
1334 the average of results from triplicate experiments. Errors represent one standard deviation. Kinetic measurements were not  
1335 performed for experiments marked with N/A. <sup>c</sup>Ratio of the normalized abundance of the 50 most abundant products to that of  
1336 total products, except for direct GUA photodegradation, GUA+VL, and GUA+AN (A13–15) whose ratios are based on the  
1337 absolute signals of products. <sup>d</sup>The normalized abundance of products was calculated using Eq. 2. The samples for experiments  
1338 without nitrate (marked with N/A) were not analyzed for N-containing compounds. For the GUA experiments, the normalized  
1339 abundance of products was calculated only for GUA+VL as the GUA signal from the UHPLC-qToF-MS in the positive ion  
1340 mode was weak, which may introduce large uncertainties during normalization. <sup>e</sup><OS<sub>c</sub>> of the 50 most abundant products.

1341  
1342

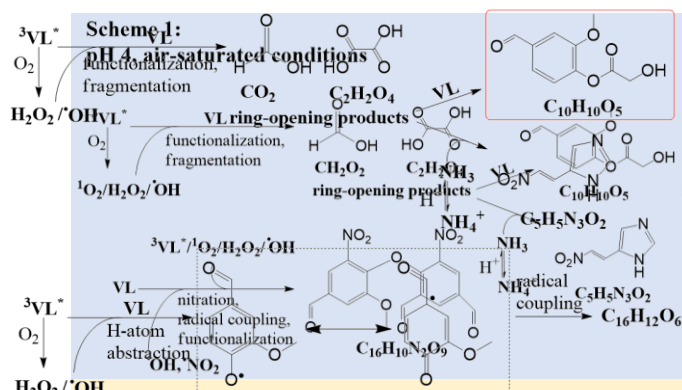


1343  
 1344 **Figure 1.** Reconstructed mass spectra of assigned peaks from (a) VL\* pH 4 ( $N_2$ -saturated; A6), (b) VL+AN pH 4 ( $N_2$ -saturated;  
 1345 A8), (c) VL\* pH 4 (air-saturated; A5), (d) VL+AN pH 4 (air-saturated; A7), (e) VL\* pH 3 (air-saturated; A3), (f) VL+AN pH  
 1346 3 (air-saturated; A4), (g) VL\* pH 2.5 (air-saturated; A1), and (h) VL+AN pH 2.5 (air-saturated; A2) after 6 h of simulated

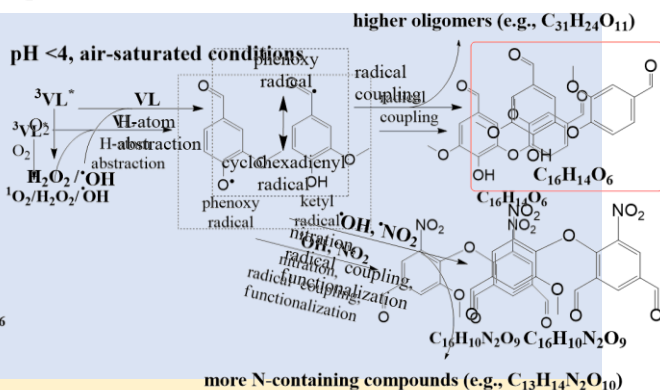
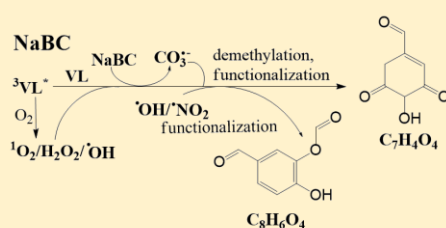
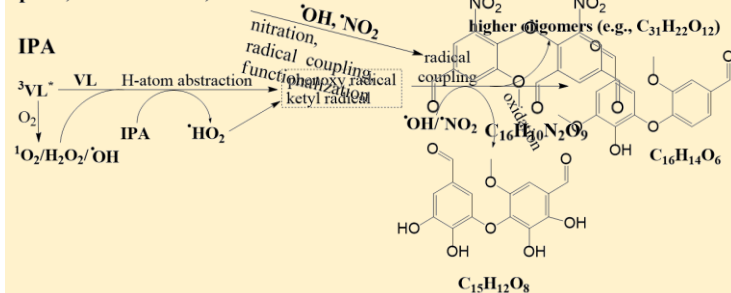


1347 sunlight irradiation. The normalized abundance of products was calculated from the ratio of the peak area of the product to  
1348 that of VL (Eq. 2). The 50 most abundant products contributed more than half of the total normalized abundance of products,  
1349 and they were identified as monomers (blue), dimers (green), trimers (red), and tetramers (orange). Grey peaks denote peaks  
1350 with low abundance or unassigned formula. Examples of high-intensity peaks were labeled with the corresponding neutral  
1351 formulas. Note the different scales on the y-axes.

## pH 4, air-saturated conditions



## pH &lt; 4, air-saturated conditions

Scheme 2:  
pH 4, IPA or NaBC, air-saturated conditions

1353

1354

1355

1356 **Figure 2.** Potential aqSOA formation pathways via direct photosensitized oxidation of VL and nitrate-mediated VL photo-  
 1357 oxidation at pH 4 and pH < 4 under air-saturated conditions. Product structures were proposed based on the molecular formulas,  
 1358 DBE values, and MS/MS fragmentation patterns. The molecular formulas presented were the major products detected using  
 1359 UHPLC-qToF-MS in positive ESI mode. The highlighted structures are the most abundant product for each condition.

1360

1361

1362

1363

1364

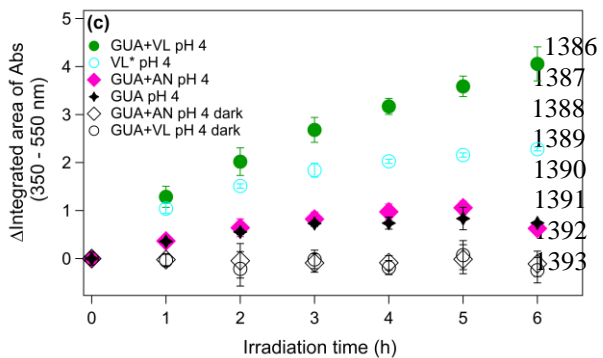
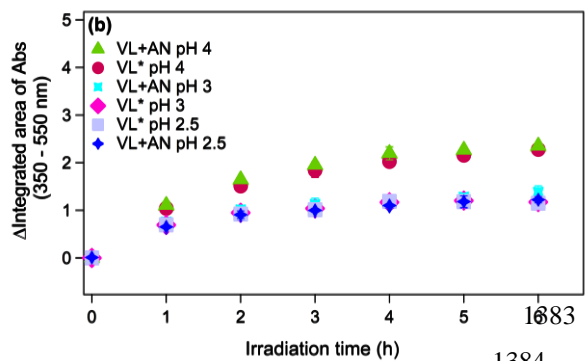
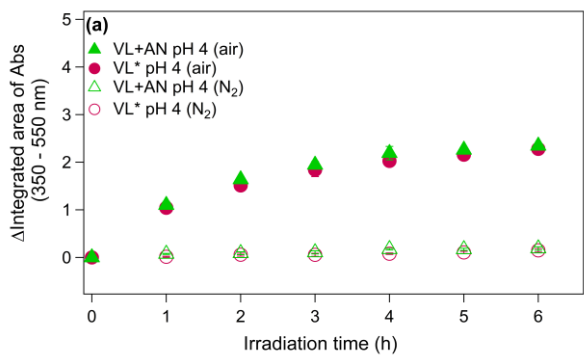
1365

1366

1367

1368

1369  
 1370  
 1371  
 1372  
 1373  
 1374  
 1375  
 1376  
 1377  
 1378  
 1379  
 1380  
 1381  
 1382

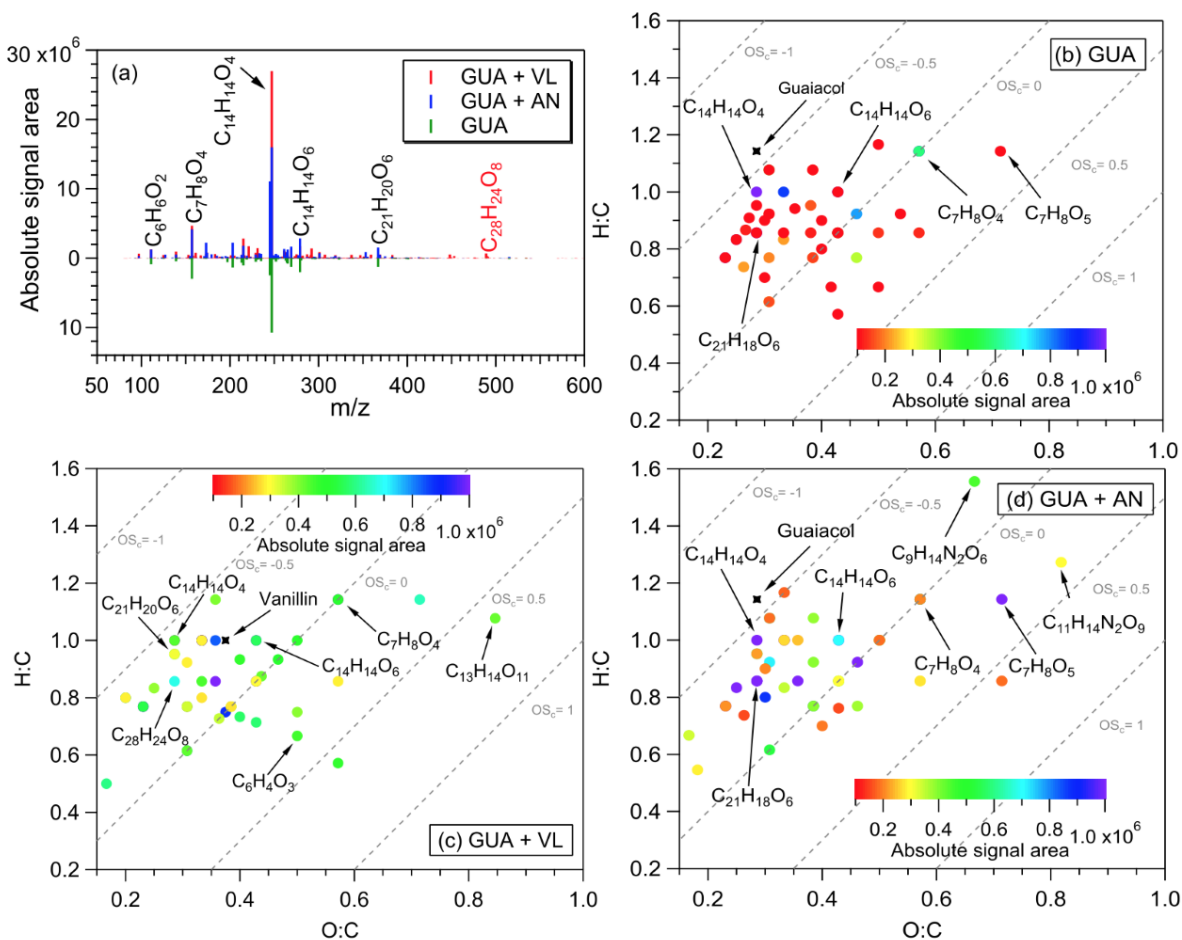


1394  
 1395  
 1396  
 1397  
 1398  
 1399  
 1400  
 1401

1385

1384

1402 **Figure 32.** (a–c*d*) Increase in light absorption under different experimental conditions for direct photosensitized oxidation of  
 1403 VL (VL\*) and nitrate-mediated VL photo-oxidation (VL+AN): (a) **Effect of secondary oxidants from VL triplets on VL\*** and  
 1404 VL+AN at pH 4 under N<sub>2</sub>- (A6, A8) and air-saturated (A5, A7) conditions. (b) Effect of pH on VL\* and VL+AN at pH 2.5  
 1405 (A1, A2), 3 (A3, A4), and 4 (A5, A7) under air-saturated conditions. (c) **Effect of VOCs and inorganic anions: IPA (A9) and**  
 1406 **NaBC (A10) on VL\* at pH 4 under air-saturated conditions.** (d) **Effect of VOCs and inorganic anions: IPA (A11) and NaBC**  
 1407 **(A12) on VL+AN at pH 4 under air-saturated conditions.** (e) Increase in light absorption during direct GUA photodegradation  
 1408 (A137) and photo-oxidation of GUA in the presence of VL (GUA+VL; A148) or nitrate (GUA+AN; A159) at pH 4 under air-  
 1409 saturated conditions after 6 h of simulated sunlight irradiation. Error bars represent one standard deviation; most error bars  
 1410 are smaller than the markers.



1411

1412

1413 **Figure 43.** (a) Reconstructed mass spectra of assigned peaks from the direct GUA photodegradation (A137) and photo-  
 1414 oxidation of GUA in the presence of VL (GUA+VL; A148) or nitrate (GUA+AN; A159) at pH 4 under air-saturated

1415 conditions after 6 h of simulated sunlight irradiation. The y-axis is the absolute signal area of the products. Examples of  
1416 high-intensity peaks were labeled with the corresponding neutral formulas. (b-d) van Krevelen diagrams of the 50 most  
1417 abundant products from the (b) direct photodegradation of GUA (A137), (c) GUA+VL (A148), and (d) GUA+AN (A159) at  
1418 pH 4 under air-saturated conditions after 6 h of simulated sunlight irradiation. The color bar denotes the absolute signal area.  
1419 The grey dashed lines indicate the carbon oxidation state values (e.g.,  $OS_c = -1, 0, \text{ and } 1$ ).

1420 ~~Figure 4. Potential photo-oxidation pathways of VL via direct photosensitized reactions and in the presence of nitrate to~~  
1421 ~~illustrate the effects of secondary oxidants from VL triplets, pH, and the presence of VOCs (IPA) and inorganic anions (NaBC).~~  
1422 ~~Product structures were proposed based on the molecular formulas, DBE values, and MS/MS fragmentation patterns. The~~  
1423 ~~molecular formulas presented were the most abundant products or products with a significant increase in normalized abun~~

1 **Supplementary material**

2  
3 **Aqueous SOA formation from the photo-oxidation of vanillin:**  
4 **Direct photosensitized reactions and nitrate-mediated reactions**

5  
6 Beatrix Rosette Go Mabato<sup>1</sup>, Yan Lyu<sup>1</sup>, Yan Ji<sup>1</sup>, [Yong Jie Li<sup>2</sup>](#), Dan Dan Huang<sup>32</sup>, Xue Li<sup>43</sup>,  
7 Theodora Nah<sup>1</sup>, Chun Ho Lam<sup>1</sup>, and Chak K. Chan<sup>1\*</sup>

8  
9 <sup>1</sup>School of Energy and Environment, City University of Hong Kong, Hong Kong, China

10 [<sup>2</sup>Department of Civil and Environmental Engineering, and Centre for Regional Ocean, Faculty of](#)  
11 [Science and Technology, University of Macau, Macau, China](#)

12 <sup>32</sup>Shanghai Academy of Environmental Sciences, Shanghai 200233, China

13 <sup>43</sup>Institute of Mass Spectrometry and Atmospheric Environment, Jinan University No. 601  
14 Huangpu Avenue West, Guangzhou 510632, China

15  
16 *Correspondence to:* Chak K. Chan (Chak.K.Chan@cityu.edu.hk)

24

25

26 **Text S1.** Materials.

27

28 Initial solutions of 0.1 mM vanillin (VL, Acros Organics, 99%, pure), 0.1 mM guaiacol (GUA,

29 Sigma Aldrich,  $\geq$  98.0%), 1 mM ammonium nitrate (AN, Acros Organics, 99+%, for analysis),

30 ~~and 1 mM sodium nitrate (SN, Sigma-Aldrich,  $\geq$  99.5%), 1 mM of 2-propanol (IPA, Optima~~

31 ~~LC/MS grade), and 1 mM of sodium bicarbonate (NaBC, Fisher BioReagents, 99.7–100.3%)~~ were

32 prepared in Milli-Q water. The pH values of the samples were adjusted using sulfuric acid (H<sub>2</sub>SO<sub>4</sub>;

33 Acros Organics, ACS reagent, 95% solution in water).

34

35 **Text S2.** UV-Vis spectrophotometric analyses.

36

37 The absorbance changes for all samples were characterized using a UV-Vis

38 spectrophotometer (UV-3600, Shimadzu Corp., Japan). The absorbance values from 200 to 700

39 nm were recorded instantly after sample collection, and measurements were done in triplicate.

40 Absorbance enhancements were calculated as the change in the integrated area of absorbance from

41 350 to 550 nm. The increase of light absorption at this wavelength range, where VL and GUA did

42 not initially absorb light, suggests the formation of light-absorbing compounds (Zhou et al., 2019).

43

44 **Text S3.** UHPLC-PDA analyses.

45

46 An ultra-high performance liquid chromatography system (UHPLC, Waters Acquity H-

47 Class, Waters, Milford, USA) coupled to a photodiode array (PDA) detector (Waters, Milford,

48 USA) was used for the quantification of VL and GUA concentrations. The drawn solutions were

49 first filtered through a 0.2  $\mu$ m Chromafil<sup>®</sup>Xtra PTFE filter (Macherey-Nagel GmbH & Co. KG,

50 Germany). Briefly, the separation of products was performed using an Acquity HSS T3 column

51 (1.8  $\mu\text{m}$ , 2.1 mm  $\times$  100 mm; Waters Corp.). The column oven was held at 30  $^{\circ}\text{C}$ , and the  
52 autosampler was cooled at 4  $^{\circ}\text{C}$ . The injection volume was set to 5  $\mu\text{L}$ . The binary mobile phase  
53 consisted of A (water) and B (acetonitrile). The gradient elution was performed at a flow rate of  
54 0.2 mL/min: 0–1 min, 10% eluent B; 1–25 min, linear increase to 90% eluent B; 25–29.9 min,  
55 hold 90% eluent B; 29.9–30 min, decrease to 10% eluent B; 30–35 min, re-equilibrate at 10%  
56 eluent B for 5 min. Standard solutions of VL and GUA ranging from 10 to 130  $\mu\text{M}$  were analyzed  
57 along with samples and blanks using the channels with UV absorption at 300 and 274 nm,  
58 respectively. The calibration curves for VL and GUA standard solutions are shown in Figure S2.

59  
60 **Text S4.** IC analyses of small organic acids.

61  
62 The small organic acids were analyzed using an ion chromatography system (IC, Dionex  
63 ICS-1100, Sunnyvale, CA) equipped with a Dionex AS-DV autosampler (Sunnyvale, CA). The  
64 separation was achieved using an IonPac<sup>TM</sup> AS15 column (4  $\times$  250 mm) with an AG15 guard  
65 column (4  $\times$  50 mm). The isocratic gradient was applied at a flow rate of 1.2 mL/min with 38 mM  
66 sodium hydroxide (NaOH) as the eluent. The total run time was set at 20 min. The standard  
67 solutions (1–50  $\mu\text{M}$ ) of formic, succinic, and oxalic acid were analyzed three times along with the  
68 samples and water blank. Formic, succinic, and oxalic acid had retention times of 3.6 min, 8.3 min,  
69 and 11.9 min, respectively.

70  
71 **Text S5.** UHPLC-qToF-MS analyses.

72  
73 The characterization of reaction products was performed using a UHPLC system  
74 (ExionLC<sup>TM</sup> AD, ABSciex, Concord, Canada) coupled to a quadrupole time-of-flight mass  
75 spectrometer (qToF-MS) (TripleTOF 6600+, ABSciex). The settings (e.g., column, mobile phase,  
76 gradient, oven temperature) in the UHPLC system were the same as those used in UHPLC-PDA



77 (Text S3). The mass spectrometer was equipped with an electrospray ionization (ESI) source and  
78 operated in the positive ion mode (the negative ion mode signals were too low for our analyses) at  
79 a resolving power (full width at half-maximum (fwhm) at  $m/z$  300) of 30000 in MS and 30000 in  
80 MS/MS (high-resolution mode). Information-dependent acquisition (IDA) scanning was adapted  
81 for product identification. The acquisition using IDA consisted of a ToF-MS scan and information-  
82 dependent trigger events. The ToF-MS scan had an accumulation time of 250 ms and covered a  
83 mass range of  $m/z$  30–700 with a declustering potential (DP) of 40 and collision energy (CE) of  
84 10 eV. The accumulation time for the IDA experiment was 100 ms, and the MS/MS scan range  
85 was set from  $m/z$  30–700 in high-resolution mode. The IDA criteria were as follows: 5 most intense  
86 ions (number of IDA experiments) with an intensity threshold above 50 cps, isotope exclusion was  
87 switched off, and dynamic background subtraction was switched on. The automated calibration  
88 device system (CDS) was set to perform an external calibration every four samples. The ESI source  
89 conditions were as follows: temperature, 500 °C; curtain gas (CUR), 25 psi; ion source gas 1 at 50  
90 psi; ion source gas 2 at 50 psi; and ion-spray voltage floating (ISVF) at 4.5 kV.

91 All parameters in the liquid chromatography system and mass spectrometer were controlled  
92 using Analyst TF Software 1.8 (ABSciex). The high-resolution LC-MS data were processed with  
93 PeakView and Analyst in the SCIEX OS software 1.5 (ABSciex). Peaks from the blank sample  
94 were subtracted from the sample signals. In addition to a minimum signal-to-noise ratio of 30, a  
95 peak was determined as a product if the difference in peak area between the samples before and  
96 after irradiation is  $\geq 10$  times. The formula assignments were carried out using the MIDAS  
97 molecular formula calculator (<http://magnet.fsu.edu/~midas/>) with the following constraints:  $C \leq$   
98 35,  $H \leq 70$ ,  $N \leq 5$ ,  $O \leq 20$ ,  $Na \leq 1$ , and the mass error was initially set as 10 ppm. The nitrogen  
99 atom was removed in the constraints for the experiments without AN or SN. The detected adducts

100 in ESI positive ion mode have several types (e.g.,  $[M+H]^+$ ,  $[M+Na]^+$ ), and their formation can be  
101 influenced by the sample matrix (Erngren et al., 2019). For simplification purposes, we mainly  
102 considered  $[M+H]^+$  adducts for formula assignments, except for specific experiments with AN or  
103 SN in which  $[M+NH_4]^+$  adducts and  $[M+Na]^+$  adducts were observed. The final assigned formulas  
104 were constrained by a mass error mostly  $< 5$  ppm, which is a requirement for product identification  
105 using positive ion mode (Roemmelt et al., 2015). The double bond equivalent (DBE) values and  
106 carbon oxidation state ( $OS_c$ ) of the neutral formulas were calculated using the following equations

107 (Koch and Dittmar, 2006):

108  
109 
$$DBE = C - H/2 + N/2 + 1 \quad (\text{Eq. S1})$$

110 
$$OS_c = 2 \times O/C - H/C \quad (\text{Eq. S2})$$

111  
112 where C, H, O, and N correspond to the number of carbon, hydrogen, oxygen, and nitrogen atoms  
113 in the neutral formula, respectively. Based on the identified products, the average oxygen to carbon  
114 (O:C) ratios,  $\langle O:C \rangle$ : ( $\langle O:C \rangle = \sum_i(\text{abundance}_i)O_i / \sum_i(\text{abundance}_i)C_i$ ) and average hydrogen  
115 to carbon (H:C) ratios,  $\langle H:C \rangle$ : ( $\langle H:C \rangle = \sum_i(\text{abundance}_i)H_i / \sum_i(\text{abundance}_i)C_i$ ) after the  
116 reactions were further estimated using the signal-weighted method (Bateman et al., 2012). The  
117 average  $OS_c$  ( $\langle OS_c \rangle$ ) was calculated as follows:

118 
$$\langle OS_c \rangle = 2 \times \langle O:C \rangle - \langle H:C \rangle \quad (\text{Eq. S3})$$

119  
120 Based on the typical MS/MS fragmentation behavior for individual functional groups (Table S1)  
121 and DBE values, examples of structures for products identified from VL (and GUA) photo-  
122 oxidation experiments were proposed (Table S23).

123

124 **Text S6.** Photon flux measurements.

125

126 In this work, 2-nitrobenzaldehyde (2NB), a chemical actinometer, was used to determine

127 the photon flux in the aqueous photoreactor. ~~We first measured the relative intensity of light~~

128 ~~passing through the empty reactor, then the reactor containing 50 μM 2NB using a high sensitivity~~

129 ~~spectrophotometer (Brolight Technology Co. Ltd, Hangzhou, China) equipped with an optical~~

130 ~~fiber (Brolight). Then, the average relative intensity absorbed by 2NB solution as a function of~~

131 ~~wavelength was calculated.~~ Briefly, the photolysis of 50 μM 2NB in the reactor was monitored by

132 determining its concentration every 5 min for a total of 35 min, during which 2NB was almost

133 completely decayed. The concentration of 2NB was measured using UHPLC-PDA, and the

134 settings (e.g., column, mobile phase, gradient, oven temperature) were the same as those for VL

135 decay analysis (Text S3). The channel with UV absorption at 254 nm was used for the

136 quantification of 2NB. The concentration of 2NB in the reactor followed exponential decay, and

137 its decay rate constant was determined using the following equation:

138 
$$\ln \left( \frac{[2NB]_t}{[2NB]_0} \right) = -j(2NB) \times t \quad (\text{Eq. S4})$$

139

140 where  $[2NB]_t$  and  $[2NB]_0$  are the 2NB concentrations at time  $t$  and 0, respectively. The calculated

141 2NB decay rate constant,  $j(2NB)$ , was  $0.0026 \text{ s}^{-1}$ . The following equation can also be used to

142 calculate  $j(2NB)$ :

143 
$$j(2NB) = 2.303 \times (10^3 \text{ cm}^3 \text{ L}^{-1} \times 1 \text{ mol}/N_A \text{ mlc}) \times \sum \left( I_{\lambda} \times \Delta\lambda \times \varepsilon_{2NB,\lambda} \times \Phi_{2NB} \right) \quad \text{-(Eq.}$$

144 S5)

145 where  $N_A$  is Avogadro's number,  $I'_\lambda$  is the actinic flux (photons  $\text{cm}^{-2} \text{s}^{-1} \text{nm}^{-1}$ ),  $\Delta\lambda$  is the  
 146 wavelength interval between actinic flux data points (nm), and  $\varepsilon_{2NB,\lambda}$  and  $\Phi_{2NB,\lambda}$  are the base-10  
 147 molar absorptivity ( $\text{M}^{-1} \text{cm}^{-1}$ ) and quantum yield (molecule  $\text{photon}^{-1}$ ) for 2NB, respectively.  
 148 Values of  $\varepsilon_{2NB,\lambda}$  (in water) at each wavelength under 298 K and a wavelength-independent  $\Phi_{2NB}$   
 149 value of 0.41 were adapted from Galbavy et al. (2010). Similar to Smith et al. (2014, 2016), we  
 150 measured the spectral shape of the photon output of our illumination system (i.e., the relative flux  
 151 at each wavelength) using a high-sensitivity spectrophotometer (Brolight Technology Co. Ltd,  
 152 Hangzhou, China). Using a scaling factor (SF), this measured relative photon output,  $I_\lambda^{\text{relative}}$ , is  
 153 related to  $I'_\lambda$  as follows:

$$154 \quad I'_\lambda = I_\lambda^{\text{relative}} \times \text{SF} \quad \text{(Eq. S6)}$$

157 Substitution of Eq. S6 into Eq. S5 and rearrangement yields:

$$160 \quad \text{SF} = \frac{j(2NB)}{2.303 \times (10^3 \text{ cm}^3 \text{ L}^{-1} \times 1 \text{ mol}/N_A \text{ mlc}) \times \sum(I_\lambda^{\text{relative}} \times \Delta\lambda \times \varepsilon_{2NB,\lambda} \times \Phi_{2NB})} \quad \text{(Eq. S7)}$$

163 and substitution of Eq. S6 into Eq. S7 yields:

$$166 \quad I'_\lambda = I_\lambda^{\text{relative}} \frac{j(2NB)}{2.303 \times (10^3 \text{ cm}^3 \text{ L}^{-1} \times 1 \text{ mol}/N_A \text{ mlc}) \times \sum(I_\lambda^{\text{relative}} \times \Delta\lambda \times \varepsilon_{2NB,\lambda} \times \Phi_{2NB})} \quad \text{(Eq. S8)}$$

167  
 168 Finally,  $I'_\lambda$  was estimated through Eq. S8. The estimated photon flux in the aqueous reactor is  
 169 shown in Figure S12.

170 The actinic flux during a haze event over Beijing (40° N, 116° E) on January 12, 2013, at  
 171 12:00 pm (GMT+8) (Che et al., 2014) estimated using the National Center for Atmospheric  
 172 Research Tropospheric Ultraviolet-Visible (TUV) Radiation Model

173 ([http://cprm.acom.ucar.edu/Models/TUV/Interactive\\_TUV/](http://cprm.acom.ucar.edu/Models/TUV/Interactive_TUV/)) is also shown in Figure S2. The  
 174 parameters used for the Quick TUV calculator were: Overhead Ozone Column: 300 du; Surface  
 175 Albedo: 0.1; Ground Elevation: 0 km asl; Measured Altitude: 0 km asl; Clouds optical depth: 0,  
 176 base: 4, top: 5; Aerosols optical depth: 2.5, single scattering albedo: 0.9, Angstrom exponent: 1;  
 177 Sunlight direct beam, diffuse down, diffuse up: 1; 4 streams transfer model. For clear days, the  
 178 actinic flux was estimated over Beijing (at the same date and time) using the default parameters.

179

180 **Text S7. Estimation of the apparent quantum efficiency of guaiacol photodegradation.**

181

182 The apparent quantum efficiency of GUA photodegradation ( $\Phi_{\text{GUA}}$ ) in the presence of  
 183 either VL or nitrate during simulated sunlight illumination can be defined as (Anastasio et al., 1996;  
 184 Smith et al., 2014, 2016):

185 
$$\Phi_{\text{GUA}} = \frac{\text{mol GUA destroyed}}{\text{mol photons absorbed}} \quad \text{(Eq. S9)}$$

186  $\Phi_{\text{GUA}}$  was calculated using the measured rate of GUA decay and rate of light absorption by either  
 187 VL or nitrate through the following equation:

188

189 
$$\Phi_{\text{GUA}} = \frac{\text{rate of GUA decay}}{\text{rate of light absorption by VL or nitrate}} = \frac{k'_{\text{GUA}} \times [\text{GUA}]}{\sum [(1 - 10^{-\varepsilon_{\lambda}[\text{C}]l}) \times I'_{\lambda}]} \quad \text{(Eq. S10)}$$

190

191 where  $k'_{\text{GUA}}$  is the pseudo-first-order rate constant for GUA decay, [GUA] is the concentration of  
 192 GUA (M),  $\varepsilon_{\lambda}$  is the base-10 molar absorptivity ( $\text{M}^{-1} \text{cm}^{-1}$ ) of VL or nitrate at wavelength  $\lambda$ , [C] is  
 193 the concentration of VL or nitrate (M),  $l$  is the pathlength of the illumination cell (cm), and  $I'_{\lambda}$  is  
 194 the volume-averaged photon flux ( $\text{mol-photons L}^{-1} \text{s}^{-1} \text{nm}^{-1}$ ) determined from 2NB actinometry:

195

196 
$$j(2\text{NB}) = 2.303 \times \Phi_{2\text{NB}} \times l \times \int_{300 \text{ nm}}^{350 \text{ nm}} (\varepsilon_{2\text{NB},\lambda} \times I'_{\lambda} \times \Delta\lambda) \quad \text{(Eq. S11)}$$

197  
198  
199  
200  
201  
202  
203  
204  
205  
206  
207

**Table S1.** Typical fragmentation behavior observed in MS/MS spectra for individual functional groups from Holčapek et al. (2010).

Functional group	Fragment ions	MS/MS loss
Nitro (RNO <sub>2</sub> )	[M+H-OH] <sup>+</sup> *	-OH
	[M+H-H <sub>2</sub> O] <sup>+</sup>	-H <sub>2</sub> O
	[M+H-NO] <sup>+</sup> *	-NO
Nitroso (RNO)	[M+H-NO <sub>2</sub> ] <sup>+</sup> *	-NO <sub>2</sub>
	[M+H-NO] <sup>+</sup>	-NO
	[M+H-H <sub>2</sub> O] <sup>+</sup>	-H <sub>2</sub> O
Carboxylic acid (ROOH)	[M+H-CO <sub>2</sub> ] <sup>+</sup>	-CO <sub>2</sub>
	[M+H-H <sub>2</sub> O-CO] <sup>+</sup>	-H <sub>2</sub> O-CO
	[M+H-H <sub>2</sub> O] <sup>+</sup>	-H <sub>2</sub> O
Phenol (ROH)	[M+H-CO] <sup>+</sup>	-CO
	[M+H-CH <sub>3</sub> ] <sup>+</sup> *	-CH <sub>3</sub>
Methoxy (ROCH <sub>3</sub> )	[M+H-CH <sub>3</sub> O] <sup>+</sup> *	-CH <sub>3</sub> O
	[M+H-CH <sub>3</sub> OH] <sup>+</sup>	-CH <sub>3</sub> OH
	[M+H-HCOH] <sup>+</sup>	-HCOH
	[M+H-R <sup>2</sup> OH] <sup>+</sup>	-R <sup>2</sup> OH
Ester (R <sup>1</sup> COOR <sup>2</sup> )	[M+H-R <sup>2</sup> OH-CO] <sup>+</sup>	-R <sup>2</sup> OH-CO
	[M+H-NH <sub>3</sub> ] <sup>+</sup>	-NH <sub>3</sub>
Amine	[M+H-CO] <sup>+</sup>	-CO
Aldehyde (RCHO)	[M+H-CO] <sup>+</sup>	-CO

208  
209  
210  
211  
212  
213  
214  
215  
216  
217  
218  
219  
220  
221  
222  
223

224  
225  
226  
227  
228  
229  
230  
231  
232  
233  
234  
235  
236

237 **Table S2.** Reaction conditions, initial VL (and GUA) decay rates, normalized abundance of  
238 products, and average carbon oxidation state ( $\langle OS_e \rangle$ ) in each experiment. Except where noted, the  
239 reaction systems consisted of VL (0.1 mM); GUA (0.1 mM); AN (1 mM); sodium nitrate (SN) (1  
240 mM); VOC (IPA) (1 mM) or inorganic anions (NaBC) (1 mM) under air-saturated conditions after  
241 6 h of simulated sunlight irradiation. Analyses were performed using UHPLC-qToF MS equipped  
242 with an ESI source and operated in the positive ion mode.

Exp no.	pH	Reaction conditions	Initial VL (and GUA) decay rates ( $\text{min}^{-1}$ ) <sup>b</sup>	Ratio of 50 most abundant products to total products <sup>e</sup>	Normalized abundance of products <sup>d</sup>	Normalized abundance of N-containing compounds <sup>d</sup>	$\langle OS_e \rangle^e$
A1	2.5	VL*	$2.8 \times 10^{-3}$	0.59	1.7	-	-0.05
A2		VL+AN	$2.5 \times 10^{-3}$	0.63	1.4	$5.3 \times 10^{-2}$	-0.04
A3	3	VL*	$2.1 \times 10^{-3}$	0.53	1.9	-	-0.04
A4		VL+AN	$2.1 \times 10^{-3}$	0.56	1.9	$3.6 \times 10^{-2}$	-0.05
A5	4	VL*	$1.9 \times 10^{-3}$	0.58	0.26	-	-0.16
A6		VL* (N <sub>2</sub> -saturated)	$4.6 \times 10^{-4}$	0.96	$4.7 \times 10^{-2}$	-	-0.24
A7		VL+AN	$1.9 \times 10^{-3}$	0.53	0.37	$1.7 \times 10^{-2}$	-0.13
A8		VL+AN (N <sub>2</sub> -saturated)	$2.9 \times 10^{-4}$	0.89	0.12	$6.3 \times 10^{-3}$	-0.21
A13		VL+SN	-	0.51	0.42	$1.7 \times 10^{-2}$	-0.07
A14		VL* (0.01 mM) <sup>d</sup>	-	0.90	0.37	-	-0.07

A15	VL (0.01 mM) + AN (0.01 mM)	—	0.77	0.40	$8.6 \times 10^{-3}$	0.12
A16	VL (0.01 mM) + AN	—	0.42	0.45	$1.2 \times 10^{-2}$	-0.06
A17	GUA only	$9.0 \times 10^{-4}$	0.77	—	—	-0.28
A18	GUA+VL	GUA: $2.0 \times 10^{-3}$ VL: $6.2 \times 10^{-4}$	0.60	2.2	—	-0.27
A19	GUA+AN	$1.1 \times 10^{-3}$	0.77	—	—	-0.26

243

244 <sup>a</sup>Irradiation time for VL\* (0.01 mM, A14) was 3 h. <sup>b</sup>The data fitting was performed in the initial  
 245 linear region. <sup>c</sup>Ratio of the normalized abundance of the 50 most abundant products to that of total  
 246 products, except for direct GUA photodegradation (A17), GUA+VL (A18), and GUA+AN (A19)  
 247 whose ratios are based on the absolute signal area of products. <sup>d</sup>The normalized abundance of  
 248 products was calculated using Eq. 2. <sup>e</sup><OS<sub>e</sub>> of the 50 most abundant products.

249

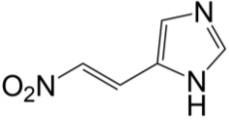
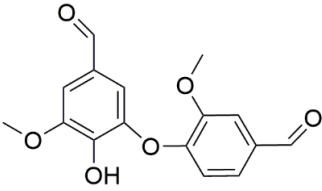
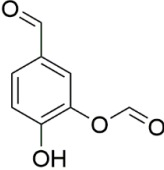
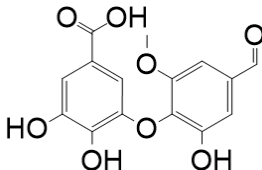
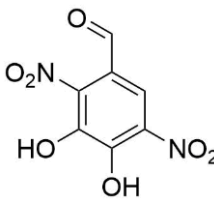
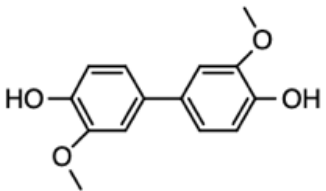
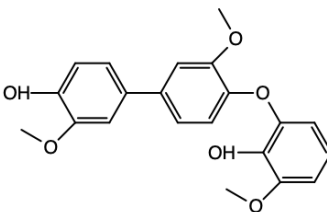
250 **Table S23.** Examples of proposed molecular structures for products identified from vanillin (and  
 251 guaiacol) photo-oxidation experiments in this study.

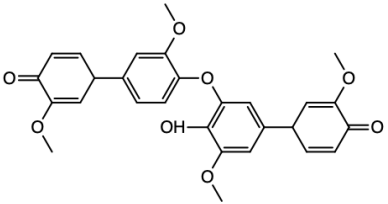
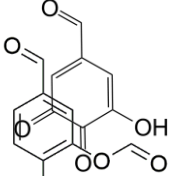
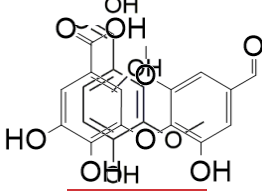
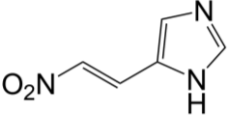
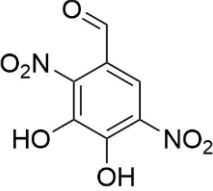
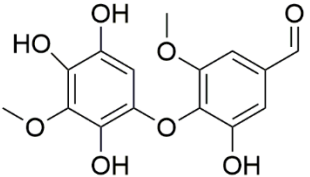
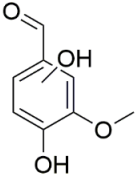
252

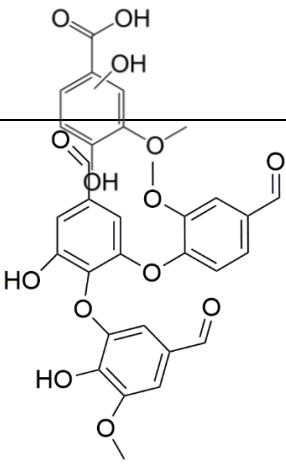
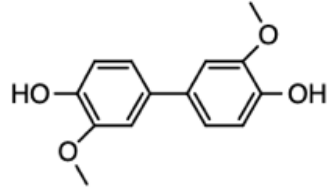
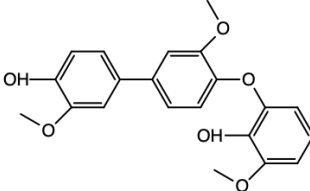
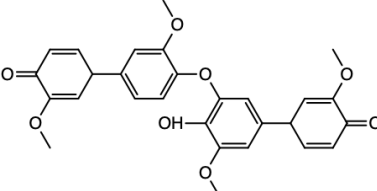
253

No.	Formula	DBE	Proposed structure	MS/MS fragment ions		
1	C <sub>8</sub> H <sub>8</sub> O <sub>3</sub> <u>(VL; the aqSOA precursor)</u>	5		-CO-CH <sub>3</sub> OH	-CO	-CO-CH <sub>3</sub> OH-CO
2	C <sub>8</sub> H <sub>9</sub> NO <sub>3</sub>	5		-CO-CH <sub>3</sub>	-NH <sub>3</sub>	
<del>3</del> 33	<del>C<sub>16</sub>H<sub>10</sub>N<sub>2</sub>O<sub>9</sub></del>	<del>13</del>		-NO <sub>2</sub>		
<u>4</u>	<u>C<sub>10</sub>H<sub>10</sub>O<sub>5</sub></u>	<u>6</u>		<u>-CH<sub>3</sub>OH</u>	<u>-CH<sub>3</sub>OH-CO</u>	
4	C <sub>10</sub> H <sub>10</sub> O <sub>5</sub>	6		-CH <sub>3</sub> OH	-CH <sub>3</sub> OH-CO	

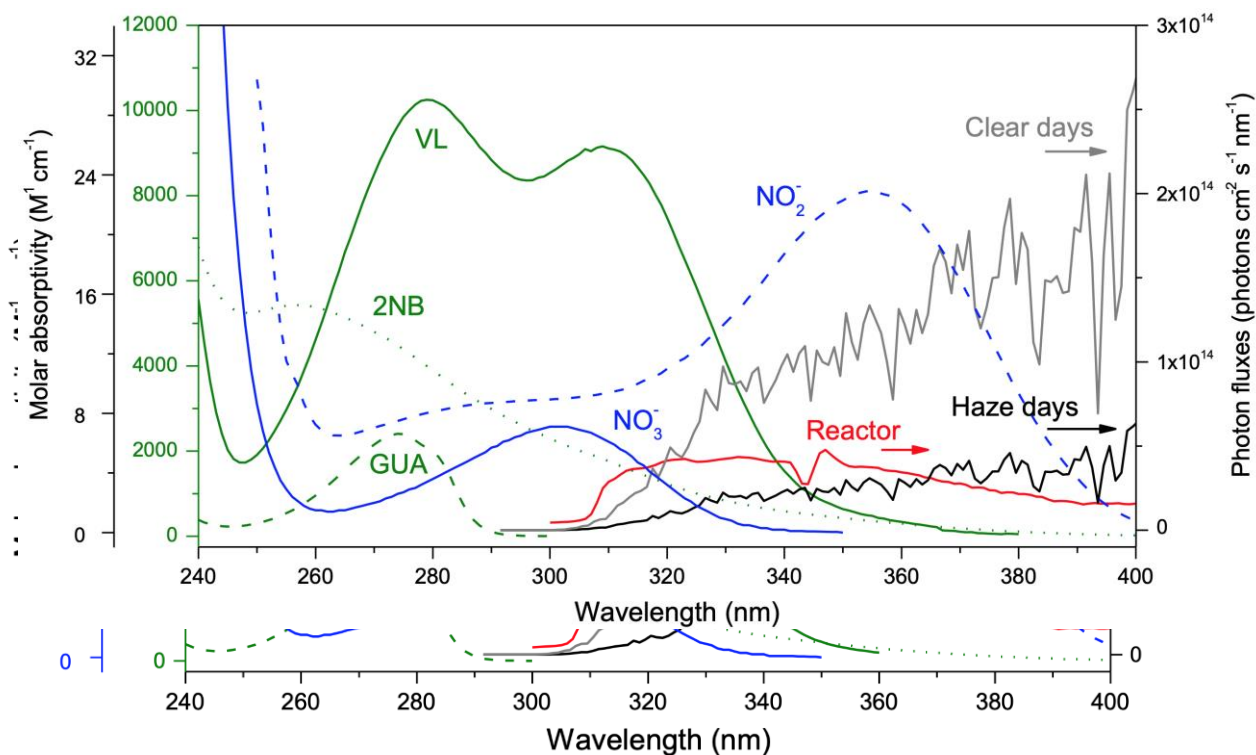


<u>5</u>	<u>C<sub>5</sub>H<sub>5</sub>N<sub>3</sub>O<sub>2</sub></u>	<u>5</u>		<u>-NH</u>		
<u>65</u>	C <sub>16</sub> H <sub>14</sub> O <sub>6</sub>	10		-CO-CH <sub>3</sub> OH- CO	-CO- CH <sub>3</sub> OH- CO-CH <sub>3</sub> OH	-CO- CH <sub>3</sub> OH- CO-CO
<u>7</u>	<u>C<sub>8</sub>H<sub>6</sub>O<sub>4</sub></u>	<u>6</u>		<u>-CO</u>	<u>-CO-CO</u>	
<u>8</u>	<u>C<sub>15</sub>H<sub>12</sub>O<sub>8</sub></u>	<u>10</u>		<u>-COOH</u>		
<u>9</u>	<u>C<sub>7</sub>H<sub>4</sub>N<sub>2</sub>O<sub>7</sub></u>	<u>7</u>				
<u>10</u>	<u>C<sub>14</sub>H<sub>14</sub>O<sub>4</sub></u>	<u>8</u>				
<u>116</u>	<u>C<sub>21</sub>H<sub>20</sub>O<sub>6</sub></u> <u>H<sub>4</sub>O<sub>4</sub></u>	<u>12</u> <u>6</u>		<u>-CO</u>	<u>-CO-CO</u>	

127	$\frac{C_{28}H_{24}O_8}{5H_{12}O_8}C_4$	1740		<del>-CO</del>	<del>-CH<sub>3</sub></del>	
138	$\frac{C_7H_4O_4}{6O_4}C_8H$	<u>6</u> 6		<del>-CO-CO</del>	<del>-CO-CO-</del> <del>CO-CO</del>	
149	$\frac{C_8H_8O_4}{H_{12}O_8}C_{15}$	<u>540</u>		<del>-CO-CH<sub>3</sub>OH-</del> <del>COOH</del>	<del>-CO</del>	<del>-H<sub>2</sub>O</del>
10	$C_5H_5N_3O_2$	5		<del>-NH</del>		
11	$C_7H_4N_2O_7$	7				
12	$C_{15}H_{14}O_8$	9		<del>-CO-CH<sub>3</sub>OH-</del> <del>CO-CO</del>	<del>-CO-</del> <del>CH<sub>3</sub>OH-</del> <del>CO-H<sub>2</sub>O</del>	<del>-CO-</del> <del>CH<sub>3</sub>OH-</del> <del>CO</del>
13	$C_8H_8O_4$	5		<del>-CO-CH<sub>3</sub>OH</del>	<del>-CO</del>	<del>-H<sub>2</sub>O</del>
14	$C_8H_8O_5$	5		<del>-CO-CH<sub>3</sub>OH</del>	<del>-CO<sub>2</sub></del>	<del>-CH<sub>3</sub>OH</del>

15	$C_{23}H_{18}O_9$	15				
19	$C_{14}H_{14}O_4$	8				
20	$C_{21}H_{20}O_6$	12				
21	$C_{28}H_{24}O_8$	17				

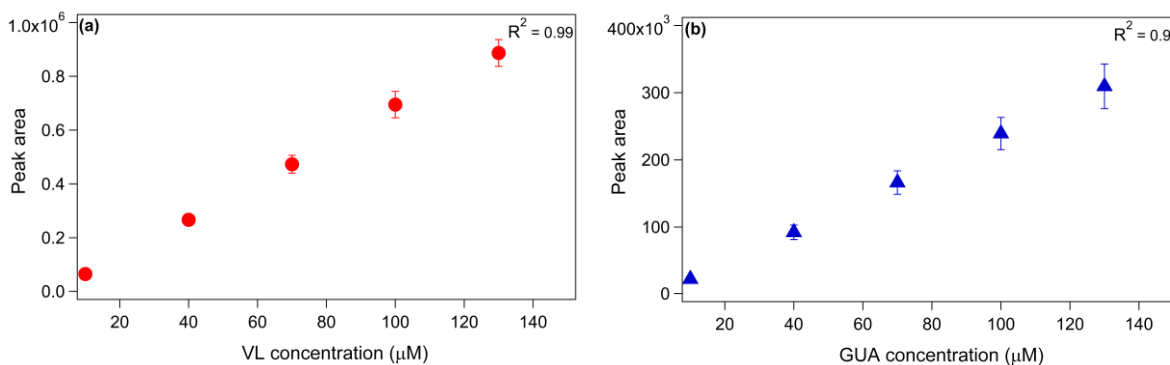
254  
255  
256  
257  
258  
259  
260  
261  
262  
263  
264



265  
266

267 **Figure S1.** The base-10 molar absorptivities ( $\epsilon$ ,  $M^{-1} cm^{-1}$ ) of vanillin (VL, green solid line), 2-  
268 nitrobenzaldehyde (2NB, green dotted line), guaiacol (GUA, green dashed line),  $NO_2^-$  (blue  
269 dashed line),  $NO_3^-$  (blue solid line), and photon flux in the aqueous reactor (red line) during typical  
270 haze days (black line) or clear days (grey line) in Beijing, China. The  $\epsilon$  values for 2NB and  $NO_2^-$   
271 were adapted from Galbavy et al. (2010) and Chu and Anastasio (2007), respectively.

272  
273



274  
275

276 **Figure S2.** Calibration curves for (a) VL and (b) GUA standard solutions (10–130  $\mu M$ ). Error  
277 bars represent one standard deviation.  
278  
279

280  
 281  
 282  
 283  
 284  
 285  
 286  
 287  
 288  
 289  
 290  
 291  
 292  
 293  
 294  
 295  
 296  
 297  
 298  
 299  
 300  
 301  
 302  
 303  
 304  
 305  
 306  
 307  
 308  
 309  
 310  
 311

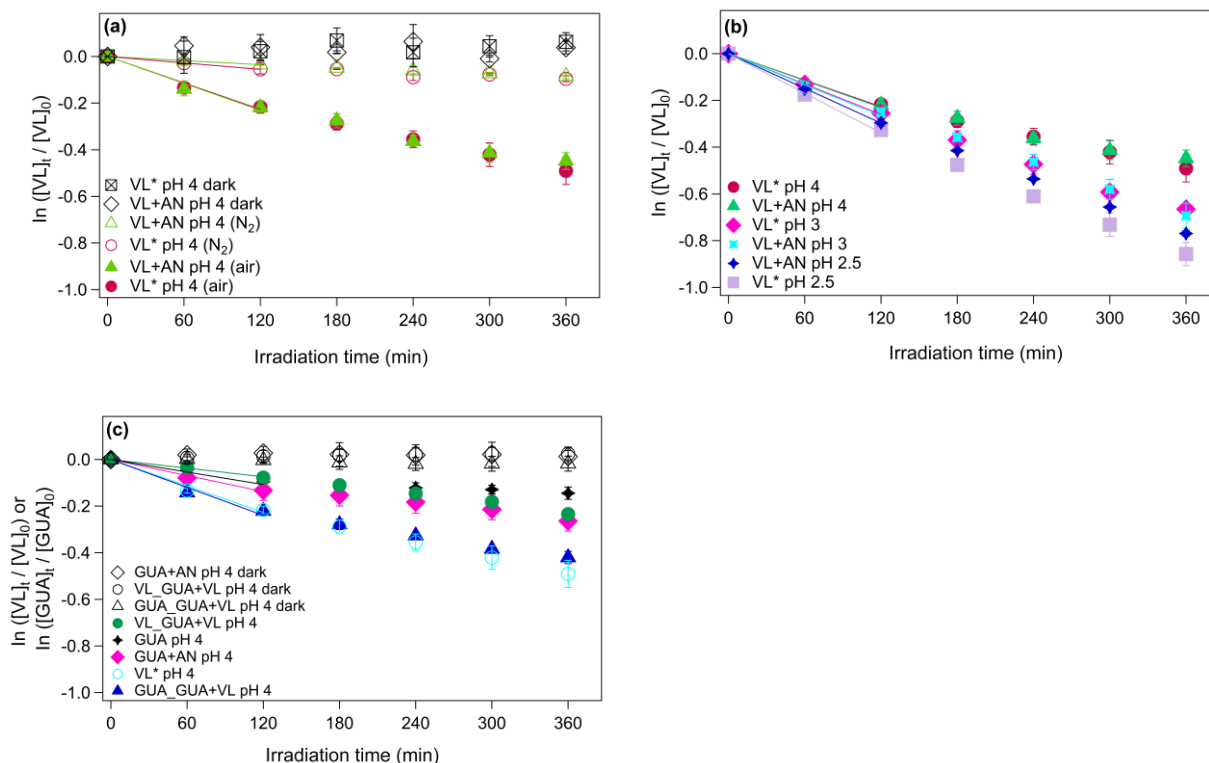
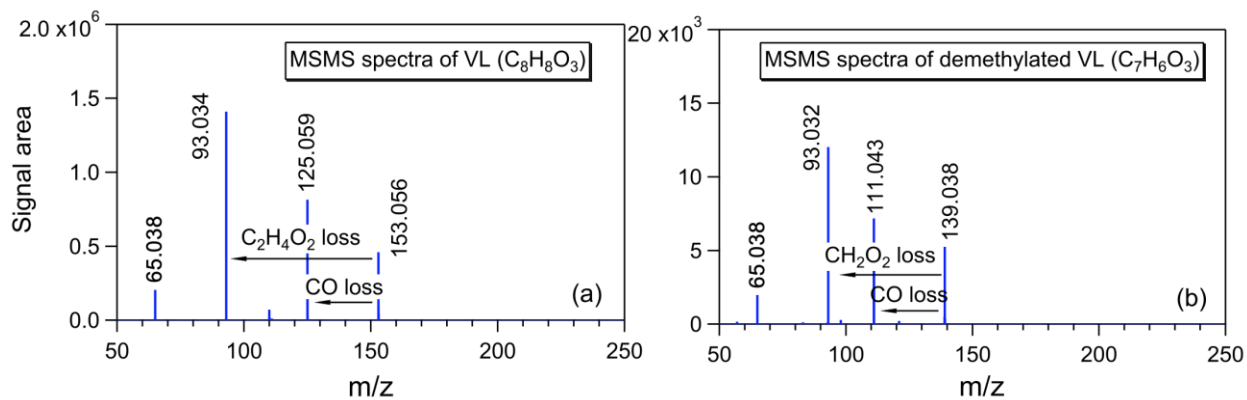
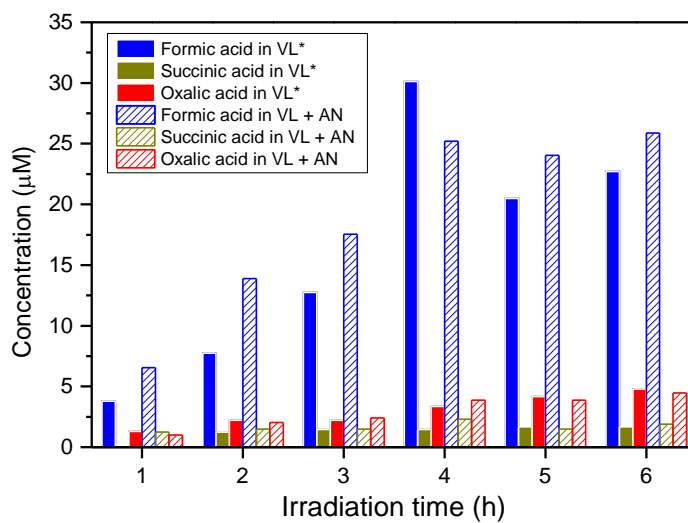


**Figure S3.** (a–c) The decay of VL under different experimental conditions for direct photosensitized oxidation of VL (VL\*) and nitrate-mediated VL photo-oxidation (VL+AN): (a) ~~Effect of secondary oxidants from VL triplets on VL\*~~ and VL+AN at pH 4 under N<sub>2</sub>- (A6, A8) and air-saturated (A5, A7) conditions. (b) Effect of pH on VL\* and VL+AN at pH 2.5 (A1, A2), 3 (A3, A4), and 4 (A5, A7) under air-saturated conditions. (c) ~~Effect of the presence of VOCs and inorganic anions: IPA (A9) and NaBC (A10) on VL\* at pH 4 under air-saturated conditions.~~ (d) ~~Effect of the presence of VOCs and inorganic anions: IPA (A11) and NaBC (A12) on VL+AN at pH 4 under air-saturated conditions.~~ (e) The decay of VL (and GUA) during direct GUA photodegradation (A137) and photo-oxidation of GUA in the presence of VL (GUA+VL; A148) or nitrate (GUA+AN; A159) at pH 4 under air-saturated conditions after 6 h of simulated sunlight irradiation. Error bars represent one standard deviation; most error bars are smaller than the markers.



312  
 313 **Figure S4.** MS/MS spectra of (a) VL and (b) demethylated VL. The arrows indicate possible  
 314 fragmentation pathways of VL and demethylated VL.

315  
 316



317  
 318 **Figure S5.** The concentration of formic, oxalic, and succinic acid at different reaction times for  
 319 VL\* (A5) and VL+AN (A7) at pH 4 under air-saturated conditions.

320  
 321  
 322

323

324

325

326

327

328

329

330

331

332

333

334

335

336

337

338

339

340

341

342

343

344

345

346

347

348

349

350

351

352

353

354

355

356

357

358

359

360

361

362

363

364

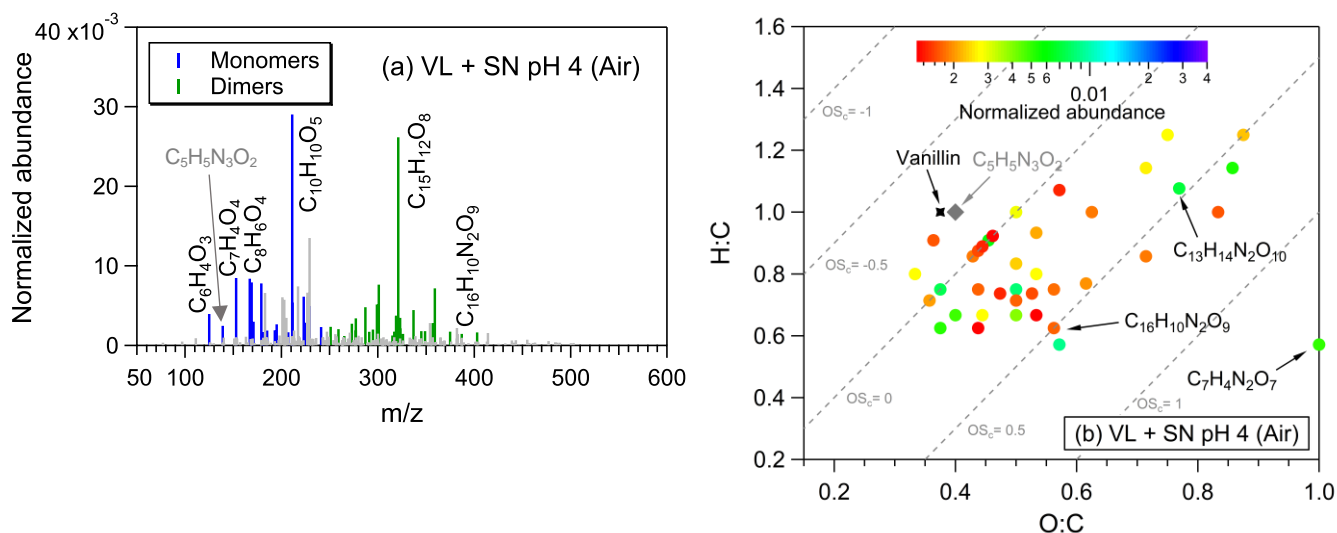
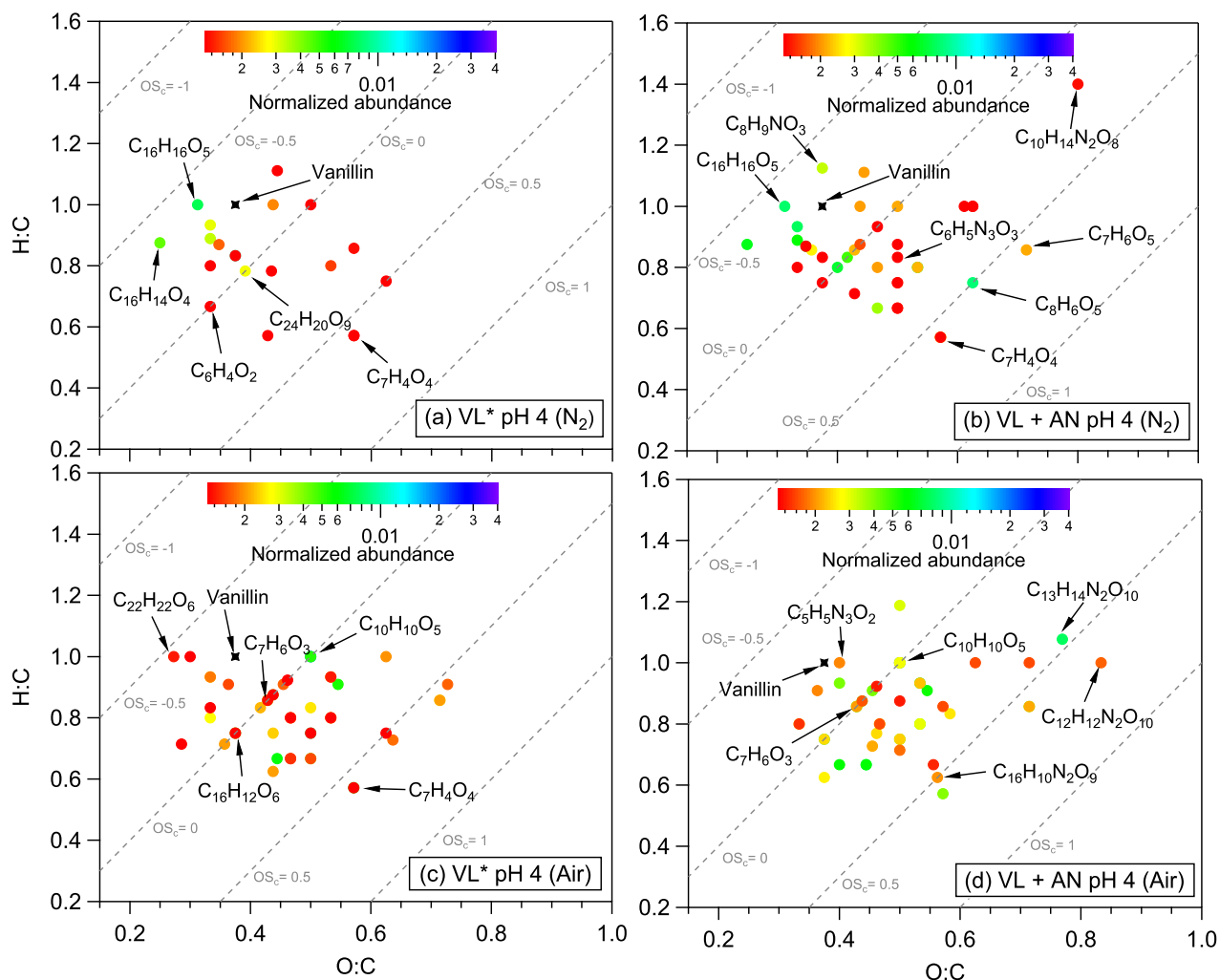


**Figure S6.** (a) Reconstructed mass spectra of assigned peaks and (b) van Krevelen diagram of the 50 most abundant products from VL+SN (A943) at pH 4 under air-saturated conditions after 6 h of simulated sunlight irradiation. The normalized abundance of products was calculated from the ratio of the peak area of the product to that of VL (Eq. 2). The 50 most abundant products contributed more than half of the total normalized abundance of products, and they were identified as monomers (blue) and dimers (green). Grey peaks denote peaks with low abundance or unassigned formula. Examples of high-intensity peaks were labeled with the corresponding neutral formulas. The color bar denotes the normalized abundance of products. The grey dashed lines indicate the carbon oxidation state values (e.g., OS<sub>c</sub> = -1, 0, and 1). The grey arrows show where the potential imidazole derivative (C<sub>5</sub>H<sub>5</sub>N<sub>3</sub>O<sub>2</sub>) from VL+AN was observed.



365

366 **Figure S7.** van Krevelen diagrams of the 50 most abundant products from (a) VL\* (N<sub>2</sub>-saturated;  
 367 A6), (b) VL+AN (N<sub>2</sub>-saturated; A8), (c) VL\* (air-saturated; A5), and (d) VL+AN (air-saturated;  
 368 A7) at pH 4 after 6 h of simulated sunlight irradiation. The color bar denotes the normalized  
 369 abundance of products. The grey dashed lines indicate the carbon oxidation state values (e.g., OS<sub>c</sub>  
 370 = -1, 0, and 1).

371

372

373

374

375

376



377

378

379

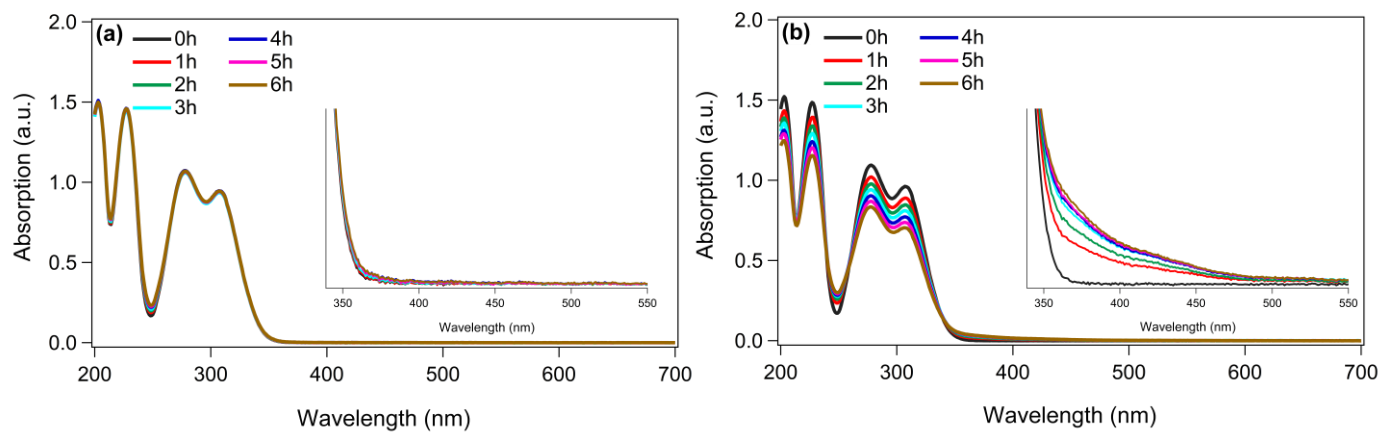
380

381

382

383

384



385

386

387

388

389

390

391

392

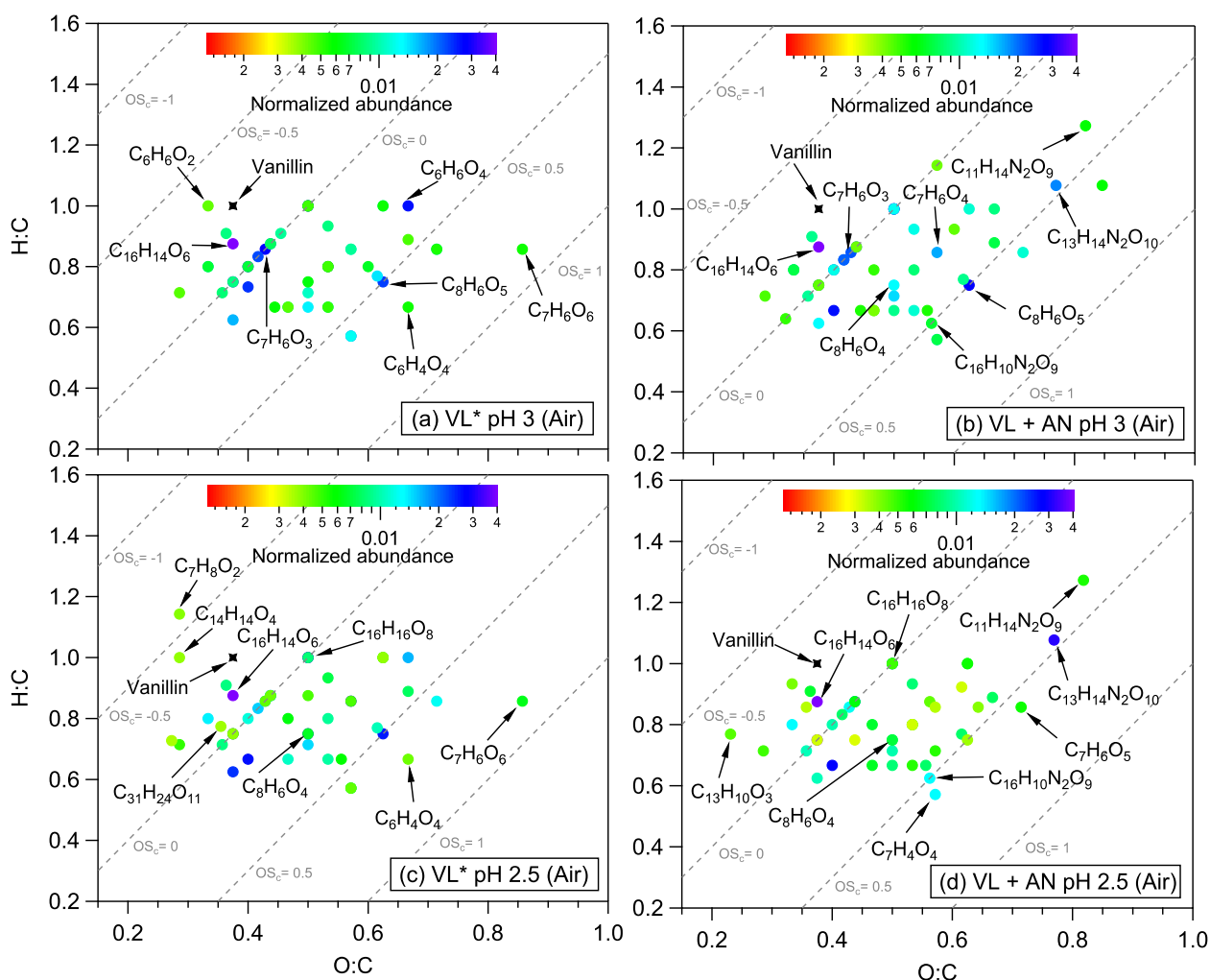
393

394

395

396

**Figure S8.** UV-Vis absorption spectra of VL\* (A6, A5; pH 4) under (a) N<sub>2</sub>- and (b) air-saturated conditions at different time intervals. The insets show the absorbance enhancement from 350 to 550 nm.



397

398

399 **Figure S9.** van Krevelen diagrams of the 50 most abundant products from (a) VL\* pH 3 (A3), (b)  
 400 VL+AN pH 3 (A4), (c) VL\* pH 2.5 (A1), and (d) VL+AN pH 2.5 (A2) under air-saturated  
 401 conditions after 6 h of simulated sunlight irradiation. The color bar denotes the normalized  
 402 abundance of products. The grey dashed lines indicate the carbon oxidation state values (e.g., OS<sub>c</sub>  
 403 =-1, 0, and 1).

404

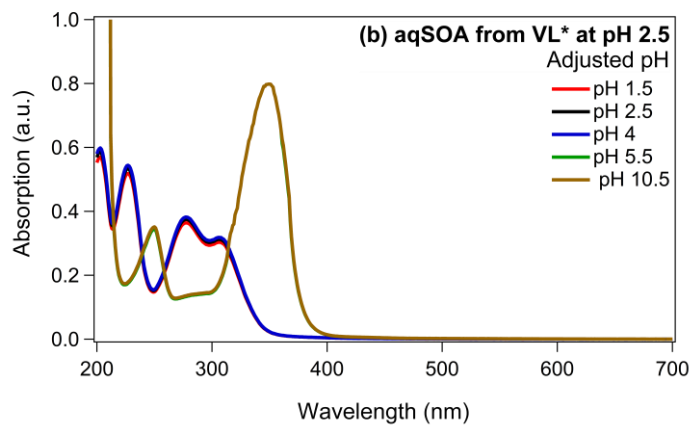
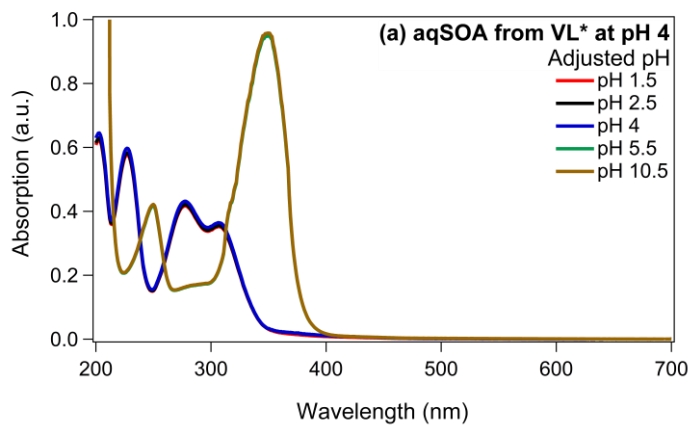
405

406

407

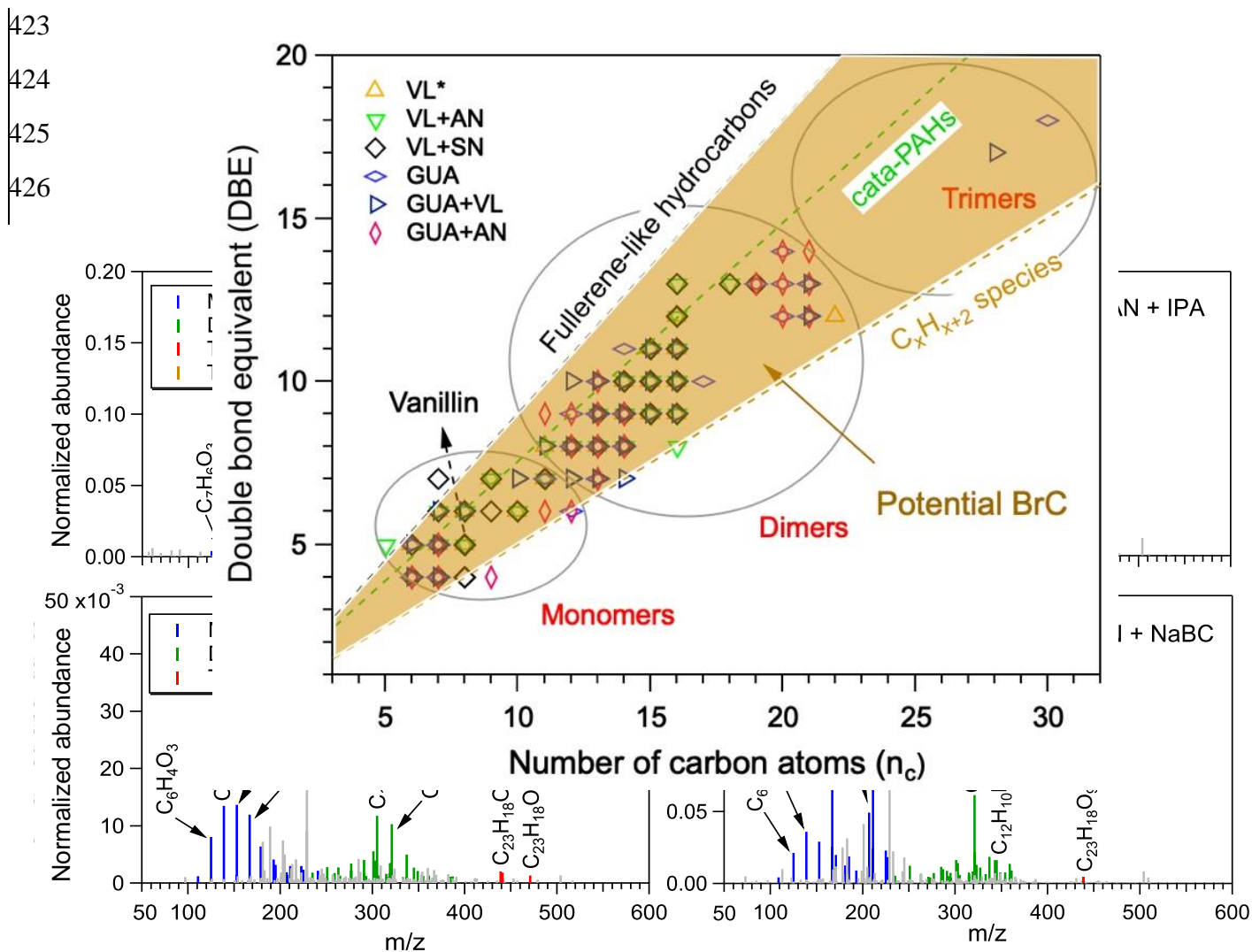
408

409



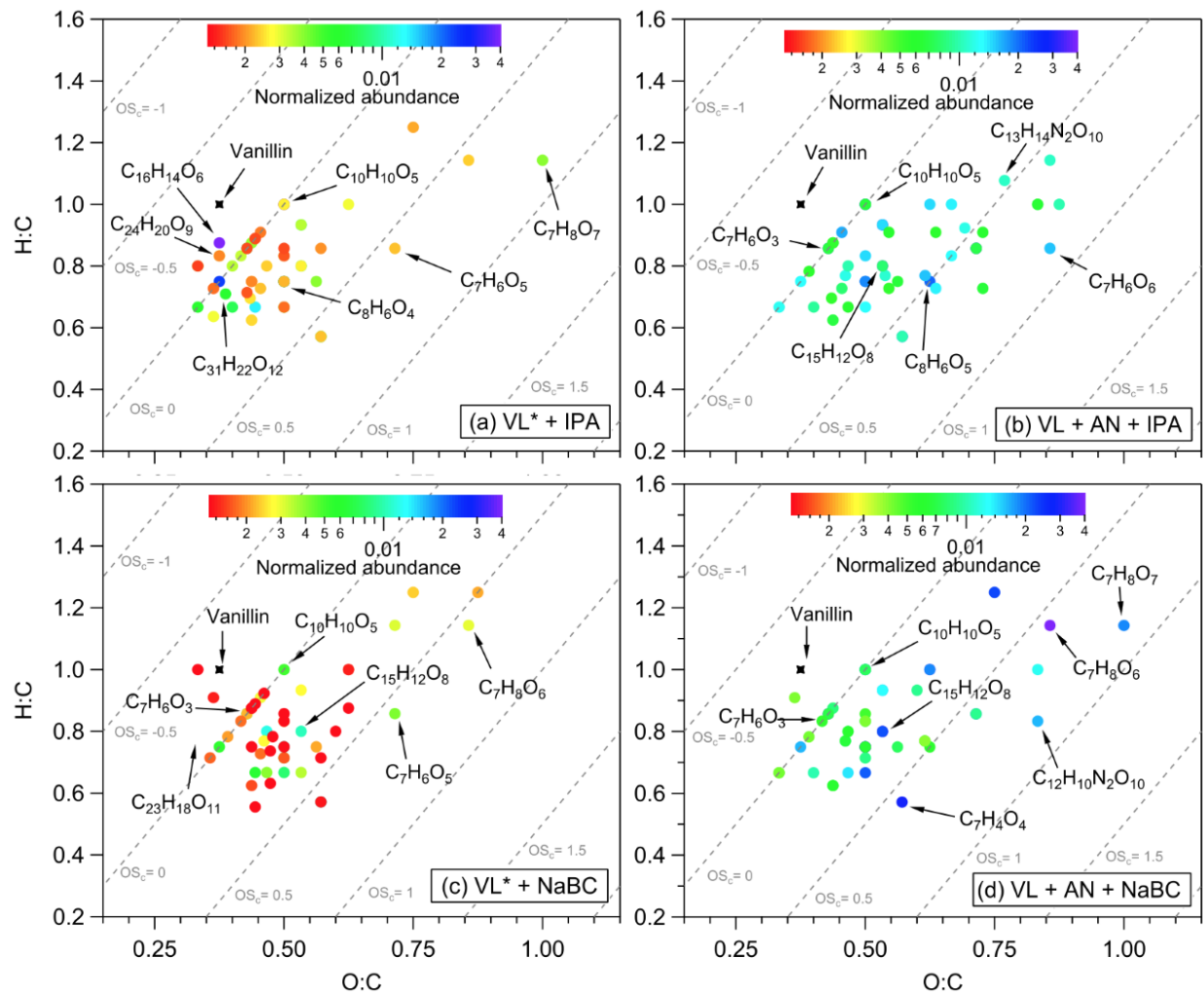
410  
411  
412  
413  
414  
415  
416  
417  
418  
419  
420  
421  
422

**Figure S10.** UV-Vis absorption spectra of VL\*-derived aqSOA formed at (a) pH 4 and (b) pH 2.5 over a range of pH conditions from 1.5 to 10.5.



427  
 428 **Figure S10.** Reconstructed mass spectra of assigned peaks from (a) VL\*+IPA (A9), (b)  
 429 VL+AN+IPA (A11), (c) VL\*+NaBC (A10), and (d) VL+AN+NaBC (A12) at pH 4 under air-  
 430 saturated conditions after 6 h of simulated sunlight irradiation. The normalized abundance of  
 431 products was calculated from the ratio of the peak area of the product to that of VL (Eq. 2). The  
 432 50 most abundant products contributed more than half of the total normalized abundance of  
 433 products, and they were identified as monomers (blue), dimers (green), trimers (red), and tetramers  
 434 (orange). Grey peaks denote peaks with low abundance or unassigned formula. Examples of high-  
 435 intensity peaks were labeled with the corresponding neutral formulas. Note the different scales on  
 436 the y axes.

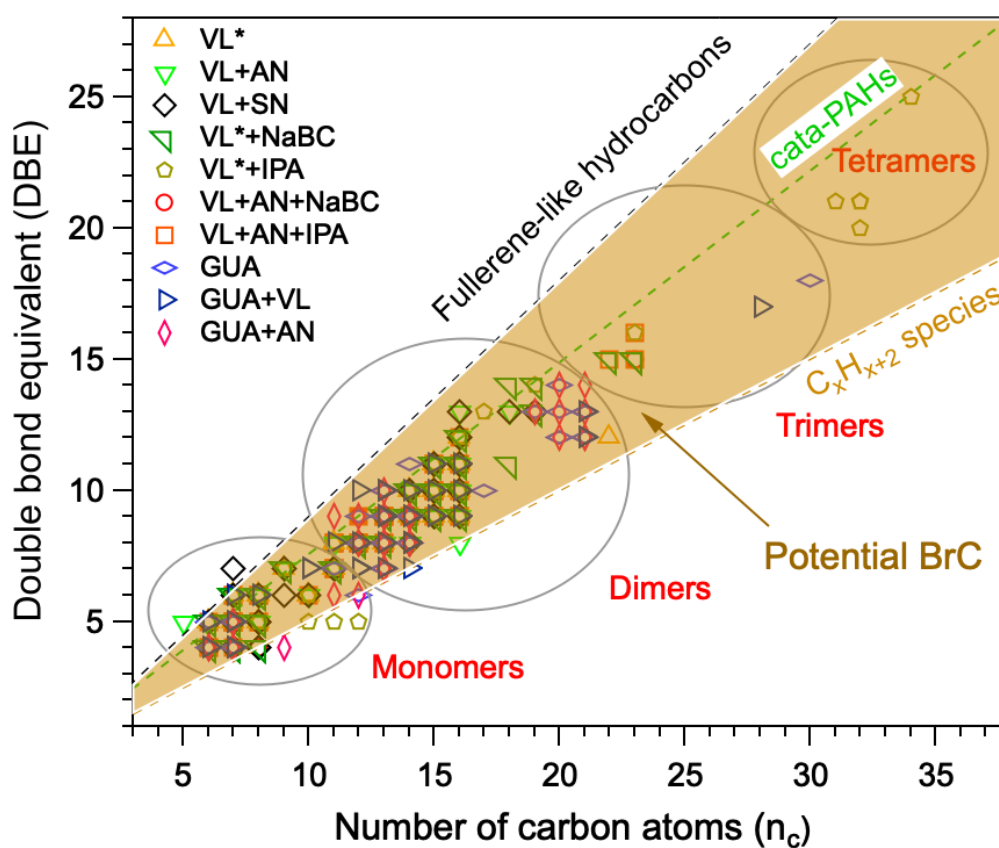
437  
 438  
 439  
 440



441  
 442  
 443  
 444  
 445  
 446  
 447  
 448  
 449  
 450  
 451  
 452  
 453

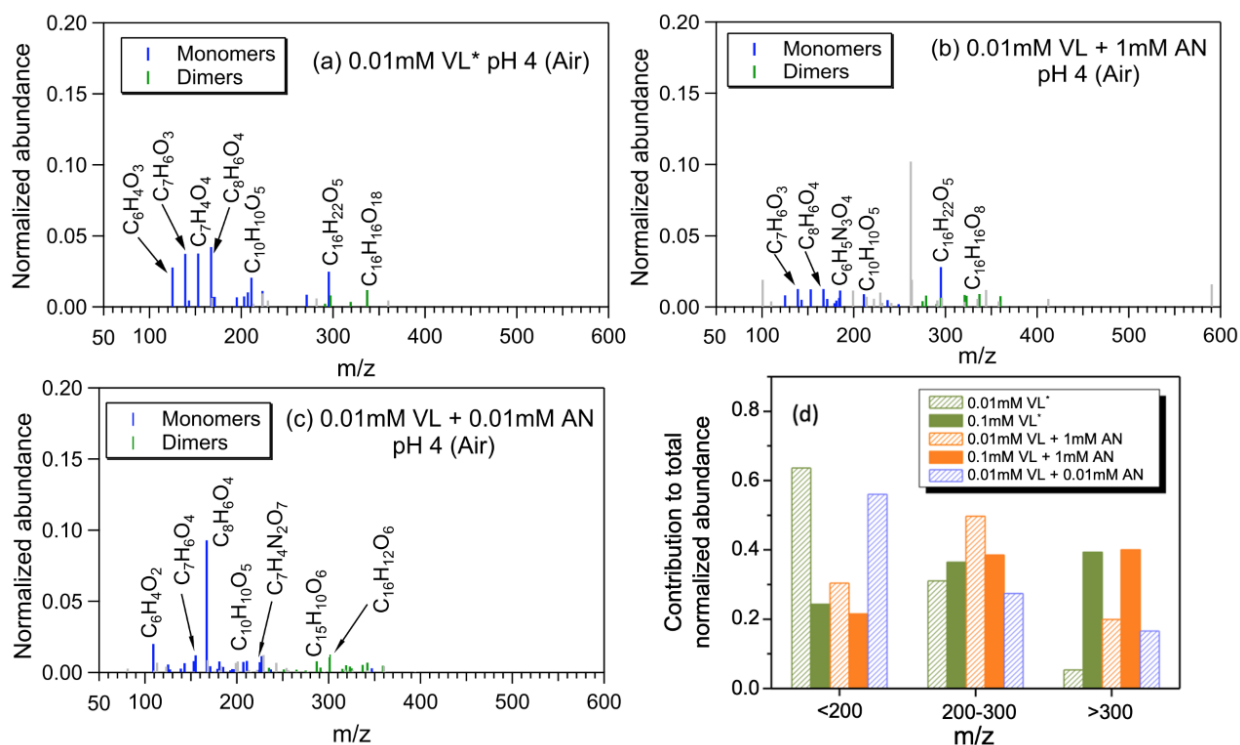
**Figure S11.** van Krevelen diagrams of the 50 most abundant products from (a) VL\*+IPA (A9), (b) VL+AN+IPA (A11), (c) VL\*+NaBC (A10), and (d) VL+AN+NaBC (A12) at pH 4 under air-saturated conditions after 6 h of simulated sunlight irradiation. The color bar denotes the normalized abundance of products. The grey dashed lines indicate the carbon oxidation state values (e.g.,  $OS_c = -1, 0,$  and  $1$ ).

454  
455  
456  
457  
458  
459  
460  
461  
462  
463  
464  
465  
466  
467  
468  
469  
470  
471  
472  
473  
474  
475  
476  
477



478 **Figure S112.** The plot of the double bond equivalent (DBE) values vs. number of carbon atoms  
479 ( $n_c$ ) (Lin et al., 2018) for the 50 most abundant products from pH 4 experiments under air-saturated  
480 conditions. Dashed lines indicate DBE reference values of fullerene-like hydrocarbons (Lobodin  
481 et al, 2012) (black dashed line), cata-condensed polycyclic aromatic hydrocarbons (PAHs)  
482 (Siegmann and Sattler, 2000) (green dashed line), and linear conjugated polyenes (general formula  
483  $C_xH_{x+2}$ ) (brown dashed line). Data points within the shaded area are potential BrC chromophores.

484 Light grey circles show the classification of the data points as monomers, dimers, trimers, or  
 485 tetramers.  
 486



487  
 488 **Figure S123.** Reconstructed mass spectra of assigned peaks from (a) 0.01 mM VL\* (A104), (b)  
 489 0.01 mM VL + 1 mM AN (A116), and (c) 0.01 mM VL + 0.01 mM AN (A125) at pH 4 under air-  
 490 saturated conditions after 6 h of simulated sunlight irradiation. The normalized abundance of  
 491 products was calculated from the ratio of the peak area of the product to that of VL (Eq. 2). The  
 492 50 most abundant products contributed more than half of the total normalized abundance of  
 493 products, and they were identified as monomers (blue) and dimers (green). Grey peaks denote  
 494 peaks with low abundance or unassigned formula. Examples of high-intensity peaks were labeled  
 495 with the corresponding neutral formulas. (d) Contributions of different m/z ranges to the  
 496 normalized abundance of products from experiments with low [VL] = 0.01 mM (A104–A126) and  
 497 high [VL] = 0.1 mM (A5 and A7) at pH 4 under air-saturated conditions after 6 h of simulated  
 498 sunlight irradiation.

499  
 500  
 501  
 502  
 503  
 504  
 505

506  
507  
508  
509  
510  
511  
512  
513  
514  
515  
516  
517  
518  
519  
520  
521  
522  
523  
524  
525  
526  
527  
528  
529  
530  
531  
532  
533  
534  
535  
536  
537  
538  
539  
540  
541  
542  
543  
544  
545  
546  
547  
548  
549  
550

## References

Anastasio, C., Faust, B. C., and Rao, C. J.: Aromatic carbonyl compounds as aqueous-phase photochemical sources of hydrogen peroxide in acidic sulfate aerosols, fogs, and clouds. 1. Non-phenolic methoxybenzaldehydes and methoxyacetophenones with reductants (phenols), Environ. Sci. Technol., 31, 218–232, <https://doi.org/10.1021/es960359g>, 1996.

Bateman, A. P., Laskin, J., Laskin, A., and Nizkorodov, S. A.: Applications of high-resolution electrospray ionization mass spectrometry to measurements of average oxygen to carbon ratios in secondary organic aerosols, Environ. Sci. Technol., 46, 8315–8324, <https://doi.org/10.1021/es3017254>, 2012.

Che, H., Xia, X., Zhu, J., Li, Z., Dubovik, O., Holben, B., Goloub, P., Chen, H., Estelles, V., Cuevas-Agulló, E., Blarel, L., Wang, H., Zhao, H., Zhang, X., Wang, Y., Sun, J., Tao, R., Zhang, X., and Shi, G.: Column aerosol optical properties and aerosol radiative forcing during a serious haze-fog month over North China Plain in 2013 based on ground-based sunphotometer measurements, Atmos. Chem. Phys., 14, 2125–2138, <https://doi.org/10.5194/acp-14-2125-2014>, 2014.

Chu, L. and Anastasio, C.: Temperature and wavelength dependence of nitrite photolysis in frozen and aqueous solutions, Environ. Sci. Technol., 41, 3626–3632, <https://doi.org/10.1021/es062731q>, 2007.

Erngren, I., Haglöf, J., Engskog, M. K. R., Nestor, M., Hedeland, M., Arvidsson, T., and Pettersson, C.: Adduct formation in electrospray ionisation-mass spectrometry with hydrophilic interaction liquid chromatography is strongly affected by the inorganic ion concentration of the samples, J. Chromatogr. A, 1600, 174–182, <https://doi.org/10.1016/j.chroma.2019.04.049>, 2019.

Galbavy, E. S., Ram, K., and Anastasio, C.: 2-Nitrobenzaldehyde as a chemical actinometer for solution and ice photochemistry, J. Photochem. Photobiol. A, 209, 186–192, <https://doi.org/10.1016/j.jphotochem.2009.11.013>, 2010.

Holčapek, M., Jirásko, R., and Lísa, M.: Basic rules for the interpretation of atmospheric pressure ionization mass spectra of small molecules, J. Chromatogr. A, 1217, 3908–3921, <https://doi.org/10.1016/j.chroma.2010.02.049>, 2010.

Koch, B. P. and Dittmar, T.: From mass to structure: an aromaticity index for high-resolution mass data of natural organic matter, Rapid Commun. Mass Spectrom., 20, 926–932, <https://doi.org/10.1002/rcm.7433>, 2006.



551 Lin, P., Fleming, L. T., Nizkorodov, S. A., Laskin, J., and Laskin, A.: Comprehensive molecular  
552 characterization of atmospheric brown carbon by high resolution mass spectrometry with  
553 electrospray and atmospheric pressure photoionization, *Anal. Chem.*, 90, 12493–12502,  
554 <https://doi.org/10.1021/acs.analchem.8b02177>, 2018.  
555

556 Lobodin, V. V., Marshall, A. G., and Hsu, C. S.: Compositional space boundaries for organic  
557 compounds, *Anal. Chem.*, 84, 3410–3416, <https://doi.org/10.1021/ac300244f>, 2012.  
558

559 Roemmelt, A. T., Steuer, A. E., and Kraemer, T.: Liquid chromatography, in combination with  
560 aquadropole time-of-flight instrument, with sequential window acquisition of all theoretical  
561 fragment-ion spectra acquisition: validated quantification of 39 antidepressants in whole blood  
562 as part of a simultaneous screening and quantification procedure, *Anal. Chem.*, 87, 9294–  
563 9301, <https://doi.org/10.1021/acs.analchem.5b02031>, 2015.  
564

565 Siegmann, K. and Sattler, K. D.: Formation mechanism for polycyclic aromatic hydrocarbons  
566 in methane flames, *J. Chem. Phys.*, 112, 698–709, <https://doi.org/10.1063/1.480648>, 2000.  
567

568 [Smith, J. D., Sio, V., Yu, L., Zhang, Q., and Anastasio, C.: Secondary organic aerosol production](#)  
569 [from aqueous reactions of 973 atmospheric phenols with an organic triplet excited state, \*Environ.\*](#)  
570 [Sci. Technol.](#), 48, 1049–1057, <https://doi.org/10.1021/es4045715>, 2014.

571

572 [Smith, J. D., Kinney, H., and Anastasio, C.: Phenolic carbonyls undergo rapid aqueous](#)  
573 [photodegradation to form low-volatility, light-absorbing products, \*Atmos. Environ.\*](#), 126, 36–44,  
574 <https://doi.org/10.1016/j.atmosenv.2015.11.035>, 2016.

575

576 Zhou, W., Mekic, M., Liu, J., Loisel, G., Jin, B., Vione, D., and Gligorovski, S.: Ionic strength  
577 effects on the photochemical degradation of acetosyringone in atmospheric deliquescent  
578 aerosol particles, *Atmos. Environ.*, 198, 83–88, <https://doi.org/10.1016/j.atmosenv.2018.10.047>,  
579 2019.  
580